AC0-1869

School of Biomedical Sciences

Structure/Function Studies of 5α- Reductase

Fiona O Baxter

This thesis is presented as part of the requirements for
the award of the degree of Doctor of Philosophy
of the Curtin University of Technology

April 2001

DECLARATION

I certify that this thesis does not incorporate, without acknowledgment, any material previously submitted for a degree or diploma from any university and that to the best of my knowledge and belief does not contain any material previously published or written by another person except where due reference is made in the text.

Signed:_____ Date:_____

Abstract

This thesis reports structure-function assessments made using site-directed mutagenesis of the human enzyme 5α-reductase (5AR), an enzyme crucial for normal masculine development. These assessments utilised the differences between the two forms of the enzyme in affinity for testosterone and sensitivity to the competitive inhibitor Finasteride.

Although first described in the 1950s, the enzyme has never been isolated and biochemical studies generated conflicting data. In some reports the enzyme was said to operate at a pH of 5.5 whereas others considered the pH optimum was more alkaline than this. Similarly, the affinity for testosterone was reported as being around 3μM and around 0.5μM and different sensitivities to the competitive inhibitor Finasteride also were reported. These differences were resolved in the period 1989-1991 by isolation of cDNAs coding for two forms of 5AR. These were termed 5AR1 and 5AR2. It is now known that 5AR1 operates at the more alkaline pH, has the lower affinity for testosterone and is the more resistant to Finasteride. 5AR1 is present to a greater extent in the periphery with 5AR2 predominating in the prostate.

Isolation of the cDNAs coding for 5AR1 and 5AR2 and the differing characteristics of the two enzymes, have provided the means to investigate structure-function relationships using site-directed mutagenesis. This approach enables identification of residues important for the binding of substrate and inhibitor by the two forms of human 5AR.

At the commencement of these studies, the residues -AVFA- had been identified as comprising part of the substrate/inhibitor binding site of human 5AR1. As the analogous residues, -VSIV- of rat 5AR1 also had been shown to contribute to this binding, it had been suggested that the analogous residues -GALA- in human 5AR2 may form its substrate/inhibitor binding domain. There was however no experimental evidence to support this suggestion. Similarly the roles of particular residues identified as being involved in substrate/inhibitor binding by 5AR had not

been subjected to significant study. Accordingly the experiments conducted were designed to address several unanswered questions. The most significant of these questions was are the residues -GALA- involved in substrate/inhibitor binding by human 5AR2 and if not what residues are in fact involved in this binding.

Rat 5AR1 exhibits a different mechanism of Finasteride inhibition than does rat 5AR2 and both of the human enzymes. This difference had been attributed to expression of a cysteine at position 146 in rat 5AR1 rather than the arginine expressed at the analogous position in rat 5AR2 and the human enzymes. The studies reported here for the mutation of the relevant arginine to cysteine do not substantiate the suggestion that cysteine 146 is responsible for the unique mechanism of inhibition by Finasteride shown by rat 5AR1

Although residues G34 and H231 in human 5AR2 had been shown important for substrate binding by this enzyme, the roles of these residues in inhibitor binding had not been examined nor had the roles of the analogous residues in human 5AR1 (G39 and H236). Experiments designed to determine these factors demonstrated a requirement of both G34 and H231 for substrate and inhibitor binding by human 5AR2. The analogous residues in 5AR1 were however only required for the binding of inhibitor.

The tetrapeptide -AVFA- had been shown to be involved in substrate/inhibitor binding by human 5AR1 but no assessment had been made of the relative roles of the individual amino acids comprising this tetrapeptide. Replacing residues in human 5AR1 with the corresponding residues from rat 5AR1 demonstrated a requirement in human 5AR1 of A26 and V27 for inhibitor but not substrate binding, possibly as a result of their conformational and electrostatic effects respectively. The branched chain residue V27 was found to be required for both substrate and inhibitor binding and the terminal alanine (A29) did not appear to play a significant role in the binding of either substrate or inhibitor. These studies also permitted an indirect assessment of the contribution of all four residues of the tetrapeptide -VSIV- to substrate binding by rat 5AR1 and showed that while the tripeptide -SIV- is important for inhibitor binding, the initial valine is not.

As mentioned above the main impetus of these studies was to determine if the residues -GALA- were involved in substrate/inhibitor binding by human 5AR2. Characterisation of mutants in which -GALA- in human 5AR2 was substituted with -AVFA- from 5AR1 and vice versa, showed these residues do not comprise the substrate/inhibitor binding site of human 5AR2.

From studies of a chimeric constructs of human 5AR1 and 5AR2 residues involved in substrate/inhibitor binding by human 5AR2 were mapped to the first 40 amino acid residues. Mutations of 6 residue clusters showed the hexapeptide -ATLVAL- (r15-20) in 5AR2 to contribute significantly to substrate/inhibitor binding. Further studies of this hexapeptide showed that residues -ATL- but not -VAL- form part of the substrate/inhibitor binding domain of human 5AR2.

Acknowledgments

I have been fortunate having had the help and support of many people throughout the duration of my PhD studies and would like to say a very big "THANK YOU" to them all. In particular I would like to acknowledge the following people;

First and foremost I would like to thank my supervisor Ian. Thank you for taking an interest in this project, your persistence for knowledge of the latest results provided me with a great deal of motivation and encouragement. Thank you for your patience, for always taking the time to listen and for all the advice and help you so willingly gave.

Thank you to all the staff at the School of Biomedical Science, Curtin University of Technology, for their support and technical assistance over the years. I would particularly like to thank Adrian Paxman for his friendly face, encouragement and willingness to help. Thanks to Katie Meehan, Fiona Lamb and Sasa Trivic for the laughter and good times we had together, you guys made it all that bit easier.

Finally I would like to thank my family and friends quite simply for just being them. You guys have provided me with all the love, encouragement and support I could possibly need. I would especially like to thank my parents for being so understanding of me and for being there through all the "ups and downs" that a PhD brings with it. But most importantly I would like to thank my Mum for keeping her fingers crossed so my mutations would work !

CONTENTS PAGE

Chapter 2.0 - Materials

Chapter 3.0 - Establishment of Cell Lines Stably Expressing Human 5α- Reductase 1 or 5α- Reductase 2

Chapter 4.0 - Mechanism of Inhibition of 5α- Reductase by Finasteride

Chapter 5.0 - Analysis of the Functional Importance of Glycine 39 and Histidine 236 in 5α- Reductase 1 and Glycine 34 and Histidine 231 in 5α- Reductase 2

Chapter 6.0 - Examining the Roles of Residues in the Tetrapeptide -AVFA- for Substrate/Inhibitor Binding in Human 5α- Reductase 1

Chapter 7.0 - Assessment of the Role of the Tetrapeptide -GALA- in Substrate/Inhibitor Binding by Human 5α- Reductase 2

Chapter 8.0 - Determination of the Substrate/Inhibitor Binding Domain of Human 5α- Reductase 2, Using Site-directed Mutagenesis

Index to Figures

Index to Tables

Publications

Publications from this study are;

Baxter, FO. and Lee, IR. 1999. Site-Directed Mutagenesis Studies of Substrate and Inhibitor Binding by Human 5α- Reductase. Combined Biological Sciences Meeting (ComBio.). Gold Coast (Qld, Australia), Abstract.

Baxter, FO., Trivic, S. and Lee, IR. 2000. Structure-Function Studies of Human 5α- Reductase 2. Eleventh Annual Combined Biological Sciences Meeting (CBSM). Perth (Western Australia), Abstract.

Baxter, FO., Trivic, S. and Lee, IR. 2001. Structure-Function Studies of Human 5α- Reductase 2, Using Site-Directed Mutagenesis. *J. Steroid Biochem. Molec. Biol.* 76(4-5). (Accepted for publication).

Abbreviations

^{14}C	*Carbon 14*
^{3}H	*Tritium*
^{32}P	*Phosphorous 32*
4-MA	*(17β-[N,N-diethyl] carbamoyl-4-methyl-4-aza-5α-androstan-3-one*
5AR	*5α- reductase*
5AR1	*5α- reductase 1*
5AR2	*5α- reductase 2*
A	*Alanine (Ala)*
AR	*Androgen receptor*
ATP	*Adenosine triphosphate*
BP	*Base pair*
BPH	*Benign prostatic hyperplasia*
BSA	*Bovine serum albumin*
cDNA	*Complementary deoxyribonucleic acid*
CHO	*Chinese hamster ovary*
CIAP	*Calf intestinal alkaline phosphatase*
CO_2	*Carbon dioxide*
cpm	*Counts per minute*
D	*Aspartate (Asp)*
Da	*Daltons*
dH_2O	*Distilled water*
DHT	*5α-Dihydrotestosterone*
DNA	*Deoxyribonucleic acid*
dNTP	*Deoxynucleotide triphosphate*
DMSO	*Dimethyl sulphoxide*
DTT	*Dithiothreitol*
E	*Glutamate (Glu)*
EDTA	*Ethylenediamine sodium tetra-acetic acid*
F	*Phenylalanine (Phe)*
FCS	*Foetal calf serum*
γ	*Gamma*
G	*Glycine (Gly)*

G418	*Geneticin (neomycin sulphate)*
GCP 53153	*N-2-[cyano-2-propyl]-3-oxo-4-aza-5α-androst-1-ene-17β-carboxamide*
H	*Histidine (His)*
hCG	*Human chorionic gonadotrophin*
HEPES	*N-[2-hydroxyethyl] piperazine N'-[2-ethane sulfonic acid]*
hpH_2O	*High pure water*
HPLC	*High performance liquid chromatography*
I	*Isoleucine (Ile)*
kb	*Kilobase*
K	*Lysine (Lys)*
Ki	*Inhibitor constant*
Km	*Affinity constant*
L	*Leucine (Leu)*
LB	*Luria bertani*
LH	*Leutinizing hormone*
LY 191704	*8-chloro-4-methyl-1,2,3,4,4a,5,6,10b-octahydro-bezol[f]quinolin-3(2H)-one*
MCS	*Multiple cloning site*
Mg	*Milligram*
Min	*Minute*
MIS	*Mullerian inhibiting substance*
MK-906	*Finasteride (17β-[N-t-butyl] carbamoyl-4-aza-5α-androst-1-ene-3-one)*
MPB	*Male pattern baldness*
mRNA	*Messenger ribonucleic acid*
N	*Asparagine (Asn)*
NADPH+	*β- Nicotinamide adenine dinucleotide phosphate*
NADP[H]	*β- Nicotinamide adenine dinucleotide phosphate (reduced form)*
nM	*Nanomolar*
nmol	*Nanomoles*
NOG	*n-octyl β-D-glucopyranoside*
ONO-3805	*4-[2-[4-(4-isobutylbenzyloxy)-2,3 dimethylbenzoylamino]phenoxy] butanoic acid*

ONPG	*o-nitrophenyl-β-D-galactopyranoside*
P	*Proline (Pro)*
PBS	*Phosphate buffered saline*
PC	*Prostate cancer*
PNK	*Polynucleotide kinase*
PSA	*Prostate specific antigen*
Q	*Glutamine (Glu)*
R	*Arginine (Arg)*
RNA	*Ribonucleic acid*
RNAse	*Ribonuclease A*
rpm	*Revolutions per minute*
S	*Serine*
SDS	*Sodium dodecyl sulphate*
SSCP	*Single stranded conformation polymorphism*
SRD5AR2	*Gene encoding 5AR2*
T	*Testosterone*
T7EEV	*T7 RNA polymerase promoter*
TAE	*TRIS/Acetic acid/EDTA buffer*
TE	*TRIS-EDTA*
Thr	*Threonine (T)*
TRIS	*Tris[hydroxymethyl] aminomethane*
TSG	*Tumour suppressor gene*
Vmax	*Maximum velocity*
μM	*Micromolar*
μmol	*Micromoles*
USA	*United states of America*
UV	*Ultraviolet*
V	*Valine (Val)*
W	*Tryptophan (Trp)*
X-gal	*5-Bromo-4-chloro-3-indolyl-β-D-galactopyranoside*
Y	*Tyrosine (Tyr)*
YENB	*Yeast extract nutrient broth*

Chapter 1.0

Literature Review

1.0 Literature Review

The enzyme 3-oxo-5α-steroid $\Delta^{4,5}$-dehydrogenase, more commonly called 5α-reductase (5AR) is a microsomal membrane protein with a central role in human male differentiation and androgen physiology[1]. It has a crucial role in the development of the male external genitalia and the prostate during embryogenesis and in the subsequent growth and maintenance of these structures during and after puberty. 5AR has both catabolic and anabolic roles of which the latter has attracted the most attention due to its association with disease. These roles of the enzyme are discussed below.

1.1 Catabolic Role of 5AR

The enzyme was first detected in rat liver slices by its ability to convert deoxycortisone to 5α- reduced metabolites[2, 3]. Subsequent studies demonstrated a requirement of 5AR for reduced pyridine nucleotide as a cofactor and the recognition of its ability to metabolise a variety of steroid substrates[4, 5, 6]. It is now known that 5AR catalyses the NADP[H] dependent 5α- reduction of $\Delta^{4,5}$ bonds in a variety of 4-ene-3-oxo steroids to give their corresponding 5α-dihydro-3-oxo form. Although the enzyme acts on gluco- and mineralo-corticoids and androgens, it acts most efficiently on progestagens such as pregn-4-ene-3,20-dione (progesterone)[7].

The 5α- reduction of the $\Delta^{4,5}$ double bond in the A-ring renders the 3-oxo group of steroid substrates more susceptible to reduction by the enzymes 3α- and 3β-hydroxysteroid dehydrogenase and to the processes of sulphation and glucuronylation[8]. Overall, this results in a reduction in affinity of binding proteins for steroid substrates, which facilitates their excretion from the body as they are no longer protein bound.

1.2 *Anabolic Role of 5AR*

The primary role of 5AR is its conversion of testosterone (T), the major circulating androgen in males, to dihydrotestosterone (DHT), the more potent by almost 50 fold, of the two androgens (Figure 1.1). It is DHT that through its effects on the male urogenital tract during embryogenesis brings about virilization of the external genitalia[9]. DHT also mediates many of the androgenic effects of male development at puberty including maturation of facial and body hair, development of acne, genital growth and the acquisition of male behaviour[10].

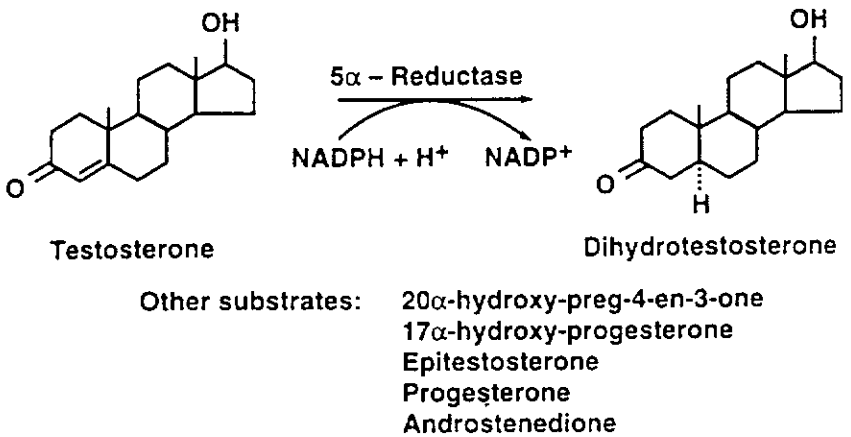

Figure 1.1: *The enzymatic reaction catalyzed by steroid 5AR[10].*

Both T and DHT mediate their effects on male sexual development by binding to the androgen receptor (AR) in the nucleus of the cell and activating androgen responsive genes[11].

1.3 *Androgens and Normal Sexual Development*

Embryonic sexual development occurs in three sequential steps[12], with the first being the establishment of chromosomal sex at fertilization ie. XX for females, XY for males. Chromosomal sex is then translated into gonadal sex, the exact mechanism of which is unknown. It is known however that the genetic determinants that induce the development of the testes, the SRY or testes

determining gene(s), are present on the Y chromosome[13]. Expression of the SRY gene transforms the bipotential gonad into a foetal testis capable of synthesizing T and other hormones. The final stage is the translation of gonadal sex into phenotypic sex and is the direct result of the type of gonad formed and the endocrine secretions of the foetal testes. During the formation of phenotypic sex, the indifferent internal and external anlage differentiate into their male or female forms. The internal genitalia arise from the Wolffian and Mullerian tissue, both of which are present in the early stages of embryogenesis. In males, the Wolffian tissue forms the epididymis, vas deferens and seminal vesicles and the Mullerian tissue disappears. In females, the Wolffian tissue degenerates or can persist as Gartner's ducts and the Mullerian tissue develops into the fallopian tubes, uterus and upper vagina[11]. Not only does differentiation of the internal and external genitalia occur during this final stage but sexual behaviour is also determined.

Virilization of the male foetus requires the production of T, DHT and anti-Mullerian hormone or Mullerian inhibiting substance (MIS). MIS is a glycoprotein produced by the sertoli cells of the foetal and newborn testes that causes regression of the Mullerian ducts preventing development of the uterus and fallopian tubes[14, 15].

T regulates gonadotrophin production and spermatogenesis. Most significantly, it promotes development of the male internal genitalia from Wolffian duct tissue and acts as a pro-hormone for DHT synthesis in the embryonic urogenital tract[11]. DHT is responsible for the differentiation of the male external genitalia (penis, scrotum and urethra) and for development of the prostate. Both T and DHT mediate their effects through the AR to which DHT binds with greater affinity than does T[16]. The mechanisms by which T and DHT bind to the same receptor yet mediate their different effects are only partially understood[11]. There are three contributing factors thought to be involved. These are that T binds less avidly to the AR than DHT due to DHT's slow dissociation rate, that formation of the DHT-receptor complex is more stable and therefore more readily transformed to the DNA-binding state and that the DHT-receptor complex activates a reporter gene system more efficiently than does the T-receptor complex.

The net effect of these three factors is that DHT formation amplifies an otherwise rather weak signal and/or that the DHT-receptor complex regulates specific genes that are unresponsive to T.

1.4 Biochemistry and Molecular Biology of 5AR

1.4.1 Characterisation Problems

The important role that androgens play in sexual differentiation has resulted in extensive study of 5AR. Insight into the biochemistry, pharmacology, regulation and physiology of 5AR has been limited by the extreme insolubility of this hydrophobic enzyme, its unstable nature and its trace-level presence in most androgen-dependent tissues[9]. There has also been considerable controversy regarding the existence of isoenzymes of 5AR and the biochemical characteristics of the human enzyme. Early studies in human skin fibroblasts demonstrated an enzyme primarily functional at neutral pH[17, 18]. Later studies from cell homogenates of genital skin fibroblasts[17], epididymis[7] and prostate[19], however suggest 5AR had an optimum pH of between 5.0-5.5 and that more than one isoform of 5AR may exist.

From 1971 to 1991 many unsuccessful attempts were made to purify 5AR from both rat and human tissues. Although solubilization of the enzyme from cell membranes using detergents was successful[20-28], activity was subsequently lost during chromatography. Chromatographic methods used for purification of 5AR include ion-exchange (DEAE-cellulose), hydrophobic (phenyl/octyl-sepharose) and affinity (NADP+-linked agarose) chromatography. All of these however have met with limited success due to a loss of enzyme activity upon binding of crude preparations to these supports[29]. This loss of activity is thought due, at least in part, to binding of partially purified enzyme to the chromatographic support matrix.

1.4.2 Expression Cloning

Much of the controversy regarding the number of isoenzymes and biochemical characteristics of 5AR has now been overcome by the use of expression cloning strategies, to isolate the cDNAs encoding rat and human 5AR. In 1988 *Xenopus laevis* oocytes injected with mRNA from rat liver and prostate were shown to express 5AR activity[30]. This approach was used by Andersson, Bishop and Russell[31] to isolate a cDNA from rat liver coding for a hydrophobic protein that catalyzed the conversion of T to DHT. In the same study a cDNA isolated from rat prostate coded for an identical protein, suggesting that there is only one form of 5AR. Differences were seen however in mRNA expression in these two tissues. mRNA in the liver increased in response to castration but remained unchanged in the prostate and T administration to castrated rats induced expression of mRNA in the prostate but not the liver. These findings led to the suggestion that T regulates the gene for 5AR differentially in androgen dependent and independent tissues[31].

The cDNA for rat 5AR was then used as a hybridization probe to screen a human prostate cDNA library and led to the isolation of the cDNA encoding human 5AR[1]. The characteristics of the human enzyme expressed by this cDNA however were not as expected as it exhibited resistance to inhibition by the 5AR inhibitor Finasteride and had an alkaline pH optimum. This was in marked contrast to earlier biochemical studies of 5AR in the prostate[19], which showed the enzyme to be sensitive to Finasteride and to have an acidic pH optimum.

These differences were explained when a second cDNA for human 5AR was cloned in 1991[32]. The enzyme coded for by this cDNA was termed 5AR2 and the enzyme coded for by the previously isolated cDNA termed 5AR1, after their chronological order of discovery. Isolation of 5AR2 also explained the differences seen in earlier biochemical studies of 5AR as it was this enzyme that exhibited an acidic pH optimum and was highly sensitive to Finasteride. In 1992 a second cDNA encoding rat 5AR was isolated[33]. The rat isoenzymes were also designated 5AR1 and 5AR2 according to their order of discovery. In both rat and man, 5AR1 and 5AR2 are different proteins that catalyze the same

biochemical reaction. Enzymes meeting this criterion can be referred to as isoenzymes[34].

1.5 Enzyme Characterisation

1.5.1 Gene Structure

The two human 5AR genes are nonsyntetic, as the genes for 5AR1 and 5AR2 are located on different chromosomes, 2 and 5 respectively. This is consistent with their divergence at the DNA sequence level[32]. The architecture and intron locations are similar in both genes suggesting the isoenzymes arose as a consequence of an ancient duplication event with subsequent evolution of their separate physiological roles.

The relative intron and exon sizes of the type 1 and type 2 genes differ. Exons 1 and 2 of the 5AR2 gene (SRD5AR2) encode proteins of 4 and 1 amino acid respectively, shorter than 5AR1, yet they share identical splice sites[35]. The sizes of introns 1, 2, 3 and 4 for the two genes also differ with those of SRD5AR2 being >29, 2.3, 2.0 and 3.0kb respectively whereas the 5AR1 gene (SRD5AR1) has introns of >14, 3.9, 6.6 and >7.0kb[35].

Studies of the human cDNAs demonstrated the existence of a 5AR pseudogene (SRD5AP1) on the X chromosome, thought to be derived from 5AR1 mRNA transcripts. This pseudogene lacks introns and although its DNA sequence within the coding region is 95% homologous with the functional SRD5AR1 gene[36], it contains a nonsense codon at residue 147. This results in premature translation termination and therefore it is believed the pseudogene encodes a non-functional protein.

1.5.2 Kinetic Constants

In cell lysates prepared from cells transfected with cDNA coding for either rat or human 5AR1, the expressed enzymes exhibit a micromolar affinity (Km = 1-

5μM) for a variety of steroid substrates including T, androstenedione and progesterone[10].

In contrast human 5AR2 has a Km for T in the submicromolar range (0.1-1.0μM) [32, 37]. This submicromolar affinity suggests that 5AR2 is more suited to act under conditions of limiting substrate, as occurs in the embryo, where T production by the testes is low and conversion of T to DHT is crucial for normal sexual development[38]. In the sexually mature male, where there are conditions of saturating substrate, a small amount of 5AR2 is capable of synthesizing large amounts of DHT.

These differences in affinity are not seen for the cofactor (NADP[H]) as for both human isoenzymes the Km is in the low micromolar range (3-10μM).

1.5.3 pH Optimum

Both rat and human 5AR1 have a broad pH optimum spanning the alkaline range 6.8-8.5, whereas the type 2 5ARs exhibit a narrow acidic optimum of between 4.9-5.1[33]. The differences in pH optima are diagnostic for the type 1 and type 2 isoenzymes and can be used to assign 5AR activity in human and rat tissue to a particular isoenzyme.

The biochemical basis for the acidic pH optimum of 5AR2 which is evolutionarily conserved in rats, mice, monkeys and humans, is puzzling. The acidic pH optimum may represent location of the protein within an acidic subcellular compartment such as the endosome or lysosome or in an unusual lipid microenvironment in a target membrane. 5AR2 activity in transfected Chinese hamster ovary (CHO) cells however, is not affected by compounds such as chloroquine, ammonium chloride and monensin[37] which neutralize the pH of acidic subcellular compartments. In addition, immunocytochemical studies have localized both 5AR1 and 5AR2 to the endoplasmic reticulum[37], a cellular compartment of neutral pH.

From these studies it has been suggested that 5AR2 may in fact display a neutral pH optimum in its native state and when cells are treated with agents

that permeabilise the plasma membrane but not endoplasmic membrane, it exhibits equivalent activity at both acidic and neutral pHs[37]. Physical lysis methods including scraping, homogenisation and perforation however result in a 5AR activity at pH 5.0 only. Observations of a higher affinity for steroid substrates and greater efficiency at a neutral pH in cell lysates expressing 5AR2, again suggest 5AR2 acts at a neutral pH within the cell[37]. This indicates the enzyme may function at a neutral pH within the cell and shift to a pH 5.0 active form upon cell lysis. This shift may reflect disruption of the lipid bilayer, an association with or dissociation from 5AR2 of an allosteric molecule or conformational changes within the enzyme itself[10].

Span and colleagues[39] provided further evidence that both 5AR isoenzymes exhibit neutral pH optima. They incubated homogenates of rat prostate and epididymis with a wide range of T concentrations and demonstrated that at a neutral pH two isoenzymes exhibiting the equilibrium constants of 5AR1 and 5AR2, were present. Similar results were obtained in a later study involving homogenates of human BPH tissue[40], suggesting 5AR2 does in fact operate at a neutral pH optimum and that the acidic optimum seen in previous studies is due to experimental artefact.

In 1996, Smith and colleagues[41] assayed transfected COS cells at 1μM and 20nM T concentrations and demonstrated a dependence of pH optimum on substrate concentration. At 1μM T a pH optimum of 5.0-5.5 was seen whereas at 20nM the optimum was 6.5. 20nM is the average plasma T concentration reported for normal males[42] and is therefore the concentration of T in which 5AR operates *in vivo*. From these results it can be concluded that 5AR2 operates most efficiently *in vivo* at a neutral pH rather than the acidic optimum seen *in vitro*.

1.5.4 Protein Structure

From their cDNA sequences it has been deduced that the rat and human isoenzymes are hydrophobic proteins of 254-260 amino acids with predicted molecular weights of 28000-29000 Da. They do not contain cleavable signal sequences or consensus sequences for either N-linked or O-linked

glycosylation. 37% of their residues have side chains common to the hydrophobic interior of globular proteins and these residues are distributed throughout the entire protein[10]. This makes it difficult to locate transmembrane regions from hydropathy plots and suggests that the isoenzymes are intrinsic membrane proteins deeply embedded in the lipid bilayer.

Human 5AR1 is a hydrophobic protein of 259 amino acids in length. Over 40% of its residues are hydrophobic with only 16% being negatively or positively charged, consistent with an intracellular membrane location[1]. It shares 50% homology with human 5AR2, also a hydrophobic protein of 254 amino acids[32].

1.5.5 Half Life

Pulse-chase experiments have shown both human 5AR isoenzymes have a half life in excess of 30 hours, which is not affected by the presence of substrate, product or competitive inhibitors. This long half-life suggests the isoenzymes are not subjected to regulation at the level of protein turnover[37]. Others however consider this an inability to detect alterations in steady-state protein levels or enzyme activity in synchronized cells at various phases of the cell cycle and the absence of any post-translational modifications including phosphorylation, fatty acylation and isoprenylation[10].

1.5.6 Rhesus Macaque 5AR

5AR1 from the Rhesus monkey, which is 94% homologous with human 5AR1 is composed of 263 residues compared with the 259 amino acids of human 5AR1. Both the Rhesus and human 5AR2 enzymes are composed of 254 amino acids[43].

Rhesus and human 5ARs share similar biochemical properties, inhibitor sensitivities and tissue distributions. Like the human enzymes, Rhesus 5AR1 has a broad pH optimum between 6.5-8.0 and 5AR2 a sharp optimum at pH 5.0. The Km for T for Rhesus 5AR1 is 3.2μM and for Rhesus 5AR2 11nM, values that are very similar to their human counterparts[43]. Time-dependent

irreversible inhibition by Finasteride is also common to both isoenzymes in both species.

1.5.7 Cynomolgus Monkey 5AR

Cynomolgus monkey steroid 5ARs have been cloned, expressed and characterized[44]. Monkey type 1 and 2 share 93% and 95% homology respectively, with their human and 61% and 71% with their rat counterparts. The type 2 isoenzymes are the same length in all three species but Cynomolgus 5AR1 is 4 and 8 amino acids longer than human and rat 5AR1 respectively.

Biochemically, monkey 5AR1 is most active at neutral pH 7.0 and type 2 at pH 4.5-5.5. The Km for T of type 1 is 2μM and for type 2 is 0.7μM. Studies with a variety of 5AR inhibitors have shown the monkey isoenzymes are functionally more similar to human than are rat 5AR's[44]. Differences between rat and human 5AR make rat a poor choice as a model for comparative *in vivo* pharmacological assessments. As the enzymes from the Cynomolgus monkey are more closely associated with the human enzymes, it is considered that these animals may be more suitable for the *in vivo* assessment of 5AR inhibitors[44].

1.6 Tissue Distribution Patterns of 5AR Isoenzymes

1.6.1 Ontogeny of Human 5AR Expression

Studies with anti-peptide antibodies directed against the carboxyl termini of both human 5AR isoenzymes[45] demonstrated that although not detectable in the foetal liver, both isoenzymes are expressed in the liver after birth and throughout life. During gestation both isoenzymes are expressed in the skin and scalp, with immunodetection studies showing 5AR1 to appear first in the early epidermis, dermis, hair follicles and sebaceous glands. 5AR2 is not detected in the epidermis and hair follicles until after week 30 suggesting 5AR1 may play a predominant role in developing skin[46]. Expression of both

isoenzymes continues until 2-3 years of age at which point it ceases. At puberty only 5AR1 is re-expressed in the skin and scalp and continues to be expressed throughout life[10].

The pattern of 5AR2 expression in the foetal genito-urinary tract was determined using immunostaining techniques with a rabbit polyclonal antibody raised against residues 227-251. 5AR2 immunostaining was evident in the foetal seminal vesicles, prostate, ejaculatory ducts, Cowper's glands, corpus cavernosum, corpus spongiosum, pendulous urethra, scrotal skin and prostatic urethra[47]. With the exception of the prostatic urethra and ejaculatory ducts, staining was evident in the stromal but not epithelial cells. 5AR2 expression was not detectable in the epithelial or stromal cells of the foetal epididymis and testis. But 5AR2 is expressed in the epithelial cells of the adult epididymis[47]. An explanation for this change in epididymal expression is that during foetal life, levels of circulating androgens are too low to stimulate the androgen dependent 5AR2 expression by the epididymis[47]. Interestingly, 5AR2 is also expressed in the medulla oblongata of the brain but why remains unclear[37].

1.6.2 Tissue Distribution of 5AR in the Rat

In situ hybridisation techniques and immunohistochemical analyses have been used to determine the cell-type specific expression pattern of rat 5AR isoenzymes. These studies demonstrated 5AR1 expression in the basal epithelial cells and 5AR2 in the stromal cells of the rat ventral prostate[48]. Subsequently, 5AR1 has been localised to the nuclear compartment of epithelial cells and 5AR2 to the microsomal compartment of stromal cells[49]. In the stromal cells, 5AR2 synthesizes DHT, which acts in part to stimulate division of the basal epithelial cells thereby forming a functional prostate. Possible mechanisms by which 5AR2 induces prostatic development have been proposed[49] and include:

1. DHT synthesis by 5AR2 acts in a paracrine manner stimulating gene expression and pattern formation in the adjacent epithelial cells.
2. DHT may act in an autocrine fashion to simulate expression of stromal cell genes that in turn drive morphogenesis of the prostate epithelial cells.

The basal epithelial cells of the rat prostate are believed to be precursor cells for the luminal epithelial cells[48]. Within the basal cells DHT is synthesized by 5AR1 and then acts in an autocrine manner to stimulate differentiation of the basal cells or in a paracrine manner to stimulate luminal cell division[11]. Neither the basal or luminal epithelial cells of the prostate undergo apoptosis under conditions of androgen deprivation. This may be due to expression of 5AR1 in the basal epithelial cells that synthesizes low levels of DHT which are sufficient to maintain the survival of the basal and luminal prostate epithelial cells[48].

Debate exists as to the expression of both 5AR isoenzymes in the rat epididymis. Immunocytochemical studies and mRNA measurements demonstrate expression of both isoenzymes in the epithelial cells in a positional gradient with highest activity in the segment closest to the testes and decreasing towards the tail. This activity gradient parallels that of sperm maturation as they travel along the epididymis and suggests an as yet unknown role for DHT in rat sperm maturation[48]. Expression of 5AR1 activity in the rat epididymis remained undetected until Span and colleagues[50] demonstrated 5AR1 activity in rat epididymis homogenates at high T concentrations.

In the rat liver only 5AR1 is expressed, also in a positional gradient where levels are highest in hepatocytes closest to the portal triad and very low surrounding the portal vein. The high concentration of 5AR around the portal triad facilitates catabolism of circulating T and other steroids as the direction of blood flow in the liver is from the portal triad to the central vein[48]. Steroid substrates catabolised by 5AR at the portal triad pass through the liver to the central vein where they are excreted via the kidneys. The pattern of expression of 5AR1 in the liver may reflect the developmental lineage of hepatocytes with hepatocyte precursor stem cells clustered around the portal triad and more differentiated hepatocytes around the central vein. This suggests an as yet unknown role for 5AR in hepatocyte differentiation.

1.6.3 Cellular Location and Tissue Distribution of Human 5AR

Immunocytochemical studies in CHO cells transfected with human 5ARs localised both isoenzymes to the endoplasmic reticulum with their carboxyl termini exposed to the cytoplasm[37].

Both rat isoenzymes of 5AR are expressed in the ventral prostate. Expression of both human isoenzymes in the prostate however, remains controversial with some authors stating that only 5AR2 is expressed, while others maintain that both isoenzymes are expressed. mRNA coding for 5AR1 has been detected in the human prostate using cDNA probes[51] and studies of affinity constants for T suggest both 5AR1 and 5AR2 are expressed in the human prostate[40]. It may be that these conflicting results are due to artefactual amplification resulting from the methods used by Hirsch and colleagues[52]. In the normal prostate there is a very low basal level of 5AR1 mRNA expression resulting in unmeasurably low enzyme levels[53]. The use of PCR techniques by Hirsch et al[52] may have resulted in the amplification of these low 5AR1 mRNA levels to a level that is measurable. As a result, these findings may not be representative of normal physiological 5AR1 levels within the prostate[53].

5AR1 expression in the prostate is reinforced from findings that the use of a selective 5AR1 inhibitor reduced 5AR activity in cultured human fibroblasts obtained from benign prostatic hyperplasia (BPH) patients, although not in freshly isolated prostate cells[52]. The selective 5AR1 inhibitor LY191704 also exhibits activity against 5AR1 in both normal and malignant prostate epithelium[54,55,56].

More recently expression of 5AR2 has been detected in the stroma and of both isoenzymes in human epithelial prostate tissue[57]. If indeed both isoenzymes of 5AR are expressed in the human prostate, this highlights the need for effective dual inhibitors for the treatment of DHT-related prostatic disease.

The cell-type specific expression pattens of 5AR1 and 5AR2 in human tissue, has been detected by immunohistochemical studies with antibodies raised against either human isoenzyme. Unlike biochemical and molecular studies,

immunoblotting studies with antibodies directed against 5AR1 have not been able to demonstrate 5AR1 expression in the human prostate[45]. These studies have however demonstrated, similar to rat 5AR1, that human 5AR1 is predominantly expressed in the liver.

In 1994, an immunochemical assay was developed[58] for the analysis of 5AR2 expression patterns in both genital and non-genital tissue. This technique employed an affinity purified polyclonal antibody directed against residues 227-252 of the carboxyl terminus of 5AR2. Expression of 5AR2 was demonstrated, using this antibody, in both the basal epithelial and stromal cells of the normal prostate but not in the luminal epithelial cells. Within these cells 5AR2 shows a perinuclear, subcellular distribution which may facilitate subsequent binding of DHT (or T) by the nuclear androgen receptor[11]. These patterns of expression suggest DHT synthesis within the prostate is mediated by 5AR2 and that once synthesized DHT may act in a paracrine fashion to stimulate growth and maintenance of the luminal epithelial cells[11].

Electron microscope and immunohistochemical studies[59] have demonstrated 5AR2 expression in smooth muscle cells of the prostate, epididymis, seminal vesicles and vas deferens. In the seminal vesicles, 5AR2 is expressed in a perinuclear pattern within the stromal cells lying adjacent to the epithelial cells. In contrast, in the epididymis 5AR2 is predominantly expressed, again in a perinuclear pattern, in the epithelial cells lining the ductules and in the myofibroblasts of the foreskin dermis[58]. The relative patterns of distribution of 5AR2 in the various genital structures suggest cell-type specific expression patterns of 5AR2 are independent of embryonic origin. The prostate and seminal vesicles originate from different anlage, the urogenital sinus and Wolffian ducts respectively, yet both have similar expression patterns of 5AR2.

In contrast, in non-genital tissue such as the liver, 5AR2 expression is confined to the hepatocytes where it shows a reticular pattern of expression throughout the cytoplasm and perinuclear membrane[58].

1.6.4 Comparison of 5AR Distribution in Rat and Human Tissue

The tissue distributions of rat and human 5AR isoenzymes differ. In the rat 5AR1 is expressed in the liver and basal epithelial prostate cells and 5AR2 in the testes, epididymis and stromal cells of the prostate. Both isoenzymes are expressed in the seminal vesicles and ventral prostate[60]. In humans, 5AR1 is predominantly expressed in the skin and 5AR2 in the genital tissue. The different tissue distributions of 5AR isoenzymes in the two species suggest they may be differentially regulated and serve different physiological functions in humans and rats[10].

1.7 5AR and Disease

Disorders associated with abnormalities of DHT production can be classified as those due to underproduction of DHT and those caused by DHT overproduction. Overproduction of DHT has been associated with acne, hirsutism, male pattern baldness (MPB), seborrhoea and androgenic alopecia[33]. Significantly, overproduction of DHT is considered responsible for benign prostatic hyperplasia (BPH) a disease prevalent in aging males[150]. In addition, it is thought DHT overproduction may be involved with the development and/or progression of prostate cancer although this remains to be proven[31].

Although altered 5AR activity has not been associated with DHT overproduction, reduced or absent 5AR activity clearly results in the underproduction of DHT[62]. This leads to a relatively rare form of male pseudohermaphroditism in which XY males fail to develop a prostate and exhibit ambiguous external genitalia at birth[1]. These individuals however have normally developed male internal genitalia. Following the isolation of cDNAs encoding 5AR1 and 5AR2, several mutations in the gene encoding 5AR2 (SRD5AR2 gene) have been described which are responsible for the reduced 5AR activity seen in pseudohermaphroditic patients[63]. These mutations are discussed in section 1.10.1.

1.7.1 5AR Deficiency

5AR deficiency is an autosomal recessive genetic disease first characterised in 1961[64] and originally termed pseudovaginal perineoscrotal hypospadias. Affected patients are 46XY males who present at birth with ambiguous genitalia resembling those of a female. Later it was determined that the phenotype expressed was due to a deficiency of DHT production from T by 5AR[65] and the disease was thereafter termed steroid 5AR deficiency.

Cloning of cDNAs for both human 5AR isoenzymes enabled identification of mutations in the SRD5AR2 gene responsible for 5AR deficiency[32]. The SRD5AR1 gene is normal in these patients but the SRD5AR2 gene displays point mutations including amino acid substitutions, splice-junction alterations, non-sense mutations and deletions[10]. Each of the amino acids affected is conserved between rat and human 5ARs indicating these residues have functional importance. Wilson et al[11] listed the four main causes of deficient 5AR activity. These are:

1. Mutations impairing T binding.
2. Mutations precluding the formation of a functional enzyme eg. deletions, premature termination codons and splice-junction abnormalities.
3. Mutations resulting in an unstable enzyme.
4. As yet uncharacterized mutations outside the coding region that impair expression of gene product.

No correlation has been detected between the severity of manifestations and the particular mutation inherited. The mutations appear to be silent in women who are asymptomatic[66].

Not all cases of pseudohermaphroditism are caused by 5AR abnormalities, as the condition is also seen in patients with androgen receptor defects, resulting from point mutations in its encoding gene. The androgen receptor forms part of the intracellular signaling system involving both T and DHT that determines the fate of cells in the bipotential anlage of the mammalian external genitalia[32].

Mutations in the AR affect its interactions with both T and DHT resulting in the inappropriate development of the male external genitalia.

5AR deficient males present at birth with a normally developed male urogenital tract but express female external genitalia ie. labia minora, labia majora and blind end vaginal pouch. The prostate is usually absent or is hypoplastic and composed of stromal tissue only[11], with prostate specific antigen (PSA) a serine protease secreted by the prostate epithelial cells not detectable[67]. The testes are often extra-abdominal, at puberty spermatogenesis is absent or greatly impaired and secondary sexual hair is sparse. These patients produce normal levels of T, which enables the male internal genitalia, seminal vesicles, epididymis and vas deferens to develop normally from Wolffian tissue.

An unusual manifestation of 5AR deficiency is that affected males virilize to different extents at puberty. At one extreme are those who are completely or predominantly female and at the other are those who have no apparent abnormalities. In between are individuals who present as females with ambiguous genitalia and those who are predominantly male but with a micropenis and hypospadia[68]. It is thought the variations in the various degrees of virilization seen may reflect low levels of circulating plasma DHT synthesized by 5AR1 in the skin and liver of these patients[11]. 5AR1 is expressed in the liver at birth and is maintained throughout life with its expression in the skin and scalp occurring at puberty and thereafter. Given the large contribution of the skin and liver to relative body mass (~25%), virilization of the external genitalia by 5AR1 production by these tissues seems feasible[45].

The variation in virilization at puberty may also be due to the fact that certain mutated forms of 5AR2 expressed in 5AR deficient patients are capable of synthesizing DHT, but at significantly lower levels than a fully functional enzyme. The low levels of DHT produced by these mutant enzymes may therefore give rise to the various degrees of virilization seen at puberty[69]. For example, patients homozygous for the substitution of arginine for histidine at residues 231 (H231R) exhibit an enzyme with 15% normal activity, this activity is sufficient to drive virilization in early infancy and in some cases *in utero*[69]. Other mutations, G196S and R246Q, which respectively express 10% and 3%

residual enzyme activity, may have similar effects to those of the H231R mutation[69].

Significantly 5AR deficient males do not tend to develop BPH, are less likely to exhibit male pattern baldness and develop less acne, confirming that DHT overproduction is involved in these disorders[10]. No defects are seen in females with 5AR deficiency, who have normal reproductive function.

The characteristic endocrinological features of 5AR deficiency have been described[11] and include:

1. Normal to high levels of male plasma T and low levels of DHT.
2. An elevated ratio of plasma T to DHT concentration in adulthood and after stimulation with human chorionic gonadotrophin (hCG) in childhood.
3. Elevated ratios of urinary 5β- to 5α-, C19 and C21 steroid metabolites.
4. Diminished conversion of T to DHT in tissues.
5. Markedly increased ratio of plasma T to DHT after T administration.
6. Normal or slightly elevated plasma LH levels.

Although plasma DHT levels are low, they are never undetectable and may fall within the normal range. The source of this DHT is that from residual mutant 5AR2 enzyme activity or type 1 activity in non-genital tissue. PSA levels are undetectable in all subjects due to the absence of a prostate.

Diagnosis is generally made at the time of puberty or in infancy. In adolescents diagnosis is straightforward, 46XY male pseudohermaphrodite displaying the characteristic female phenotype, normal plasma T levels and abnormal plasma T to DHT ratios or urinary 5β- to 5α- reduced steroid metabolites[11].

In infancy, diagnosis is more problematic, particularly if there is no family history and involves determination of plasma T to DHT ratios both before and after hCG administration or the measurement of 5β-/5α- glucocorticoid metabolites. In some cases measurement of 5AR activity in cultured genital skin fibroblasts may provide diagnosis, but enzyme activity may be within the normal range[70].

Knowledge of significant mutations in the SRD5AR2 gene responsible for 5AR deficiency provides a means for the development of genetic screening techniques to identify these mutations. The use of such techniques may enable early diagnosis in pseudohermaphroditic patients and determination of the carrier status of prospective parents for SRD5AR2 gene mutations.

Removal of the testes to prevent partial virilization at puberty, oestrogen/progesterone therapy to promote feminization and vaginoplasty when appropriate are undertaken, only after intense psychological and psychiatric evaluation of patients choosing to live their lives as females[71].

Individuals raised as males or those raised as females who elect to function as males, undergo corrective genital surgery and androgen supplementation to replenish DHT levels. Many forms of androgen supplementation have been trialed. DHT enanthate has been administered by injection and a sustained elevation in plasma DHT levels observed[72], however DHT enanthate is not available for general use. Topical administration of DHT raises plasma DHT levels, producing significant phallic growth[73], however the long-term efficacy and safety of this therapy are not known. T esters have been administered at levels sufficient to elevate plasma T to supraphysiological levels, concurrently raising DHT levels within the normal range and promoting virilization[74]. Again, the safety of treatment with supraphysiological T levels is unknown. Finally, androgens have been administered in a form that doesn't require 5AR to be active eg. 19-nortestosterone, which is active in the absence of 5α- reduction and can be administered by injection in an esterified form[75].

1.7.2 Male Pattern Baldness

MPB is the progressive loss of scalp hair in males under androgen control. Male pseudohermaphrodites with 5AR deficiency do not develop MPB suggesting a role for DHT in its pathogenesis[62]. Increased formation of 5α-reduced metabolites in bald scalp compared to "hairy" scalp has been demonstrated[76, 77] with 5AR1, but not 5AR2 activity detected in non-balding scalp[78]. Yet no differences exist in this 5AR1 expression both between adult balding and "hairy" scalp and male and female scalp[79].

1.7.3 Hirsutism

Hirsutism is excessive hair growth and refers to a condition in women where there is growth of unwanted excess facial hair resulting from androgen overproduction. DHT is essential for hair growth and it has been suggested increased 5AR activity in the skin may play a role in the pathogenesis of hirustism[80, 81]. Increased 5AR activity has been demonstrated in hirsute females[82], with a significant correlation between increased 5AR activity and severity of hirsutism, as assessed by the Ferriman-Galleway score[83].

1.7.3 Acne

Acne is the active inflammation of sebaceous glands accompanied by pimples (pustules or cysts) on the skin. Acne was not seen in earlier reports of 5AR deficient patients and its development was thought therefore to be DHT-dependent. Acne has since been reported in 5AR deficient patients with DHT synthesis by 5AR1 believed responsible[84].

The therapeutic use of 5AR inhibitors in acne is limited. The T to DHT ratio in sebum is similar to serum demonstrating sebum production is a T and not DHT-dependent process[85]. Studies have also demonstrated sebum production in men is not affected by the 5AR inhibitor Finasteride[86], possibly as the major isoenzyme expressed in the skin, 5AR1, is relatively insensitive to this inhibitor.

1.7.5 Benign Prostatic Hyperplasia

BPH is the most common benign proliferative disorder in men over 50 years old, with a 2% incidence in all males born[53]. DHT synthesis is essential for both the embryonic differentiation and postnatal growth of the prostate epithelial and stromal cells, but unregulated DHT production is believed responsible for the pathogenesis of hyperplastic prostate growth in BPH[61]. Androgen deprivation studies in BPH cell lines have demonstrated a reduction in prostate size[67] and in the absence of androgens the prostate epithelial cells undergo apoptopic cell death. These studies demonstrate a requirement of androgens for the survival

of prostate cells and also provide significant evidence that DHT overproduction causes BPH.

The human prostate comprises four glandular zones, the periurethral, transition, central and peripheral zones[53], which differ histologically and biochemically. The periurethral and transition zones are the main sites of hyperplastic origin suggesting 5AR activity may differ between the four zones. The prostate is also composed of epithelial and stromal tissue with the growth and integrity of epithelial cells strongly dependent on the stroma[87]. Stromal enlargement is the first step in the development of BPH, which suggests increased 5AR activity in the stroma of BPH. Several investigations have demonstrated increased stromal and epithelial 5AR activity in BPH[88-92], however marked DHT accumulation in BPH stroma is not evident[93]. Studies of 5AR activity in primary cultures of epithelial and stromal cells from the four prostate zones of normal and hyperplastic prostates showed no significant differences in DHT production between the four normal and hyperplastic zones, nor between epithelial and stromal cells within the same prostate[53].

BPH clinically presents with symptoms relating to obstruction of urinary flow and bladder dysfunction[94]. Symptoms include hesitancy, dribbling, decreased size or force of urine stream, incomplete emptying, urgency, dysuria and straining. It is for these reasons treatment of BPH is required.

1.7.6 Prostate Cancer

Prostate cancer (PC) is the second leading cause of male cancer deaths in the USA, being responsible for nearly 4% of all male deaths over the age of 55[95]. Prostate cancer is most commonly diagnosed in African/American males (116/100 000 persons per year), has an intermediate incidence in Caucasian males (71/100 000 persons per year) and lowest rate among Asian males (Japanese: 39/100 000 persons per year, Chinese: 28/100 000 persons per year). Epidemiological studies clearly demonstrate prostate cancer has an inherited component, with the current understanding that accumulation of multiple genetic alterations is important for cancer to occur. Males inheriting one of these alterations are thought to be predisposed to cancer development and

at higher risk for cancer at an early age than those acquiring alterations later in life[95].

A number of somatic genetic alterations have been demonstrated in prostate cancer including alterations in DNA methylation, oncogenes, tumor suppressor genes (TSGs), metastasis suppressor genes (MSGs), telomerase activity and the androgen signaling cascade[95]. In human cancer cells, some genomic alterations are characterized by abnormal DNA methylation including hypermethylation, redistribution of methylation and demethylation of normally methylated regions. Hypomethylation has been reported in prostate cancer but its significance is unclear[95]. Genomic regions of hypermethylation are of greater significance particularly in or near the 5' region and/or in regions that may contain the promoter and one or more exons of its associated gene. Methylation of these regions can be associated with transcription inactivation of associated genes. An example of this is the CDKN2 gene, which encodes a cyclin-dependent kinase-inhibitory protein controlling passage of cells through the G_1 phase of the cell cycle. CDKN2 gene inactivation may induce progression through the cell cycle and homozygous deletions of this gene have been detected in ~20% of prostate cancer patients[95].

Certain oncogenes including the *myc* oncogene (*c-myc*), have been associated with prostate cancer with significantly higher levels of *c-myc* transcripts seen in prostate cancer specimens than in BPH samples[95]. Malignant progression not only involves the enhancement of oncogene-derived transformation but also requires the loss of regulatory function by TSGs. Before a cell is at risk for malignant transformation however, both copies of TSGs must be inactivated. The acquisition of metastatic ability is the biological hallmark for the aggressiveness of prostate cancer, the genetic control of metastasis may be exerted by increased expression of specific genes involved in transformation to the metastatic phenotype. It is possible that inactivation of specific MSGs may promote evolution of metastasis in a manner similar to the effects on tumour initiation due to TSG inactivation.

The androgen signalling cascade involves unbound T, which enters the cell and of which >90% is irreversibly converted to DHT by the action of 5AR. The

androgen receptor (AR) is normally associated with heat shock proteins and unless liganded with steroid, is unable to bind with androgen response elements in the cell nucleus. Both T and DHT can bind to the androgen receptor (AR), with DHT binding with five times the affinity of T. This binding induces dissociation of the AR from heat shock proteins, hyperphosphorylation, conformational changes and its dimerization. The AR is now capable of binding with specific DNA sequences termed androgen-response elements, within the promoter region of androgen responsive genes. In conjunction with cofactor proteins and other transcription factors, the AR is now able to up- or down-regulate gene transcription.

Through the reduction of T or DHT levels, the AR is the target of endocrine therapy for PC. This reduction can be achieved using surgical castration and/or the administration of anti-androgen therapy. Blockade of the androgen signal kills PC cells through induction of programmed cell death. This suggests androgens play at least a permissive role in the pathogenesis of prostate cancer[31]. DHT is the main androgen stimulating and maintaining benign growth of the prostate but it is unclear whether the androgen dependence of prostate cancer is also related to DHT[67].

Studies of 5AR activity between races demonstrate young Japanese men express lower activity than Caucasian-Americans and African-American men[96]. This pattern of 5AR expression parallels that of prostate cancer risk with Japanese men having the lowest risk and lowest levels of 5AR. Also, the DHT to T ratio is highest in African-American, intermediate in Caucasian and lowest in Asian-American males, corresponding with their respective risk of prostate cancer development. The missense substitution, V89L, of the SRD5AR2 gene is differentially distributed among races and is associated with reduced 5AR activity *in vivo*[97]. African-Americans have the highest risk of prostate cancer development and the highest expression of the V89 allele of the V89L substitution, whereas Asians have the lowest risk of prostate cancer development and express the highest frequency of the L89 allele.

It has been suggested that 5AR overactivity is responsible for neoplastic prostate growth through the effects of increased DHT levels on the androgen

receptor. Comparisons of normal and neoplastic prostate tissue however, have demonstrated increased 5AR activity in some[98, 99] but not all studies[53, 100, 101, 102]. Also lower serum and intraprostatic DHT levels are seen in cancerous as opposed to normal or hyperplastic prostates[103], suggesting the androgen dependence of prostate cancer is not related to DHT.

Further support that DHT does not play a role in the pathogenesis of PC is provided from studies with the Copenhagen rat Dunning prostatic adenocarcinoma model R-3327 and the competitive 5AR inhibitor Finasteride. In these studies, a reduction in ventral prostate size without concurrent suppression of the Dunning-H adenocarcinoma tumour was seen. As Finasteride inhibits 5AR and therefore DHT production, these results demonstrate normal growth of the prostate is DHT dependent, yet growth of the prostatic tumour is not. Similar results have been obtained from studies with the non-competitive 5AR inhibitor F-105657[104].

Although the majority of studies suggest development of prostate cancer is not androgen dependent, androgen deprivation studies in BPH and PC cell lines indicate this may not be entirely the case. These studies have demonstrated the development of prostate cancer is an androgen dependent process, as the greatest reduction in prostate size was seen in cancerous cell lines[67].

1.8 Inhibitors of 5AR

Studies of disorders of DHT production are of scientific value as they aid in understanding the roles of T and DHT in sexual differentiation, male behaviour and androgen action in general. The evidence that 5AR deficient individuals lack a prostate and DHT mediates prostate growth, together with the high incidence of prostatic disease has generated considerable interest in the development of pharmacological inhibitors of 5AR. A variety of compounds have been synthesized and their inhibitory effect on 5AR activity assessed.

Inhibitors of 5AR are based on steroid structures as these compounds are the natural substrates of the enzyme. A structural requirement for synthetic 5AR

inhibitors is that they contain a stable configuration in the A-ring enabling them to mimic the transition state in the conversion of T to DHT and bind tightly to the active site. As 5AR is not inhibited by product the first developed inhibitors were substrate analogues.

5AR inhibitors can be divided into two categories the steroidal and non-steroidal inhibitors. These are discussed below. Studies of the various inhibitors have demonstrated that although 5AR1 and 5AR2 are inhibited to a similar degree by some of these compounds, their sensitivities to others differ significantly. As both human isoenzymes contribute to serum DHT levels and as most inhibitors demonstrate isoenzyme selectivity, this has generated the need for effective dual isoenzyme inhibitors.

1.8.1 Steroidal Inhibitors

This is the largest class of 5AR inhibitors of which the most significant compounds are 4-MA (17β-[N,N-diethyl] carbamoyl-4-methyl-4-aza-5α-androstan-3-one) and Finasteride (17β-[N-t-butyl] carbamoyl-4-aza-5α-androst-1-ene-3-one) or MK-906. Both of these compounds have been extensively studied and both are competitive inhibitors of the natural substrate testosterone.

The compound 4-MA was synthesized in 1981 by Brooks and colleagues[105] and inhibits both human and rat 5AR1. Significantly 4-MA has a low affinity for the androgen receptor[10], which has the advantage that undesirable anti-androgenic effects including impotence, impairment of muscle growth and gynaecomastia are less likely. A disadvantage of 4-MA however is its inhibition of the enzyme 3β- hydroxysteroid dehydrogenase, which can cause hepatotoxicity[106].

Finasteride, which was developed in 1984 by Rasmussen and colleagues[107], is a potent inhibitor of both rat and human 5AR. It differs from 4-MA in that there is a double bond in the A-ring, no 4-methyl group and a C17 t-butyl amide group (Figure 1.2).

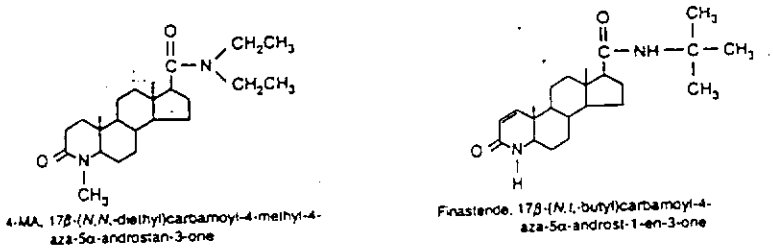

Figure 1.2: *Structural comparison of the Steroidal Inhibitors*[10].

As Finasteride has a slow association rate and an even slower dissociation rate it is considered a time dependent inactivator of 5AR[108]. It is unclear if inactivation of 5AR results from the covalent attachment of Finasteride so it can no longer bind substrate or if Finasteride binding to 5AR leads to irreversible conformational changes.

CGP 53153 (N-2-[cyano-2-propyl]-3-oxo-4-aza-5α-androst-1-ene-17b-carboxamide) shares structural similarity with Finasteride and is a potent competitive inhibitor of 5AR *in vivo* and *in vitro* (Figure 1.3). Both Finasteride and CGP 53153 produce a significant reduction in prostate volume without any undesirable anti-androgenic side effects[109]. *In vitro*, CGP 53153 less potently inhibits 5AR in rat and human microsomal preparations than does Finasteride. However, *in vivo* it is almost ten times more potent than Finasteride in the reduction of rat prostate growth, suggesting CGP 53153 is either more effectively taken up by the prostate, has an improved bioavailability or a prolonged half-life[109].

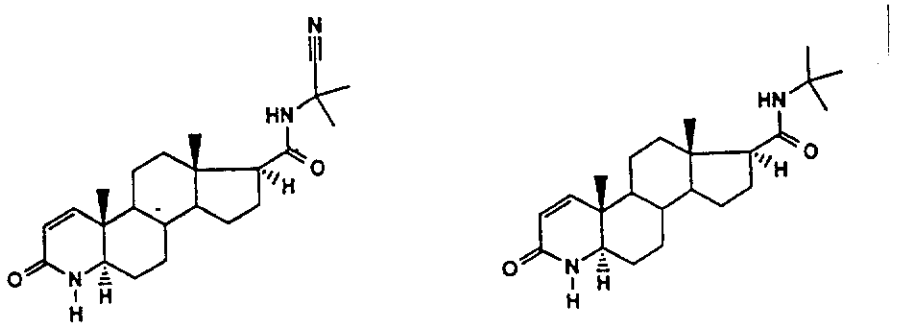

CGP 53153 **Finasteride**

Figure 1.3: *Structural comparison of CGP 53153 and Finasteride*[109].

Unlike inhibitors such as 4-MA and Finasteride, SK-105657 is a steroidal inhibitor lacking the heterocyclic A-ring common to other 4-azasteroids, but share the t-butyl amide substituent at position 17 of the D-ring. It is a non-competitive inhibitor with respect to substrate and is thought to bind an enzyme-NADP+ intermediate, mimicking an enzyme-bound enolate[110].

The hormones progesterone, megesterol acetate and other gestagens inhibit 5AR[67]. Progesterone is a physiological substrate for 5AR but although it has inhibitory action against 5AR it is metabolized too quickly to be an effective inhibitor *in vivo*[94].

1.8.2 Non-steroidal Inhibitors

The non-steroidal inhibitors share similar features with the 4-aza steroids in that they have a heterocyclic ring containing nitrogen and 3-oxo groups, but unlike the 4-azasteroids they lack a fourth steroid ring (Figure 1.4).

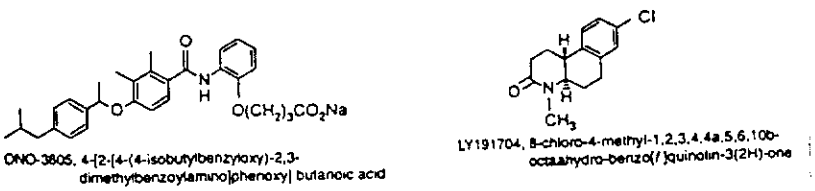

Figure 1.4: *Structures of the Non-steroidal Inhibitors*[10].

The non-steroidal inhibitors include the benzoylaminophenoxybutanoic acid derivatives such as 4-[2-[4-(4-isobutylbenzyloxy)-2,3-dimethylbenzoylamino]phenoxy] butanoic acid (ONO-3805), which is a potent inhibitor of both rat isoenzymes and human 5AR2[111]. Another class of non-steroidal inhibitors are the benzoquinolones, of which the compound 8-chloro-4-methyl-1,2,3,4,4a,5,6,10b-octaahydro-bezol[*f*]quinolin-3(2H)-one (LY 191704) has attracted some interest. LY 191704 is a potent inhibitor of human 5AR1 and as a result may have potential therapeutic use in the treatment of androgen-dependent dermatological conditions like MPB.

LY 320236 is a benzoquinolone that inhibits 5AR in the human scalp, skin and prostatic homogenates. It contains the benzoquinolone ring nucleus common to LY 191704 and is a competitive inhibitor of 5AR1 (Ki = 3.39±0.38nM) and a non-competitive inhibitor of 5AR2 (Ki = 29.7±3.4nM)[112]. Structural modification of the benzoquinolone ring nucleus increases potency against 5AR2, whilst retaining anti-5AR1 activity. LY 320236 is a potent dual inhibitor of human 5AR that doesn't exhibit *in vivo* or *in vitro* toxicology and has potential therapeutic use in the treatment of androgen dependent disorders[112].

1.8.3 Androgen Inhibitors

The anti-androgens cyproterone acetate and flutamide reduce T and DHT levels in prostatic tissue but as they bind to the androgen receptor they also affect normal androgen dependent functions[67]. Other approaches to inhibiting 5AR activity such as castration, LHRH antagonists and anti-androgens have been superseded by compounds like Finasteride. These compounds generally have the same effects as the older forms of treatment but have the significant advantage that they cause no unwanted side effects on male sexual behaviour[67].

1.9 Finasteride

Human 5AR1 is relatively resistant to Finasteride whereas 5AR2 is markedly sensitive but why the two isoenzymes vary in their sensitivity to Finasteride is

unknown. Despite this difference, Finasteride is widely used in the treatment of prostatic disease and its use has been extensively studied. These studies are discussed below.

1.9.1 Mechanism Based Finasteride Inhibition of Rat and Human 5AR

Preliminary studies of Finasteride demonstrated its competitive reversible mode of inhibition[19]. The differences between the Ki for Finasteride, which is much less than the Km for T, show Finasteride efficiently competes with the natural substrate (T) for binding by 5AR.

Finasteride is an irreversible slow time-dependent mechanism based inhibitor of both human isoenzymes. It is a potent inhibitor of 5AR2 where it is accepted as an alternative substrate and is ultimately reduced to dihydrofinasteride via an enzyme-bound NADP-dihydrofinasteride intermediate. The binding of Finasteride by human 5AR1 has been shown to involve an initial rapid binding of the inhibitor followed by a relatively slow step leading to the formation of the final enzyme-inhibitor (E-I) complex[113]. Inability of 5AR1 to recover activity after Finasteride exposure suggests Finasteride binding by 5AR is covalent in nature and is responsible for the slow kinetics seen[113]. However although enzyme denaturation studies have shown non-covalent binding of Finasteride, covalent binding to 5AR1 has yet to be demonstrated[114].

From figure 1.5, it can be seen that the reduction of T and mechanism based inhibition by Finasteride follow parallel reactions that proceed through closely related enolate intermediates. The two reactions diverge at the final step where Finasteride aborts the process by translocating the enolate/carbanion centre to a position where normal proton transfer cannot take place[114]. Finasteride is processed much slower by 5AR1 than 5AR2 and as a result, adduct formation during 5AR1inhibition occurs at a much slower rate constant.

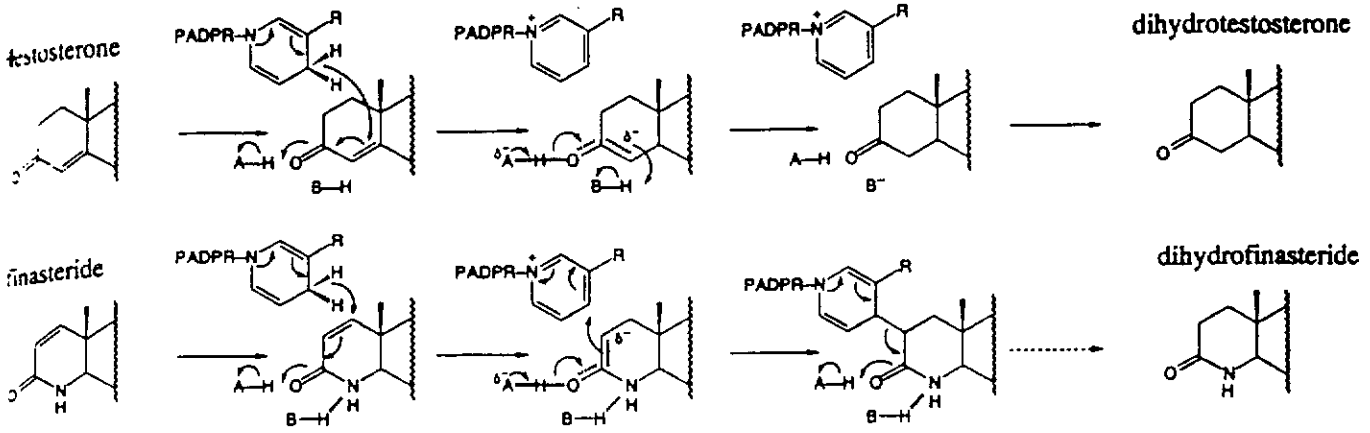

Figure 1.5: Proposed mechanism of 5AR inhibition by Finasteride[114].

Differences in the potency and mechanisms of Finasteride inhibition are seen between rat and human 5AR isoenzymes. Finasteride is a potent, time independent and reversible inhibitor of rat 5AR1 but is a potent, time-dependent and irreversible inhibitor of rat 5AR2 and of both the human isoenzymes[115]. In Rhesus macaque monkeys[43], time-dependent irreversible Finasteride inhibition of both isoenzymes also is seen. Why reversible inhibition only occurs in rat 5AR1 remains unknown although two possibilities have been suggested. One possibility is that 5AR requires recognition of Finasteride as an alternative substrate to enable reduction in the A-ring of the azasteroid. If the enzyme is incapable of catalyzing this reaction, reversible inhibition results. It could be however that reduction of Finasteride does occur but the partitioning of the enolate may favour proton transfer to yield dihydrofinasteride rather than collapsing with NADP+ to form a stable adduct. Incubating rat 5AR1 with ^{3H}Finasteride and analysis of product formation with high performance liquid chromatography (HPLC) showed Finasteride was not converted to dihydrofinasteride, indicating that 5AR cannot reduce the A-ring of the inhibitor[115].

The distinct mechanism of inhibition seen for rat 5AR1 suggests there may be subtle differences in the NADP[H] binding site that may interfere with the

enzyme-catalyzed reduction of $\Delta^{1,4}$-azasteroids eg. Finasteride, but not $\Delta^{4,3}$-keto-steroids such as T. What these differences might be are unknown as 5AR does not contain a consensus NADP[H]-binding site and as the enzyme has yet to be purified, there is only very limited structural information. Characterisation of naturally occurring mutations in the SRD5AR2 gene tentatively identified eight amino acids (R145, R171, P181, G183, N193, G196, R246W and R246Q) contributing to cofactor binding[63]. Strict conservation is seen in seven of these eight residues between rat, human and monkey isoenzymes, with R145 being the exception. Arginine is expressed at the analogous residues in both 5AR1 and 5AR2 across species except rat 5AR1, where the arginine is replaced by a cysteine. It has been proposed that this substitution may contribute to the distinct mechanism of Finasteride inhibition seen for rat 5AR1[115].

1.9.2 Finasteride and BPH

Finasteride was approved in 1992, for use in the treatment of BPH in the USA. Its inhibition of 5AR results in lower serum and intraprostatic DHT levels and apoptosis of the epithelial prostate cells with a subsequent reduction in prostate size[102]. Finasteride is a selective but not specific inhibitor of human 5AR2 and a poor inhibitor of 5AR1[53], which in the presence of normal to elevated T levels elicits a reduction in prostate size. If administered early enough to males with prostatic enlargement, Finasteride may prevent more serious progression of disease[67].

T to DHT conversion by 5AR is a sequential reaction where NADP[H] binding precedes that of T. Inhibition studies in prostatic stromal cells suggest Finasteride simultaneously competes with T at the same binding region of 5AR[116]. Sequential binding is also seen in the epithelial cells, only here Finasteride binds to 5AR after T and as a result the effects of Finasteride on 5AR1, the major isoenzyme expressed in the epithelial cells, are reduced[116].

DNA cleavage is a well-known marker of cellular apoptosis and can be demonstrated histologically. This is by staining using biotin labelled nucleotides and the enzyme terminal deoxytransferase, which adds the labelled nucleotides to the cleaved DNA ends[117]. Increased staining with this method has been

1.9.3 Finasteride and Prostate Cancer

Studies of 5AR activity in prostate tumours have lead to conflicting results with some claiming increased activity[121] whereas others consider this increase not to occur[122, 123]. Studies of the DU145 androgen insensitive human prostatic adenocarcinoma cell line demonstrated only 5AR1 mRNA expression and enzyme activity that was potently and selectively inhibited by LY306089, a selective non-competitive 5AR1 inhibitor[55]. This suggests that 5AR1 may have a role in prostate cancer whereas 5AR2 seems to play an important role in the development of prostatic hyperplasia[41].

The value of 5AR inhibitors in the management of prostate cancer appears limited but requires further investigation. Combining 5AR inhibitors with other substances like pure anti-androgens, to enhance their effectiveness is one possibility[67]. It remains undetermined whether early application of 5AR inhibitors may play a preventative role in the development of prostate cancer. As inhibitors of 5AR2 only, may not be effective for prostate cancer treatment, it seems possible that development of equally efficient dual 5AR inhibitors is required[41].

Clinical experience of the treatment of prostate cancer with Finasteride is very limited. In a study of prostatic volume, PSA and prostatic acid phosphatase levels of patients with asymptomatic D stage prostate cancer treated with Finasteride, the only statistically significant results seen were a decrease in PSA levels in comparison with placebo and a 77-79% reduction in plasma DHT[124]. This indicates limited effectiveness of Finasteride but the effects were much less than those seen with castration or total androgen blockage[124]. A clinical trial determining the efficacy of Finasteride in prostate cancer in 18000 men is currently being undertaken in America and it is hoped this trial will provide further insight into the mechanisms involved in the aetiology of prostate cancer as well as the therapeutic effectiveness of Finasteride.

1.9.4 Finasteride and MPB

Dallob and colleagues[79] assessed the effects of Finasteride on the levels of T and DHT in scalp skin of men with MPB. They concluded DHT levels in balding scalp were significantly higher than levels in hair-containing scalp from the same patient, although no significant differences in circulating T levels were seen. Some patients were treated with 5mg Finasteride for 28 days and others with a placebo. After treatment DHT levels were measured in scalp samples. A significant reduction in DHT levels in bald scalp samples from Finasteride treated subjects was seen compared with DHT levels in the placebo group[79]. The mean DHT levels in bald scalp of Finasteride treated patients were similar to levels in hair containing scalp from placebo treated patients. These findings suggest Finasteride may be valuable for the treatment of MPB. It is unclear however whether complete inhibition of both 5AR isoenzymes is necessary to promote hair growth.

1.9.5 Finasteride and Hirsutism

The short-term effects of Finasteride on circulating androgens and gonadotrophin secretions in hirsute females given 5mg Finasteride a day for 3 months were assessed[125]. Most significantly, plasma DHT levels decreased, plasma T levels increased and the Ferriman-Galleway score decreased by 27.8% in treated subjects. These results indicate Finasteride treatment reduces hirsutism in females without affecting gonadotrophin secretions.

In a similar study, the tolerability of Finasteride, its effects on sex hormones and its efficacy in the treatment of hirsutism were assessed[126]. Following 3 months of therapy a 50% reduction in the Ferriman-Galleway score was seen, menstrual cycles remained ovulatory, serum DHT decreased and there were slight increases in serum gonadotrophin, T and SHBG levels. Interestingly from this study it was determined that combining the oral contraceptive pill with Finasteride resulted in a more pronounced improvement in hirsute patients[126].

1.10 Structure/Function Analyses

Inability to isolate 5AR together with its very low expression levels, has prevented characterisation of its substrate/inhibitor and cofactor binding domains. Isolation of the cDNAs encoding human 5AR by expression cloning has lead to the discovery that mutations in isoenzyme 2 were associated with 5AR deficiency. This led to investigations of these mutations and to elucidation of their effects on 5AR activity.

1.10.1 Mutations of 5AR2

Using standard methods of molecular genetic analysis, twenty-nine mutations of the SRD5AR2 gene have been identified and characterized in 5AR deficient patients (Figure 1.6). These mutations all prevent the formation of a fully functional enzyme, generate an unstable enzyme or impair enzyme ability to bind T or NADP[H]. It is feasible that as yet uncharacterized mutations outside the coding region of SRD5AR2 may impair 5AR2 expression[10]. These mutations have been classified as point mutations including amino acid substitutions, splice junction alterations, deletions and nonsense mutations[69]. Mutations are evenly distributed throughout the five exons, show prevalence among particular ethnic groups and there are mutational hot spots[10]. All of the point mutations identified in a study of New Guinea families altered amino acid residues conserved between rat and human 5AR2, indicating the importance of these residues for enzyme function[32].

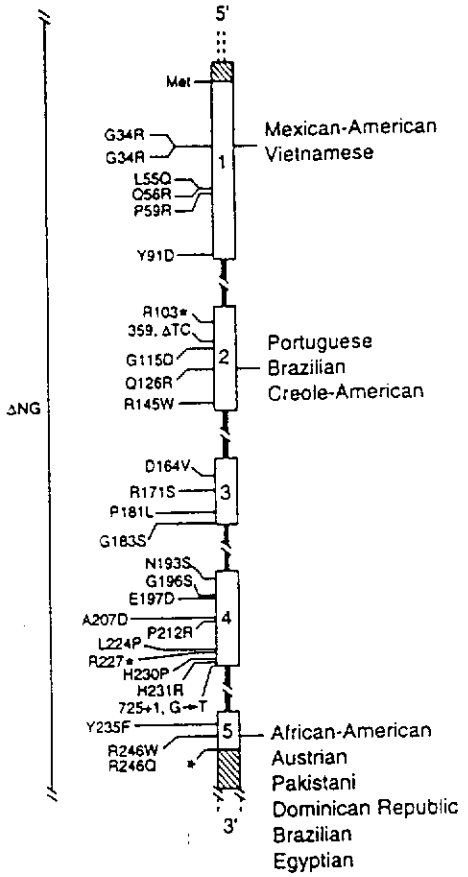

Figure 1.6: *Mutations in the SRD5AR2 gene responsible for 5AR deficiency*[10].

5AR expression in mammalian cells transfected with mutant cDNAs has enabled biochemical characterisation of twenty-two missense mutations of SRD5AR2. Twelve mutations resulted in enzyme inactivation while the remaining ten severely reduced enzyme activity by affecting either substrate (T) or cofactor (NADP[H]) binding[63]. How all of these ten mutations result in enzyme inactivation is unknown but they do not appear to be related to a failure of 5AR synthesis, as the protein is immunologically detectable. Mutations

affecting cofactor binding were mapped to its conserved carboxyl terminus and those affecting substrate binding to its two ends[10], the locations of these mutations are shown in figure 1.7. These mutations disrupt either substrate or cofactor binding but not both, demonstrating the amino acid determinants of each binding domain are unique. Of the ten mutations impairing enzyme activity two were found to affect substrate binding. These were the G34R (substitution of arginine for glycine at residue 34) and H231R (substitution of arginine for histidine at residue 231) mutations.

The remaining eight mutations appear to reduce the ability of 5AR to bind with cofactor[63]. These mutations are R145W (tryptophan for arginine at residue 145), R171S (serine for arginine at residue 171), P181L (leucine for proline at residue 181), Q183S (serine for glutamine at residue 183), N193S (serine for asparagine at residue 193), G196S (serine for glycine at residue 196), R246W (tryptophan for arginine at residue 246) and R246Q (glutamine for arginine at residue 246). It is unknown how these mutations affect NADP[H] binding, but as substrate binding is unaffected this suggests mutations affecting cofactor binding do not affect substrate binding and do not cause enzyme denaturation[63].

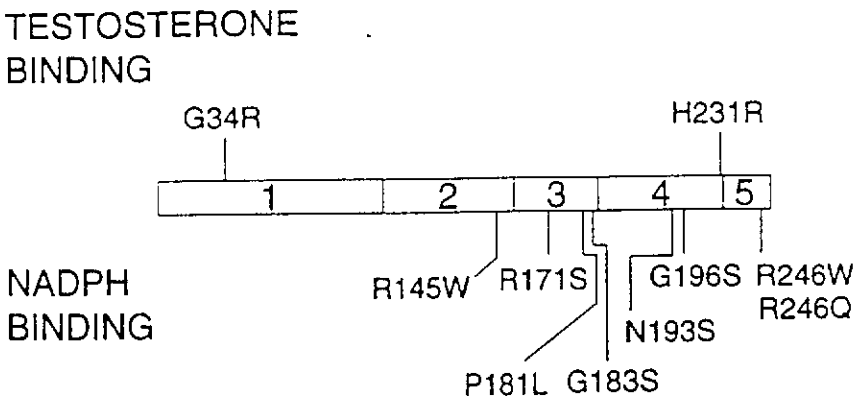

Figure 1.7: *Location of ten mutations affecting substrate or cofactor binding by 5AR2[10].*

As well as affecting substrate and cofactor binding, all but one (R145W) of the ten mutations affecting enzyme activity also altered the pH optimum of 5AR2, shifting if from an acidic to a more basic optimum[63].

More recently single strand conformation polymorphism (SSCP) gel electrophoresis was used to detect single nucleotide substitutions of the SRD5AR2 gene[127]. A further thirteen mutants were identified in this study, one resulting in unaltered 5AR activity, three increasing and nine decreasing 5AR activity. The sensitivity of these mutants to the pharmacological inhibitors Finasteride, PNU-157706 and GG-745 were also determined. From these studies the substrate and inhibitor (Finasteride and GG-745) binding sites were found to be bipartite with distinct residues from both the amino and carboxyl termini involved[127]. The binding site for PNU-157706 spanned a larger part of the amino and smaller part of the carboxyl termini. Alternatively it was thought possible residues within the carboxyl terminus alone, are involved in cofactor binding.

Characterisation of the effects on 5AR activity of the mutations in the SRD5AR2 gene has provided information regarding the structure-function relationships of 5AR. The locations of point mutations responsible for 5AR deficiency are conserved in primate 5AR2 and all but 2 mutations (G115 and H230), are conserved between monkey, rat and human 5AR2. As these mutated residues are conserved between rat, monkey and human isoenzymes, this suggests they are important for enzyme activity[63]. Characterisation of the mutational effects on 5AR activity has also provided information useful for the experimental determination of the substrate, inhibitor and cofactor binding domains of 5AR. This is of significance not only for furthering understanding of how the enzyme operates but also for providing information useful for the development of new enzyme inhibitors designed to interact with residues that contribute significantly to enzyme function. At present there are only a few reports of studies designed to determine structure-function relationships of 5AR.

1.10.2 Substrate Binding

To date the only studies providing information on the steroid-binding domain of 5AR, are those of Thigpen and Russell[128] who determined the sensitivity to Finasteride of chimeras of rat and human 5AR1. For this study the differing sensitivities of rat and human 5AR1 to Finasteride were exploited as rat 5AR1

has greater sensitivity (Ki= 12nM) than does its human counterpart (Ki= 330nM).

The rat/human chimera containing exon 1 of rat 5AR1 attached to the remainder of human 5AR1, yielded an enzyme with a rat-like sensitivity to Finasteride demonstrating the major determinants of Finasteride binding are located within exon 1[128]. Exchanging progressively smaller segments located these determinants to within the first 44 amino acid residues of rat 5AR1. Alignment of rat and human sequences identified two regions of non-identity, from which an eleven amino acid segment incorporating residues 16-27 in rat and 20-30 in human 5AR1 was selected. Tri and tetra-peptide segments were then substituted. When residues 22-25 of rat 5AR1 were replaced with residues 26-29 of human 5AR1, the expressed enzyme exhibited reduced sensitivity to Finasteride. Similarly, replacing residues 26-29 of human 5AR1 with residues 22-25 from rat 5AR1 resulted in an expressed enzyme with increased sensitivity to Finasteride. From these studies it was concluded that residues 22-25 (VSIV) in the amino terminus of rat and the analogous residues 26-29 (AVFA) of human 5AR1 are involved in Finasteride binding[128]. As Finasteride is a competitive 5AR inhibitor, this indicates that residues 22-25 in rat and 26-29 in human 5AR1 form part of the substrate binding domain of these isoenzymes.

Some support for this is given by findings of a two-fold reduction in Km for T in chimeras of human 5AR1 in which amino terminus residues were replaced with their analogous residues from rat 5AR1[128]. This indicates exchange of these residues affects both substrate and inhibitor binding. Interestingly some chimeras had greater affinities for T, suggesting some disorders of DHT overproduction may be due to mutations causing a gain of function[128]. Recent studies of genetic variants of the SRD5AR2 gene and their association with prostate cancer have demonstrated that substitution of alanine at residue 49, with threonine results in increased enzymatic activity *in vitro*[97]. This effect seems to be an inherent gain of function encoded by the amino acid substitution, as steady state concentrations of the normal and mutant enzyme were identical[97]. As a result of this mutation the inhibitory effects of Finasteride were also significantly reduced, suggesting Finasteride therapy in prostate cancer patients expressing the A49T genotype may be ineffectual.

It has also been suggested that the analogous residues in 5AR2 (-GALA-, r21-24) form part of its substrate binding domain[44, 128] but this has yet to be determined experimentally. The analogous tetrapeptides in rat (-GTLI-) and monkey (-GALV-) 5AR2 are not conserved across the three species, reflecting differences seen in the steroid and inhibitor affinities[44].

Interestingly, the G34R mutation lies adjacent to the proposed substrate binding site of human 5AR2 (r21-24). This mutation reduces the affinity of 5AR2 for substrate and suggests an extended sequence of amino acids form the substrate binding domain in the amino terminus[128]. As little is currently known of the tertiary structure of 5AR, these studies have to treat 5AR as a linear molecule. It is probable however that residues involved in substrate/Finasteride binding will map to regions other than the amino terminus.

The amino acid residues in the tetrapeptides VSIV and AVFA consist of hydrophobic residues making it difficult to predict the relative contributions of the individual amino acids. Extensive structure-activity studies among 4-azasteroid inhibitors demonstrate substitution at carbon 17 dramatically affects the ability of a compound to inhibit an isoenzyme of 5AR[19]. The bulkier t-butyl group at carbon 17 in Finasteride may therefore determine the sensitivity to Finasteride of a particular 5AR. This suggests the large phenylalanine residue at position 3 of the tetrapeptide -AVFA-, in human 5AR1 may be the most likely single amino acid determinant of its Finasteride resistance[128].

Recent studies in rat 5AR1 with a competitive photoactive probe, [1,2 ^{3}H]N-4(benzylbenzoyl)-3-oxo-4-aza-4-methyl-5α-androstan-17β-carboxamide, identified an N-terminal tetrapeptide -LEGF- (residues 15-18) thought to comprise its substrate binding domain[129]. Further analyses with identical digestion and chromatography conditions led to the identification of a slightly longer peptide including residues 15-21 (-LEGFMAF-). Interestingly, this sequence lies immediately adjacent to the tetrapeptides identified as contributing to substrate binding by Thigpen and Russell[128], lending further support for their involvement in steroid binding.

A strong preference for aromatic substitutions is seen within this region of 5AR among the different isoenzyme and species (Figure 1.8). This demonstrates they share a common structural feature that permits tight binding of aromatic groups[129]. Substitution of F18 for leucine in rat 5AR1 (F18L), resulted in an almost twelve fold decrease in substrate affinity[129], reinforcing the importance of this residue for substrate binding.

Human 5AR1	^{9}LLVAEERLLAALAYLQCAVGCAVFAR$^{34??}$
Rat 5AR1	^{1}MELDELCLLDELVY^{15}LEGFMA^{21}FVSIVG^{26}
Human 5AR2	^{1}MQVQCQQSPVLAGS^{15}ATLVT^{20}LGALAL^{25}
Rat 5AR2	^{1}MQIVCHQVPVLAGS^{15}ATLAT^{20}MGTLIL^{25}

Figure 1.8: *Sequence comparison between rat and human 5ARs.*

1.10.3 Cofactor Binding

Early studies[130] observed functional domains of membrane proteins are often encoded by discrete exons within a gene. Residues involved in substrate binding by 5AR lie within exon 1[128], therefore other functional domains such as the cofactor binding domain also may be encoded by a single exon.

Studies by Wigley and associates[63] identified several mutations occurring within the C-terminus of 5AR resulting in a reduction in affinity for cofactor and suggesting the cofactor binding domain of 5AR lies within the C-terminus. Although NADP[H] is the only cofactor for 5AR, the amino acid sequence of rat and human 5AR isoenzymes do not contain consensus adenine dinucleotide binding sequences or NADP[H] binding residues identifiable in other reductase enzymes[131]. Studies of the mutations in 5AR indicate it has a novel structure with residues contributing to NADP[H] binding spread throughout the C-terminus. With the exception of R145, all mutations show conservation between rat, human and monkey 5AR. The G196 and R246 mutations reduce affinity for cofactor almost 100-fold. Interestingly glycines and arginines are often found at crucial positions in NADP[H] cofactor binding domains in other proteins[131], suggesting 5AR may share tertiary structure homology with other enzymes. To

date however primary structural identities between 5AR and other NADP[H]-utilising proteins remains elusive[32].

Using the photolabelled [2'-^{32}P]-2-azido-NADP+ probe as a competitive NADP[H] inhibitor Bhattacharyya and colleagues[29] identified an eleven amino acid peptide in rat 5AR1, residues 170-180 (-NLRKPGETGYK-), believed to form part of its NADP[H] binding site. These eleven residues lie within a highly conserved region of rat 5AR1 (r160-190) that has 97% homology with human 5AR1 (r164-194). There is only a single residue that differs between the two isoenzymes, glutamate 176 in rat and aspartate 180 in human 5AR1. Hydropathy plots demonstrate this peptide is located in a solvent-exposed region of 5AR1[29] and as such can directly interact with NADP[H], a hydrophilic molecule.

The sequence -Gly-XX-Gly-XXXXX-Gly-Gly- has been identified as the nucleotide binding sequence unique to 5AR1 isoenzymes[29]. In the type 2 isoenzymes although the third and fourth glycine residues are conserved, the second glycine residue is not. In human type 2 this second glycine has been replaced with a serine and with isoleucine in rat type 2. Overall however, there are marked similarities in the putative cofactor binding regions between and within species as is evident from comparisons of these regions:

Rat 5AR1	^{170}N-L-R-K-P-G-E-T-G-Y-K-I-P-R-G-G-L-F-E-Y-V^{190}
Human 5AR1	^{174}N-L-R-K-P-G-**D**-T-G-Y-K-I-P-R-G-G-L-F-E-Y-V^{190}
Human 5AR2	^{169}Q-L-R-K-P-G-E-**I**-**S**-Y-**R**-I-P-**Q**-G-G-L-F-**T**-Y-V^{189}
Rat 5AR2	^{169}Q-L-R-K-P-G-E-**V**-**I**-Y-**R**-I-P-R-G-G-L-F-**T**-Y-V^{189}

In all of these enzymes an acidic residue follows the first glycine and may be involved in hydrogen bonding with the ribose moiety or to the ring of nitrogens in the adenine ring of NADP[H] [29]. All sequences contain conserved aromatic residues, which are possibly involved in aromatic and hydrogen bonding interactions with the adenine ring of NADP[H].

The sequence -Gly-X-X-Gly-X-X-X-X-X-Gly-Gly- identified as the 5AR1 nucleotide binding sequence[29] differs significantly from the signature motif -Gly-

X-Gly-X-X-Gly/Ala- normally associated with βαβ fold in most NAD+/NADP+ binding sites[132], again suggesting a unique cofactor binding site for 5AR.

Of the ten mutations affecting NADP[H] binding[63] R171S, P181S and G183S in human 5AR2 lie within the proposed adenine binding domain[29]. The R145W, N193S, G196S and R246Q mutations also affect NADP[H] binding and therefore may also form part of the adenine binding domain.

Using site-directed mutagenesis[133] the roles of residues Y179, Y189, F187 and S164 within the NADP[H] binding site of rat 5AR1 were investigated. Studies of other NADP[H]-requiring enzymes[134] have demonstrated an involvement of the hydroxyl function of tyrosyl residues in mediating hydride transfer from cofactor to substrate. The Y179F mutation significantly reduced affinity for cofactor but Vmax was unchanged, suggesting the hydroxyl function of tyrosine is not involved in the reaction but is essential for maximal NADP[H] binding[133]. The Y189F mutation significantly increased cofactor affinity but did not alter the affinity for substrate. This demonstrates the involvement of hydroxyl function for cofactor but not substrate binding[133]. The Y189S mutant, in which the hydroxyl function is preserved exhibited similar kinetics to wild type 5AR1 and supports a role for hydroxyl function in cofactor binding.

Although the mutation F187Y did not affect cofactor binding it did cause an 18-fold reduction in substrate affinity[133], suggesting F187 plays an important role in substrate binding. As discussed earlier, it is thought the phenylalanine residue in the tetrapeptide AVFA also may be of particular significance in substrate binding. The S164A mutation slightly decreased affinity for cofactor and reduced Vmax, it was therefore concluded that although hydroxyl function affects cofactor binding it is not necessary for substrate binding[133].

Serine residues also play a role in the recognition of 2'-phosphate groups in NADP[H][135]. The Y179S mutation resulted in complete loss of enzyme activity, despite preservation of hydroxyl function in this mutant. Replacement with a non-aromatic residue however has resulted in disruption of the binding domain and has thus prevented binding of cofactor[133].

1.11 Conclusion

It has been conclusively demonstrated that 5AR is an enzyme of importance in androgen metabolism and in the development and maintenance of the male external genitalia and prostate during embryogenesis and subsequent life. Both the overproduction and underproduction of DHT are associated with endocrine abnormalities in man. Those of most significance are abnormalities of masculine development, benign prostatic hyperplasia and prostate cancer.

Identification of the cDNAs coding for the rat and human isoenzymes of 5AR has lead to a significant increase in the understanding of the enzyme and of its associations with disease. Identification of the various mutations in 5AR and correlation of these with the symptoms of the disease they cause has enabled greater understanding of the structure/function relationships of the enzyme.

As yet there have been few reports of the experimental determination of these relationships. That identifying residues involved in Finasteride binding however is of particular importance and showed that residues in rat and human 5AR1 involved in binding of Finasteride are analogous and as Finasteride is a competitive inhibitor, these residues may also be part of the substrate binding domain. This suggests the analogous region of 5AR2 may also form part of its Finasteride/substrate binding domain.

These discussions above have shown that the associations of 5AR2 with human disease are of more significance than are those of 5AR1. It is apparent therefore that studies designed to determine residues of 5AR2 involved in inhibitor/substrate binding are of merit. However despite the greater significance of 5AR2 to human disease, the association of 5AR1 with dermatological conditions including male pattern baldness, also warrants further investigation of residues comprising its inhibitor/substrate binding domain.

Chapter 2.0

Materials

2.1 REAGENTS

Reagent	Supplier
5α- Reductase 1 cDNA	Dr DW Russell, Southwest Medical Centre, Dallas, Texas, USA
5α- Reductase 2 cDNA	Dr DW Russell
5-Bromo-4-chloro-3-indolyl-β-D-galactopyranoside (X-gal)	Promega Corporation, Madison, Wisconsin, USA
6X Blue/orange sample loading buffer	Promega
Agar	Oxoid Ltd, Hampshire, England
Agarose	Pharmacia Biotech. AB, Uppsala, Sweden
Ammonium sulphate	Ajax Chemicals, Sydney, Australia
Amphotericin B (25mg/mL)	Trace Bioscience Pty Ltd, Australia
Ampicillin	Sigma Chemical Co. St Louis, Michigan, USA
Bacto-tryptone	Oxoid

Bacto yeast extract	Oxoid
β- Galactosidase enzyme assay kit	Promega
β- Galactosidase expression vector	Promega
β- Mercaptoethanol	British Drug Houses (BDH) Chemicals, Victoria, Australia
Bovine serum albumin (BSA)	Commonwealth Serum Laboratories (CSL), Melbourne, Australia
Calcium chloride	BDH
Calcium phosphate transfection kit	Pharmacia Biotech.
Calf intestinal alkaline phosphatase (CIAP)	Promega
Carbon-14 labelled dihydrotestosterone (^{14C}-DHT), 53.6mCi/mmol	NEN, Boston, Massachusetts, USA
Chinese hamster ovary (CHO) cells	American Type Culture Collection, USA
Copper sulphate	BDH
Developer (Film)	Kodak Australasia Pty Ltd, Victoria, Australia
Dichloromethane	BDH
Diethyl ether	BDH

Dihydrotestosterone (DHT)	Sigma
Dimethylformamide	BDH
Dimethyl sulphoxide (DMSO)	Ajax
Dipotassium hydrogen orthophosphate	BDH
Disodium hydrogen Orthophosphate	BDH
Dithiothreitol (DTT)	Sigma
Deoxy nucleotide triphosphate (dNTPs)	Stratagene Cloning Systems, California, USA
Dpn I restriction enzyme	Stratagene
E.coli strain DH5α	Promega
Electroporation cuvettes	Biorad Laboratories, California, USA
Epicurian coli XL-1 blue supercompetent cells	Stratagene
Ethanol	BDH
Ethidium bromide	Sigma
Ethylenediamine disodium tetra-acetic acid (EDTA)	BDH

Finasteride	Merck-Sharpe and Dohme, Germany
Fixer (Film)	Kodak
Foetal calf serum (FCS)	Trace Bioscience
Formaldehyde	BDH
Gamma adenosine triphosphate ($^{32P}\gamma$-ATP), 25Ci/mmol	ICN-Radiochemicals, Ohio, USA
Geneticin 418 (Neomycin sulphate)	Gibco BRL Life-Technologies, New York, USA
Glacial acetic acid	BDH
Glucose	BDH
Glucose-6-phosphate	Sigma
Glucose-6-phosphate dehydrogenase	Sigma
Glutaraldehyde	BDH
Glycine	Sigma
Glycerol	Ajax
Ham's F12 tissue culture medium	Trace Bioscience
Hybond ECL nitrocellulose membrane	Amersham Pharmacia Biotech. Buchinghamshire, England

Isopropanol	BDH
Isopropyl-thiogalactoside (IPTG)	Promega
L-glutamine	ICN Biomedicals Inc. Ohio, USA
Lambda DNA markers	Promega
Magnesium chloride	Ajax
Magnesium sulphate	Ajax
Methanol	Scot Scientific Pty Ltd. Perth, Western Australia
N-[2-hydroxyethyl] piperazine-N'-[2-ethane sulfonic acid] (HEPES)	Sigma
β- Nicotinamide adenine dinucleotide phosphate (NADP+)	Sigma
β- Nicotinamide adenine dinucleotide phosphate, reduced form (NADP[H])	Sigma
n-octyl *β-D*-glucopyranoside (NOG)	Sigma
Not I restriction enzyme	Promega
Nutrient broth	Oxoid
NZ amine (casein hydrochloride)	Sigma

Oligonucleotide primers/probes (These were obtained from the several sources listed).	Life Technologies, Operon Technologies, Genset Pacific Oligonucleotides and Pacific Oligonucleotides
o-nitrophenyl-β-D-galactopyranoside (ONPG)	Sigma
Optifluor-O organic scintillant	Canberra-Packard, Packard Instrument Co. Meridian, Connecticut, USA
pADVantage co-expression vector	Promega
pCI-neo mammalian expression vector	Promega
Penicillin	Trace Bioscience
Pfu DNA polymerase	Promega
Phenol reagent of folin and ciocalteau	BDH
Potassium acetate	BDH
Potassium dihydrogen orthophosphate	BDH
Potassium chloride	Ajax
pUC18 control vector	Stratagene
pWhitescript control vector	Stratagene

Ribonuclease A (RNAse)	Promega
Sal I restriction enzyme	Promega
Scintillation vials	Canberra-Packard
Quickchange™ site-directed mutagenesis kit	Stratagene
Sodium acetate	Ajax
Sodium bicarbonate	BDH
Sodium carbonate	BDH
Sodium chloride	BDH
Sodium citrate	BDH
Sodium dihydrogen orthophosphate	BDH
Sodium dodecyl sulphate (SDS)	BDH
Sodium hydroxide	BDH
Sodium tartrate	BDH
Spermidine	Sigma
Streptomycin	Trace Bioscience
Sulphuric acid	BDH
T_4 DNA ligase	Promega
T_4 polynucleotide kinase (PNK)	Promega

Testosterone (T)	Sigma
Thin layer chromatography (TLC) plates	Merck, Germany
TRIS	Sigma
TRIS-Cl	Sigma
Tritiated Testosterone (^{3}H-T) 80mCi/mmol	Amersham Life Science, Buckinghamshire, England
Triton-X	Sigma
Trypsin	Sigma
Yeast extract	Oxoid
X-ray Film	Fuji Pty Ltd. Japan
Zinc Chloride	BDH

2.2 BACTERIAL CULTURE

All filter sterilisation was through a 0.22μM filter and autoclaving was at 121^{o}C for 20 minutes.

Ampicillin (100μg/mL)

250mg Ampicillin

* Dissolve in 25mL of phosphate buffer (pH 8.0) and filter sterilise

Dipotassium hydrogen orthophosphate (1M)

174.2g Dipotassium hydrogen orthophosphate

* Make to 1L with dH_2O

Glucose (2M)

360.3g Glucose

* Make to 1L with dH_2O and filter sterilise

IPTG (20mg/mL)

2g IPTG

* Make to 100mL with dH_2O and filter sterilise

Luria bertani (LB) broth

10g Bacto-Tryptone
5g Yeast extract
10g Sodium chloride

* Make to 1L with dH_2O and sterilise by autoclaving

LB-agar

10g Bacto-Tryptone
5g Yeast extract
10g Sodium chloride
15g Agar

* Make to 1L with dH_2O and sterilise by autoclaving

LB-ampicillin broth

1mL Ampicillin (10mg/mL)

* Add to 100mL of autoclaved LB broth
* The final concentration of ampicillin is 100μg/mL

LB-ampicillin agar

1mL Ampicillin (10mg/mL)

* Add to 100mL of melted LB agar ($50^{O}C$)
* The final concentration of ampicillin is 100μg/mL

LB-ampicillin-X-gal-IPTG agar

1mL Ampicillin (10mg/mL)
100μL X-gal (100mg/mL)
500μL IPTG (20mg/mL)

* Add to 100mL of melted LB agar ($50^{O}C$)
* The final concentration of ampicillin, X-gal and IPTG is 100μg/mL

Magnesium chloride (1M)

203.3g Magnesium chloride ($MgCl_2.6H_2O$)

* Make to 1L with dH_2O and sterilise by autoclaving

Magnesium sulphate (1M)

120.4g Magnesium sulphate

* Make to 1L with dH_2O and sterilise by autoclaving

NZY+ Broth

10g	NZ amine (casein hydrochloride)
5g	Yeast extract
5g	Sodium chloride

* Make to 1L with dH_2O and sterilise by autoclaving
* Immediately prior to use add (per 100mL):
    a) 1.25mL magnesium chloride (1M)
    b) 1.25mL magnesium sulphate (1M)
    c) 1mL glucose (2M)
    d) Filter sterilise the resulting solution

Phosphate buffer (0.1M, pH 8.0)

5.5mL	Potassium dihydrogen orthophosphate (1M)
94.5mL	Dipotassium hydrogen orthophosphate (1M)

* Make to 1L with dH_2O

Potassium dihydrogen orthophosphate (1M)

131.6g	Potassium dihydrogen orthophosphate

* Make to 1L with dH_2O

X-gal (100mg/mL)

10g	X-gal

* Make to 100mL in dimethylformamide
* Store in a light-proof container

2.3 CELL CULTURE REAGENTS

Complete Ham's F12 tissue culture medium

Per litre;

10.63g	Ham's F12 medium (with L-glutamine, without sodium bicarbonate)
2g	Sodium bicarbonate

* Filter sterilise, then add aseptically:

4mL	L-glutamine (0.5M)
10mL	Penicillin/streptomycin (100μg/mL)
50mL	Foetal calf serum

Geneticin 418 (600μg/mL)

1.2mL	G418 (50mg/mL)
98.8mL	Complete Hams F12

* Filter sterilise

L- glutamine (0.5M)

2.92g	L-glutamine

* Make to 40mL with hpH_2O and filter sterilise
* Store as 2mL aliquots at -20^{o}C

Phosphate buffered saline (PBS) (pH 7.4)

8g	Sodium chloride
0.2g	Potassium chloride

1.44g	Disodium hydrogen orthophosphate
0.24g	Potassium dihydrogen orthophosphate

* Adjust pH to 7.4 then make to 1L with hpH_2O and sterilise by autoclaving

PBS-EDTA (pH 7.4)

8g	Sodium chloride
0.2g	Potassium chloride
1.44g	Disodium hydrogen orthophosphate
0.24g	Potassium dihydrogen orthophosphate
0.2g	EDTA

* Adjust pH to 7.4 then make to 1L with hpH_2O and sterilise by autoclaving

Trypsin (0.5%)

5g	Trypsin

* Make to 1L with PBS-EDTA and filter sterilise
* Store at $4^{O}C$

2.4 BUFFERS

2.4.1 Plasmid DNA Extraction

This was performed using either the commercially available BRESAspin™ plasmid mini kit, the individual constituents of the various buffers for which were not provided in the manufacturer's protocol. Or the alkaline lysis method[136] the reagents for which are given below.

Ethanol (70%)

700mL 100% Ethanol

* Make to 1L with hpH_2O

RNAse

10mg RNAse (50-100 units/mg)

* Make to 1mL with hpH_2O

Solution 1 (50mM Glucose, 25mM TRIS-Cl [pH8.0], 10mM EDTA [pH8.0])

905mg	Glucose
394mg	TRIS-Cl
292mg	EDTA

* Prepare in 100mL batches and sterilise by autoclaving
* Store at 4^{O}C

Solution 2 (0.2M Sodium hydroxide, 1% SDS)

0.8g	Sodium hydroxide
0.1g	SDS

* Prepare fresh daily in 10mL batches

Solution 3 (5M Potassium acetate, Glacial acetic acid)

49.05g	Potassium acetate
11.5mL	Glacial acetic acid

* Make to 100mL with hpH_2O and store at 4^{O}C

* The resulting concentrations of potassium and acetate in solution 3 are 3M and 5M respectively

2.4.2 DNA Purification Methods

DNA purification was required following the CIAP-dependent dephosphorylation of *Not I* digested pCI-neo vector, to remove any residual CIAP activity. Dephosphorylation of *Not I* digested pCI-neo vector was necessary to prevent vector self re-ligation during ligation of *Not I* digested vector with the 5AR1 insert.

DNA purification was also required to remove an 11bp fragment excised from the vector pCI-neo following its digestion with both *Sal I* and *Not I*. This was again required to prevent vector self-religation during the religation of *Sal I/Not I* digested pCI-neo with the 5AR2 insert.

The Promega Wizard DNA Clean-Up System was used both for the purification of *Not I* digested pCI-neo following dephosphorylation and *Sal I /Not I* digested pCI-neo before ligation with the 5AR1 and 5AR2 cDNA inserts respectively. The reagents required are listed below.

<u>Isopropanol (80%)</u>

800mL 100% Isopropanol

* Make to 1L with dH_2O

2.4.3 Restriction Digests

10X Buffer D (6mM TRIS-Cl [pH7.9], 100mM Sodium chloride, 6mM Magnesium chloride, 1mM DTT)

94.6mg	TRIS-Cl
584.4mg	Sodium chloride
57.1mg	Magnesium chloride
15.4mg	DTT

* Make to 100mL with hpH_2O, sterilise by autoclaving

2.4.4 Agarose Gel Electrophoresis

Agarose gel (1%)

1g	Agarose
100mL	1X TAE buffer

* Dissolve agarose either by steaming for 60 minutes or using a microwave oven

6X Blue/orange sample loading buffer

This was obtained from Promega, the components of which are;

15%	Ficoll 400
0.03%	Bromophenol blue
0.03%	Xylene cyanol FF
0.4%	Orange G

Ethidium bromide stain (25mM)

1g	Ethidium bromide

* Make to 100mL with dH_2O
* (NB: Ethidium bromide is a mutagen)

50X TAE buffer

242g	TRIS
57.1mL	Glacial acetic acid
100mL	EDTA (0.5M, pH 8.0)

* Make to 1L with hpH_2O

1X TAE buffer

200mL	50X TAE
9800mL	hpH_2O

2.4.5 DNA Extraction from Agarose Gels

2.4.5a Extraction from Lyophilised Agarose Gels[137]

This method was used initially to isolate the cDNA inserts for 5AR1 and 5AR2 for subsequent ligation with appropriately digested pCI-neo vector.

Low TE buffer, pH 7.4 (10mM TRIS-Cl [pH7.4], 1mM EDTA [pH8.0])

1.58g	TRIS-Cl
292mg	EDTA

* Adjust pH to 7.4 then make to 1L with hpH_2O
* Sterilise by autoclaving

Sodium acetate (3M, pH 5.2)

245.7g Sodium acetate

* Adjust pH to 5.2 then make to 1L with dH_2O
* Sterilise by autoclaving

TE buffer (10mM TRIS-Cl [pH7.5], 1mM EDTA)

1.58g TRIS-Cl
292mg EDTA

* Make to 1L with hpH_2O and sterilise by autoclaving

2.4.5b BRESAspin™ Gel Extraction Kit

This commercial kit became available during the course of these studies and was found simpler and more effective than the previous method. The individual constituents of the various buffers used were not provided in the manufacturers protocol.

2.4.6 Dephosphorylation of 5α- Reductase 1

10X CIAP buffer (500mM TRIS-Cl [pH9.0], 10mM Magnesium chloride, 1mM Zinc chloride, 10mM Spermidine)

7.88g TRIS-Cl
95.2mg Magnesium chloride
13.63mg Zinc chloride
145.2mg Spermidine

* Make to 100mL with hpH_2O and sterilise by autoclaving

2.4.7 Ligation Reaction

This was used as a general method to ligate excised inserts into the vector pCI-neo.

10X T4 DNA ligase buffer (300mM TRIS-Cl [pH7.8], 100mM Magnesium chloride, 100mM DTT, 5mM ATP)

4.73g	TRIS-Cl
952mg	Magnesium chloride
1.54g	DTT
250mg	ATP

* Make to 100mL with hpH_2O and sterilise by autoclaving

2.4.8 Electroporation

This was used both to transform plasmid DNA into bacteria and to transfect mammalian CHO cells.

2.4.8a Preparation of Electrocompetent E.coli

Glycerol (10%)

100mL	100% Glycerol

* Make to 1L with dH_2O and filter sterilise

Yeast extract nutrient broth

7.5g	Yeast extract
8g	Nutrient agar (1.5%)

* Make to 1L with dH_2O and sterilise by autoclaving

2.4.8b Electroporation of E.coli

SOC Broth (2% Bacto-Tryptone, 0.5% Bacto yeast extract, 10mM Sodium chloride, 2.5mM Potassium chloride, 10mM Magnesium chloride, 10mM Magnesium sulphate, 20mM Glucose)

20g	Bacto-Tryptone
5g	Bacto yeast extract
584.4mg	Sodium chloride
186.4mg	Potassium chloride
952mg	Magnesium chloride
1.2g	Magnesium sulphate
3.62g	Glucose

* Make to 1L with dH_2O and sterilise by autoclaving

2.4.8c Electroporation of CHO Cells

* Cell culture reagents used for the electroporation of CHO cells were as described section 2.3.

2.4.9 Hybridisation

2.4.9a 5' End Labelling of Primers

EDTA (0.5M, pH 8.0)

93.05g	EDTA

* Adjust pH to 8.0 and make to 500mL with hpH_20
* Sterilise by autoclaving

10X PNK buffer (500mM TRIS-Cl, 10mM Magnesium chloride, 1mM Zinc chloride, 10mM Spermidine)

7.88g	TRIS-Cl
95.2mg	Magnesium chloride
13.6mg	Zinc chloride
145.2mg	Spermidine

* Make to 100mL with hpH_2O and sterilise by autoclaving

2.4.9b Hybridisation with End Labelled Primers

SDS (10%)

100g	SDS

* Make to 1L with dH_20

20X Sodium chloride, tri sodium citrate (SSC) (150mM Sodium chloride, 15mM Sodium citrate)

8.77g	Sodium chloride
4.41g	Sodium citrate

* Adjust pH to 7.4 and make to 1L with dH_2O

2X SSC

100mL	20X SSC

* Make to 1L with dH_20

2X SSC 0.1% SDS

100mL	20X SSC
10mL	10% SDS

* Make to 1L with dH_20

1X SSC 0.1% SDS

50mL	20X SSC
10mL	10% SDS

* Make to 1L with dH_20

0.5X SSC 0.1% SDS

25mL	20X SSC
10mL	10% SDS

* Make to 1L with dH_20

0.1X SSC 0.1% SDS

5mL	20X SSC
10mL	10% SDS

* Make to 1L with dH_20

20X Sodium chloride, sodium dihydrogen orthophosphate, ethylenediamine disodium tetra-acetic acid (SSPE) (3.6M Sodium chloride, 0.2M Sodium dihydrogen orthophosphate, 25mM EDTA)

210.38g	Sodium chloride
31.2g	Sodium dihydrogen orthophosphate

7.44g EDTA

* Adjust pH to 7.4 and make to 1L with dH_20

Hybridisation Buffer

7g	SDS
1g	BSA
25mL	20X SSPE
1mL	EDTA (0.5M, pH 8.0)

* Dissolve BSA first, gradually add SDS whilst stirring over low heat
* Add hpH_20 to 100mL and filter sterilise the resulting solution

Southern blotting transfer buffer (0.4M Sodium hydroxide, 0.6M Sodium chloride)

16.04g	Sodium hydroxide
35.16g	Sodium chloride

* Make to 1L with dH_20

TRIS (1M, pH 8.0)

121.1g	TRIS

* Adjust pH to 8.0 and make to 1L with dH_20

2.4.9c Developing Autoradiographs

X-ray film was from Fuji. Developer and fixer were supplied by Kodak Australia and used according to the manufacturers protocol.

2.4.10 Site-Directed Mutagenesis

During the course of these studies primers were synthesized and purified by several different companies. These were Gibco BRL, Operon Technologies, Pacific Oligonuclelotides and Genset Pacific Oligonucleotides. The Quickchange™ site-directed mutagenesis kit is commercially available from Stratagene Cloning Systems.

dNTP Mix (10mM)

2.5mM	adenosine triphosphate
2.5mM	guanosine triphosphate
2.5mM	thymidine triphosphate
2.5mM	cytosine triphosphate

10X Reaction buffer (100mM Potassium chloride, 60mM Ammonium sulphate, 200mM TRIS-Cl [pH8.0], 20mM Magnesium chloride, 1% Triton-X, 100µg/mL BSA)

745.5mg	Potassium chloride
792.6mg	Ammonium sulphate
3.15g	TRIS-Cl
190.4mg	Magnesium chloride
1mL	Triton X-100
10mg	BSA

* Make to 100mL with hpH_2O and sterilise by autoclaving

2.4.11 Calcium Phosphate Transfection

Buffer A (0.5M Calcium chloride)

5.55g Calcium chloride

* Make to 100mL with 0.1M HEPES buffer (pH 7.0) and filter sterilise

Buffer B (0.28M Sodium chloride, 0.75mM Sodium dihydrogen orthophosphate, 0.75mM Disodium hydrogen orthophosphate)

1.64g Sodium chloride
9.0mg Sodium dihydrogen orthophosphate
10.65mg Disodium hydrogen orthophosphate

* Make to 100mL with 0.05M HEPES buffer (pH 7.0) and filter sterilise

HEPES buffer (0.05M, pH7.0)

1.19g HEPES

* Make to 100mL with hpH_2O and filter sterilise

HEPES buffer (0.1M, pH7.0)

2.38g HEPES

* Make to 100mL with hpH_2O and filter sterilise

HEPES buffer (25mM, pH 7.5) with sodium chloride(0.85%) and glycerol (15%)

25mM HEPES
8.5g Sodium chloride

150mL Glycerol

* Adjust pH to 7.5, make to 1L with hpH_20 and filter sterilise

2.4.12 Determination of β- Galactosidase Activity

2X Assay buffer (200mM Sodium dihydrogen orthophosphate [pH7.3], 2mM Magnesium chloride, 100mM β- Mercaptoethanol, 0.13% ONPG)

2.4g	Sodium phosphate buffer
19.04mg	Magnesium chloride
700µL	β- Mercaptoethanol
133mg	ONPG

* Make to 100mL with dH_2O

1X PBS buffer (Magnesium and Calcium free)

0.8g	Sodium chloride
0.02g	Potassium chloride
0.12g	Disodium hydrogen orthophosphate
0.02g	Potassium dihydrogen orthophosphate

* Adjust pH to 7.4 and make to 1L with hpH_20

Reporter lysis buffer

* Commercially prepared 5X stock solution that is diluted to a 1X solution, with hpH_20, prior to use

Sodium bicarbonate (1M)

106.2g Sodium bicarbonate

* Make to 1L with dH_20

2.4.13 Characterisation of Stably Transfected Cells - 5α-Reductase Activity Assays

2.4.13a Characterisation of Stably Transfected Cells - pH Studies

Cell sonication buffer (0.1M Sodium citrate, 0.1M TRIS, 0.1% NOG, 0.1% BSA)

2.94g	Sodium citrate
1.21g	TRIS
100mg	NOG
100mg	BSA

*Make to 100mL with dH_2O

* Split into 10mL aliquots and adjust pH to the desired value between pH4.0-12.0

* Add ~5nM ^{3H}T

Glucose-6-phosphate (100mg/mL)

100mg	Glucose-6-Phosphate

* Make to 1mL with dH_20

Glucose-6-phosphate dehydrogenase (690 units/mL)

3mg	Glucose-6-phosphate dehydrogenase (230 units activity per milligram)

* Resuspend in 1mL of hpH_2O

NADP+ (65mM)

50mg NADP+

* Make to 1mL with dH_20

NADP[H] (14mM)

10mg NADP[H]

* Make to 1mL with dH_20

Sodium phosphate buffer (50mM, pH 7.0) with 20% glycerol

7.098g Sodium dihydrogen orthophosphate

* Adjust pH to 7.0
* Add 200mL of glycerol, then make to 1L with dH_20

2.4.14 Protein Measurement by the Method of Folin and Lowry

Alkaline tartrate solution (190mM Sodium carbonate, 2mM Sodium tartrate)

20g Sodium carbonate
0.5g Sodium tartrate

* Dissolve in 1L of 0.1M Sodium hydroxide

BSA protein standard

1g BSA

* Make to 100mL in cell lysis buffer or sodium phosphate buffer (50mM, pH 7.0) with 20% glycerol, where appropriate

Cell lysis buffer (0.2M Sodium hydroxide, 1% SDS)

8g	Sodium hydroxide
10g	SDS

* Make to 1L with dH_20

Copper sulphate solution (6mM)

1g	Copper sulphate

* Make to 1L with dH_20

Folin and ciocalteau reagent

* The constituents of the commercially prepared phenol reagent of folin and ciocalteau were not provided
* Dilute 1:1 with dH_20 prior to use

Sodium hydroxide (0.1M)

4g	Sodium hydroxide

* Make to 1L with dH_2O

Working alkaline tartrate solution

9 parts	Alkaline tartrate solution
1 part	Copper sulphate solution

* Make immediately prior to use

Chapter 3.0

Establishment of Cell Lines Stably Expressing Human 5α- Reductase 1 or 5α- Reductase 2

3.1 INTRODUCTION

Inability to isolate 5α- Reductase (5AR) has meant that the many biochemical studies of the enzyme have not been made on the pure enzyme. These biochemical studies have generated a large amount of data, much of it contradictory. These early studies have been comprehensively reviewed relatively recently[78]. In essence, the biochemical studies have indicated that 5AR is both resistant and sensitive to the competitive inhibitor Finasteride, has a Km for testosterone (T) in the micromolar and submicromolar range and an acidic and alkaline pH optimum. Although these contradictory findings suggested the existence of more than one enzyme, the inability to isolate 5AR precluded definite confirmation of this.

With the advent of expression cloning techniques much of the early confusion generated by the reported biochemical differences was overcome. In 1989, the cDNA encoding a rat 5AR was isolated using an expression cloning technique in *Xenopus laevis* oocytes[31]. A cDNA encoding human 5AR was isolated from a human prostate cDNA library soon after[1]. This enzyme exhibited a Km for T in the micromolar range, an alkaline pH optimum and was relatively resistant to Finasteride. Most significantly, a second cDNA encoding human 5AR was isolated in 1991[32]. This enzyme exhibited a Km for T in the submicromolar range, an acidic pH optimum and was very sensitive to inhibition by Finasteride. The isoenzymes encoded by these cDNAs were termed 5AR1 and 5AR2 after the chronological order of their discovery and their identification resolved the differences reported in the earlier biochemical studies. Biochemical characterisation of the enzymes coded for by these cDNAs showed 5AR1 exhibited an alkaline pH optimum, had a Km for T of ~3μM and was relatively resistant to Finasteride, whereas 5AR2 was markedly sensitive to Finasteride, had a Km for T of ~0.1μM and an acidic pH optimum. These findings clearly showed that the conflicting results of earlier biochemical studies were due to two separate isoenzymes with distinct characteristics.

Knowledge of the amino acid sequences of the two forms of 5AR plus the well-documented differences in their biochemical properties has permitted studies designed to identify residues involved in substrate and cofactor binding.

Identification of these residues enables structure-function analyses of the enzyme and will assist both in understanding of the role of 5AR in androgen action and in the design of inhibitors of the enzyme.

Site-directed mutagenesis has been used in this project to gain further insight into the structure/function relationships of human 5α- reductase isoenzymes. For this cDNAs were mutated, stably transfected into Chinese hamster ovary (CHO) cells and the characteristics of the expressed enzymes determined. It is apparent that to identify the effects of changes made by site-directed mutagenesis, determination of the characteristics of the wild type enzymes under the same conditions as those used for the mutant enzymes is required. To enable this, cell lines stably expressing the wild type human 5AR isoenzymes were established, their characteristics determined and compared with those in the literature.

3.2 METHODS

3.2.1 PLASMID DNA EXTRACTION

3.2.1.1 BRESAspin™ Plasmid Mini Kit (Bresatec)

A 2mL overnight culture of *E.coli* expressing the plasmid of interest was grown at 37°C in Luria Bertani broth containing 100μg/mL ampicillin. Bacteria were pelleted by centrifugation at 13000rpm for 30 seconds, the supernatant removed and the bacteria recentrifuged for a further 10 seconds at 13000rpm. Residual supernatant was then removed and the bacterial pellet resuspended, by vortexing, in 50μL of re-suspension buffer. Lysis buffer (100μL) then was added and the tubes mixed by repeated inversion before the addition of 325μL of neutralization buffer and the tubes again mixed by inversion. The precipitate was then pelleted by centrifugation at 13000rpm for 5 minutes.

The resultant supernatant was transferred to a spin-column plasmid isolation unit and centrifuged for 30 seconds at 13000rpm. The flow-through was

discarded before adding 300μL of wash buffer and recentrifuging for 30 seconds. The spin-column was then transferred to a fresh collection tube and the plasmid DNA eluted by adding 50μL of high pure water and centrifuging at 13000rpm for 30 seconds. The plasmid DNA was stored at -20°C until required.

3.2.1.2 Alkaline Lysis Method[136]

An overnight culture (1.5mL) of plasmid-containing *E.coli* grown in the presence of ampicillin (100μg/mL) was pelleted by centrifugation at 13000rpm for one minute. The supernatant was removed and the bacteria completely resuspended by vortexing vigorously in 100μL of ice cold solution#1. 200μL of freshly prepared solution#2 was added and rapidly mixed by inverting the tube 5 times. Ice cold solution#3 (150μL) was then added before vortexing the tubes gently in an inverted position for 10 seconds prior to incubation on ice for 3-5 minutes and centrifugation at 13000rpm for 5 minutes.

The supernatant was transferred to a fresh tube, an equal volume of phenol:chloroform added and the tube then vortexed before centrifuging at 13000rpm for 2 minutes. The supernatant was again transferred to a fresh tube, an equal volume of chloroform added and after vortexing was centrifuged for 2 minutes. Ice cold 100% ethanol (2 volumes) was added to the supernatant, mixed and the DNA precipitated by incubation on ice for 30 minutes. The DNA was recovered by centrifugation at 13000rpm for 15 minutes at 4°C, the supernatant removed and the tube half-filled with 70% ethanol before recentrifuging for 2 minutes. The supernatant was removed and any excess ethanol allowed to evaporate before the DNA was re-dissolved in 50μL of sterile high pure water. RNAse (~1ng/50μL) was added prior to storage at -20 °C.

3.2.2 DNA PURIFICATION METHODS

3.2.2.1 Wizard™ DNA Clean-Up System

Plasmid DNA was resuspend in high pure water to a final volume of 50μL before adding 1mL of Wizard DNA clean-up resin and mixing by inversion. A minicolumn was attached to the end of a 2.5mL syringe barrel and the resin/DNA mixture forced through the column. The minicolumn was then washed with 2mL of 80% isopropanol before drying by centrifugation at 13000rpm for 20 seconds. Elution of DNA from the minicolumn was with 50μL of sterile hi-pure water pre-heated to 70°C and incubation for one minute at room temperature before centrifuging for 20 seconds at 13000rpm. Purified DNA was stored at -20°C.

3.2.3 RESTRICTION ENZYME DIGESTS

3.2.3.1 Not I Restriction Digest of pBluescript and pCI-neo Vectors Containing cDNA Insert for 5α- Reductase 1

To a solution containing 1μg of the DNA to be digested, *Not I* restriction enzyme (1μL) was added along with a sufficient volume of sterile high pure water and 10X buffer D to give a final concentration of 1X buffer D. For example if the final reaction volume was 20μL, then 2μL of 10X buffer D was added along with the required volume of sterile high pure water to give a total volume of 20μL and a final concentration of 1X buffer D. A typical reaction mix is shown below.

5μL	1μg sample DNA
1μL	*Not I* restriction enzyme
2μL	10X buffer D *
12μL	sterile high pure water
20μL	

* This gives 2μL of 10X buffer D in a total reaction volume of 20μL and a final concentration of buffer D of 1X.

Tubes were incubated at 37°C for 2 hours and the reaction then immediately stopped by placing all tubes on ice.

3.2.3.2 Sal I/ Not I Restriction Digest of pBluescript and pCI-neo Vectors Containing cDNA Insert for 5α- Reductase 2

Digestion of 5AR2 was essentially as for 5AR1, except two enzymes were required and the reaction components and volumes differed slightly.

To a solution containing 1μg of the DNA to be digested, 1μL of *Not I* and 1μL of *Sal I* restriction enzymes were added. A volume of sterile high pure water and 10X buffer D was also added to give a final concentration of 1X buffer D. Tubes were then incubated at 37°C for 2 hours and the reaction immediately stopped by placing all tubes on ice.

3.2.4 AGAROSE GEL ELECTROPHORESIS

3.2.4.1 Preparation of a 1.0% Agarose Gel

1 gram of agarose (nucleic acid grade) was added to 100mL of 1X TAE buffer and dissolved either by steaming or in a microwave oven. The melted agarose was then poured into an appropriate gel cast and the well comb inserted prior to the agarose setting.

3.2.4.2 Agarose Gel Electrophoresis

DNA samples to be electrophoresed were added to an appropriate volume of loading buffer (5μL of loading buffer for ~1μg of sample) and loaded into a freshly prepared agarose gel. Samples were electrophoresed in 1X TAE buffer, containing ethidium bromide, at 40 volts for 2.5-3 hours or at 60 volts for 1 hour.

The resulting DNA bands were visualized using a UV transilluminator and their molecular size calculated from λ Hind III standard markers.

3.2.5 DNA EXTRACTION FROM AGAROSE GELS

3.2.5.1 Extraction from Lyophilised Agarose Gels[137]

DNA samples were electrophoresed at 40 volts for 2 hours in a 1% gel in 1X TAE buffer. The DNA bands of interest were then excised from the gel with a scalpel blade and placed into a sterile microfuge tube before overnight lyophilization. The DNA was eluted from the lyophilised gel by adding a mixture of equal volumes of TE buffer and ethanol (typically 300μL) and incubating at room temperature for 1 hour with constant mixing. The DNA was then forced out of the agarose slice by compression with a small metal spatula and the agarose discarded before centrifugation for 5 minutes at 13000rpm.

The supernatant was transferred to a fresh microfuge tube and ethanol (2 volumes) and 3M sodium acetate (1/20 volumes) added before pelleting the DNA by centrifugation at 13000rpm for 15 minutes. The supernatant was carefully removed and excess ethanol allowed to evaporate before resuspending the DNA in 20μL of low TE buffer. Recovered DNA was quantitated from absorbance measurements at 260nM and ~1μg DNA electrophoresed in a 1% agarose gel in 1X TAE buffer for 60 minutes at 60 volts, stained with ethidium bromide and visualized.

3.2.5.2 BRESAspin™ Gel Extraction Kit

DNA samples were electrophoresed at 40 volts for 2 hours on a 1% gel in 1X TAE buffer. The DNA bands of interest were then excised from the gel with a scalpel blade and placed into a sterile microfuge tube. The gel slice volume was ascertained by weighing the sample and assuming 100mg equates to 100μL, 3 gel slice volumes of gel solubilisation buffer were added. The sample was incubated at 50°C until the agarose had completely dissolved (5-10 minutes), then applied to a BRESAspin filter unit and centrifuged at 13000rpm

for 30 seconds. The liquid was discarded from the collection tube and the unit recentrifuged for sixty seconds. The BRESAspin filter unit was then transferred to a fresh tube, 50μL of hpH_2O added and centrifuged at 13000rpm for 30 seconds. DNA samples were store at -20^{O}C until required.

To ensure DNA excised from pBluescript vector was of the correct size (2100bp for 5AR1 and 2400bp for 5AR2), comparisons were made with simultaneously run λ DNA markers. These cDNA inserts were then sub-cloned into the vector pCI-neo for enzyme expression in mammalian cells.

3.2.6 DEPHOSPHORYLATION

3.2.6.1 Dephosphorylation of Not I Digested pCI-neo

The 5AR1 cDNA received from Dr Russell, was cloned into the *Not I* site of the pBluescript vector. Consequently the pCI-neo vector also had to be digested with *Not I* before ligation of the 5AR1 insert. This however gives complementary ends of the vector, which can lead to vector self-religation, preventing ligation of the insert into the vector. To prevent self-religation, the vector was dephosphorylated with the enzyme calf intestinal alkaline phosphatase (CIAP). This removes 5'-phosphate groups and prevents vector self-religation as without these 5'-phosphate groups, the vector cannot interact with the 3'-hydroxyl group to form a phosphodiester bond. Addition of the 5AR1 cDNA, which has a 5'-phosphate group, facilitates phosphodiester bond formation between vector and insert in the presence of DNA ligase.

For dephosphorylation, 2μg of *Not I* digested pCI-neo was suspended in sterile hpH_2O to give a final volume of 50μL and then purified and concentrated as previously described (Section 3.2.2.1). To 50μL of the purified pCI-neo DNA then was added 6 μL of 10X CIAP buffer, 0.2 units (2 μL) of CIAP enzyme and 2μL of sterile high pure water giving a final concentration of 1X CIAP buffer in a total volume of 60μL.

The reaction mixture was incubated at 37°C for 30 minutes before adding a further 2μL of CIAP enzyme and re-incubating at 37°C for a further 30 minutes. The reaction was stopped by placing the tubes immediately on ice and any residual CIAP activity removed using a Wizard Clean-Up column (Section 3.2.2.1).

The dephosphorylated pCI-neo was then used to create the construct required to express 5AR1 in mammalian cells (section 3.2.7.1).

3.2.7 LIGATION

3.2.7.1 Ligation of 5AR1 with pCI-neo

Between 50-100ng of 5AR1 insert, excised from pBluescript and isolated as previously described (section 3.2.5.1), was mixed with dephosphorylated *Not I* digested pCI-neo vector at a ratio of 2:1 before adding T4 DNA Ligase, 10X ligase buffer and if required sufficient high pure water to give a final concentration of 1X ligase buffer. The ligation reaction was incubated at 15°C for 4 hours or at 4°C overnight.
A typical reaction mixture is shown below.

5AR1 insert	5μL (~1μg DNA)
pCI-neo vector	20μL (~400ng DNA)
Ligase 10X buffer	3μL
T_4 DNA Ligase	2μL
Final volume	30μL

Control reactions including 40-100ng of undigested vector (pCI-neo) only or vector (pCI-neo) digested with *Not I* were performed in parallel.

3.2.7.2 *Ligation of 5AR2 with pCI-neo*

The vector pCI-neo was digested with both *Sal I and Not I* prior to its ligation with the 5AR2 insert. This dual digestion generates a vector with non-compatible "sticky ends" which prevents vector self-religation. However an 11bp fragment is excised during digestion of pCI-neo vector with *Sal I and Not I*. This fragment requires removal before ligation of digested vector with the 5AR2 insert to prevent its religation into *Sal I/ Not I* digested pCI-neo, which would prevent ligation of vector with the 5AR2 insert. Removal of the 11bp fragment was with the Wizard Clean-Up system (Section 3.2.2.1).

For a typical ligation, 150-300ng of 5AR2 insert, was extracted from lyophilised agarose gel (Section 3.2.5.1), and added to digested vector at a ratio of 2 parts DNA:1 part vector. T4 DNA ligase, 10X ligase buffer and sufficient high pure water to give a final concentration of 1X ligase buffer also were added. The ligation reaction was then incubated at 15^{O}C for 4 hours or at 4^{O}C overnight.

A typical reaction mixture is shown below.

5AR2 insert	5μL (approx. 150ng of DNA)
pCI-neo vector	4μL (approx. 80ng of DNA)
Ligase 10X buffer	2μL
T_4 DNA Ligase	1μL
Sterile hpH_2O	8μL
Final volume	20μL

Control reactions including 40-100ng of undigested vector (pCI-neo) only or vector (pCI-neo) digested with *Sal I* and *Not I* were performed in parallel.

3.2.8 BACTERIAL ELECTROPORATIONS

To generate sufficient constructs for subsequent experiments the ligation reaction mixtures were transformed into *E.coli* strain DH5α by electroporation.

3.2.8.1 *Preparation of Electrocompetent E.coli Strain DH5α*

1L of yeast extract nutrient broth (YENB) was inoculated with a 10mL overnight broth culture of *E.coli* strain DH5α and incubated with constant mixing at 37 ^{o}C. The absorbance was monitored at 600nM and bacteria harvested when an absorbance between 0.5-0.9 was obtained. For harvesting, the broth culture of bacteria was chilled on ice for 5 minutes before centrifuging at 3500rpm for 10 minutes at 4^{o}C. The supernatant was discarded and the bacterial pellet washed twice with 10mL of ice-cold sterile high pure water before resuspending in 2-3mL of sterile ice cold 10% glycerol in hpH_2O and storage in 40μL aliquots at -70^{o}C.

3.2.8.2 Protocol for Electroporation of E.coli (DH5α)

This protocol was used when electroporating pBluescript, pCI-neo, pADVantage or β-Galactosidase vectors into *E.coli* strain DH5α. It was also used when electroporating pBluescript and pCI-neo vectors containing either 5AR1 or 5AR2 inserts into bacteria.

Aliquots of *E. coli* were washed twice with 50μL of sterile ice cold 10% glycerol in high pure water before resuspending in a final volume of 40μL of 10% glycerol. DNA (~1μg) was added and the whole mixture stood on ice for at least 5 minutes before transferring to a sterile ice cold electroporation cuvette with a 0.1cm gap. The bacteria/DNA mixture was electroporated at 1.8kV, 200 Ohms and 25μFarads (F), 1mL of SOC broth was immediately added before incubation at 37^{o}C for at least one hour with shaking. The entire reaction mixture was plated onto LB plates containing ampicillin (100μg/mL). For this four plates were set up on one of which was plated 200μL of undiluted SOC

broth and on the others 50μL of either a $^{1}/_{10}$, $^{1}/_{100}$ or $^{1}/_{1000}$ dilution of the SOC broth. A control electroporation of *E. coli* strain DH5α only also was included.

3.2.9 5' END LABELLING OF HYBRIDISATION PROBES

Although selection with ampicillin enables isolation of those bacteria containing the pCI-neo vector it does not identify which bacteria have taken up pCI-neo vector containing 5AR insert. To identify these bacteria, hybridisation studies with suitable probes were used. These probes were based on those used by others[53], these probes were synthesized by Life Technologies and their sequences are given below. Before use the probes were labelled with $^{32P}\gamma$ATP (section 3.2.9.1).

5AR1 Hybridisation Probes;

5AR11 probe

5'- CAT CAG AAA CGG GTA AAT TAA GC -3'

5AR12 probe

5'- GCT CGC CTA CCT GCA GTG -3'

5AR2 Hybridisation Probes;

5AR21 Probe

5'- GCC ACC GGC GAG GAA CAC -3'

5AR22 Probe

5'- GTG CAG AAG GCA GTG CCT CTG-3'

3.2.9.1 End Labelling Protocol

This protocol was used to 5' end label the probes for both 5AR1 and 5AR2. 2μL of probe was incubated at 37°C for 10 minutes with 5μL of ^{32}P gamma labelled ATP (50μCi), 1μL of T4 polynucleotide kinase (PNK) enzyme, 2μL of

10X PNK buffer and 10μL of sterile hpH_2O to give a final volume of 20μL. The reaction was terminated by the addition of 2μL of 0.5M EDTA (pH 8.0).

3.2.10 HYBRIDISATION

3.2.10.1 *Colony and DNA Transfer to Membranes*

Colonies resulting from electroporation of pCI-neo containing either 5AR1 or 5AR2 inserts (Section 3.2.8.2), were picked onto grided LB plates containing ampicillin (100μg/mL) and grown overnight at 37°C. Positive controls were colonies containing pBluescript vector with the appropriate insert [5AR1 or 5AR2] and the negative control was pCI-neo vector with no insert. Following incubation, colonies were transferred to a Hybond N+ nylon membrane by placing the membrane directly onto the colonies and leaving for 2 minutes before lifting. The membranes were then dried at 60°C for 30 minutes.

After drying, membranes were placed colony side up, onto filter paper soaked with 10% SDS for 10 minutes at room temperature before transferring to filter paper soaked with transfer buffer and incubating for a further 30 minutes at room temperature. The membranes were then washed twice for 10 minutes at room temperature using filter paper soaked with TRIS buffer (1M, pH 8.0) before being blotted with filter paper (3MM) to remove any colony debris and dried at 60°C for one hour.

3.2.10.2 Pre-Hybridisation, Hybridisation and Membrane Washing

Membranes were prehybridised in hybridisation buffer at 50°C with shaking for one hour before the addition of labelled probe (section 3.2.9.1) and re-incubation overnight, again with shaking at 50°C.

Following hybridisation membranes were washed as follows:

* 2XSSC (0.1% SDS) at 50°C for 10 minutes
* 2XSSC (0.1% SDS) at 50°C for 10 minutes

* 1XSSC (0.1% SDS) at 50°C for 10 minutes
* 0.5XSSC (0.1% SDS) at room temperature for 10 minutes
* 0.1XSSC (0.1% SDS) at room temperature for 10 minutes
* 2XSSC at room temperature for 10 minutes

Membranes were then placed onto Fuji X-ray film (Fuji, Japan) in a light tight cassette and incubated overnight at -70°C. Autoradiographs were developed by placing films in developer, water and fixer for 2 minutes each, before rinsing and drying. Positive clones were identified by areas of blackening on the film.

3.2.11 CHINESE HAMSTER OVARY CELL ELECTROPORATIONS

3.2.11.1 Cell Preparation

Electroporation was also used to transfect Chinese hamster ovary (CHO) cells with the 5AR constructs. Electroporations typically were performed using ~10^6 cells and ~5μg of DNA. Flask cultures of CHO cells were trypsinised and harvested with 9mL of Ham's F12 culture media containing 10% FCS and centrifuged in a sterile tube at ~1000rpm for 3 minutes. The cell pellet was then washed in 9mL of sterile PBS, re-centrifuged and resuspended in sterile PBS to a final volume of 1mL.

3.2.11.2 Cell Electroporation

This protocol was used for all cell electroporations. The DNA for transient transfection was mixed with pADVantage co-transfection vector, which enhances transient expression of DNA in mammalian cells by increasing translation initiation. DNA and co-transfection vector were mixed in a 1:1 ratio (typically 5μg:5μg), added to 200μL of CHO cell suspension and incubated on ice for 10 minutes. The mixture then was transferred into an ice cold electroporation cuvette (0.4cm electrode gap) and electroporated at 300 volts, 100 ohms and 1μF to soften the cell membrane. Electroporation at 300 volts, 100 ohms and 250μF was then performed immediately and the cuvette stood on

ice for 5-10 minutes. Electroporated cells were transferred into individual wells of a 6 well tray, each containing 2mL of complete Ham's F12 media. Cells were incubated at 37°C, 5% CO_2 for approximately 48 hours before testing for 5AR expression.

3.2.12 CALCIUM PHOSPHATE TRANSFECTION

3.2.12.1 Calcium Phosphate Transfection of CHO Cells

Approximately $3x10^5$ CHO cells were grown to 60% confluence in a 5cm tissue culture dish in Ham's F12 complete medium. Just prior to transfection, medium was replaced with fresh medium and cells allowed to settle for approximately 2 hours. For DNA preparation 120μL of buffer A (0.5M calcium chloride) was mixed with 120μL of sterile hipure water containing 5μg of plasmid DNA, vortexed for 5 seconds and incubated at room temperature for 10 minutes. 240μL of buffer B (0.28M sodium chloride, 0.75mM sodium dihydrogen orthophosphate, 0.75mM disodium hydrogen orthophosphate) were then added drop wise to the mixture using a 2.5mL syringe fitted with a 26 gauge needle, with vortexing following the addition of every 2-3 drops. Calcium phosphate precipitates of DNA were incubated at room temperature for 15 minutes before adding drop wise with a pasteur pipette to a 6cm culture dish containing CHO cells. During this addition mixing was made after every 2-3 drops of precipitate, to ensure even distribution. The cultures were incubated overnight at 37°C and 5% CO_2, then washed twice with 5mL of Ham's F12 medium without foetal calf serum (FCS) and shocked by incubation with 3mL of 25mM HEPES buffer (pH7.5, 0.85% sodium chloride and 15% glycerol) at room temperature for 3 minutes. Cells were again washed twice with 5mL of Ham's F12 medium (without FCS), before the addition of 4mL of Ham's F12 medium (with 10% FCS) and incubation at 37°C and 5% CO_2 for approximately 60 hours before medium replacement. Selection of cells containing insert was made by incubation with medium containing 600μg/mL geneticin 418 (G418). Assessment of cells for β- Galactosidase activity was made after 5 days incubation (section 3.2.13) and after 16 days for 5AR activity (section 3.2.14.1).

3.2.12.2 *Cell Harvesting*

Petri dishes of cells stably transfected with β- Galactosidase were directly assayed for enzyme activity following 5 days incubation. Individual clones of cells transfected with either 5AR1 or 5AR2 construct were harvested with a sterile pasteur pipette after 16 days incubation. Harvested cells were placed into wells of a 24 well micro titre tissue culture tray and incubated for 2-4 days in medium containing G418 (600μg/mL). Cells were then screened for 5AR activity as described below (section 3.2.14.1) and those cells expressing 5AR activity were harvested and expanded in tissue culture flasks.

3.2.13 DETERMINATION OF β- GALACTOSIDASE ACTIVITY

To determine if CHO cells were capable of both transient and stable transfection with and expression of foreign DNA, the Promega PSV-β-Galactosidase vector and β- Galactosidase enzyme assay system were used. β- Galactosidase activity of transfected CHO cells was determined 48 hours post-electroporation or 5 days after calcium phosphate transfection with the β-Galactosidase vector. For this, stably or transiently transfected cells were rinsed twice with 1mL of 1X PBS buffer before incubation with an appropriate volume of Promega's reporter lysis buffer (400μL for a 60mm dish, 900μL for a100mm dish) for 15 minutes, agitating the cells after approximately 8 minutes incubation. Cells were dislodged from the well with a "hockey stick" prepared from a glass pasteur pipette and transferred to a sterile microfuge tube before centrifuging at 13000rpm for 2 minutes.

To 150μL of supernatant an equal volume of 2X Assay buffer was added then incubated at 37°C until a yellow colour change was evident (typically the time required ranged from 30 minutes to 3 hours). The reaction was stopped by the addition of 500μL of sodium carbonate (1M) and the absorbance at 420nM measured against a blank of hpH_2O.

3.2.14 5α- REDUCTASE ACTIVITY ASSAYS

3.2.14.1 Cell Screening

Following stable transfection, cells were grown in medium containing 600μg/mL G418 for a period of 14 days following which G418 resistant clones were selected and expanded in 24 well tissue culture trays. The various clones of cells selected for with G418 medium, were screened for 5AR activity to identify their relative expression of 5AR. For this culture medium was replaced with 0.5-1mL of medium containing ~5nM labelled (^{3}H) testosterone (T) and the cells incubated for one hour at 37^{O}C/5%CO_2. The labelled medium was then removed and 20μL of hpH_2O containing 1000-2000dpm of radiolabelled (^{14}C) dihydrotestosterone added before extracting with 1mL of diethyl ether. This mixture was vortexed and incubated at -70^{O}C for 20-30 minutes or until the aqueous layer was frozen. The ether layer was removed, dried down either *in vacuo* or under nitrogen and steroids taken up by vortexing in 70μL of acetone. The acetone was spotted onto a thin layer chromatography plate as a tight spot with unlabelled testosterone and dihydrotestosterone (100mg/dL) standard spotted in separate tracks before developing in dichloromethane:diethyl ether (4:1). After development the tracks containing standards, which were at each end of the TLC plate, were cut from the plate and the steroids visualized by spraying with 40% sulphuric acid and heating at 90^{O}C until visible. These tracks were then realigned on the TLC plate and used to identify the regions of DHT and T in the sample tracks. The relevant regions of the sample tracks were then scraped into scintillation vials, Optifluor organic scintillant added and the vials counted in a liquid scintillation counter set to count both ^{3}H and ^{14}C.

Appropriate volumes of the radiolabelled ^{3H}-T media and 20μL of the ^{14C}-DHT media are also counted. Counting the volume of ^{3H}T media added to each well of cells (typically 0.5-1.0mL), enables determination of the amount of radiolabelled substrate (T), in cpm, added to each well. This method of measuring 5AR activity is extremely troublesome and has many associated procedural losses, for which it is necessary to account. For this a known amount of ^{14C}-DHT (~1500cpm/20μL) was added to the media recovered from each well of cells. Comparison of ^{14C}-DHT recovered in the samples with a 20μL

sample of ^{14C}-DHT permits the percentage recovery of ^{14C}-DHT to be determined for each sample. It is assumed as there has been procedural loss of ^{14C}-DHT that similar loss of ^{3H}-T will also have occurred. To determine the actual ^{3H}-T counts of the sample therefore the ^{3H}-T counts obtained are corrected for this loss.

3.2.14.2 Characterisation of Stably Transfected Cells - Determination of Km and Vmax for Testosterone

Assessment of Km and Vmax for wild type 5AR1 and 5AR2 and the various mutants was made using 0.5-1.0mL of medium containing ~5nM ^{3H}T and unlabelled substrate (T) at 0.025, 0.05, 0.0625, 0.1, 0.125, 0.25, 0.5, 1, 1.25, 1.67, 2.5, 5, 10 and 20μM. Either stably or transiently transfected CHO cells growing in 24 well micro titre tissue culture trays were incubated for 1 hour at 37^{O}C/5%CO_2 with 0.5-1.0mL of medium. 5AR activity at each substrate concentration was determined by thin layer chromatography (Section 3.2.14.1) and duplicate wells were used for each substrate concentration. Cell lysis buffer (100μL) then was added and the total protein concentration for individual wells determined by the method of Folin and Lowry (Section 3.2.15). This enables determination of 5AR activity as nanomoles of DHT per minute per milligram of cell protein and compensates for any differences in cell numbers between individual wells. The Enzyme Kinetics V1.5 program (Trinity software) was used to construct Lineweaver-Burke plots from which Km and Vmax values were determined.

3.2.14.3 Characterisation of Stably Transfected Cells - Inhibitor Studies

The Ki for Finasteride for the wild type enzymes and for all mutants was measured with cells incubated as described in the previous section (3.2.14.2) at T concentrations of 0.05, 0.1, 0.5, 1, 5 and 20μM. Finasteride concentrations were 0, 300 and 600nM for 5AR1 and 0, 20 and 40nM for 5AR2.
Ki values were determined with the Enzyme Kinetics V1.5 program (Trinity software), from the slopes of Lineweaver-Burke plots constructed at each concentration of Finasteride.

3.2.14.4 Characterisation of Stably Transfected Cells - IC_{50} Studies

The IC_{50} is defined as the concentration of inhibitor required to inhibit enzyme activity by 50%, at a fixed concentration of substrate. The IC_{50} value for all enzymes was determined by incubating cells expressing the enzyme with media containing ~5nM ^{3H}T, a fixed concentration of unlabelled T (1μM) and Finasteride at 0, 1, 2.5, 5, 10, 20, 50, 100, 300, 600nM. Cells were incubated for one hour before determination of 5AR activity (Section 3.2.14.1) and cell protein (Section 3.2.15). Duplicate wells of cells were assayed at each inhibitor concentration. 5AR activity, expressed as nanomoles of DHT formed per minute per milligram of cell protein, was plotted versus inhibitor concentration and IC_{50} values determined from these plots.

3.2.14.5 pH Optima of Stably Transfected Cells

Unlike measurements of Km, Ki and IC_{50} values, pH optima were determined using protein preparations from sonicated cells rather than on live cells.

3.2.14.5.a Cell Sonicate Preparation

Sonicates were prepared from cells grown to confluence in five tissue culture dishes (5cm diameter). Cells were removed by adding ice cold PBS (2mL) to each petri dish and mechanically scraping cells from the bottom of the petri dish with a plastic cell scraper. After pelleting by centrifugation at 3000rpm for 5 minutes at 4°C, supernatant was removed and cells resuspended in 1mL of 50mM sodium phosphate buffer (pH 7.0) containing 20% glycerol and 12mM NADP[H]. The cell suspension was then placed on ice and sonicated at 8-10 microns for 8 x 10 seconds with a one minute interval between each period. Cells were left on ice until required.

3.2.14.5b 5α- Reductase Assay

Unlike measurements of 5AR in living cells, measurement of 5AR in cell sonicates required the addition of NADP[H]. For these assays 50μL of a

10mg/mL NADP[H] solution was added to 410μL of assay buffer at various pH values (pH 4, 5, 5.5, 6, 6.5, 7, 7.5, 8, 9, 10, 11 or 12) containing ~5nM ^{3H}-T and a fixed concentration of unlabelled T (typically 1μM). This was then pre-incubated at 37°C for 5-10 minutes before the addition of 40μL of sonicate (section 3.2.14.5a) and incubation at 37°C for 30 minutes. Tubes were then placed immediately on ice and steroids extracted and chromatographed as described in Section 3.2.14.1. On some occasions an NADP[H] regenerating system consisting of 5μM glucose-6-phosphate, 3μM NADP+ and 0.7 units of glucose-6-phosphate dehydrogenase was used.

Cell protein concentrations were determined by the method of Folin and Lowry (Section 3.2.15) except that the bovine serum albumin standards were prepared in cell sonication buffer. Plots of pH vs 5AR activity, expressed as nanomoles of DHT formed per minute per milligram of cell protein, were constructed and the pH optima determined as the pH of the buffer in which maximum 5AR activity was observed.

3.2.15 FOLIN AND LOWRY PROTEIN ASSAY

3.2.15.1 Protein Measurement by the Method of Folin and Lowry[151]

For this, freshly prepared alkaline tartrate working solution (5mL) was added to 100μL of standard (BSA) or sample, mixed and incubated at room temperature for 10 minutes. Folin and Ciocalteau reagent (500μL) was then added before vortex mixing and incubating at room temperature for a further 30 minutes. Absorbances were measured at 750nM against blanks prepared from 100μL of lysis or sonication buffer treated as above. Protein concentrations of samples were determined from a standard curve prepared using a stock solution of BSA (10g/L) diluted in the appropriate buffer to give standards ranging from 25-500μg/L.

On occasion a modified method utilizing smaller volumes of both sample and reagents also was used. For this sample volumes were reduced to 20μL, alkaline tartrate to 1mL and Folin and Ciocalteau reagent to 100μL.

3.2.16 CELL CULTURE METHODS

3.2.16.1 Cell Trypsinisation

Cells were washed with 2-3mL of PBS (pH 7.4, 0.05mM EDTA), before covering the cell surface with 2-3mL of trypsin (0.5% in PBS [pH7.4], 0.05mM EDTA). The trypsin solution was removed after ~30 seconds and the cells incubated at $37^{O}C/5\%CO_2$ until the cells were detached. Cells were resuspended in Ham's F12 tissue culture medium containing 10% FCS, penicillin/streptomycin (10,000 units of each) and glutamine (2mM), before transferring to other culture flasks or trays.

3.2.16.2 Cell Storage in Liquid Nitrogen

Trypsinised cells were pelleted in a sterile centrifuge tube at ~1000rpm for 5 minutes before removal of the supernatant and resuspension in 1mL of DMSO:FCS (1:9) at a concentration of $\sim 10^6$ cells/mL. The cell suspension was then dispensed into cryogenic vials, which were placed at $-80^{O}C$ overnight before transfer to liquid nitrogen storage cylinders.

3.2.16.3 Recovery of Cells from Liquid Nitrogen

Frozen cells were rapidly thawed and transferred to a sterile centrifuge tube containing 9mL of prewarmed culture media containing 10% FCS, penicillin/streptomycin (10,000 units of each) and glutamine (2mM), then centrifuged at ~1000rpm for 5 minutes. The supernatant was removed and the cell pellet resuspended in 9mL of culture media containing 10% FCS before recentrifuging. The cell pellet then was resuspended in 5mL of Ham's F12 tissue culture media containing 10% FCS, penicillin/streptomycin (10, 000 units of each) and glutamine (2mM) and the cells transferred to the required tissue culture flask/tray.

3.3 RESULTS

3.3.1 Recovery of cDNAs for 5AR1 or 5AR2

Amplification of the pBluescript vector plus 5AR1 or 5AR2 cDNA inserts by electroporation into *E.coli* (strain DH5α) was successful as determined by blue-white selection on LB agar plates containing ampicillin, X-gal and IPTG. To confirm the presence of the vector plus insert, plasmid DNA isolated from selected bacteria was digested with either *Not I* or *Sal I* and *Not I* for 5AR1 and 5AR2 inserts respectively. The electrophoretic patterns obtained for digested DNA confirmed the presence of vector plus inserts in these bacteria (Figures3.3.1a and 3.3.1b).

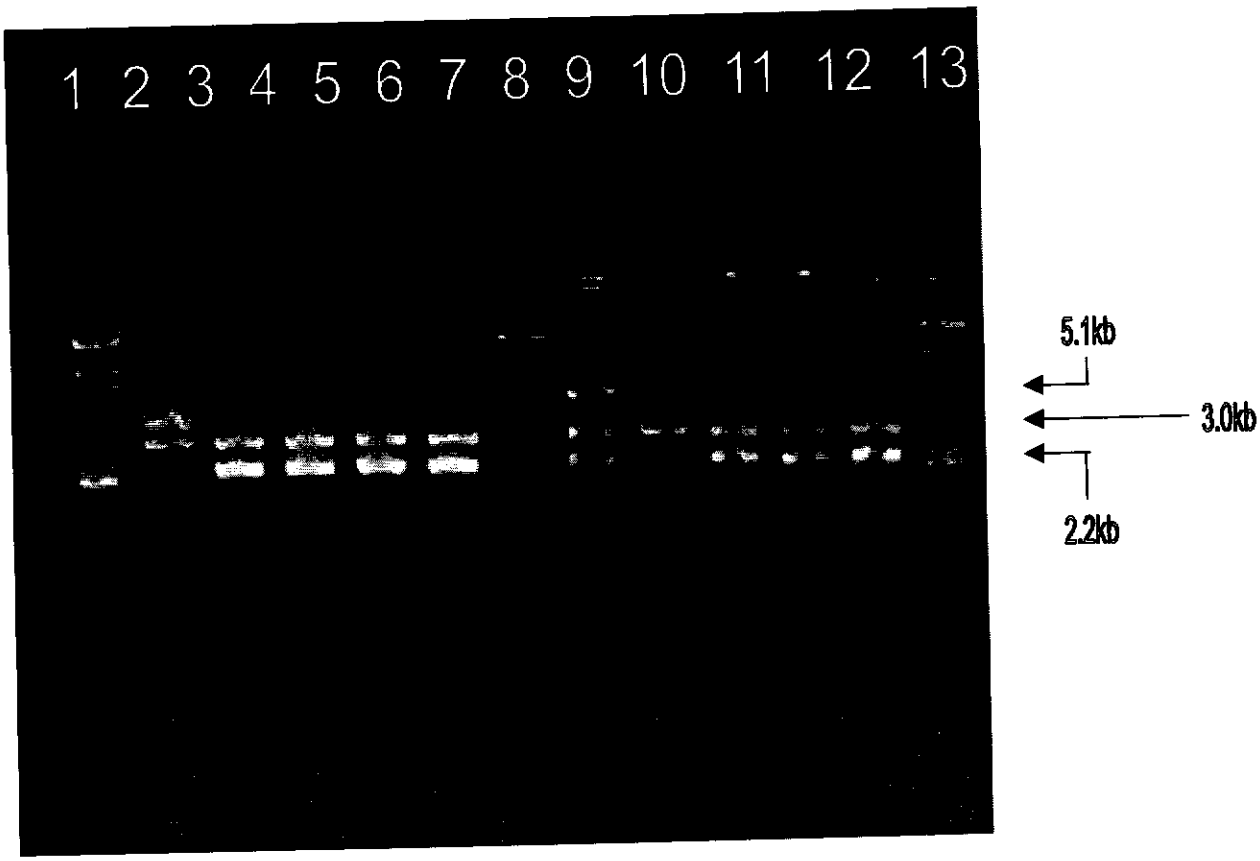

Figure 3.3.1a *Plasmid DNA (lanes 3-6 and 8-12) isolated from E.coli (DH5α) transfected with pBluescript containing 5AR1 cDNA insert and digested with Not I restriction enzyme and electrophoresed (1% agarose gel) at 40 volts for 2.5 hours before staining with ethidium bromide. Undigested DNA in lane 2 and molecular size markers (λ DNA digested with Hind III) are in lanes 1, 7 and 13. The molecular sizes of the DNA bands in the digested sample are ~3.0Kb and ~2.2Kb which respectively correspond to the molecular sizes of the pBluescript vector (2.9Kb) and the cDNA insert for 5AR1 (2.1Kb). Undigested sample is ~5.1Kb, the combined molecular size of vector plus insert.*

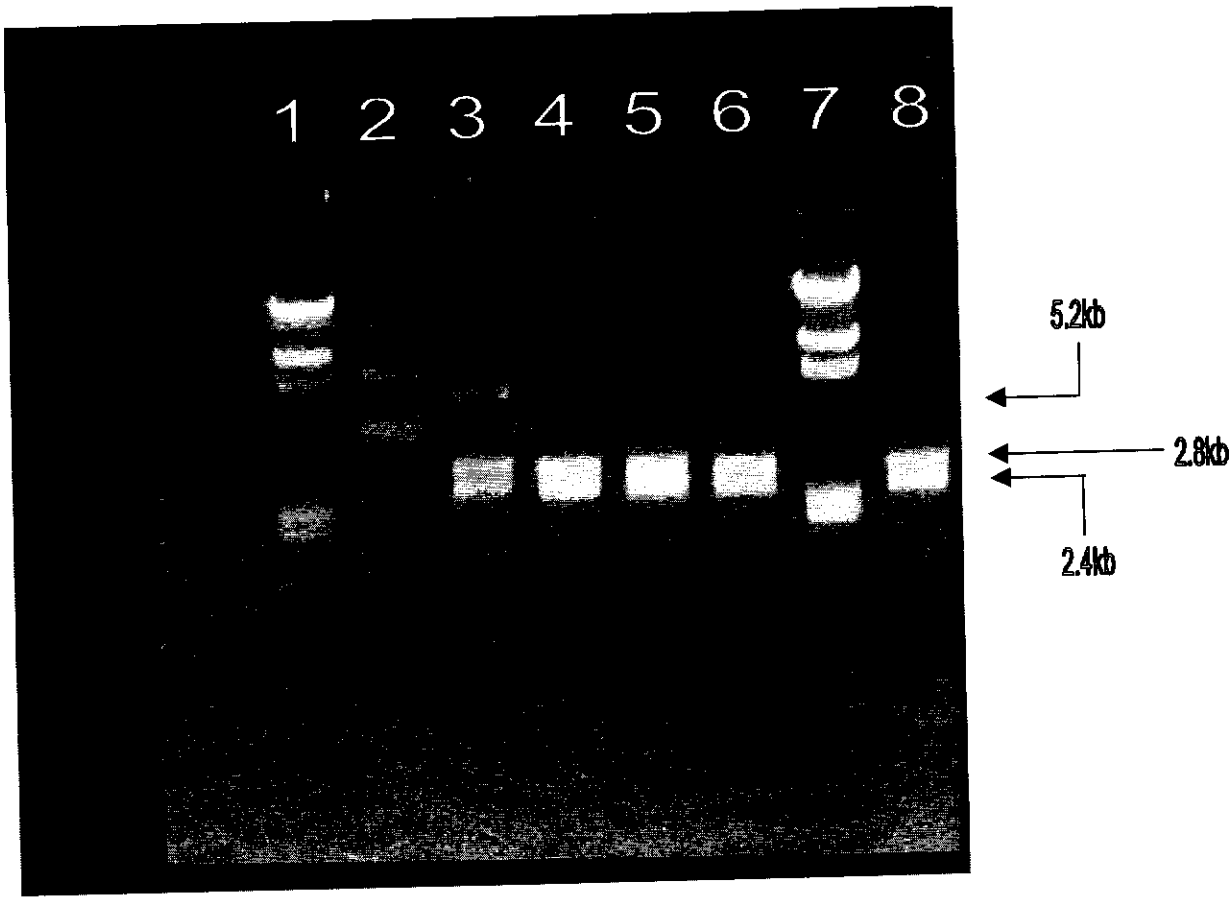

Figure 3.3.1b *Plasmid DNA (lanes 3-6 and 8) isolated from E.coli (DH5α) transfected with pBluescript vector containing the cDNA insert for 5AR2, digested with Sal I and Not I restriction enzymes and electrophoresed (1% agarose gel) at 40 volts for 2.5 hours before staining with ethidium bromide. Undigested DNA is in lane 2 and λ Hind III marker in lanes 1 and 7. The molecular sizes of the DNA bands in the digested samples (lanes 3-6 and 8) are ~2.8Kb and ~2.4Kb which are those expected for pBluescript (2.9Kb) and the cDNA insert for 5AR2 (2.4Kb). Undigested sample is ~5.2Kb, the combined molecular size of vector plus insert. The extra band present in lane 3 is partially digested vector plus insert.*

3.3.2 Isolation of cDNA inserts for 5AR1 and 5AR2

Homogeneity of inserts excised from pBluescript and isolated as described (Section 3.2.5.1) was determined by electrophoresis. The single band of DNA seen for 5AR1 and 5AR2 inserts confirmed their homogeneity (Figures 3.3.2a and 3.3.2b).

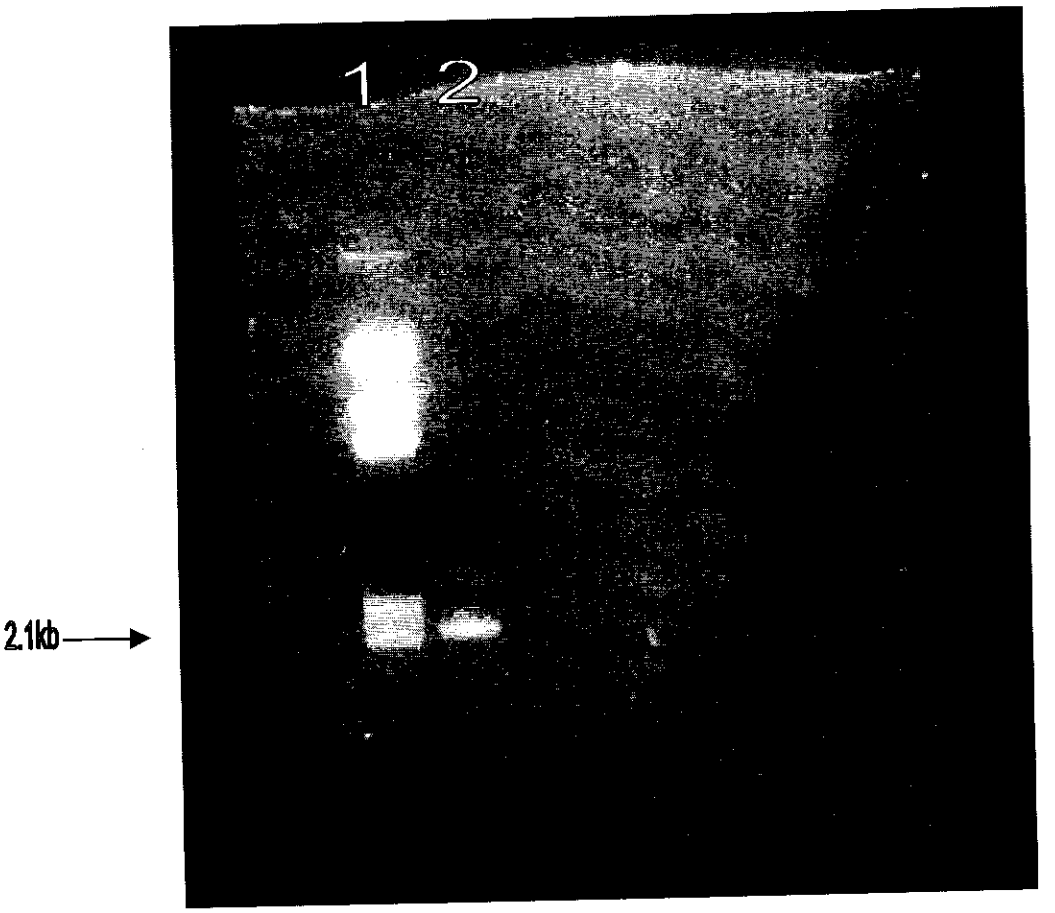

Figure 3.3.2a *Electrophoresis in a 1% agarose gel at 60 volts for 60 minutes of cDNA for 5AR1 excised from pBluescript vector using Not I, shows a single band of DNA of ~2.1Kb (lane 2). λ Hind III DNA markers are in lane 1.*

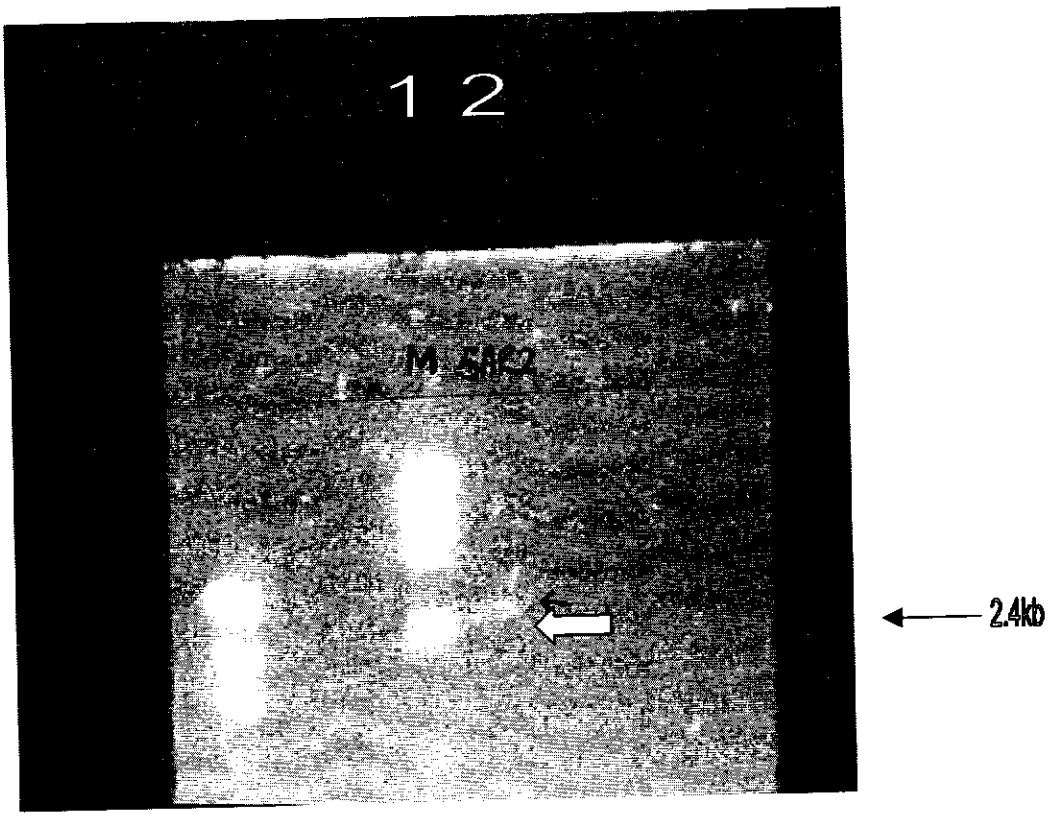

Figure 3.3.2b *Electrophoresis in a 1% agarose gel at 60 volts for 60 minutes of cDNA for 5AR2 excised from pBluescript vector with Sal I and Not I, shows a single band of DNA of ~2.4Kb (lane 2,denoted by arrow). λ Hind III DNA markers are in lane 1.*

3.3.3 Restriction digestion of the vector pCI-neo

The inserts isolated as above (section 3.3.2) were ligated into appropriately digested pCI-neo vector. This digestion facilitated ligation by generating compatible "sticky ends". Agarose gel electrophoresis was used to determine that successful digestion of the vector had occurred (Figures 3.3.3a and 3.3.3b).

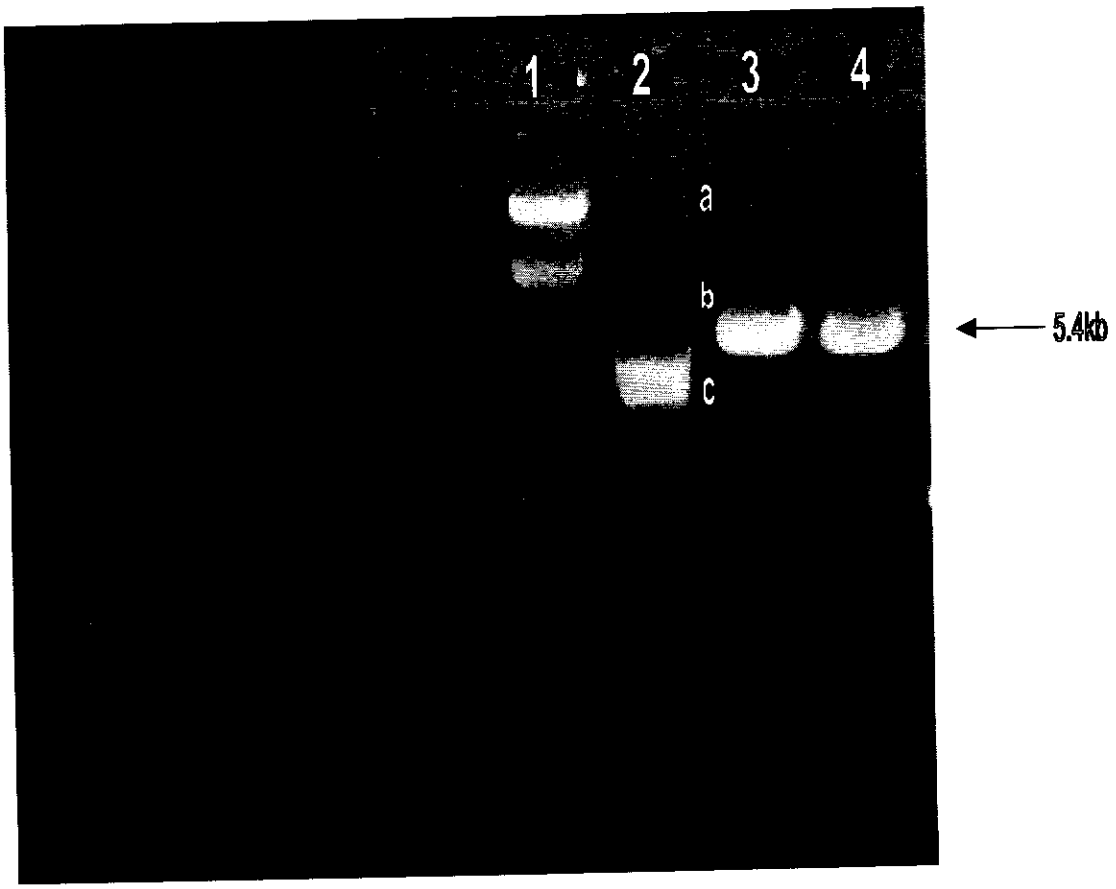

Figure 3.3.3a *Electrophoresis of undigested vector (pCI-neo) in a 1% agarose gel for 2.5 hours at 40 volts showed three bands of DNA (lane 2). In descending order of molecular size these are (a) open circular, (b) linear and (c) closed circular forms of the vector. In contrast, Not I digested pCI-neo (lanes 3&4) showed only a single band of DNA of ~5.4Kb which is that expected for the linear form of the vector. λ Hind III DNA markers are in lane 1.*

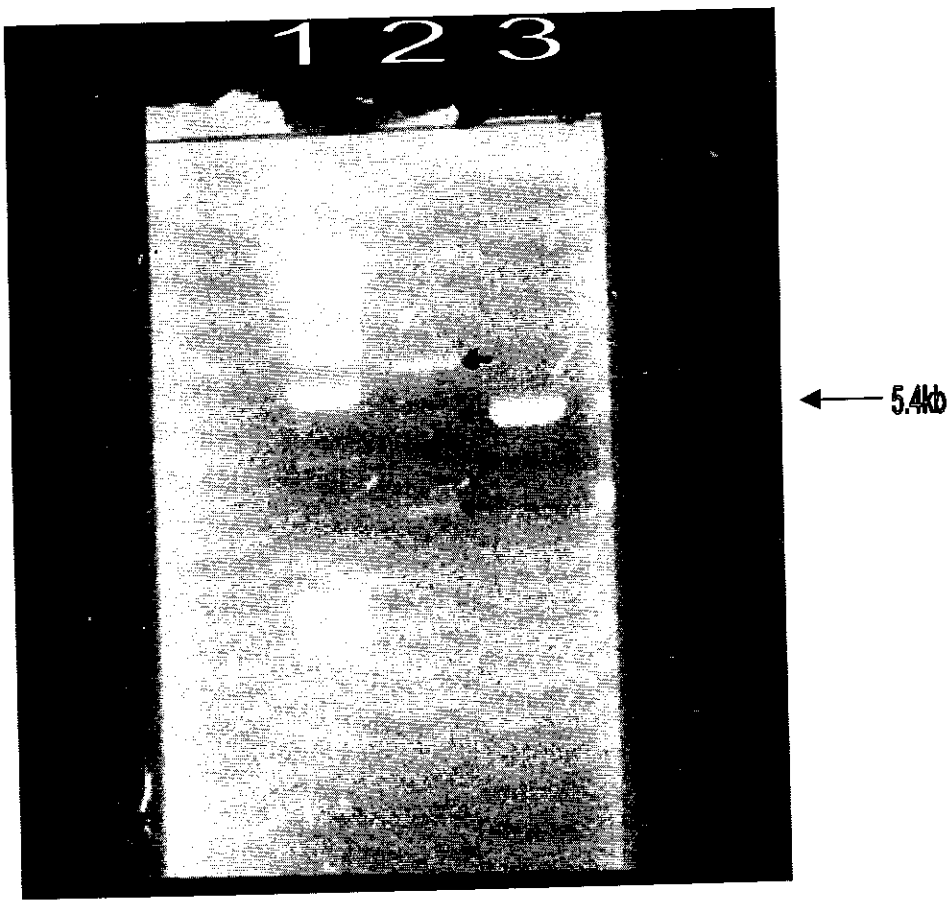

Figure 3.3.3b *Sal I/Not I digestion of the pCI-neo vector gave a single band of DNA (lane 3) with a molecular size of 5.4Kb which is that expected for the linear form of pCI-neo. λ Hind III markers are in lane 1 and undigested vector (pCI-neo) in lane 2.*

3.3.4 Generation of pCI-neo/5α- Reductase Constructs

Bacteria (*E.coli* strain DH5α) transformed with pCI-neo/5AR constructs by electroporation were identified initially by ampicillin resistance followed by transfer to nylon membranes and hybridisation with radiolabelled ($^{32P}\gamma$ATP) probes specific for 5AR1 or 5AR2. Initially, labelled probe was separated from free $^{32P}\gamma$ATP using a Biorad-50 gel filtration column. This however proved to be both time consuming and unnecessary as similar results were obtained with label probe separated from free $^{32P}\gamma$ATP and labelled probe not separated from free $^{32P}\gamma$ATP.

Autoradiographs from hybridisation experiments are shown in figures 3.3.4a and 3.3.4b. As a final check of the constructs, positive clones were digested and electrophoresed (Figures 3.3.4c and 3.3.4d).

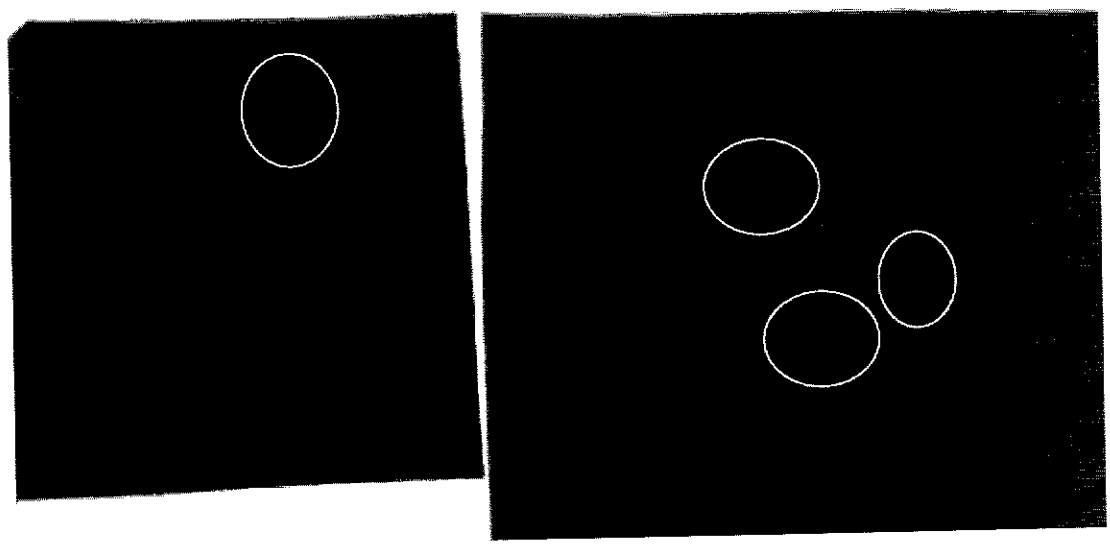

Figure 3.3.4a *Autoradiograph of ampicillin resistant bacteria generated from electroporation of the pCI-neo/5AR1 ligation and detected with a $^{32P}\gamma$ATP labelled 5AR1 hybridisation probe. Positive clones containing pCI-neo vector ligated with 5AR1 insert are circled.*

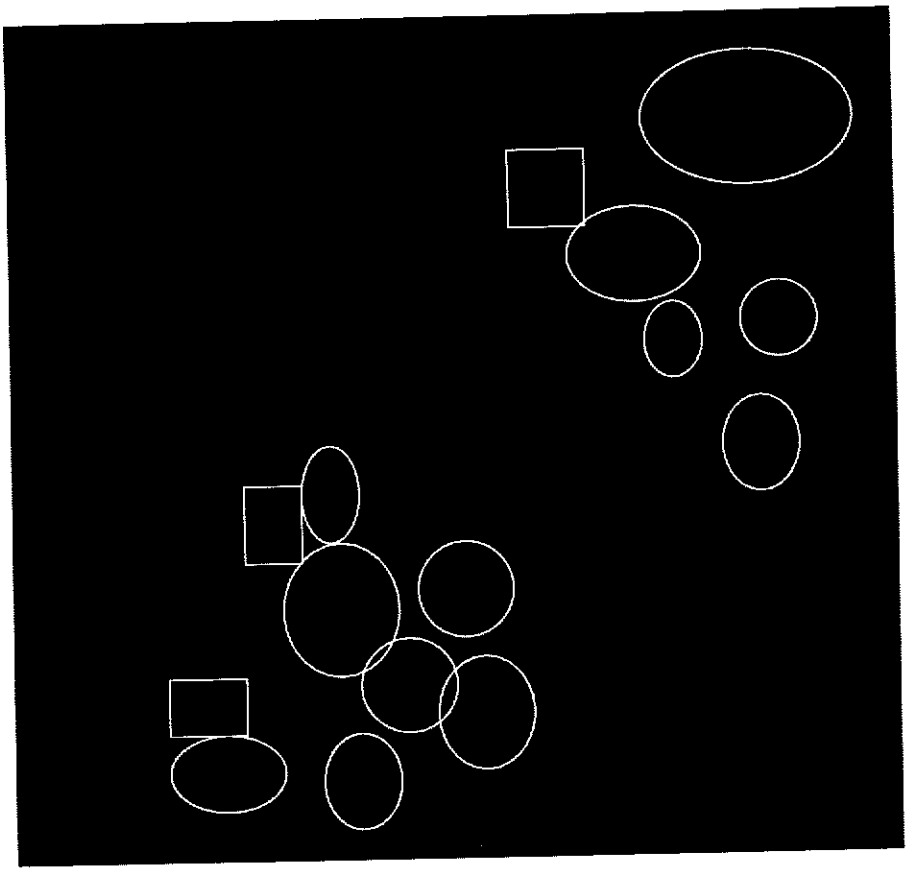

Figure 3.3.4b *Autoradiograph of pCI-neo/5AR2 ligation detected by hybridisation with a $^{32P}\gamma$ATP labelled 5AR2 probe. Positive clones containing pCI-neo vector ligated with 5AR2 insert are circled. Positive controls of pBluescript containing 5AR2 are boxed.*

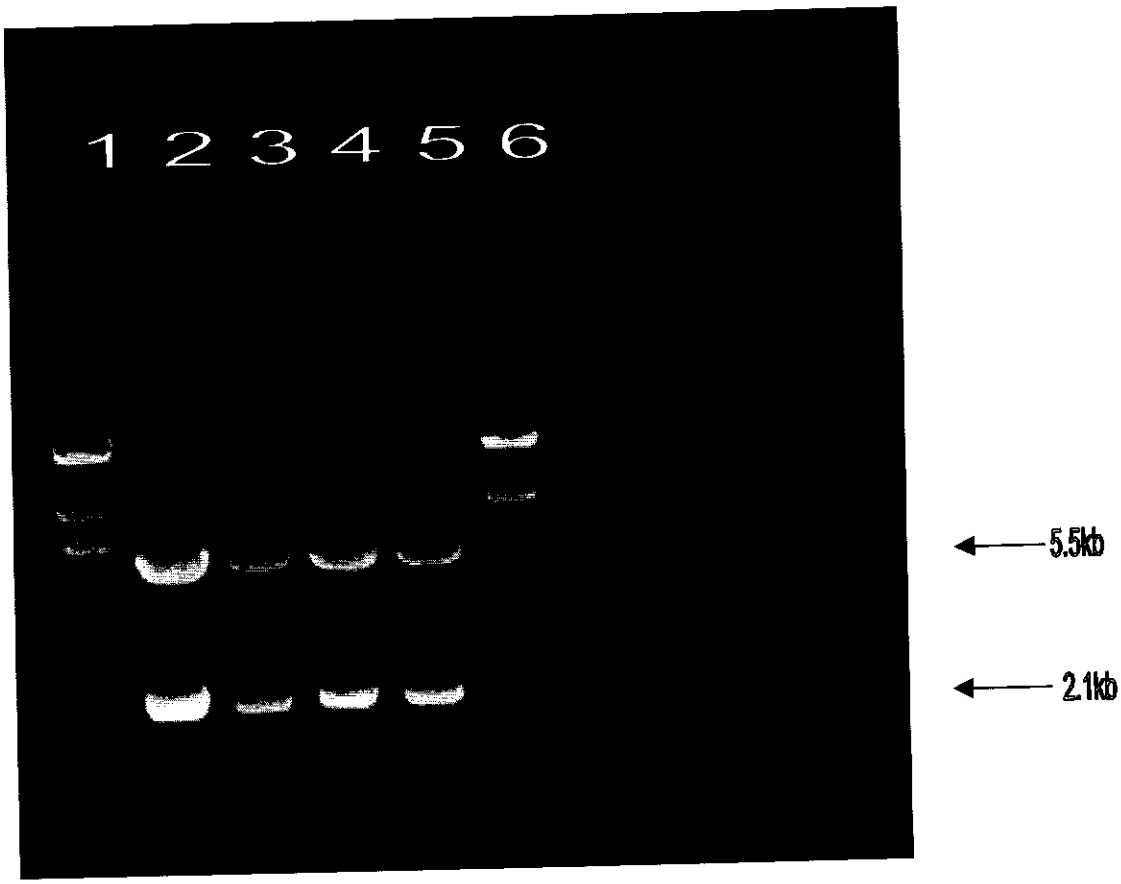

Figure 3.3.4c *Not I digested clones containing pCI-neo/5AR1 electrophoresed at 40 volts for 2.5 hours in 1% agarose gave DNA bands of 5.5 and 2.1Kb (lanes 2-5). These are the sizes expected for the pCI-neo vector and the 5AR1 insert respectively. λ Hind III size markers are in lanes 1 and 6.*

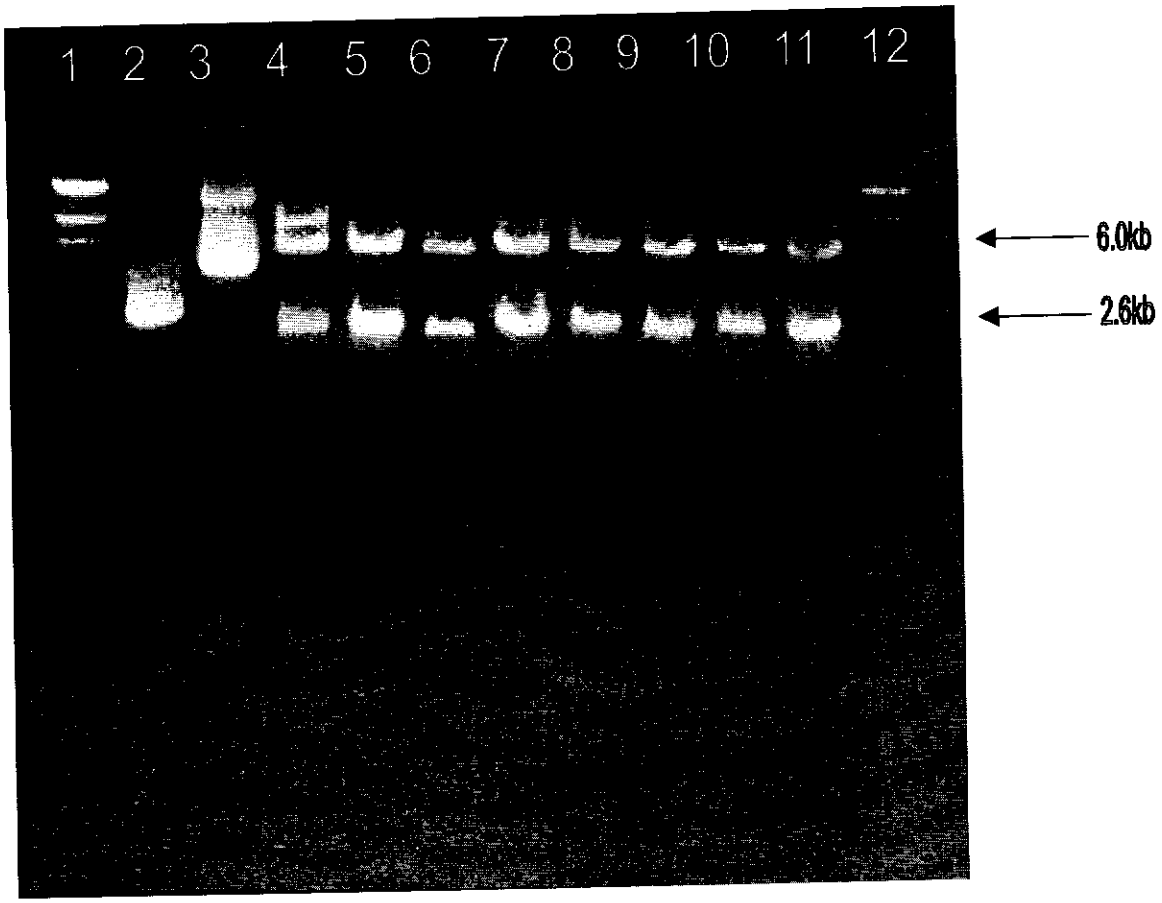

Figure 3.3.4d *Sal I/ Not I digested clones containing pCI-neo/5AR2 electrophoresed at 40 volts for 2.5 hours in 1% agarose gave DNA bands of 6.0 and 2.6Kb (lanes 4-11). These are the sizes expected for the pCI-neo vector and the 5AR2 insert respectively. λ Hind III DNA size markers are in lanes 1 and 12.*

3.3.5 Transfection of Chinese hamster ovary (CHO) cells with β- Galactosidase vector

CHO cells transfected with the PSV-β-Galactosidase vector by electroporation or by calcium phosphate transfection were shown to express the enzyme as determined by β-Galactosidase activity measured with the Promega β-Galactosidase enzyme assay system (Table 3.3.5).

	β- Galactosidase activity (milliunits)
Blank (hpH_2O)	0.000
CHO cell control	0.45±0.10
CHO cells electroporated with β- Galactosidase vector	1.02±0.01
CHO cells transfected with β- Galactosidase vector by calcium phosphate method	3.84±0.06

Table 3.3.5 *CHO cells electroporated with β- Galactosidase vector expressed β- Galactosidase with an activity of 1.02 milliunits, twice that of mock transfected CHO cells (0.45 milliunits). CHO cells transfected by calcium phosphate precipitation with β- Galactosidase vector expressed eight and a half times the β- Galactosidase activity (3.84 milliunits) of mock transfected CHO cells and ~3 times the activity of cells transfected by electroporation.*

3.3.6 Electroporation of Chinese hamster ovary cells with pCI-neo/5α-Reductase constructs

CHO cells transiently transfected, by electroporation, with pCI-neo vector plus insert (5AR1 or 5AR2) confirmed the functional integrity of the sub-cloned inserts. 5AR activity of cell lines electroporated with 5AR1 or 5AR2 respectively, is shown in tables 3.3.7a and 3.3.7b.

Sample	^{3H}-T cpm	^{14C}-DHT cpm	^{3H}-T corrected cpm	DHT/min (nmol)
1μM T	493621	16	-	-
DHT	1281	2247	-	-
CHO control	1764	773	5128	0.17
5AR1-1	2248	703	7825	0.26
5AR1-2	2441	902	6081	0.21
5AR1-3	2911	890	7349	0.25
5AR1-4	2592	701	8309	0.28

Table 3.3.6a *5AR activity (nanomoles of DHT formed per minute) of CHO cells electroporated with 5AR1 in pCI-neo and cotransfected with pADVantage vector. On average transfected cells express 5AR activity one and a half times that of untransfected control cells.*

Sample	^{3H}-T cpm	^{14C}-DHT cpm	^{3H}-T corrected cpm	DHT/min (nmol)
1μM T	352431	16	-	-
DHT	1676	2586	-	-
CHO control	1126	586	4696	0.22
5AR2-1	2444	311	7825	0.96
5AR2-2	2568	298	6081	1.05
5AR2-3	3074	394	7349	0.95
5AR2-4	6387	881	8309	0.89

Table 3.3.6b *5AR activity (nanomoles of DHT formed per minute) of CHO cells transfected with 5AR2 in pCI-neo vector and co-transfected with pADVantage. 5AR2 transfected cells on average express four and a half times the activity of control cells.*

3.3.7 Calcium phosphate transfection of Chinese hamster ovary cells with pCI-neo/5α- Reductase constructs

CHO cells transfected, by calcium phosphate precipitation, with pCI-neo vector containing either 5AR1 or 5AR2 insert were selected by incubation in medium containing geneticin 418 (neomycin sulphate [G418]). G418 resistant cells were harvested and assayed for 5AR activity. 5AR activity determined in transfected cells was compared with 5AR activity in cells transfected with vector (pCI-neo) only and in non-transfected CHO cells.

Table A: 5AR activity of CHO cells transfected with 5AR1

Sample	^{3H}-T cpm	^{14C}-DHT cpm	^{3H}-T corrected cpm	DHT/min (nmol)
1μM T	98175	7	-	-
DHT	766	2029	-	-
CHO control	2330	454	12800	0.60
pCI-neo control	828	373	4451	0.76
AA2	633	72	17750	3.01
AA6	665	64	20979	3.56
AB4	753	115	13220	2.24
AD1	1476	99	30102	5.11
AD2	2370	240	19938	3.39
BA1	1632	187	17620	2.99
BA2	401	31	26117	4.43
BA3	1370	156	17731	3.01
BA4	1335	110	24503	4.16
BC2	891	106	16971	2.88
CA3	575	47	24701	4.19
CB1	2063	222	18762	3.19

Table B: 5AR activity of CHO cells transfected with 5AR2

Sample	^{3H}-T cpm	^{14C}-DHT cpm	^{3H}-T corrected cpm	DHT/min (nmol)
1μM T	358732	9	-	-
DHT	1773	2412	-	-
CHO control	2330	454	12800	0.60
pCI-neo control	828	373	4451	0.76
DC2	39160	246	383959	17.84
DC6	21816	179	298968	13.89
EA2	21776	199	263938	12.26
EA4	71406	518	332793	15.54
EA6	52915	286	446262	20.73
FA1	35834	311	277915	12.91
FA6	15428	130	286249	13.30
FC6	31418	165	459274	21.34
GA2	51106	280	440242	20.45
GA3	35319	253	336717	15.64

Table 3.3.7a and b *CHO cells stably transfected with 5AR1 (Table A) and 5AR2 (Table B) expressed on average 5 times and 30 times the 5AR activity (nmol of DHT formed per minute) of control cells for 5AR1 and 5AR2 respectively.*

3.3.8 Characterisation of Stably Transfected Cells - Determination of Km and Vmax for testosterone

Lineweaver-Burke plots for 5AR1 and 5AR2 transfected cells showed characteristics for the expressed enzymes comparable with those in the literature (Figure 3.3.8a and 3.3.8b). Michaelis-Menton plots of these data

showed saturation of the enzymes (Figure 3.3.8a and 3.3.8b). *Nb*. All Km values are the calculated mean plus or minus the standard deviation.

A

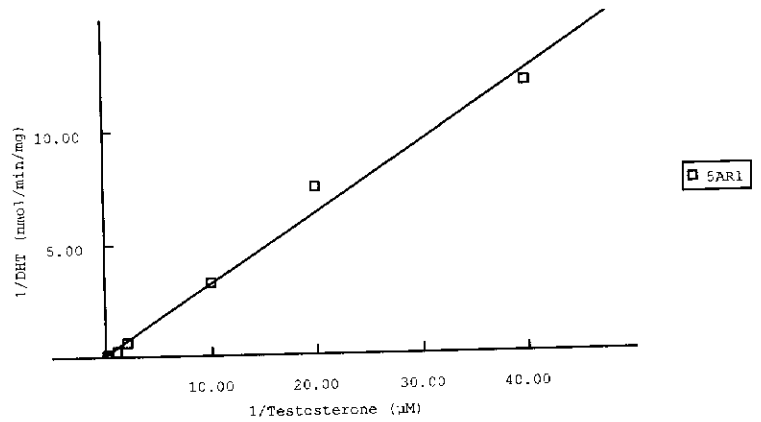

B

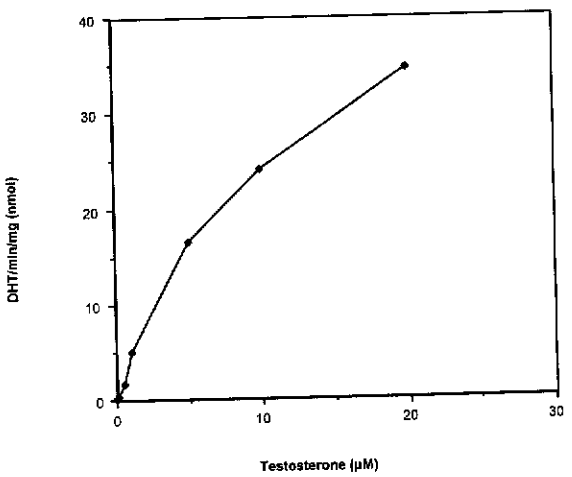

Figure 3.3.8a *Km and Vmax values of 2.80±0.60µM and 9.35nmol of DHT/min/mg of cell protein respectively, were calculated from Lineweaver-Burke plots (A) of 5AR1 transfected CHO cells incubated at T concentrations from 0.025-20µM for one hour at 37°C. The Michaelis-Menton plot for 5AR1 transfected CHO cells (B) demonstrates enzyme saturation.*

C

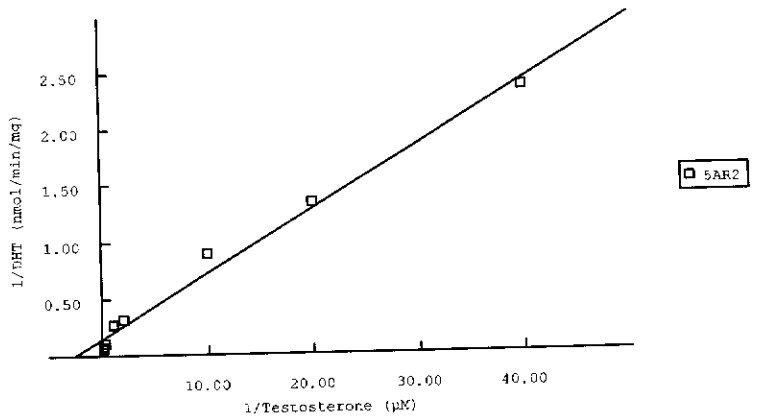

D

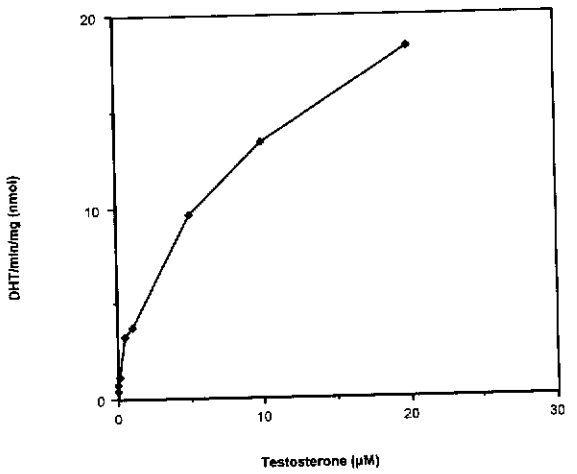

Figure 3.3.8b *Km and Vmax values of 0.45±0.31μM and 6.58nmol of DHT/min/mg of cell protein respectively, were calculated from Lineweaver-Burke plots (C) of 5AR2 transfected CHO cells incubated at T concentrations from 0.025-20μM for one hour at 37°C. The Michaelis-Menton plot for 5AR2 transfected CHO cells (D) demonstrates enzyme saturation.*

3.3.9 Characterisation of Stably Transfected Cells - Inhibitor plots and IC_{50} studies

Inhibitor plots for 5AR1 and 5AR2 (Figure 3.3.9a) gave Ki values of 327.8nM and 11.8nM respectively, these were as expected from previously published data. The relative resistance of 5AR1 and marked sensitivity of 5AR2 to Finasteride was further substantiated from IC_{50} values of 125nM and 19nM respectively (Figure 3.3.9b).

D

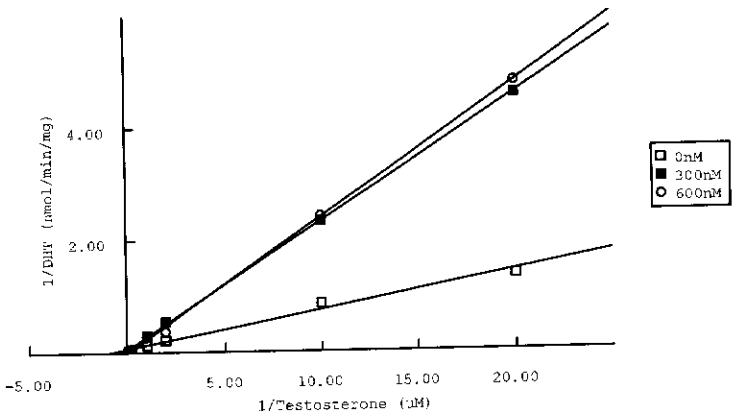

E

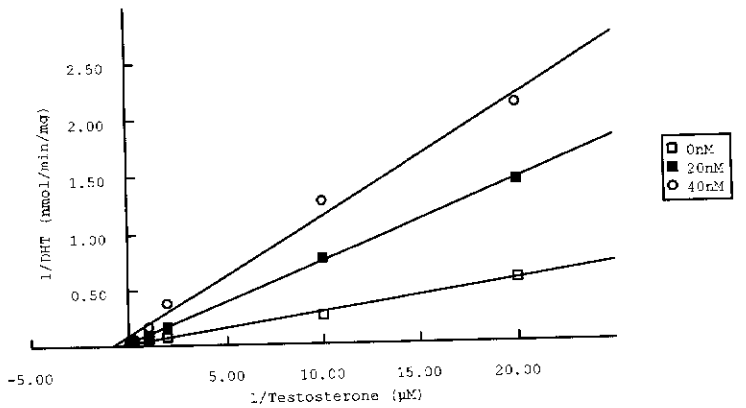

Figure 3.3.9a *Inhibitor plots for CHO cells stably transfected with 5AR1 (D) or 5AR2 (E) in pCI-neo. At 0, 300 and 600nM Finasteride, a Ki of 327.8nM was calculated for 5AR1 transfected cells. For 5AR2 transfected cells a Ki of 11.8nM was determined at 0, 20 and 40nM Finasteride.*

F

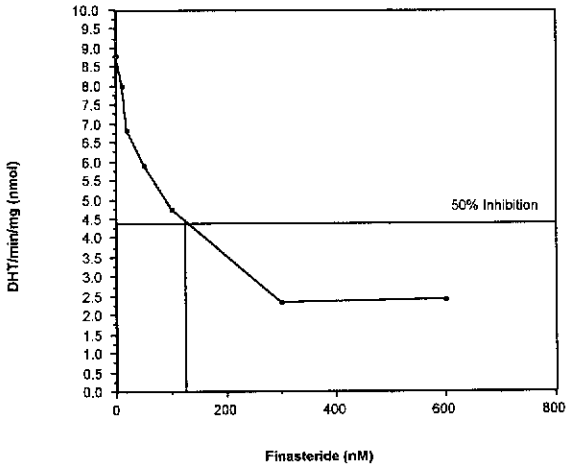

G

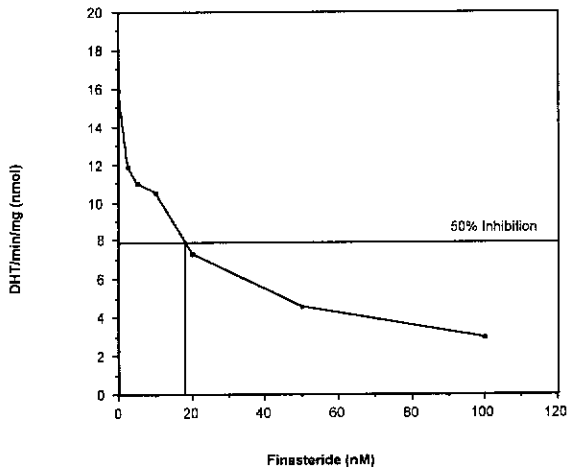

Figure 3.3.9b *CHO cells stably transfected with 5AR1 (F) or 5AR2 (G) were incubated for 60 minutes at 1μM T and Finasteride concentrations between 0-600nM. The concentration of inhibitor required to inhibit 5AR activity by 50% was interpolated as 125nM for 5AR1 and 19nM for 5AR2.*

3.3.10 pH Optima of Stably Transfected Cells

As is shown in figure 3.3.10a, cells stably transfected with 5AR1 showed a broad peak of activity over the pH range 5.5-7.0 with an optimum at pH 6.0. In contrast, cells expressing 5AR2 showed a more acidic pH optimum of 5.5.

H

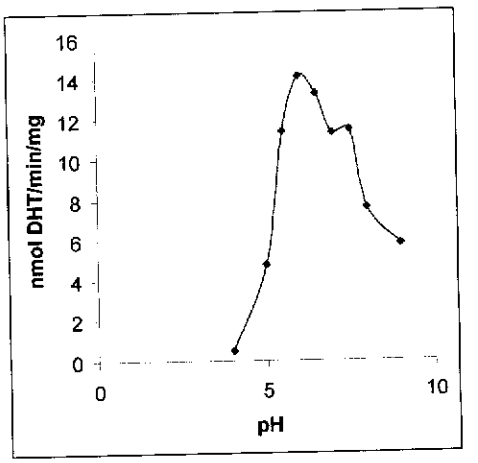

I

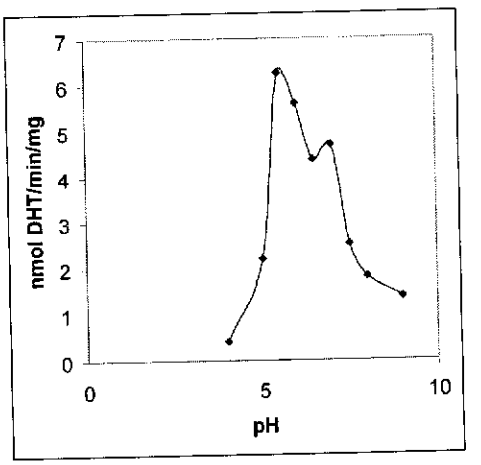

Figure 3.3.10a *The 5AR activity of CHO cells stably transfected with 5AR1 (H) or 5AR2 (I) was determined using sonicated cells incubated for 30 minutes at 37^{O}C with 1μM T in buffers ranging in pH from 4.0-9.0. For 5AR1, a broad peak of maximum activity was seen between pHs 5.5-7.0 with an optimum occurring at pH 6.0, whereas for 5AR2 a peak of maximum activity was seen at pH 5.5.*

Cell Line Expressing	Average % Conversion T to DHT	Km for T (μM)	Vmax (nmol/min/ mg)	Vmax/Km Ratio	Ki for Finasteride (nM)	IC_{50} (nM)	pH optimum
CHO cell control	0.85	18.67± 1.19	42.07	2.25	-	-	-
Wild type 5AR1	3.5	2.80± 0.60	9.35	3.36	327.8	125	6
Wild type 5AR2	20.8	0.45± 0.31	6.58	13.20	11.8	19	5.5

Table 3.3.8: *Characteristics of wild type human 5AR enzymes.*

3.4 DISCUSSION

Only 5μg of pBluescript plasmid plus inserted cDNAs for each of 5AR1 and 5AR2 was received from Dr D.W. Russell, therefore it was necessary to obtain more plasmid DNA for this project. For this, bacteria were electroporated with the plasmid and glycerol stocks made of bacteria containing the plasmid were stored at -70^{O}C. These glycerol stocks were used to provide plasmid DNA when required.

Electroporation of the pBluescript plasmid was not easily achieved, with the major problem being "sparking" in the electroporation cuvettes resulting in very little or no bacterial growth post-electroporation. It was thought the "sparking" was the result of small amounts of sodium acetate present in the plasmid preparations even though only very small amounts of plasmid (~100ng) were used. To overcome this, plasmid DNA was washed three times with 70% ethanol prior to electroporation. This proved successful as evidenced by the growth of some white colonies on selective agar plates. The pBluescript vector contains a gene encoding resistance to ampicillin so that only those colonies expressing the plasmid will grow on agar plates containing ampicillin. It also has a LacZ gene enabling blue-white selection on agar plates containing X-gal and IPTG, with those colonies expressing the vector appearing white. The LacZ gene codes for the enzyme β-Galactosidase which breaks-down lactose to glucose and galactose. β-Galactosidase also catalyses the simplified reaction in

which the lactose analogue X-gal (5-bromo-4-chloro-3-indolyl-β-D-galactopyranoside) is converted to a deep blue product[138]. In the presence of an inducer of the enzyme (IPTG) and X-gal, transformants expressing the LacZ gene appear blue. Recombinants for which the LacZ gene has been disrupted by the insertion of the 5AR cDNA will appear white, as they no longer express a functional β-Galactosidase enzyme and can't convert X-gal to its blue derivative. Therefore colonies expressing the pBluescript vector plus insert appear white when grown on LB agar plates containing ampicillin, X-gal and IPTG.

To ensure the blue/white selection was in fact functioning as expected, white colonies were picked, grown in broths and their plasmid DNA isolated. This was then digested with *Not I* for 5AR1 and *Sal I/ Not I* for 5AR2 and electrophoresed with undigested plasmid DNA and DNA from pBluescript containing no insert. The resultant gel showed that undigested pBluescript plus either 5AR1 or 5AR2 insert had the expected molecular sizes. Significantly the digested DNA showed the presence of DNA with the molecular sizes expected for 5AR1 and 5AR2 inserts, confirming the results of the blue/white selection.

The pBluescript vector does not contain a mammalian origin of replication and is therefore not suitable for use with mammalian cells. It was necessary therefore to excise the inserts from pBluescript and religate them into a vector suitable for use with mammalian cells. As future experiments required selection of cells transfected with plasmid plus insert, it was decided at the time to use the newly developed pCI-neo vector. pCI-neo contains the human cytomegalovirus (CMV) immediate/early enhancer/promoter sequence, an SV40 origin of replication, which enables replication in cells expressing the SV40 large T antigen, an ampicillin resistance gene and the neomycin phosphotransferase gene. The ampicillin resistance gene permits identification of bacteria containing the plasmid following its electroporation into *E.coli* to amplify the plasmid. The neomycin phosphotransferase gene enables selection of mammalian cells transfected with the plasmid by the incorporation of neomycin (Geneticin 418 [G418]) into the culture medium.

There are several ways to religate the excised DNA inserts into the new vector. Religation can be performed using a mixture of pBluescript plus insert, pCI-neo, restriction enzymes and T_4 DNA ligase. With this method however, excised insert may religate back into pBluescript. Additionally for 5AR2, for which an 11bp fragment is excised from pCI-neo during *Sal I/ Not I* digests, religation of the 11bp fragment back into pCI-neo may occur thereby preventing religation of the 5AR2 insert into pCI-neo. For 5AR1, although *Not I* digestion does not excise nucleotides, it does lead to the generation of compatible sticky ends in the digested vector, enabling vector self-religation. For these reasons it was decided to first isolate the inserts from pBluescript and then add these to pCI-neo previously digested with the appropriate restriction enzymes.

There are numerous methods for the recovery of DNA fractionated on agarose gels. These include extraction of DNA from low-melting-temperature agarose, DNA extraction from agarose gels by electrophoresis onto DEAE-cellulose membranes and extraction by electroelution into dialysis bags[136]. Using low-melting-temperature agarose, gel slices containing the DNA bands of interest are excised following electrophoresis and then digested with the enzyme agarase before purification of the recovered DNA. Although this method has proved successful, there are some associated problems. The enzyme agarase may not completely digest the agarose, which as a result is extracted along with the DNA. As the polysaccharide content of agarose is a potent inhibitor of many enzymes used in cloning steps including T_4 DNA ligase[136], this is a particular disadvantage of the method. Additionally, low-melting-point agarose is very expensive. For isolation of DNA by electrophoresis onto DEAE-cellulose membranes, the sample is electrophoresed and located by staining with ethidium bromide. A slit is then cut in the gel immediately ahead of the band of interest into which a small piece of DEAE-cellulose membrane is inserted and electrophoresis is continued until the DNA band has migrated onto the membrane. The membrane is then washed and the DNA eluted using a buffer of high ionic strength[136]. This method also has its problems in that it is unsuitable for extracting DNA fragments larger than 15Kb and single stranded DNA fragments are difficult to elute from the membrane[136]. Like the two methods described above, electroelution into dialysis bags also has not proved entirely satisfactory due to low yields of DNA[136].

A new extraction method[137] appeared promising and was therefore tried and evaluated. In this method DNA is electrophoresed in normal agarose, following which gel slices containing the DNA bands of interest are excised and subsequently lyophilised. This results in a gel of a more open porous structure from which the DNA is easily eluted. It was found that this method was simple to perform and yielded sufficient quantities of DNA for use in subsequent ligations. This method however was eventually discarded when a commercially available system (BRESAtec) became available.

Prior to its ligation with the 5AR1 insert, pCI-neo was digested with *Not I*, which generates a vector with compatible 5' and 3' sticky ends. Due to the close proximity of the compatible ends during ligation, vector self religation is more efficient than is vector religation with insert, which occurs purely by chance when the vector and insert are in close proximity to one another[138]. In order to minimise self religation and therefore enhance vector religation with the 5AR1 insert, digested vector was treated with calf intestinal alkaline phosphatase (CIAP) prior to ligation. CIAP removes the 5' phosphate group from the digested vector so that self religation cannot occur. The insert has a 5' phosphate group and can therefore ligate with the treated plasmid.

pCI-neo was digested with both *Sal I* and *Not I* prior to ligation with the insert for 5AR2. Digestion with both restriction enzymes does not result in compatible 5' and 3' restriction sites however, vector self religation is still possible. During digestion an 11bp fragment is excised from the vector. If this fragment is not removed prior to ligation it is possible the vector will self religate with its excised 11bp fragment, reducing the chance of insert religation with pCI-neo. To enhance vector religation with insert, following digestion pCI-neo was purified using a Wizard clean up column (Section 3.2.2.1), which removes the 11bp fragment.

The quantity of digested vector required for ligation with either insert varied depending on the amount of insert recovered from lyophilised agarose gels. It is necessary to maintain the vector to insert ratio of 1:2 and this accounts for the

difference in ligation volumes used for the ligations of pCI-neo with 5AR1 and 5AR2.

Selection of pCI-neo clones ligated with either insert was achieved by electroporation of *E. coli* strain DH5α with the resulting pCI-neo/insert ligations. Transformants were selected with ampicillin, the resistance to which is encoded in the pCI-neo vector, as described previously. As both open and closed circular forms of plasmid DNA are more readily transformed than linear plasmid DNA, most transformants grown should contain vector ligated with insert (closed circular DNA). Digested vector which has not religated with insert will be linear DNA and thus less likely to transform. However, not all the vector DNA is completely digested during a restriction digest. As the vector expresses the ampicillin resistance gene it is possible that some transformants contain undigested vector (closed circular DNA) or partially digested (open circular DNA) present in the ligation mixture prior to electroporation. Selection of transformants containing vector with ligated insert consequently could not be based solely on ampicillin resistance.

Differentiation between transformants containing vector only from those containing vector and religated insert was achieved by hybridisation of DNA isolated from ampicillin resistant bacteria. For this, radiolabelled ($^{32}P_{\gamma}ATP$) probes specific for 5AR1 or 5AR2 were used. Although the radiolabelling of the probes was easily accomplished, many problems were encountered with the hybridisation process. Initially, the positive controls included in each hybridisation did not generate a positive result. It was thought this was due to ineffective transfer of DNA to the membranes. Probing of DNA directly transferred to membranes however also gave no signal.

It was then thought that perhaps the hybridisation temperature of 60^{o}C was too high, preventing the labelled probe annealing with the DNA bound to the membranes. Theoretically the ideal temperature of hybridisation is 5^{o}C below the melting point (T_m) of the probe[136]. As the T_m of the 5AR1 and 5AR2 probes were 64^{o}C and 68^{o}C respectively, then a hybridisation temperature of 60^{o}C appeared suitable. However, as hybridisations at 60^{o}C had not been

successful, it was decided to lower the hybridisation temperature to 37°C, a temperature at which hybridisation should occur. The results remained negative. Using double the quantity of labelled probe was tried, as was the use of labelled probe not separated from unincorporated $^{32}P_{\gamma}ATP$ in case probe was being lost during the separation process. Results were still negative

The probe sequences were then studied to determine with which region of the sequence of the respective insert they are complementary. This led to the resolution of the problem. It was discovered that the probes designed for the 5AR2 insert, the sequences for which were obtained from the literature[53], were in fact complementary for the 5AR1 insert and vice versa.

Once the correct probes were used for hybridisations the positive controls finally generated a positive result. However, in contrast to the previous experiments there were no negative colonies. This included the negative controls used, which were bacteria transformed with pCI-neo only. This was due to using the hybridisation temperature of 37°C, which had been chosen as a result of the problems previously encountered. This temperature enables significant mismatching between the probe and its target DNA. As a result the hybridisation temperature was increased to 50°C in order to try and reduce the amount of mismatching. With hybridisation at 50°C negative controls were negative and positive controls positive. Most significantly, some transformants from pCI-neo ligations with either 5AR1 or 5AR2 also generated positive signals.

To ensure that those clones positive on hybridisation did in fact contain vector ligated with insert, restriction digests on plasmid DNA isolated from these transformants were performed. After electrophoresis of the four positive 5AR1 clones digested with *Not I* and the nineteen positive 5AR2 clones digested with *Sal I* and *Not I*, DNA bands of the appropriate molecular sizes were obtained. This confirmed the clones selected as positive from the hybridisations contained vector ligated with insert.

Restriction digests of positive hybridisation clones partially resolved another problem that it was thought might be encountered. Ethidium bromide, which was used to stain and visualise DNA bands following electrophoresis, binds and stains DNA by intercalating between adjacent base pairs[138]. This intercalation may lead to the partial unwinding of the double helix resulting in nicked DNA. As a result, exposure of the 5AR inserts to ethidium bromide may have resulted in a nicked insert that encodes a non-functional enzyme. However, as the insert encoding sequences were successfully excised from pCI-neo following ligation, this suggests that damage, at least to the 5' and 3' ends of the inserts, due to ethidium bromide exposure had not occurred.

This, of course, did not show if ethidium bromide had damaged other areas of the inserts. To determine if this had occurred it was decided to screen Chinese hamster ovary (CHO) cells transiently transfected by electroporation with pCI-neo plus 5AR1 or 5AR2 for enzyme expression. Before this however, it was necessary to determine both that CHO cells could be successfully transfected with foreign DNA and that the cells do not naturally express large amounts of 5AR.

To determine if the technique used for transient transfection was operating correctly and that the CHO cells used here could express foreign DNA, the Promega PSV-β-Galactosidase vector and β-Galactosidase enzyme assay system were used. This system, which was found simple to use, showed that CHO cells transfected with the vector had significantly (~240%) greater β-Galactosidase activity than control cells. This demonstrated both that the transient transfection procedures was operating as expected and that CHO cells can be transfected with and express foreign DNA. CHO cells after electroporation with buffer only, demonstrated insignificant 5AR activity indicating they are suitable for transfection with 5AR1 and 5AR2 encoding inserts.

As a preliminary experiment, CHO cells were initially transiently transfected by electroporation with plasmid DNA isolated from individual hybridisation positive 5AR2 clones. The pADVantage cotransfection vector, which enhances transient protein expression by increasing translation initiation, was

simultaneously electroporated. Control CHO cells not electroporated with DNA were included for comparison. Transfected cells however, showed no increase in expression of 5AR activity. It was thought this might be due to insufficient DNA in the electroporation mixture. The plasmid DNA preparations from eight of the nineteen positive 5AR2 clones therefore were pooled prior to electroporation and electroporations of the pooled plasmid DNA performed in quadruplicate. All of the cultures prepared from the electroporated cells expressed significant 5AR activity, on average 440% greater than that of non-transfected control CHO cells. This demonstrated that these 5AR2 inserts did encode a fully functional 5AR isoenzyme and therefore had not been significantly damaged by exposure to ethidium bromide. The success of this experiment meant that the pooled DNA was satisfactory for stable transfection of the CHO cells.

Electroporation was also used for functional assays to determine if the 5AR1 insert had been ligated correctly into pCI-neo. As the 5AR1 insert is excised from pBluescript with only a single enzyme (*Not I*) both the 5' and 3' restriction sites of the insert are identical. Similarly, digestion of the recipient vector with this enzyme generates identical 5' and 3' restriction sites. Although self religation could not occur as the vector was dephosphorylated after digestion, it is possible for the insert to religate into the vector in the wrong orientation. If this occurs then the insert encoding sequence will be read "back to front" during translation and a functional enzyme will not be produced. The orientation of the insert cannot be determined either by hybridisation or by electrophoresis of *Not I* restriction digests of positive 5AR1 hybridisation clones. To determine orientation requires either sequencing or digestion of the vector with insert using restriction enzymes that give different sized fragments depending on the orientation of the insert. These two procedures are both time consuming and expensive to perform and an easier approach was utilised. It was decided to electroporate CHO cells with plasmid DNA from each of the four positive 5AR1 hybridisation clones and assess transfected cells for expression of 5AR. All of the transiently transfected cells expressed significant 5AR activity, on average 150% greater than non-transfected control CHO cells. This showed that in each of the four individual 5AR1 clones, the 5AR1 insert had orientated correctly when religated into pC1-neo and had not been significantly damaged by

exposure to ethidium bromide. As each individual clone expressed 5AR activity, pooled plasmid DNA isolated from the four positive clones was used for the stable transfection of CHO cells.

Electroporation cannot be used to give stable transfectants, which requires other procedures such as calcium phosphate precipitation[139]. A commercially available calcium phosphate precipitation method (Cellphect; Pharmacia) was used for the establishment of stably transfected CHO cells. Like most of the commercially prepared methods used, this system was found simple and effective. Initial assessments, again using the Promega PSV-β-Galactosidase system, gave β-Galactosidase activity of vector transfected cells about 800% greater than control mock transfected cells. To achieve effective transfection with the method however, it is necessary to ensure a fine precipitate is prepared and is well dispersed over the recipient cells. This requires careful attention to the mixing procedures during precipitate preparation and maximum cell surface area for the recipient cells. These criteria were met by vigorous vortexing during precipitate preparation and growing cells in petri-dishes rather than in the wells of tissue culture trays.

Selection of cells containing vector was made with Geneticin (G418) an aminoglycoside, which rapidly kills cells not expressing the neomycin resistance gene. Control cells began to die within 2-3 days and within 7 days clones of actively growing cells were readily seen. Stable transfection of cells requires that the plasmid DNA is incorporated into the cell chromosomal DNA and cultures therefore were left for 14-16 days before harvesting individual clones. For this, individual colonies of cells transfected either with vector alone or with vector plus insert were harvested to 24 well plates and assayed for 5AR activity. Of the fifty-eight separate clones screened from cells transfected with vector plus 5AR1 insert, many had 5-6 times the 5AR activity of cells transfected with vector only. Of these 12 were selected for expansion. Sixty six separate clones from cells transfected with vector plus 5AR2 insert were screened, many expressed 5AR activity in the range 4-44 fold greater than that of cells transfected with vector alone. 10 of these clones were selected for further culture.

Following the establishment of CHO cell lines stably expressing 5AR1 or 5AR2, the enzyme kinetics of these transfected cells were characterised. The equilibrium constant (Km) and maximum velocity (V_{max}) were determined from assays in which transfected cells were incubated at various substrate (T) concentrations, following which 5AR activity was determined (Section 3.2.14.2). The pH optimum for wild type 5AR isoenzymes were determined from cell sonicates (Section 3.2.14.5) and the inhibitory effects of the competitive 5AR inhibitor Finasteride determined from both Ki (Section 3.2.14.3) and IC_{50} studies (Section 3.2.14.4). Duplicate wells were assayed at each substrate concentration and pH. Cell protein estimations were determined by the method of Folin and Lowry (section 3.2.15) and compensated for differences in 5AR activity due to differences in cell numbers between wells. All data was analysed using the Enzyme Kinetics V1.5 program and Km, Vmax, Ki, and IC_{50} values as well as pH optima were calculated from pooled data from two or more experiments.

Data from Km and Vmax studies were analysed from Lineweaver-Burke plots constructed with the Enzyme Kinetics V1.5 program. Cells expressing 5AR1 demonstrated a Vmax of 9.35nmol of DHT/min/mg of cell protein and Km of 2.80±0.60μM, while those expressing 5AR2 a Vmax of 6.58nmol of DHT formed/min/mg of cell protein and a Km of 0.45±0.31μM. The Vmax/Km ratio gives an indication of the relative efficiency of a 5AR enzyme in converting T to DHT. Vmax/Km ratios for the wild type enzymes were 3.36 for 5AR1 and 13.20 for 5AR2. This greater efficiency of 5AR2 (4-fold) is in accord with its ability to work best under conditions of limiting substrate where T to DHT conversion is crucial for normal sexual development[38].

Various values have been published for the Km and Vmax of 5AR. Thigpen et al, 1993b[37], state a Km and Vmax of human 5AR1 as 1.7μM and 2.8nM DHT/min/mg cell protein respectively. Levy et al, 1995[44] report a Km of 3.5-5.2μM and Vmax of 220 pmol DHT/(min.mg) and Russell and Wilson (1994)[10] give a Km of 1-5μM. The Km of 2.80±0.60μM obtained here for 5AR1 is within the range of these published values. Comparison of the value obtained here for Vmax with previously published data is made difficult by the differing units in which 5AR activity has been expressed. However, comparing the values for

Vmax of 5AR1 and 5AR2 obtained here shows these are similar, which is in accord with the results reported by Thigpen and associates[37] for the Vmax values of the two isoenzymes.

The Km and Vmax for human 5AR2 have been reported as 0.2μM and 2.4 nM of DHT/min/mg cell protein[37], 0.7μM and 88pmol/(min.mg)[44], 0.5-1.0μM and 2.0-5.0nmol min^{-1} mg^{-1} [63] and a Km of 0.1-1.0μM[10]. The Km of 0.45±0.31 μM for 5AR2 obtained here falls within these previously published values and as for 5AR1, comparisons of Vmax are made difficult by the different units of expression for 5AR activity.

It is widely established throughout the literature that the pH optima of the human 5AR isoenzymes differ greatly. 5AR1 exhibits a broad alkaline peak from pH 6.0-8.5[1, 33] and 5AR2 a narrow acidic peak at pH 5.0[32, 33]. The pH optima determined here for wild type 5AR1 (pH 6.0-7.5) and 5AR2 (pH 5.5) are in agreement with published values.

The ability of Finasteride (MK-906) to inhibit the action of human 5AR1 was also assessed and a Ki (inhibition constant) of 327.8nM for Finasteride was obtained. This value is similar to those of 325 nM[37], 340-620nM[1] and 330nM[128] but is a little higher than 100-120nM reported by Levy et al, 1995[44]. In similar studies of human 5AR2, a Ki value of 11.8nM was obtained. This value is similar to that reported by Thigpen et al, 1993b[37], of 12nM but is higher than 1-3nM reported by Levy et al, '95[44].

Andersson et al in 1991[32], reported IC_{50} values of 900nM and 30nM for human 5AR1 and 5AR2 respectively. Although the IC_{50}s calculated here are lower (125nM for 5AR1 and 19nM for 5AR2), they clearly reflect the relative sensitivities of the two enzymes to Finasteride.

Overall the kinetic characteristics obtained for CHO cells expressing 5AR1 and 5AR2 fall within the range of values previously reported by other researchers. These results not only validate the 5AR assay system used but more importantly demonstrate successful re-ligation of the cDNA inserts for 5AR1 and 5AR2 into pCI-neo without altering the functional properties of the encoded

isoenzymes. The establishment of cells stably expressing wild type 5AR1 and 5AR2 provides the basis for comparison of the effects of mutation of these enzymes.

The experiments reported here have been discussed at some length as the entire project rested on the expression and characterisation of wild type 5AR1 and 5AR2 under the conditions to be used. Without this, comparisons of mutated enzymes with the wild type enzymes would not have been possible and the effects of the mutations on enzyme activity could not have been determined.

Chapter 4.0

Mechanism of 5α- Reductase Inhibition by Finasteride

4.1 INTRODUCTION

In the early 1990s two cDNAs encoding 5α- reductase (5AR) were isolated in rat and man using expression cloning techniques[1, 31, 32, 33]. The two isoenzymes were termed 5AR1 and 5AR2 after the chronological order of their discovery. The human isoenzymes are encoded by different genes and differ with respect to their protein structure, relative tissue distributions, biochemical properties and sensitivity to pharmacological inhibitors.

The gene encoding human 5AR1 (SRD5AR1 gene) is located on chromosome 5 and encodes a protein of 259 amino acids. The SRD5AR2 gene, which codes for human 5AR2, is expressed on chromosome 2 and encodes a protein of 254 amino acids. The two human isoenzymes share 50% homology, with 5AR1 predominantly expressed in non-genital tissue, including the skin and liver and 5AR2 in the genital tissues including the prostate[10]. 5AR1 exhibits a neutral pH optimum (6.8-8.5) and a substrate affinity for testosterone (T) in the micromolar range (Km=1-5μM). 5AR2 exhibits a narrow pH optimum (pH 4.9-5.1) and substrate affinity in the nanomolar range (Km=0.1-1μM) [10]. Most significantly, the two isoenzymes differ in sensitivity to pharmacological inhibitors. The most widely used inhibitor of 5AR is the competitive inhibitor Finasteride, a 4-aza steroid widely used for the treatment of benign prostatic hyperplasia (BPH) and more recently for male pattern baldness (MPB). Notably, human 5AR2 is markedly more sensitive to Finasteride than is 5AR1.

As in the human, there are two 5ARs in the rat with the type 1 enzyme in rat and human having 60% homology and the type 2 enzymes having 77% homology. In general the rat and human 5ARs share similar tissue distributions, pH optima and substrate affinities although rat 5AR2 has a lower Km for T than 5AR1[33]. A significant difference between the enzymes from the two species is their sensitivity to pharmacological inhibitors including Finasteride. Although both rat and human 5AR2 are equally sensitive to inhibition by Finasteride, rat 5AR1 is almost 50-fold more sensitive than is human 5AR1[44]. This difference makes the rat a poor choice as a model for the comparison of the effectiveness of pharmacological inhibitors between the rat and human 5ARs[44].

In 1995, two 5ARs from the *Cynomolgus* monkey were cloned, expressed and characterised[44]. Monkey 5AR1 and 5AR2 share 93% and 95% homology respectively with their human counterparts and they also exhibit similar pH optima (5AR1=7.0, 5AR2=4.5-5.5) and substrate affinities for testosterone (5AR1=2 μM, 5AR2=0.7μM). Studies with pharmacological inhibitors have demonstrated monkey 5ARs are more similar to human than are rat 5ARs[44].

As mentioned previously the competitive inhibitor Finasteride (17β-[N-t-butyl] carbamoyl-4-aza-5α-androst-1-ene-3-one) is currently widely used. It contains a stable configuration in its A-ring enabling it to mimic the transition-state in the conversion of testosterone (T) to dihydrotestosterone (DHT) and to bind tightly to the active site of the enzyme[94]. Finasteride competes with the natural substrate T for the enzyme, resulting in a reduction in conversion of T to DHT. The mechanism of action of Finasteride is time-dependent and irreversible with respect to both human 5AR1 and 5AR2. It displays a slow K_{on} rate and an even slower dissociation rate ($T_{1/2}$ >30 days), essentially leading to irreversible inhibition of the enzyme[108]. It is unclear if inactivation is due to covalent attachment of Finasteride preventing 5AR from binding substrate or if Finasteride binding leads to conformational changes in the enzyme[10].

Finasteride is an extremely potent inhibitor of human 5AR2 but is less effective against human 5AR1 whereas in rats it is an equally potent inhibitor of both isoenzymes. Mechanistic studies of Finasteride inhibition in rat and human isoenzymes demonstrate differences both within and between species[115]. Finasteride is a time-dependent irreversible inhibitor of both human 5ARs and rat 5AR2 but is a time-independent reversible inhibitor of rat 5AR1. The reasons for this unique inhibitory mechanism of rat 5AR1 are unknown but are thought to involve subtle differences in its NADP[H]-binding site.

To date a consensus NADP[H]-binding site for 5AR has not been described. Studies of naturally occurring mutations in the human SRD5AR2 gene have tentatively identified seven amino acids thought to contribute to this binding[63]. These residues are:

- Arginine (R) 145
- Arginine 171

- Proline (P) 181
- Glycine (G) 183
- Asparagine (N) 193
- Glycine 196
- Arginine 246

All of these residues except R145 show strict conservation in rat, human and monkey 5AR[115]. Unlike the other three isoenzymes (human 5AR1 and 5AR2 and rat 5AR2), all of which have an arginine at positions analogous to R145 in human 5AR2, rat 5AR1 has a cysteine at this position. It has been suggested this cysteine may be associated with the differences in Finasteride binding exhibited by rat 5AR1[115].

To determine if in fact cysteine 146 is at least partly associated with the difference in Finasteride binding, the analogous residues R150 and R145, in human 5AR1 and 5AR2 respectively, were mutated to cysteine using site-directed mutagenesis. For this the 5AR1 and 5AR2 cDNAs sub-cloned into the pCI-neo expression vector were mutated to give mutants named 5AR1RC and 5AR2RC respectively.

The commercially available Quickchange™ site-directed mutagenesis kit (Stratagene) was used for this site-directed mutagenesis and subsequently to create all human 5AR mutants used in this study. *In vitro* site-directed mutagenesis is frequently used to study protein structure-function relationships and to identify intramolecular regions or amino acids mediating function. Most methods for site-directed mutagenesis require single-stranded DNA (ssDNA) templates and are usually very labour intensive and difficult to perform[140]. For these reasons Stratagene developed the Quickchange™ site-directed mutagenesis kit, a non-PCR method claimed to be fast and easy to use enabling highly efficient site-directed mutagenesis to be performed in a single day. It was also claimed that with this kit >80% efficiency of mutagenesis is achievable and the potential for unwanted second site mutations diminished.

The Quickchange™ procedure[140] uses a supercoiled double stranded DNA (dsDNA) template and two synthetic oligonucleotide primers complementary to

opposite strands of the vector and which contain the desired mutation. Primer extension during temperature cycling is achieved using of *Pfu* DNA polymerase. This generates copies of the plasmid by linear amplification whilst at the same time incorporating the mutation of interest. Although the primers can sit down on each mutant strand, the direction in which they can extend only allows for extension of the parental strand and therefore no re-amplification occurs. Treatment of the reaction after temperature cycling with *Dpn I* endonuclease digests the parental DNA template strand and this selects for the newly synthesised DNA containing the desired mutation. DNA isolated from almost all *E.coli* is *dam* methylated and is therefore digested by *Dpn I*, which is specific for methylated, and hemimethylated DNA. The parental strand DNA was isolated from DH5α *E.coli* and as all DNA isolated from *E.coli* is *dam* methylated, the parental strand is susceptible to digestion by *Dpn I*. The newly synthesised DNA is cloned and not isolated from *E.coli* therefore it is not methylated nor susceptible to digestion by *Dpn I*. Following treatment of the mutagenesis reaction mixture with *Dpn I*, an aliquot is transformed, by heat pulsing, into Epicurian Coli XL-1 Blue supercompetent *E.coli*.

The Quickchange™ method had only recently been introduced when this project commenced. It was considered therefore that replacement of arginine by cysteine in the cDNAs for human 5AR1 and 5AR2 would enable both familiarisation with the method and assessment of this change on Finasteride binding.

As replacing arginine with cysteine involved only a single amino acid substitution, this was thought suitable to test this newly available method. To effect this change required mutation of only one nucleotide in 5AR1 and two nucleotides in 5AR2. Mutant clones obtained were fully sequenced both to identify the presence of the desired mutation and to ensure unexpected changes had not been incorporated into the entire cDNA. Mutant cDNAs then were stably transfected into Chinese hamster ovary (CHO) cells, which were used for the studies of Finasteride inhibition.

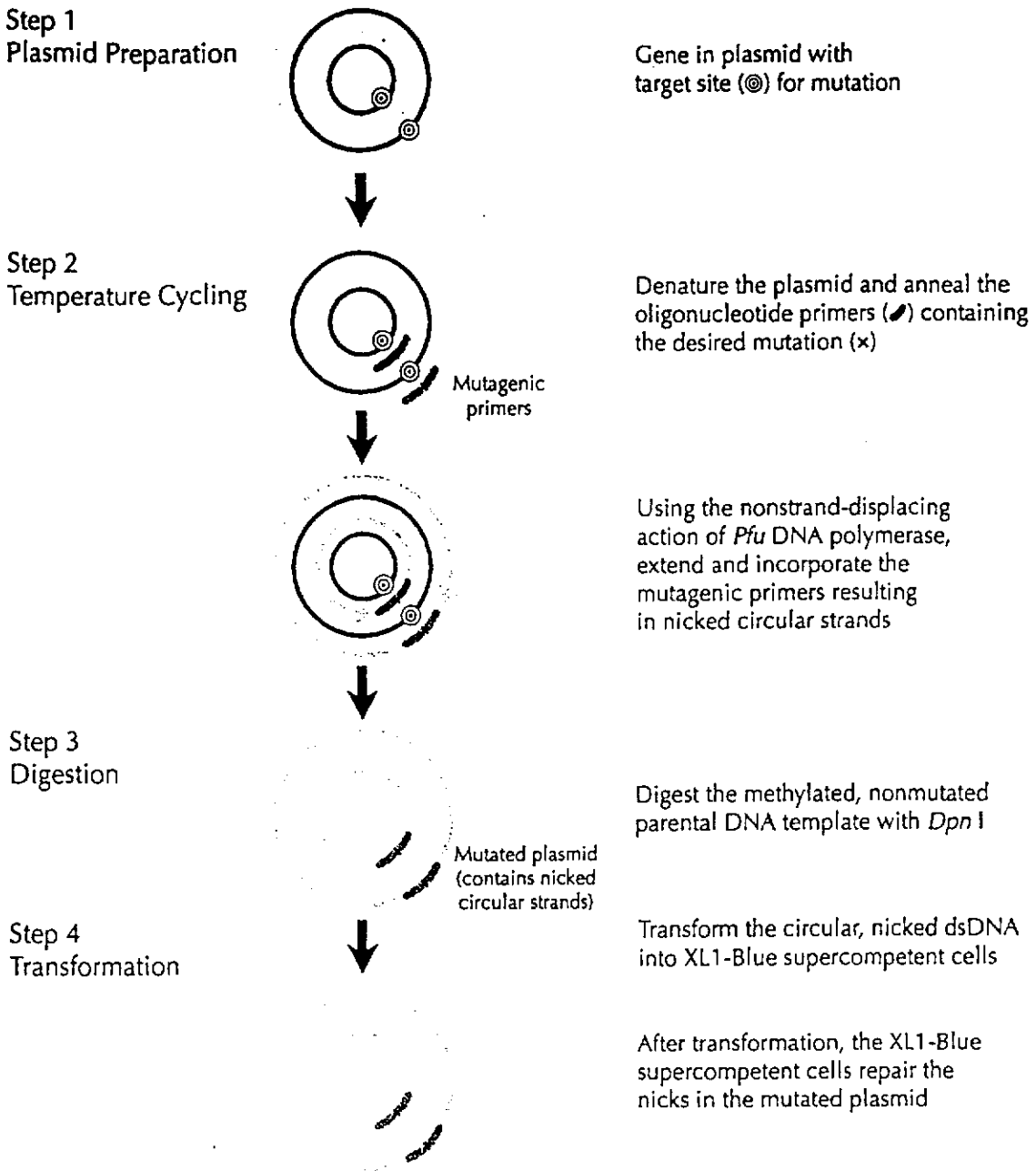

Figure 4.1 *The Quickchange™ mutagenesis procedure[140].*

4.2 METHODS

4.2.1 PLASMID DNA EXTRACTION

The BRESAspin™ Plasmid Mini Kit (Bresatec) was used to extract all plasmid DNA using the method described in section 3.2.1.1.

4.2.2 SITE-DIRECTED MUTAGENESIS

4.2.2.1 *Reaction Components*

Two complementary oligonucleotide primers containing the desired mutation and flanked by unmodified nucleotide sequences were synthesized and purified by reverse phase liquid chromatography to ensure maximal efficiency of mutagenesis. The sample reaction was set up by adding 125ng of both forward and reverse oligonucleotide primers to 50-100ng of dsDNA template, 5μL of 10X reaction buffer, 1μL of dNTPs (10mM) and sufficient sterile high pure water to give a final concentration of 1X reaction buffer. 1 μL of native *Pfu* DNA polymerase (2.5U/ μL) was added before thermocycling.

4.2.2.1a Primers

DNA sequences for the 5AR1RC and 5AR2RC mutagenesis primers, which were synthesized by Operon Technologies (California), are given below with mutated residues in bold type.

5AR1RC Primer Pair

5'- ^{146}GTA ACA GAT CCC **T**GT TTT CTA ATA GGT TTT GGC^{156} -3'

5'- ^{146}CAT TGT CTA GGG **A**CA AAA GAT TAT CCA AAA CCG^{156} -3'

5AR2RCF Primer Pair

5'- ^{140}TGG TAC ACA GAC ATA **T**GT TTT AGC TTG GG^{149} -3'

5'- ^{140}ACC ATG TGT CTG TAT ACA AAA TCG AAC CC^{149} -3'

4.2.2.1b pWhitescript™ mutagenesis control

The pWhitescript control was cycled to ensure the mutagenesis kit was functioning as specified by the manufacturer. For this the reaction mix listed below was prepared.

5μL	10X reaction buffer
2μL	pWhitescript™ 5.7kb control plasmid (10ng)
1.25μL	oligonucleotide control primer#1 (125ng) (5'-CCA TGA TTA CGC CAA GCG CGC AAT TAA CCC TCA C -3')
1.25μL	oligonucleotide control primer#2 (125ng) (5'- GTG AGG GTT AAT TGC GCG CTT GGC GTA ATC ATG G -3')
1μL	dNTPs
39.5μL	sterile hpH_2O
50μL	

* Add 1 μL of native *Pfu* DNA polymerase (2.5U/ μL), prior to cycling.

4.2.2.2 Cycling Conditions

Each mutagenesis reaction was cycled according to the cycling parameters outlined by the manufacturer (Table 4.2.2.2a).

Step	Number of Cycles	Temperature	Time
1	1	95°C	30 seconds
2	12-18**	95°C	30 seconds
3	12-18**	55°C	1 minute
4	12-18**	68°C	2minutes/kb of plasmid length

Table 4.2.2.2a *Cycling Parameters for the Quickchange™ Site-Directed Mutagenesis Method*

** The cycle number for steps 2-4 was adjusted in accordance with the type of mutation desired (Table 4.2.2.2b)

Type of mutation desired	Number of cycles
Point mutations	12
Single amino acid changes	16
Multiple amino acid deletions or insertions	18

Table 4.2.2.2b *Cycle Numbers for Types of Mutations Desired*

* Following cycling, reactions were cooled to 37°C by placing them on ice or more commonly, stored at 4°C overnight

The 5AR1RC and 5AR2RC mutagenesis reactions were cycled as below:

1. 1 cycle at 95°C for 30 seconds.
2. 16 cycles at 95°C for 30 seconds.
3. 16 cycles at 55°C for 1 minute.
4. 16 cycles at 68°C for 14 minutes.
5. 4°C overnight.

The pWhitescript mutagenesis control was cycled as below:

1. 1 cycle at 95°C for 30 seconds.
2. 12 cycles at 95°C for 30 seconds.
3. 12 cycles at 55°C for 1 minute.
4. 12 cycles at 68°C for 12 minutes.
6. 4°C overnight.

4.2.2.3 Product Digestion and Transformation into Bacteria

Following cycling, 1μL of *Dpn I* restriction enzyme (10U/μL) was added directly to each sample and control amplification reaction before mixing and centrifugation at 13000rpm for 1 minute. Reactions were then incubated at 37°C for 1 hour and stopped by immediately placing reaction tubes on ice.

Epicurian Coli XL1-Blue supercompetent cells were gently thawed on ice before placing 50μL into a prechilled Falcon® 2059 polypropylene tube. *Dpn I*-treated DNA from each sample or control reaction (1μl) was added to a separate aliquot of bacteria, mixed by gently swirling and incubated on ice for 30 minutes. The transformation reactions were heat-pulsed at 42 °C for 45 seconds to transfer the plasmid DNA into the bacterial cells. Reactions were then immediately placed on ice for 2 minutes before the addition of 0.5mL of NZY+ broth, preheated to 42 °C and incubation at 37 °C for 1 hour with shaking. The entire volume of each sample transformation was plated onto LB agar plates containing ampicillin (100μg/mL) and incubated at 37 °C for >16 hours. The pWhitescript™ control transformation mixture (250μL) was plated onto LB plates containing ampicillin (100μg/mL), X-gal (100μg/mL) and IPTG (100μg/mL) then incubated as above.

4.2.2.4a pUC18 Transformation Control

To establish if the transformation procedure was working effectively, the pUC18 transformation control was performed in parallel. For this, 1μL of the pUC18 control plasmid was added to 50μL of Epicurian Coli XL1-Blue supercompetent

cells. These cells were then transformed as described in section 4.2.2.4 and 5μL of the pUC18 control plated onto LB plates containing ampicillin (100μg/mL), X-gal (100μg/mL) and IPTG (100μg/mL), before incubating at 37^{O}C for >16 hours.

4.2.3 DNA SEQUENCING FOR MUTATION IDENTIFICATION

All DNA sequencing was performed (Royal Perth Hospital Immunology Department) using the dideoxytermination method and an ABI Prism automated DNA sequencer. Sequencing was performed not only to ensure the desired mutations had been made, but also to ensure integrity of the entire cDNA was maintained following mutagenesis. Sequencing primers were specifically designed for the multiple cloning site of the pCI-neo expression vector (T7EEV) and for the two 5AR cDNAs. Primers were synthesized by Operon Technologies (California) and their sequences are listed below.

T7EEV Sequencing Primer
5'- AAG GCT AGA GTA CTT AAT ACG A -3'

AR1RC Sequencing Primer
5'- ^{84}AAC TGC ATC CTC CTG GC^{89} -3'

AR2RC Sequencing Primer
5'- ^{78}CCA CCT GGG ACG GTA CTT^{83} -3'

4.2.4 CALCIUM PHOSPHATE TRANSFECTION

Calcium phosphate transfection of CHO cells with pCI-neo vector containing either the 5AR1RC or 5AR2RC mutant cDNA was as described in section 3.2.12.

4.2.5 CHARACTERISATION OF STABLY TRANSFECTED CELLS - 5α- REDUCTASE ACTIVITY ASSAYS

Determination of the 5AR activity of transfected cells and of Km, Vmax, Ki, pH optima, total protein assays and cell culture procedures were as described in sections 3.2.14 to 3.2.16.

4.2.5.1 Characterisation of Stably Transfected Cells - Time Dependence of Inhibition

These studies were performed to determine if Finasteride inhibits the 5AR1RC and 5AR2RC mutant cDNAs in a time dependent manner. Cells expressing wild type isoenzymes were also assayed for comparison. Cells were incubated with medium containing ^{3H}T (5nM), 0.5μM unlabelled testosterone for 5AR1 and 0.1μM for 5AR2, 0nM or 50nM Finasteride for 5AR1 and 0nM or 10nM for 5AR2. 3mL of medium was added per well of a 24 well tray and a 300μL aliquot removed following 2.5, 5, 10, 30, 45, 60, 80 and 110 minutes incubation. Each aliquot was then extracted with ether and chromatographed as described in section 3.2.14.1 to determine 5AR activity. Conversion of T to DHT vs time was plotted in both the absence and presence of Finasteride and the time dependence of inhibition determined.

4.2.5.2 Characterisation of Stably Transfected Cells - Reversibility of Inhibition

To determine if removal of Finasteride reversed its inhibitory effects on wild type and mutant cells lines, cells were incubated with medium containing ^{3H}-T (5nM), 0.5μM unlabelled T for 5AR1 and 0.1μM for 5AR2, and 0nM or 50nM Finasteride for 5AR1 and 0nM or 10nM for 5AR2. 3mL of media was added per well of a 24 well tray and 300μL aliquots removed at 2.5, 5, 10, 15, 30, 45 and 60 minutes. At 60 minutes remaining media was removed and cells were then incubated with 3mL of media containing ^{3H}-T and unlabelled T only again with removal of 300μL aliquots at each time interval as before. All aliquots were extracted with ether and subjected to thin layer chromatography as described in section 3.2.14.1. Conversion of T to DHT versus time was plotted and the

reversibility of inhibition determined.

4.3 RESULTS

4.3.1 Site-directed mutagenesis of Wild Type 5AR1 and 5AR2 cDNAs

Using the Quickchange™ site-directed mutagenesis kit and appropriate oligonucleotide primers, the 5AR1RC and 5AR2RC mutant cDNAs were created and sequenced for the presence of the desired mutation. Bacterial colony numbers resulting from each transformation reaction are given in Table 4.3.1. Blue/white selection of the pWhitescript mutagenesis and pUC18 transformation controls are demonstrated in Figures 4.3.1a and 4.3.1b respectively. Sequences of the mutants 5AR1RC and 5AR2RC showing the presence of the desired mutations are shown in Figures 4.3.1c and 4.3.1d respectively. No mutations other than those expected are seen in either of the cDNAs.

Mutation	**Transformation colony numbers**
pWhitescript mutagenesis control	222 colonies (8 white, 214 blue phenotype)
pUC18 transformation control	>250 colonies (>98% blue phenotype)
5AR1RC	>250
5AR2RC	18

Table 4.3.1 *Ampicillin resistant colony numbers resulting from the transformation of pWhitescript and pUC18 controls and 5AR1RC and 5AR2RC mutagenesis reactions.*

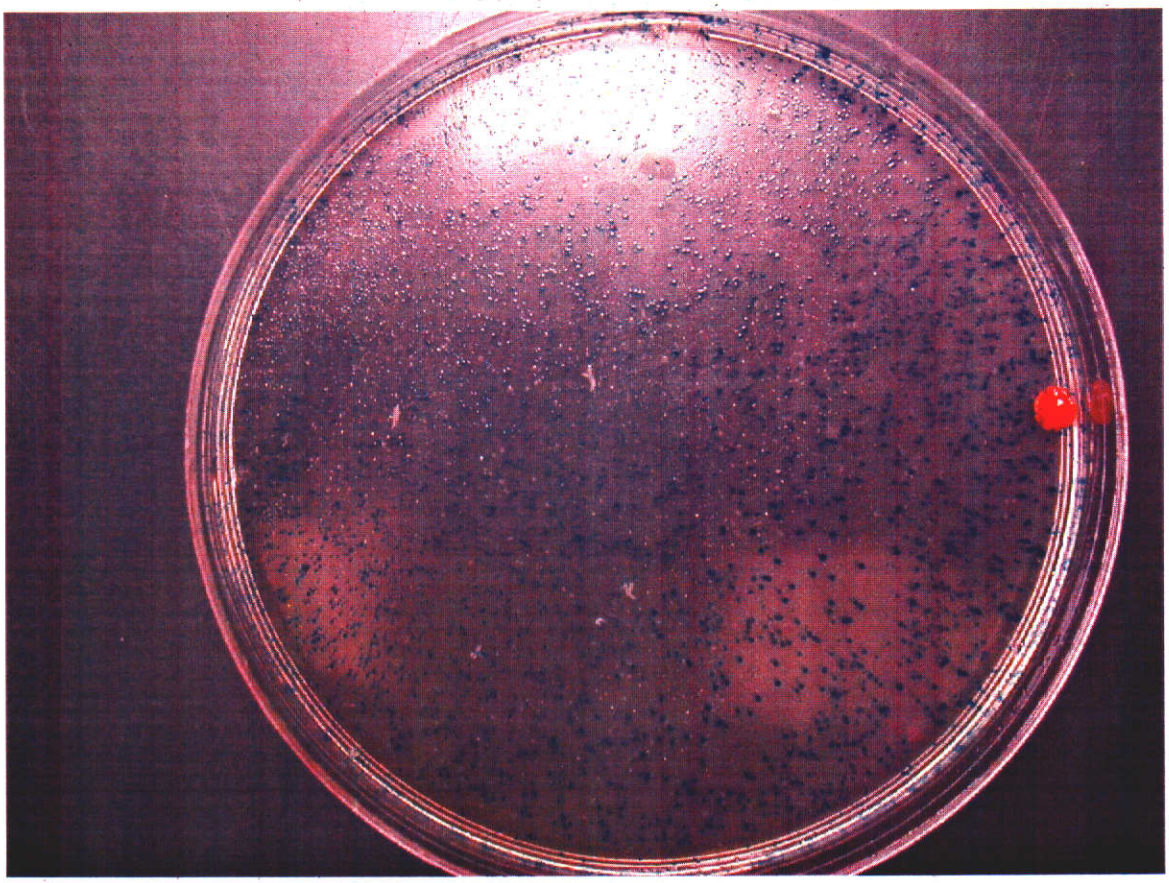

Figure 4.3.1a *Blue/White selection of pWhitescript mutagenesis control, 222 colonies were evident upon transformation of which 214 expressed a blue phenotype giving a mutagenesis efficiency of 96%. These results are in accordance with the manufacturer's recommendations.*

Figure 4.3.1b *Blue/White selection of pUC18 transformation control. On transformation, >250 colonies were seen of which >98% expressed a blue phenotype. These results are in agreement with the recommendations of the manufacturer of the method.*

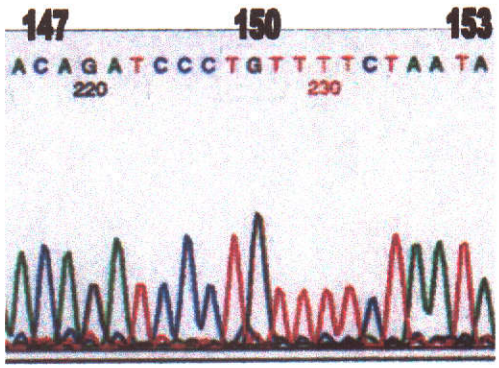

Figure 4.3.1c *DNA sequence chromatograph of 5AR1RC mutant clone using T7EEV primer. Residue 150 has been mutated from -CGT- to -**T**GT- and now codes for cysteine. The entire cDNA sequence is given in appendix A and shows no other alterations to the wild type cDNA have occurred.*

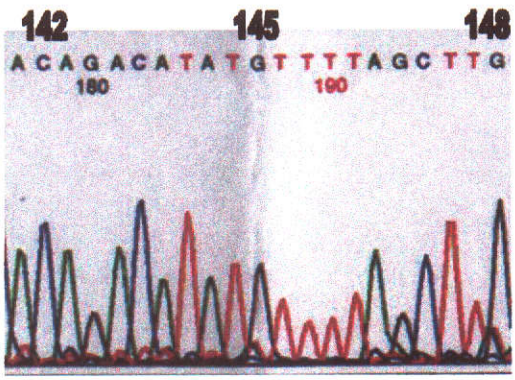

Figure 4.3.1d *DNA sequence chromatograph of 5AR2RC mutant clone using T7EEV primer. Residue 145 has been mutated from -CGG- to -**T**GT- and now encodes cysteine. The entire cDNA sequence is given in appendix A and shows no other alterations to the wild type cDNA have occurred.*

4.3.2 Characterisation of Stably Transfected Cells - Km and Vmax

Comparisons of Figures 3.3.8a and 3.3.8b with Figure 4.3.2a shows the arginine to cysteine mutation at residue 150 for 5AR1 and residue 145 for 5AR2, did not change the Km for either enzyme. (*Nb*. All Km values are the calculated mean plus or minus the standard deviation). The Vmax value for 5AR2RC was more than double that of wild type 5AR2, whereas that of 5AR1RC remained unaltered, indicating the mutations did not disrupt enzyme conformation.

A

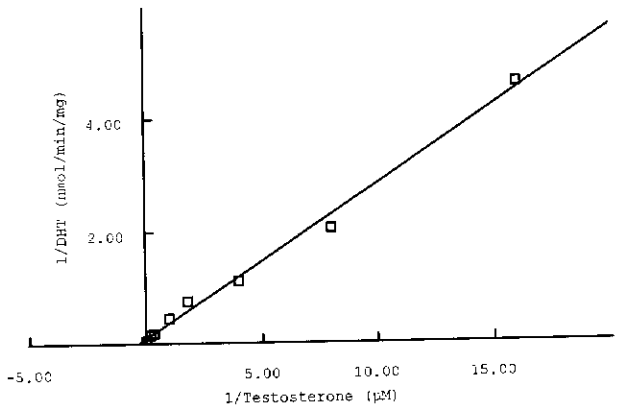

B

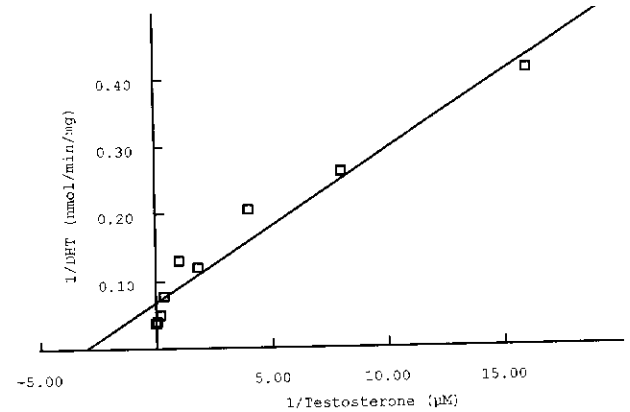

Figure 4.3.2a *Lineweaver-Burke plot of 5AR1RC (A) or 5AR2RC (B) transfected CHO cells, each derived from 2 separate experiments. Km and Vmax values were 2.3±1.5μM and 8.8nmol of DHT/min/mg of cell protein (A) and 0.3±0.03μM and 14.0nmol of DHT/min/mg of cell protein (B).*

4.3.3 Characterisation of Stably Transfected Cells - Inhibitor Studies

Figure 4.3.3a shows the inhibitor plots for the 5AR1RC and 5AR2RC mutants. In comparison with the wild type isoenzymes a 2.5-fold decrease in Ki was seen for the 5AR1RC mutant, whereas the Ki of the 5AR2RC mutant was not affected.

C

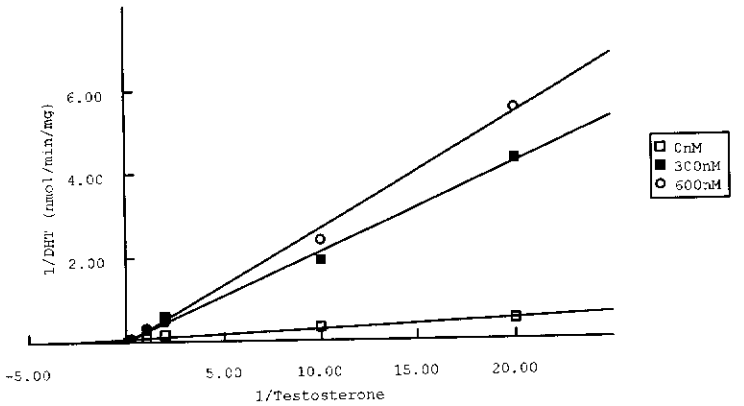

D

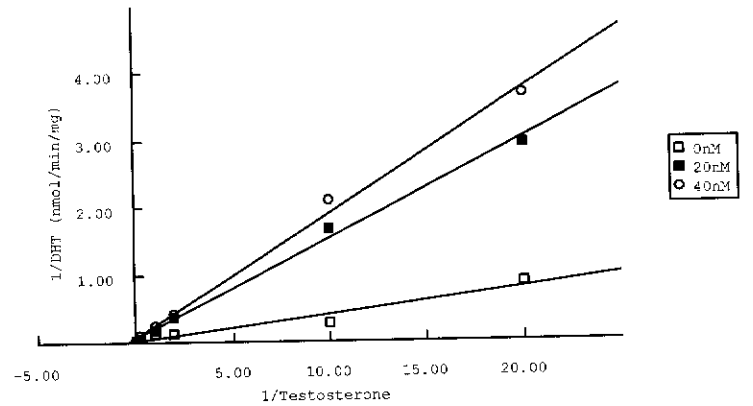

Figure 4.3.3a *Inhibitor plots for cells stably transfected with 5AR1RC (C) or 5AR2RC (D). 5AR1RC transfected cells were incubated at 0, 300 and 600nM Finasteride and a Ki of 131.0nM was obtained. 5AR2RC transfected cells were incubated at 0, 20 and 40nM Finasteride with a Ki of 15.6nM obtained.*

4.3.4 Characterisation of Stably Transfected Cells - Time Dependence of Inhibition

Assessments of time dependence of Finasteride inhibition for CHO cells stably transfected with wild type and mutant 5ARs are shown respectively in Figures 4.3.4a and 4.3.4b. Finasteride inhibited both wild type enzymes and the 5AR1RC and 5AR2RC mutants in a time dependent manner.

E

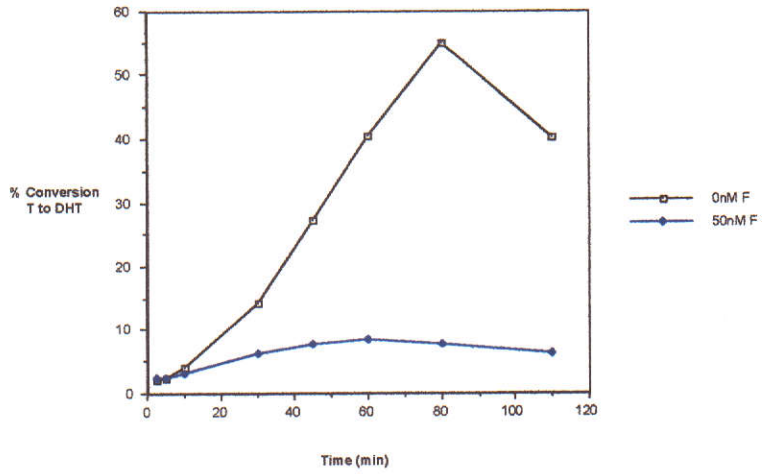

F

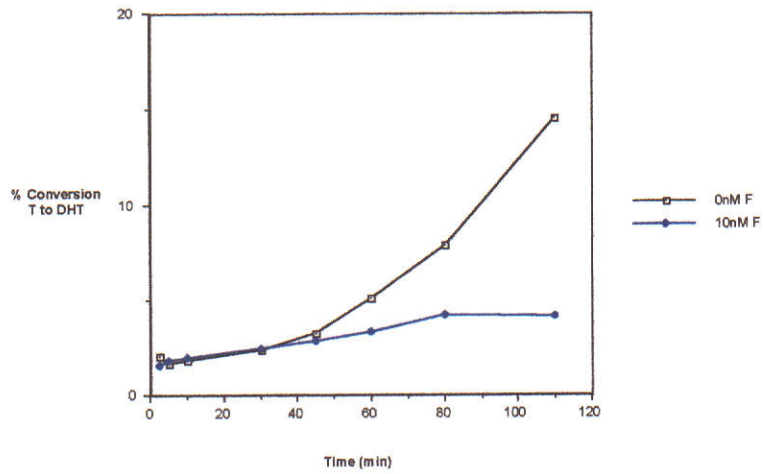

Figure 4.3.4a CHO cells stably transfected with wild type 5AR1 (E) were incubated with 0.5μM T and 0 or 50nM Finasteride. Cells transfected with wild type 5AR2 (F) were incubated with 0.1μM T and 0 or 10nM Finasteride. Aliquots were withdrawn at 2.5, 5, 10, 30, 45, 60, 80 and 120 minutes

then assayed for 5AR activity. As is shown Finasteride inhibits both 5AR1 and 5AR2 in a time dependent manner.

G

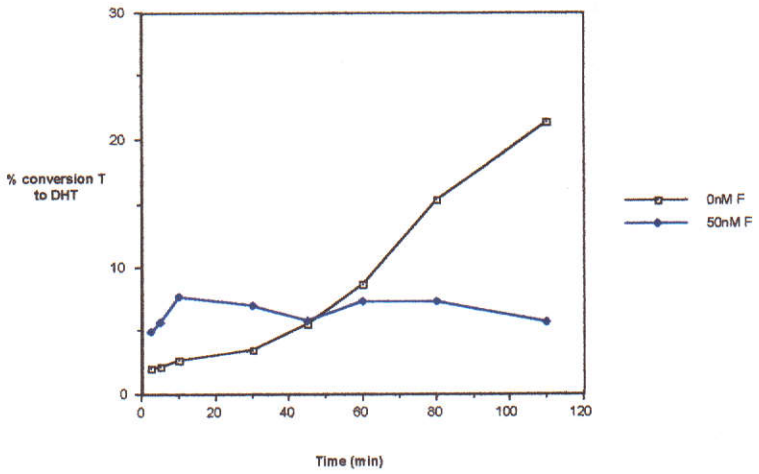

H

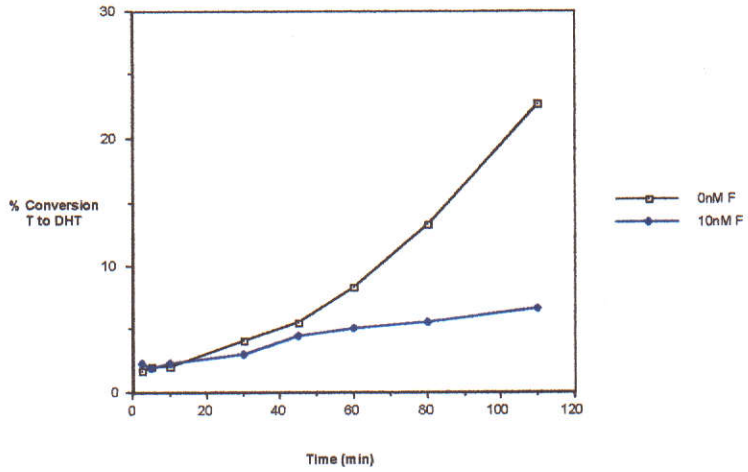

Figure 4.3.4b *CHO cells stably transfected with 5AR1RC (G) were incubated with 0.5μM T and 0 or 50nM Finasteride. Cells transfected with 5AR2RC were incubated with 0.1μM T and 0 or 10nM Finasteride. Aliquots were withdrawn at 2.5, 5, 10, 30, 45, 60, 80 and 120 minutes and assayed for 5AR activity. As with the wild type enzymes, time dependent inhibition of the 5AR1RC and 5AR2RC mutants by Finasteride was seen.*

4.3.5 Characterisation of Stably Transfected Cells - Reversibility of Inhibition

Transfected cells were incubated in media both with and without Finasteride and aliquots withdrawn at each time interval. Following 60 minutes incubation remaining media was removed and replaced with media without Finasteride. Aliquots were again removed and 5AR activity determined. Plots of time versus % conversion of T to DHT were obtained and the ability of 5AR to recover from the inhibitory effects of Finasteride determined (Figures 4.3.5a and 4.3.5b).

I

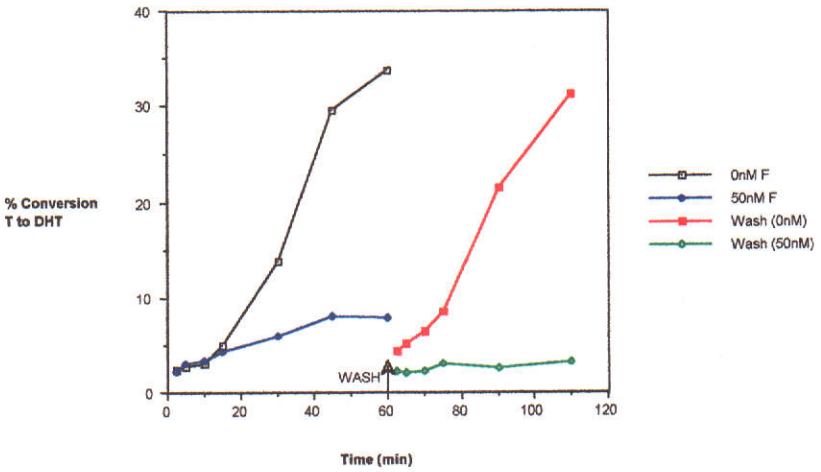

J

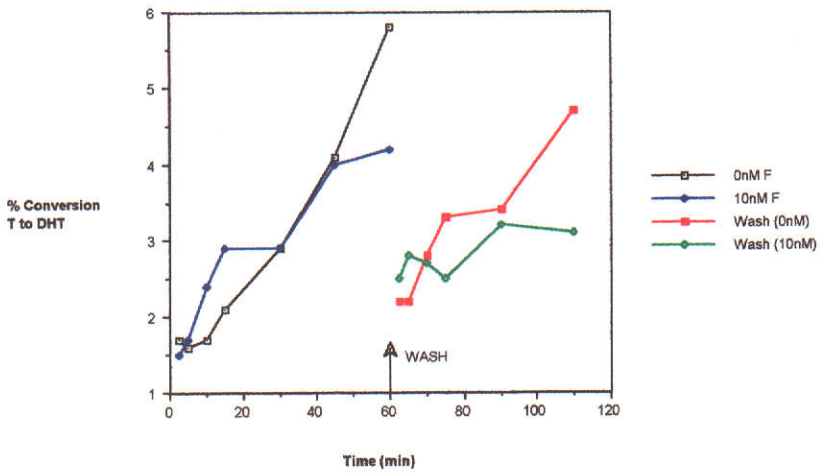

Figure 4.3.5a *CHO cells transfected with wild type 5AR1 (I) were incubated with 0.5μM T and 0 or 50nM Finasteride. Cells transfected with wild type 5AR2 (J) were incubated with*

0.1μM T and 0 or 10nM F. At 60 minutes, fresh media containing no Finasteride (wash) was added to all cells and the ability of 5AR1 and 5AR2 to recover from the inhibitory effects of Finasteride determined. Irreversible inhibition of both 5AR1 and 5AR2 by Finasteride is clearly demonstrated.

K

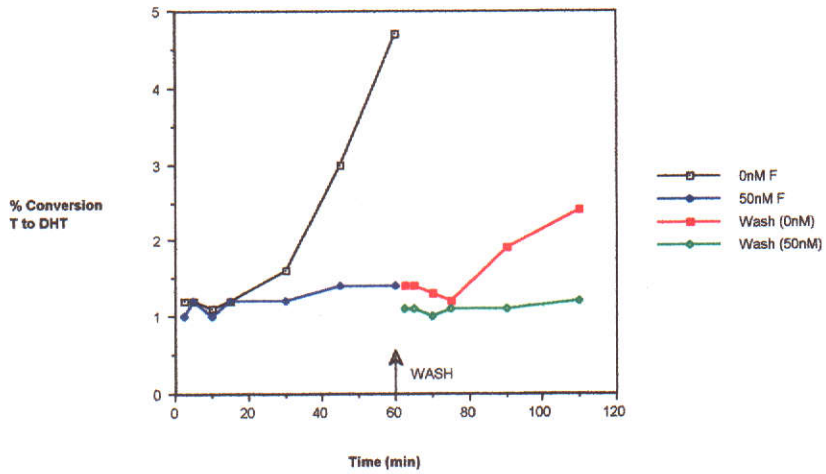

L

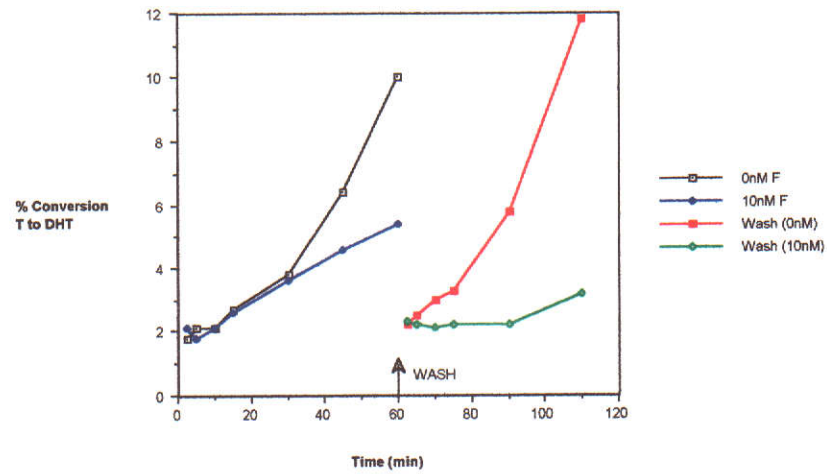

Figure 4.3.5b *5AR1RC transfected CHO cells (K) were incubated with 0.5μM T and 0 or 50nM F. 5AR2RC transfected CHO cells (L) were incubated with 0.1μM T and 0 or 10nM Finasteride. At 60 minutes, fresh media containing no Finasteride (wash) was added to all cells and the ability of the expressed 5AR1RC and 5AR2RC mutants to recover*

from the inhibitory effects of Finasteride determined. As with both wild type enzymes, the 5AR1RC and 5AR2RC mutants show irreversible inhibition by Finasteride.

CHO cells Expressing	Average % Conversion T to DHT	Km for T (μM)	Vmax (nmol/min/mg)	Vmax/Km	Ki for Finasteride (nM)	Time-Dependent Inhibition?	Reversible Inhibition?
CHO cell control	0.85	18.67±1.19	42.07	2.25	-	-	-
Wild Type 5AR1	3.5	2.8±0.6	9.4	3.36	327.8	Yes	No
5AR1RC	5.8	2.3±1.5	8.8	3.82	131.0	Yes	No
Wild Type 5AR2	20.8	0.5±0.3	6.6	13.20	11.8	Yes	No
5AR2RC	44.0	0.3±0.03	14.0	46.7	15.6	Yes	No

Table 4.3.2: *Comparisons of the characteristics of mutant and wild type 5α- reductase enzymes*

4.4 DISCUSSION

At the time these experiments were performed the Quickchange™ site-directed mutagenesis procedure was newly developed and required initial testing to determine its suitability for future experiments. The pWhitescript mutagenesis and pUC18 transformation controls were first performed to test the efficiency of the mutagenesis kit itself. The manufacturer state expected colony numbers are between 50 and 800 for the pWhitescript control with greater than 80% containing the mutation and expressing a blue phenotype on agar plates containing X-gal and IPTG. The pWhitescript control plasmid contains a stop codon (TAA) at amino acid nine where a glutamine codon (CAA) normally appears in the β- Galactosidase gene of the pBluescript II SK(-) phagemid[141]. The presence of this stop codon inactivates the β- Galactosidase gene producing white colonies in the presence of X-gal and IPTG. The control primers create a point mutation reversing the T residue of the stop codon back to a C residue reinstating the glutamine codon and β- Galactosidase gene

expression. When transformed into supercompetent *E.coli* and plated onto agar plates containing X-gal and IPTG, colonies expressing the mutation now appear blue.

The pWhitescript control yielded 222 colonies falling within the range stipulated by the manufacturer (50-800 colonies). Of these colonies only 8 expressed a white phenotype from which a mutagenesis efficiency (ME) of 96% can be calculated, which was again in accordance with manufacturer's specifications. The formula for calculating the ME is;

$$ME = \frac{\textit{Number of blue colony forming units (214)}}{\text{Total number of colony forming units (222)}} \textit{ X 100\%}$$

The pUC18 transformation control functions to assess the viability of the supercompetent *E.coli*, which are highly sensitive to small variations in storage temperature. Successful transformation of the pUC18 control reinforces viability of the supercompetent *E.coli* and should yield >250 colonies of which >98% express a blue phenotype upon transformation. Transformation of the pUC18 control yielded >250 colonies of which >98% expressed a blue phenotype, these results were in accordance with the manufacturer's specifications.

Once it had been established that the mutagenesis kit was functioning optimally it was decided to perform a simple mutation, namely the mutation of a single residue from arginine to cysteine, to determine the suitability of the procedure. Single amino acid mutations involve mutating up to three base pairs within a codon, such that it now encodes a different amino acid residue. The 5AR1 and 5AR2 DNA templates were cycled with oligonucleotide primers containing the necessary mutation for converting residues 150 and 145 respectively, from arginine to cysteine. For 5AR1 this required the changing of **C**GT to **T**GT (5AR1RC mutation) a single base pair change, while for 5AR2 two base pair changes were made, **CGG** to **TGT** (5AR2RC mutation). Following temperature cycling the reactions were digested with *Dpn I* and transformed into supercompetent *E.coli*. Colony numbers for 5AR1RC and 5AR2RC respectively were >250 and 18. Why the differences in colony number occurred is unknown,

initially it was thought possible that it could be due to having a single mutation in 5AR1RC and a double mutation in 5AR2RC. Subsequent experiments where larger numbers of colonies were obtained when mutating several bases indicate this is not a likely explanation.

From the 5AR1RC mutation 5 colonies were sent for sequence analysis while 10 were sent from the 5AR2RC mutation. In each case at least one clone with the desired mutation was identified. Sequencing of the entire cDNA of colonies containing the desired mutation showed no unwanted secondary mutations had occurred. These findings confirmed the ability of the Quickchange™ method to generate 5AR1 and 5AR2 mutants expressing the arginine to cysteine mutation only. This preliminary study demonstrated the effectiveness of the method and it was decided to continue with its use for future mutational experiments.

CHO cells stably transfected with calcium phosphate precipitates of the mutant 5AR1RC and 5AR2RC cDNAs were selected with geneticin (G418), the resistance to which is encoded by the pCI-neo vector into which the 5AR cDNAs were sub-cloned prior to mutagenesis. Many G418 resistant clones were produced for both mutant isoenzymes and those expressing greatest 5AR activity were expanded in tissue culture and the expressed enzyme kinetically characterised.

The affinity for (Km) and maximum velocity (Vmax) of the mutant enzymes with T as substrate were determined as was the inhibitory constant (Ki) for Finasteride and compared with corresponding values for the wild type enzymes. These characteristics were used as a basis for comparison of mutant isoenzymes and their wild type counterpart. The Km and Vmax calculated for 5AR1RC were 2.25±1.47μM and 8.79nmol DHT/min/mg respectively and closely resemble those of wild type 5AR1 (Km = 2.80±0.60μM, Vmax = 9.36nmol DHT/min/mg). The Ki for Finasteride of 5AR1RC although lower (Ki = 131.0nM) than the value obtained for wild type 5AR1 (Ki = 327.8nM), still falls within the range 100-620nM obtained by others[1, 37, 44, 128]. These findings indicate exchanging arginine for cysteine at residue 150 in 5AR1 does not alter either the Km for T or the Ki for Finasteride.

As the Vmax/Km ratios of the mutant (5AR1RC) and wild type enzyme (5AR1) were similar, 3.82 and 3.36 respectively, the mutation had no discernible effect on the efficiency of T to DHT conversion.

The Km, and Ki values derived for the 5AR2RC mutant of 0.32±0.03μM, and 15.6nM respectively, correlate well with those of wild type 5AR2 (Km = 0.45±0.31μM, Ki = 11.8nM). However, the Vmax of the 5AR2RC mutant (13.99nmol DHT/min/mg) was 2-fold greater than the Km for the wild type enzyme (6.58nmol DHT/min/mg). Comparison of the Vmax/Km ratios for mutant (5AR2RC) and wild type 5AR2, 46.7 and 13.2 respectively, shows the mutant to be more efficient than the wild type enzyme. In view of the similarities in the other characteristics assessed, it seems more likely this difference is due to variation in transfection efficiency rather than that the mutation of residue 145 from arginine to cysteine has significantly altered enzyme characteristics.

Rat 5AR1 expresses a cysteine at residue 146, unlike the strict conservation of arginine seen at the analogous residues in rat 5AR2 and both human 5ARs. Rat 5AR1 displays a unique mechanism of Finasteride inhibition in that it is both reversible and time-independent. Although it is thought cysteine 146 may contribute to its unique mechanism of inhibition[115] the studies reported here, admittedly on human enzymes, suggest this may not be the case.

As with wild type 5AR1, time dependent inhibition by Finasteride of the 5AR1RC mutant was seen. In the absence of Finasteride, 5AR activity levels for both wild type and mutant 5AR1 enzymes were seen to increase with time. In comparison, in the presence of 50nM Finasteride reduced activity was seen for wild type 5AR1 following 10 minutes incubation. For the 5AR1RC mutant this reduction in activity occurred slightly later at 45 minutes incubation. In contrast although time dependent inhibition by Finasteride was also seen for wild type 5AR2 and the 5AR2RC mutant, in the presence of 10nM Finasteride reduction in enzyme activity was seen earlier (30 minutes) in the mutated enzyme than in the wild type enzyme (45 minutes.). In the absence of Finasteride, levels of 5AR activity for both wild type and mutant 5AR2 again increased with time.

Irreversible inhibition by Finasteride was seen for both wild type 5AR1 and the 5AR1RC mutant. In the absence of Finasteride, cells expressing wild type 5AR1 demonstrated increased 5AR activity with time, whereas with 50nM Finasteride, 5AR activity was seen to diminish following 15 minutes incubation. After the wash step where all media was replaced with that not containing Finasteride, levels of 5AR activity did not recover to the levels of cells not exposed to Finasteride. Similar results were seen for cells expressing the 5AR1RC mutant with 5AR activity again diminishing after 15 minutes incubation with 50nMF and not recovering after replacement with media not containing Finasteride.

Irreversible inhibition by Finasteride was also seen for wild type 5AR2 and the 5AR2RC mutant. Cells expressing wild type 5AR2 demonstrated diminished 5AR activity in the presence of 10nM Finasteride following 15 minutes incubation. As before following the addition of media without Finasteride to cells previously exposed to 10nM Finasteride, levels of 5AR activity did not recover to those of cells not exposed to Finasteride. Similar results were seen for the 5AR2RC mutant, although levels of 5AR activity did not fall until 30 minutes incubation with 10nM Finasteride.

Substitution of cysteine for arginine at residues 150 and 145 in human 5AR1 and 5AR2 respectively, did not alter the time-dependent irreversible inhibition seen for the wild type enzymes. These studies do not substantiate the suggestion[115] that the replacement of arginine by cysteine at residue 146 in rat 5AR1 is responsible for its unique mechanism of inhibition by Finasteride. Exchanging the appropriate residues in rat 5AR1 and 5AR2 was not possible in this study, as the cDNAs for the rat enzymes were not available. However this particular region is highly conserved in the 5AR enzymes from all species, with the only variation being the R146C exchange in rat 5AR1. Thus if this R146C is significant for rat 5AR1 it is probable exchanging arginine for cysteine would have some demonstrable effect on 5AR from other species. This was not the case.

Chapter 5.0

Analysis of the Functional Importance of Glycine 39 and Histidine 236 in 5α- Reductase 1 and Glycine 34 and Histidine 231 in 5α- Reductase 2

5.1 INTRODUCTION

The enzyme 5α- Reductase (5AR) catalyses the conversion of testosterone (T) to dihydrotestosterone (DHT), with DHT mediating the embryonic development of the male external genitalia and prostate and maintaining their growth and integrity thereafter. Both DHT overproduction and underproduction have been associated with a number of endocrine abnormalities and disorders in man. DHT overproduction is implicated in the pathogenesis of benign prostatic hyperplasia (BPH), male pattern baldness (MPB), seborrhoea, acne, androgenic alopecia and possibly prostate cancer. DHT underproduction results in a rare form of male pseudohermaphroditism, termed 5AR deficiency, in which 46XY males fail to develop a prostate and present at birth with ambiguous genitalia resembling those of a female[1].

Following the expression cloning and isolation of the cDNAs for both human 5AR isoenzymes (5AR1 and 5AR2), it was determined mutations in the gene encoding 5AR2, the SRD5AR2 gene, were responsible for 5AR deficiency[32]. These mutations occur naturally and have been studied through their recreation in an expressible cDNA with subsequent transfection of and kinetic characterisation in mammalian cells[63]. Twenty-two mutations were characterised twelve of which resulted in complete enzyme inactivation and the remaining ten severely impaired enzyme activity by affecting either substrate or cofactor binding[63].

Mutations affecting cofactor binding, R145W, R171S, P181L, G183S, N193S, G196S, R246W and R246Q mutations have been shown to map to the carboxyl terminus of 5AR (Figure 5.1). In contrast two mutations primarily affecting substrate binding, the G34R and H231R mutations map to the amino and carboxyl termini respectively.

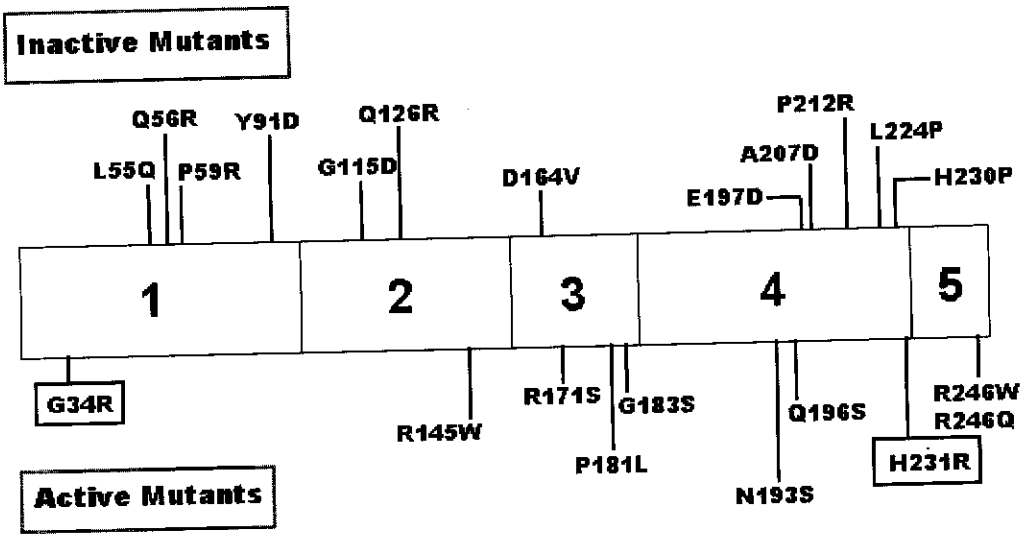

Figure 5.1: *Location of mutations inactivating or impairing 5AR2 activity*[63].

Studies by Wigley and colleagues (1994)[63] determined the affinity constants of the mutant enzymes for the natural substrate (T) and cofactor (NADP[H]). Although their pH optima and half-lives were determined, analysis of the interaction between the mutant enzymes and 5AR inhibitors, such as Finasteride, were not performed. Identification of individual residues that interact with inhibitors of 5AR may provide information useful for the production of new and improved inhibitors for the treatment of disorders associated with DHT overproduction. For this reason it was decided to recreate the G34R and H231R mutations in 5AR2 and determine their effects on inhibitor (Finasteride) binding using IC_{50} studies.

IC_{50} values indicate the concentration of inhibitor required to inhibit enzyme activity by 50%, at a fixed substrate concentration. These values are determined by incubating cells expressing 5AR with media containing a constant amount of substrate (typically 1μM unlabelled testosterone) in the presence of various concentrations of inhibitor (Finasteride, 0-5000nM) and

determining enzyme activity at each concentration of inhibitor. The effects of the various concentrations of inhibitor on enzyme activity are then evaluated to determine IC_{50} values.

Whether the G34R and H231R mutations have similar effects in human 5AR1 as in 5AR2 remains to be determined. G39 and H236 are the analogous residues in 5AR1 and determination of their relative contribution to substrate/inhibitor binding may facilitate the production of more efficient pharmacological inhibitors for the treatment of 5AR1-associated conditions such as male pattern baldness. Therefore G39 and H236 were both mutated to arginine, using site-directed mutagenesis with primers expressing the desired mutation. The affinity constant for T, IC_{50} for Finasteride and pH optima were determined for CHO cells stably expressing these mutant enzymes and compared with cells transfected with wild type 5AR1.

A significant reduction in substrate affinity in human 5AR2 is evident upon mutation of G34 to arginine[63]. Why this occurs is unknown but it is thought to relate to substitution of the smaller glycine residue with the bulkier and charged arginine. Assessment of the influences of size and charge on the reduced substrate binding due to the 5AR2G34R mutation was made from mutations of G34 to alanine, aspartate, glutamate, asparagine or glutamine. The effect of these mutations on inhibitor binding by 5AR2 also was assessed. Studies of similar substitution of the analogous residue G39 in 5AR1 were also performed.

5.2 METHODS

5.2.1 PLASMID DNA EXTRACTION

The BRESAspin^{TM} Plasmid Mini Kit (Bresatec) was used to extract all plasmid DNA, as described in section 3.2.1.1.

5.2.2 SITE-DIRECTED MUTAGENESIS

5.2.2.1 Reaction Components

Each reaction was set up as described section 4.2.2.1. Reaction components used in each reaction were:

5μL	10X Reaction buffer
75ng	dsDNA template **
125ng	Oligonucleotide forward primer
125ng	Oligonucleotide reverse primer
1μL	dNTPs (10mM)
XμL	Sterile hpH_2O
50μL	

* 1μL of native Pfu DNA polymerase (2.5U/μL) was added prior to cycling.

** 75ng of template DNA was cycled for all reactions except the 5AR1G39D, 5AR2G34R and 5AR2H231R reactions for which 50ng was cycled.

Nb. As each primer preparation had a different concentration, the amount rather than volume of primer used is given. The value of XμL for the volume of water used reflects the different volumes of primer solution added.

5.2.2.1a Primers

DNA sequences for the various mutagenesis primers are given below with mutated residues in bold type. All primers were synthesized by Life Technologies (Queensland).

5AR1G39A Primer Pair
5'- ^{34}CG AAC TCA GTG TAC **GCC** CGC CAC GCG C^{43} -3'
3'- ^{34}GC TTG AGT CAC ATG **CGG** GCG GTG CGC G^{43} -5'

5AR1G39D Primer Pair
5'- ^{34}CG AAC TCA GTG TAC **GAC** CGC CAC GCG C^{43} -3'
3'- ^{34}GC TTG AGT CAC ATG **CTG** GCG GTG CGC G^{43} -5'

5AR1G39E Primer Pair
5'- ^{34}CG AAC TCA GTG TAC **GAA** CGC CAC GCG C^{43} -3'
3'- ^{34}GC TTG AGT CAC ATG **CTT** GCG GTG CGC G^{43} -5'

5AR1G39N Primer Pair
5'- ^{34}CG AAC TCA GTG TAC **AAC** CGC CAC GCG C^{43} -3'
3'- ^{34}GC TTG AGT CAC ATG **TTG** GCG GTG CGC G^{43} -5'

5AR1G39Q Primer Pair
5'- ^{34}CG AAC TCA GTG TAC **CAG** CGC CAC GCG C^{43} -3'
3'- ^{34}GC TTG AGT CAC ATG **GTC** GCG GTG CGC G^{43} -5'

5AR1G39R Primer Pair
5'- ^{34}CG AAC TCA GTG TAC **CGC** CGC CAC GCG C^{43} -3'
3'- ^{34}GC TTG AGT CAC ATG **GCG** GCG GTG CGC G^{43} -5'

5AR1H236R Primer Pair

5'- ^{231}GGT AGA GCA AAA GAG **CGT** CAT GAG TGG TAC CTC CGG^{242} -3'

3'- ^{231}CCA TCT CGT TTT CTC **GCA** GTA CTC ACC ATG GAG GCC^{242} -5'

5AR2G34A Primer Pair

5'- ^{30}CC TCC GGC TAC **GCG** AAG CAC ACG GAG AGC^{39} -3'

3'- ^{30}GG AGG CCG ATG **CGC** TTC GTG TGC CTC TCG^{39} -5'

5AR2G34D Primer Pair

5'- ^{30}CC TCC GGC TAC **GAC** AAG CAC ACG GAG AGC^{39} -3'

3'- ^{30}GG AGG CCG ATG **CTG** TTC GTG TGC CTC TCG^{39} -5'

5AR2G34E Primer Pair

5'- ^{30}CC TCC GGC TAC **GAA** AAG CAC ACG GAG AGC^{39} -3'

3'- ^{30}GG AGG CCG ATG **CTT** TTC GTG TGC CTC TCG^{39} -5'

5AR2G34N Primer Pair

5'- ^{30}CC TCC GGC TAC **AAC** AAG CAC ACG GAG AGC^{39} -3'

3'- ^{30}GG AGG CCG ATG **TTG** TTC GTG TGC CTC TCG^{39} -5'

5AR2G34Q Primer Pair

5'- ^{30}CC TCC GGC TAC **CAG** AAG CAC ACG GAG AGC^{39} -3'

3'- ^{30}GG AGG CCG ATG **GTC** TTC GTG TGC CTC TCG^{39} -5'

5AR2G34R Primer Pair

5'- ^{30}CCC TCC GGC TAC **CGG** AAG CAC ACG GAG^{38} -3'

3'- ^{30}GGG AGG CCG ATG **GCC** TTC GTG TGC CTC^{38} -5'

5AR2H231R Primer Pair

5'- ^{227}CGA GCT TTT CAC **CGC** CAT AGG TTC TAC C^{236} -3'

3'- ^{227}GCT CGA AAA GTG **GCG** GTA TCC AAG ATG G^{236} -5'

5.2.2.2 *Cycling Conditions*

All mutagenesis reactions were cycled as follows:

1. 1 cycle at 95^{O}C for 30 seconds.
2. 16 cycles at 95^{O}C for 30 seconds.
3. 16 cycles at 55^{O}C for 1 minute.
4. 16 cycles at 68^{O}C for 14 minutes.
5. 4^{O}C overnight.

5.2.2.3 *Product Digestion and Transformation into Bacteria.*

Dpn I digestion and transformation of each 5AR1 mutagenesis reaction into Epicurian supercompetent *E.coli* were as described in sections 4.2.2.3 and 4.2.2.4 respectively.

5.2.3 DNA SEQUENCING FOR MUTATION IDENTIFICATION

Automated DNA sequencing with primers specifically designed for the pCI-neo multiple cloning site and for each 5AR cDNA was as described in section 4.2.3.

For the 5AR1H236R and 5AR2H231R mutations clones expressing the desired mutation were initially identified by sequencing with the AR1H and AR2H primers. These primers were synthesised by Operon Technologies (California) and their DNA sequences are given below. Due to the limited read out of the sequencing method used, sequencing of the entire cDNA for clones expressing the 5AR1H236R and 5AR2H231R mutations required additional primers. These were the AR1R or AR2R primers and the T7EEV primer, the sequences of which are listed in section 4.2.3.

AR1H Sequencing Primer

5'- ^{168}CA GAT CAT ATC CTA AGG^{173} -3'

AR2H Sequencing Primer

5'- ^{166}ATA TTG CGC CAG CTC AG^{171} -3'

For all 5AR1G39 and 5AR2G34 mutations initial identification of clones expressing the desired mutation was achieved by sequencing with the T7EEV primer. Again due to the limited read out of the sequencing method used, clones expressing the desired mutation were then sequenced in their entirety using the AR1R and AR2R primers, for 5AR1 and 5AR2 clones respectively.

5.2.4 CALCIUM PHOSPHATE TRANSFECTION

Calcium phosphate transfection of CHO cells with pCI-neo vector containing mutated 5AR1 or 5AR2 cDNAs was as described in section 3.2.12.

5.2.5 CHARACTERISATION OF STABLY TRANSFECTED CELLS - 5α- REDUCTASE ACTIVITY ASSAYS

Determination of 5AR activity of transfected cells and of Km, Vmax, IC_{50}, pH optima, total protein assays and cell culture procedures were as described in sections 3.2.14 to 3.2.16.

5.3 RESULTS

5.3.1 Site-directed Mutagenesis of Wild Type 5AR1 and 5AR2 cDNAs

Mutations of the 5AR1 and 5AR2 cDNAs to give each of the 5AR1G39, 5AR1H236, 5AR2G34 and 5AR2H231 mutant cDNAs were made with the Quickchange^{TM} site-directed mutagenesis kit and appropriate oligonucleotide primers. Plasmid DNA isolated from ampicillin resistant bacteria from all

transformations (Table 5.3.1) was sequenced for the presence of the desired mutation. Sequence chromatographs for the various mutant cDNAs are shown in Figures 5.3.1a to 5.3.1n.

Mutation	Colony Numbers on Transformation
5AR1G39A	>250
5AR1G39D	>250
5AR1G39E	>250
5AR1G39N	>250
5AR1G39Q	>250
5AR1G39R	~100
5AR1H236R	2
5AR2G34A	100-200
5AR2G34D	150-200
5AR2G34E	>250
5AR2G34N	10
5AR2G34Q	>250
5AR2G34R	5
5AR2H231R	40

Table 5.3.1 *Ampicillin resistant colony numbers resulting from the transformation of the various mutagenesis reactions.*

Figures 5.3.1a to 5.3.1n show the sequences, which confirm that the various mutations have been achieved. For each mutation shown the entire sequence data is given in appendix A.

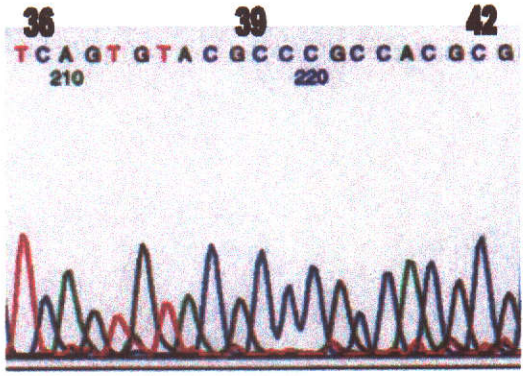

Figure 5.3.1a *Sequence chromatograph of 5AR1G39A mutant clone showing the mutation of glycine 39 (-GGC-) to alanine (-GCC-).*

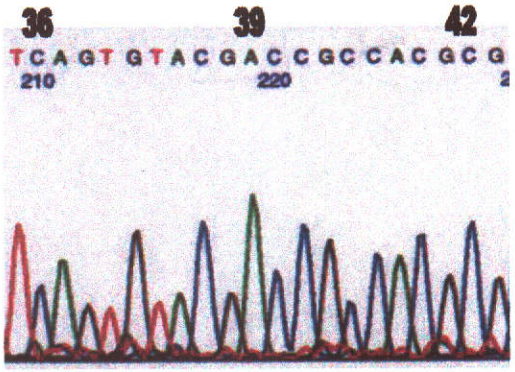

Figure 5.3.1b *Sequence chromatograph of 5AR1G39D mutant clone showing the mutation of glycine 39 (-GGC-) to aspartate* (-GAC-).

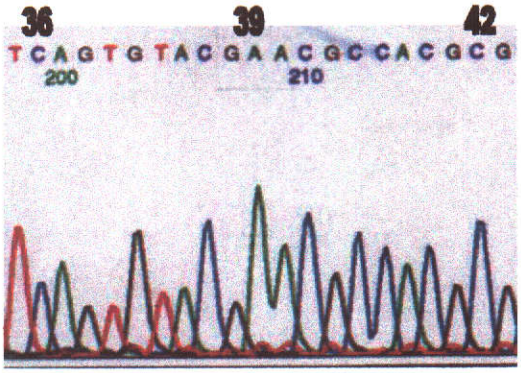

Figure 5.3.1c *Sequence chromatograph of 5AR1G39E mutant clone showing the mutation of glycine 39 (-GGC-) to glutamate (-**GAA**-).*

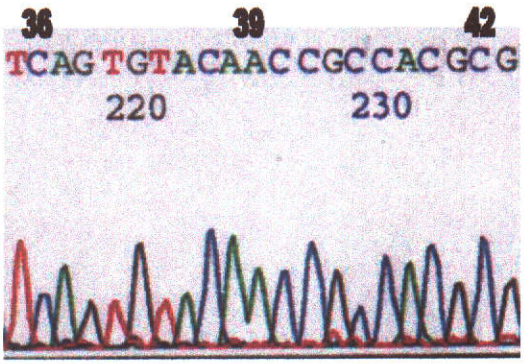

Figure 5.3.1d *Sequence chromatograph of 5AR1G39N mutant clone showing the mutation of glycine 39 (-GGC-) to asparagine (-**AAC**-).*

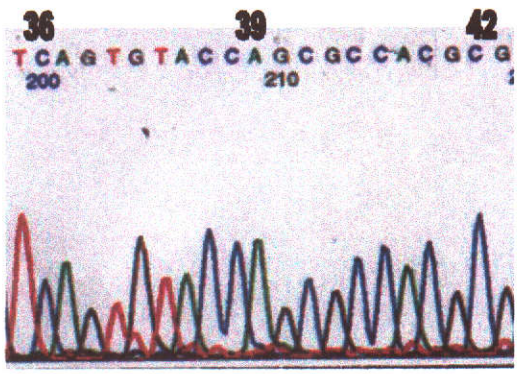

Figure 5.3.1e *Sequence chromatograph of 5AR1G39Q mutant clone showing the mutation of glycine 39 (-GGC-) to glutamine (-**CAG**-).*

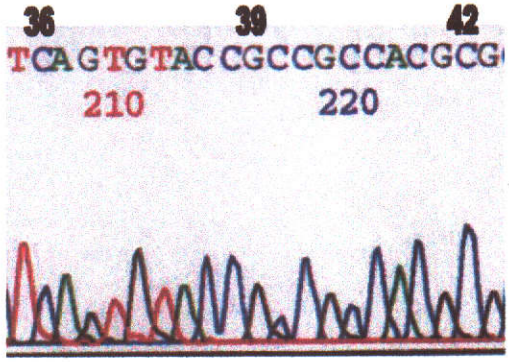

Figure 5.3.1f *Sequence chromatograph of 5AR1G39R mutant clone showing the mutation of glycine 39 (-GGC-) to arginine (-**C**GC-).*

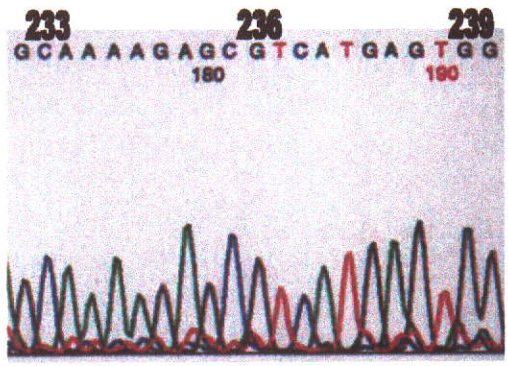

Figure 5.3.1g *Sequence chromatograph of 5AR1H236R mutant clone showing the mutation of histidine 236 (-GGT-) to arginine (-**C**GT-).*

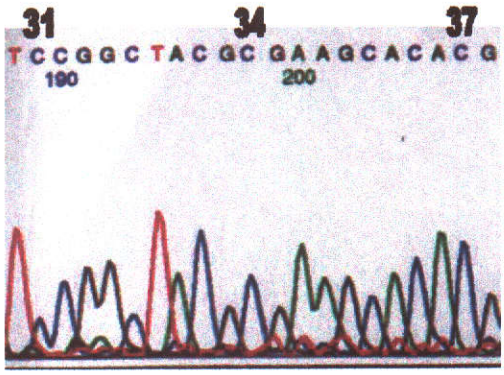

Figure 5.3.1h *Sequence chromatograph of 5AR2G34A mutant clone showing the mutation of glycine 34 (-GGG-) to alanine (-G**C**G-).*

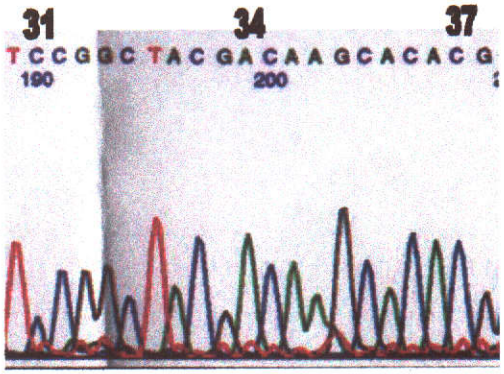

Figure 5.3.1i *Sequence chromatograph of 5AR2G34D mutant clone showing the mutation of glycine 34 (-GGG-) to aspartate (-**GAC**-).*

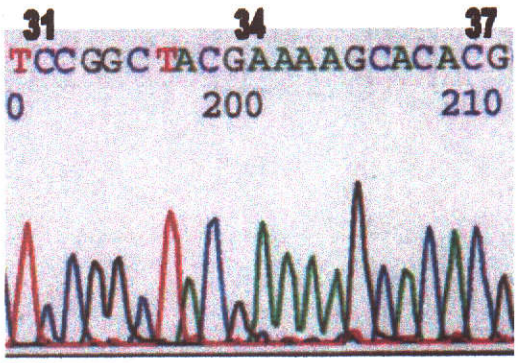

Figure 5.3.1j *Sequence chromatograph of 5AR2G34E mutant clone showing the mutation of glycine 34 (-GGG-) to glutamate* (-**GAA**-).

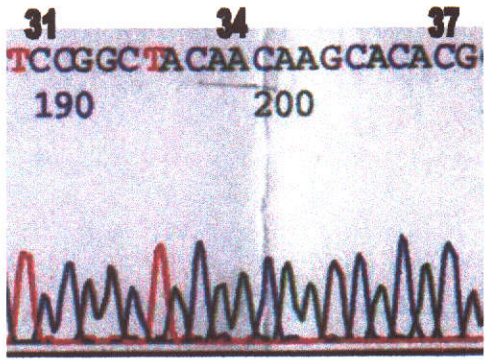

Figure 5.3.1k *Sequence chromatograph of 5AR2G34N mutant clone showing the mutation of glycine 34 (-GGG-) to asparagine (-**AAC**-).*

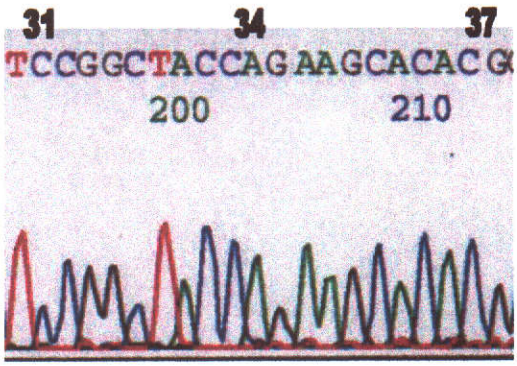

Figure 5.3.1l *Sequence chromatograph of 5AR2G34Q mutant clone showing the mutation of glycine 34 (-GGG-) to glutamine (-CAG-).*

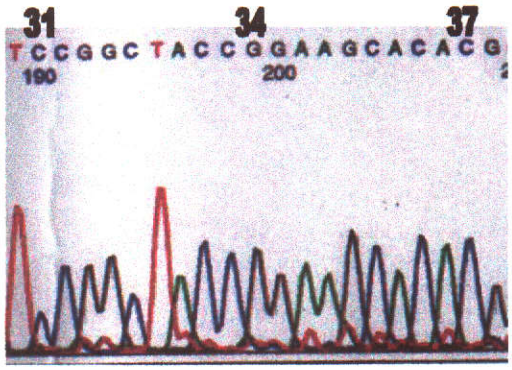

Figure 5.3.1m *Sequence chromatograph of 5AR2G34R mutant clone showing the mutation of glycine 34 (-GGG-) to arginine (-CGG-).*

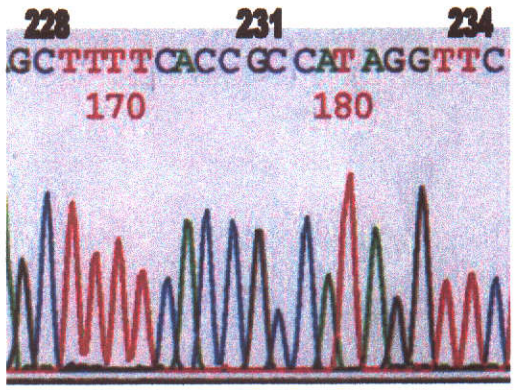

Figure 5.3.1n *Sequence chromatograph of 5AR2H231R mutant clone showing the mutation of histidine 231 (-CAC-) to arginine (-CGC-).*

5.3.2 Characterisation of Stably Transfected Cells - Km and Vmax Studies

The affinity constants (Km) and maximum velocities (Vmax) for cells stably expressing each of the mutant cDNAs were determined as described in section 3.2.14.2. Figures 5.3.2a to 5.3.2h are the Lineweaver-Burke plots from which these values were determined, all Km values are the calculated mean plus or minus the standard deviation.

A

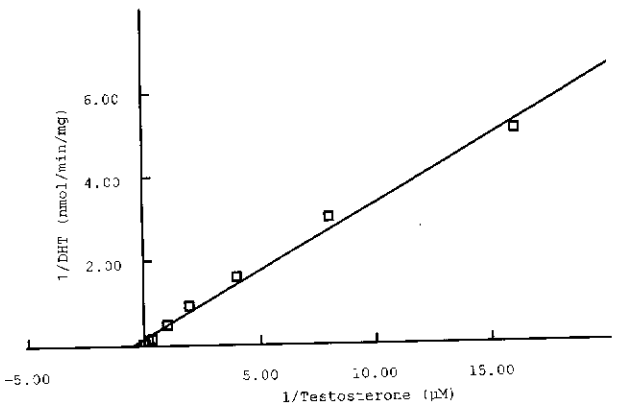

B

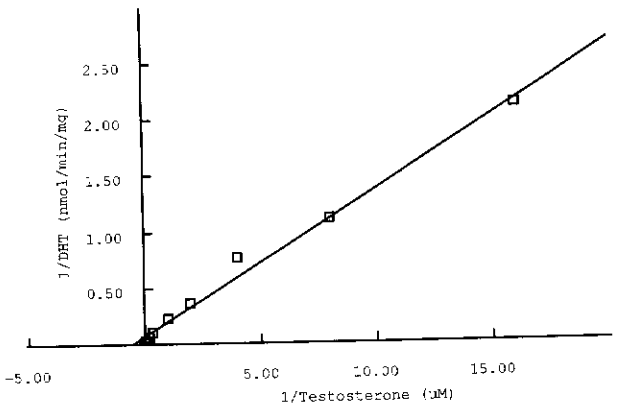

Figure 5.3.2a *Lineweaver-Burke plots of 5AR1G39A (A) or 5AR1G39D (B) transfected CHO cells, derived from 3 and 2 separate experiments respectively. Km and Vmax values were 3.87±0.08μM and 10.90nmol DHT/min/mg (A) and 1.76±0.11μM and 13.68nmol DHT/min/mg (B).*

C

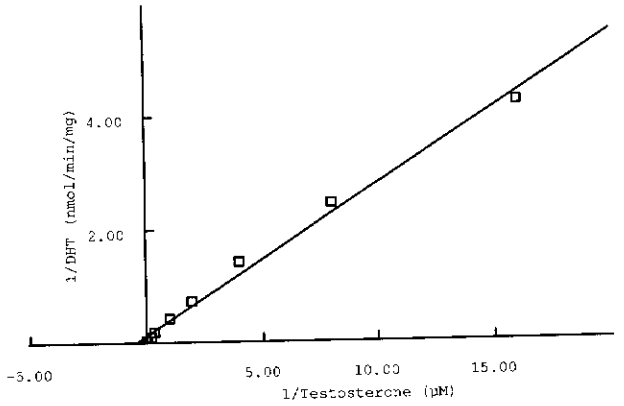

D

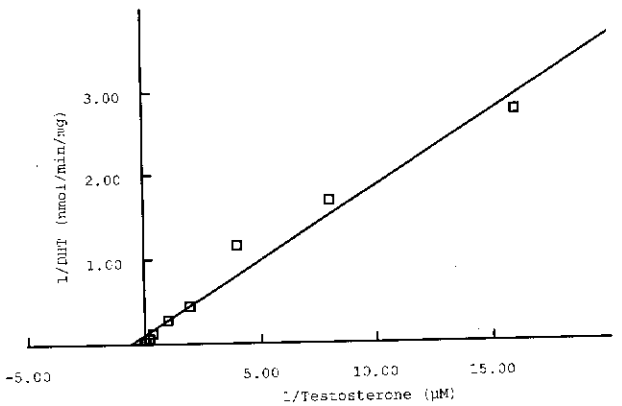

Figure 5.3.2b *Lineweaver-Burke plots of 5AR1G39E (C) or 5AR1G39N (D) transfected CHO cells, derived from 3 and 2 separate experiments respectively. Km and Vmax values were 2.12±0.30μM and 8.27nmol DHT/min/mg (C) and 1.66±0.15μM and 9.34nmol DHT/min/mg (D).*

E

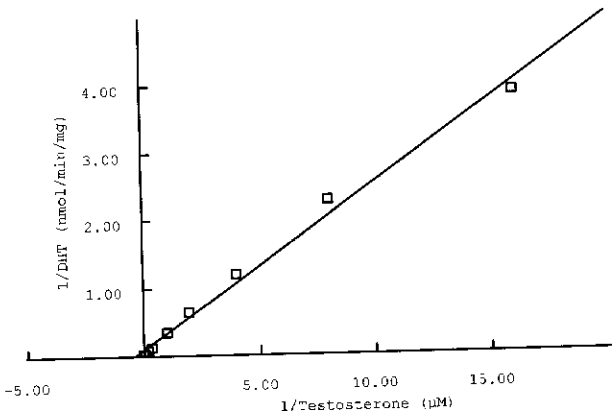

F

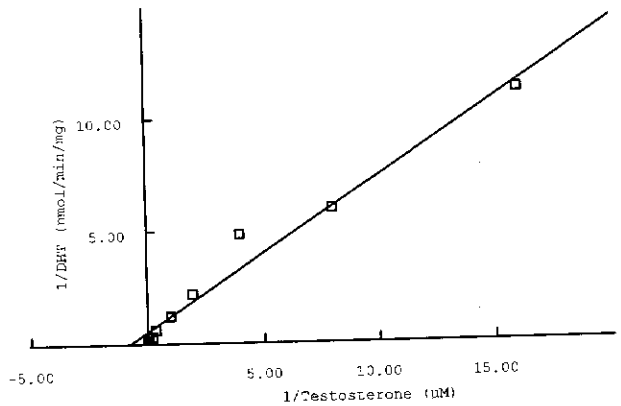

Figure 5.3.2c *Lineweaver-Burke plots of 5AR1G39Q (E) or 5AR1G39R (F) transfected CHO cells, derived from 3 and 2 separate experiments respectively. Km and Vmax values were 3.06±0.60μM and 11.85nmol DHT/min/mg (E) and 1.32±0.29μM and 1.90nmol DHT/min/mg (F).*

G

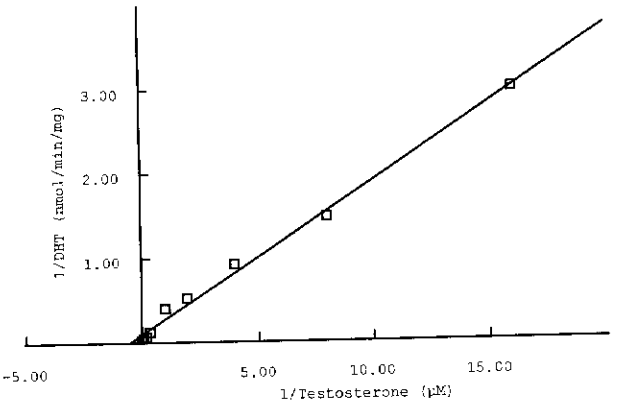

H

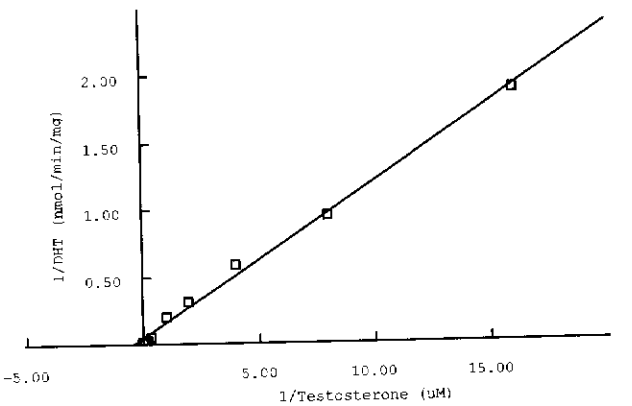

Figure 5.3.2d *Lineweaver-Burke plot of 5AR1H236R (G) 5AR2G34A (H) transfected CHO cells each derived from 2 separate experiments. Km and Vmax values were 2.73±1.84μM and 11.70nmol DHT/min/mg(G) and 2.45±0.64μM and 22.94nmol DHT/min/mg (H).*

I

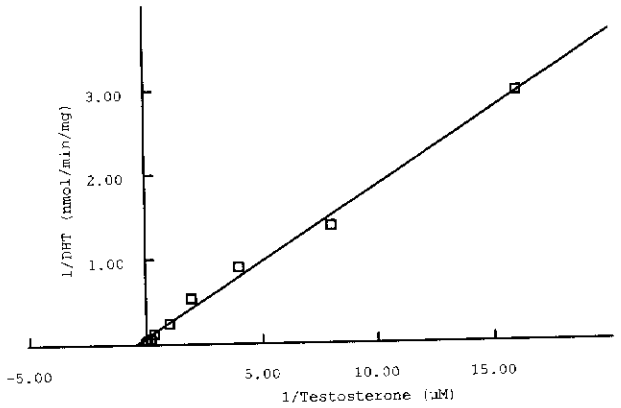

J

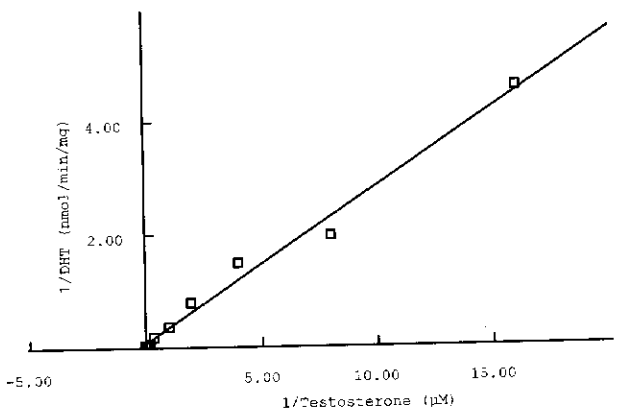

Figure 5.3.2e *Lineweaver-Burke plots of 5AR2G34D (I) or 5AR2G34E (J) transfected CHO cells, each derived from 2 separate experiments. Km and Vmax values were 2.83±0.63μM and 14.55nmol DHT/min/mg (I) and 2.01±0.64μM and 8.29nmol DHT/min/mg (J).*

K

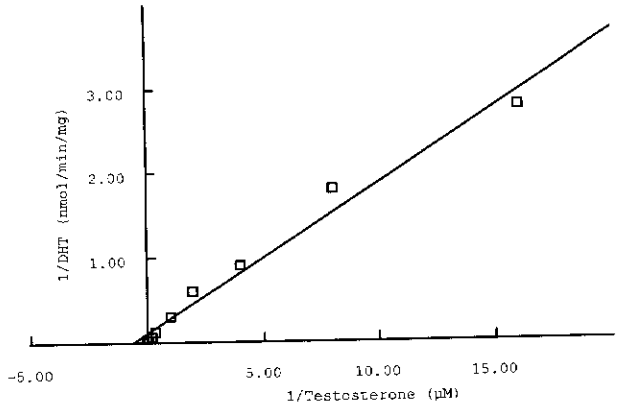

L

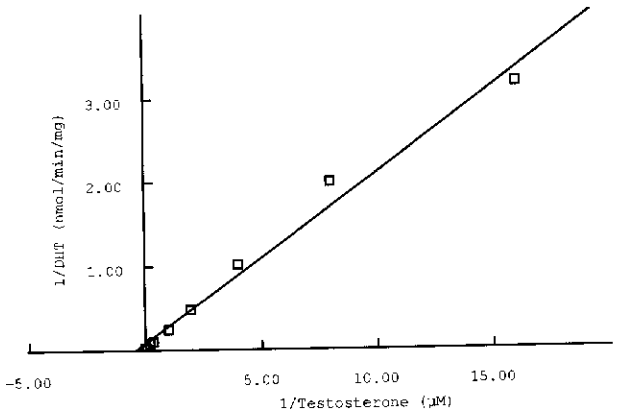

Figure 5.3.2f *Lineweaver-Burke plots of 5AR2G34N (K) or 5AR2G34Q (L) transfected CHO cells, derived from 2 and 3 separate experiments respectively. Km and Vmax values were 1.63±0.17μM and 9.00nmol DHT/min/mg (K) and 2.87±0.04μM and 13.88nmol DHT/min/mg (L).*

M

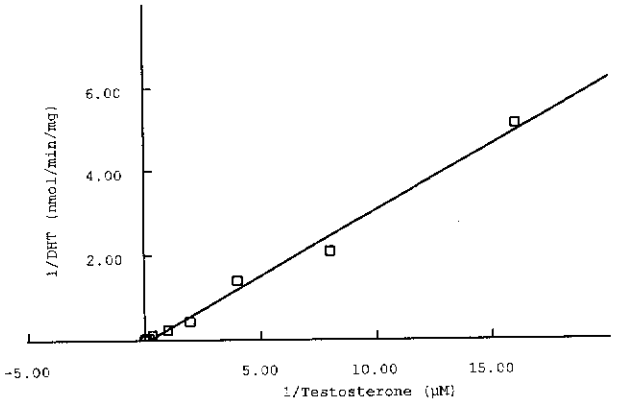

N

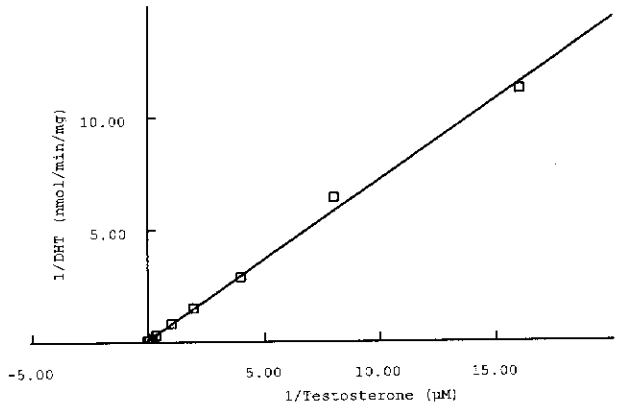

Figure 5.3.2g *Lineweaver-Burke plots of 5AR2G34R (M) or 5AR2H231R (N) transfected CHO cells each derived from 2 separate experiments. Km and Vmax values were 11.35±0.41µM and 42.69nmol DHT/min/mg (M) and 12.51±2.88µM and 16.10nmol DHT/min/mg (N).*

5.3.3 Characterisation of Stably Transfected Cells - IC_{50} Studies

IC_{50} values were determined by incubating CHO cells expressing wild type or mutant 5AR1 or 5AR2 enzymes in media containing a constant amount (1μM) of testosterone and Finasteride concentrations ranging from 0 to 5000nM. IC_{50} plots for both 5AR1 and 5AR2 wild type and mutant enzymes are given in Figures 5.3.3a to 5.3.3p. For these experiments IC_{50} values were used in preference to Ki values, as several attempts to determine Ki values were unsuccessful.

A

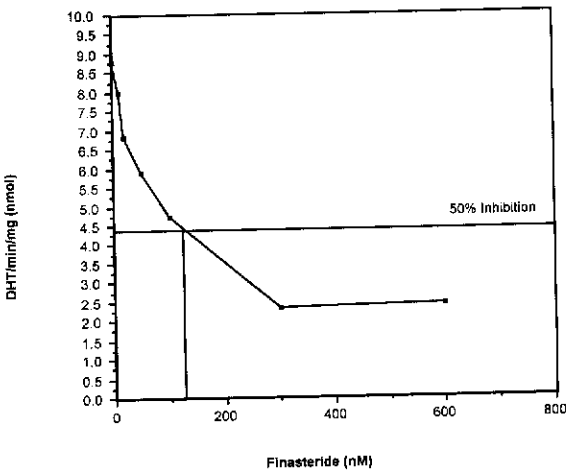

B

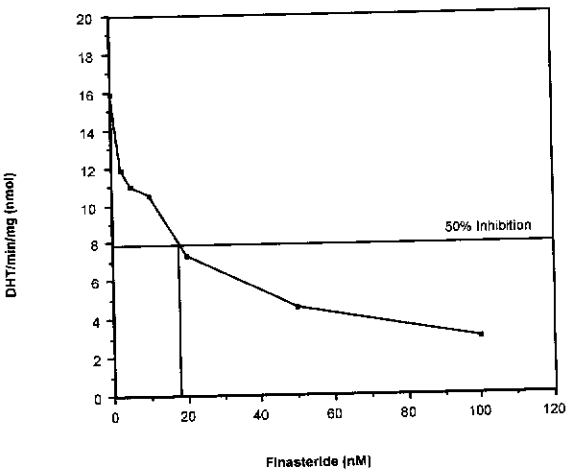

Figure 5.3.3a *Analysis of data (from 2 separate experiments) showed that 125nM of Finasteride was required for 50% inhibition of the 5AR activity of CHO cells stably transfected with wild type 5AR1 (A). 19nM of Finasteride was required to inhibit the 5AR activity of CHO cells stably transfected with wild type 5AR2 (B) by 50%.*

C

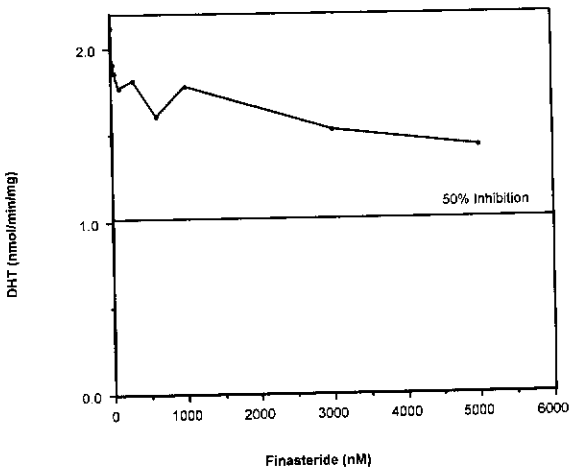

D

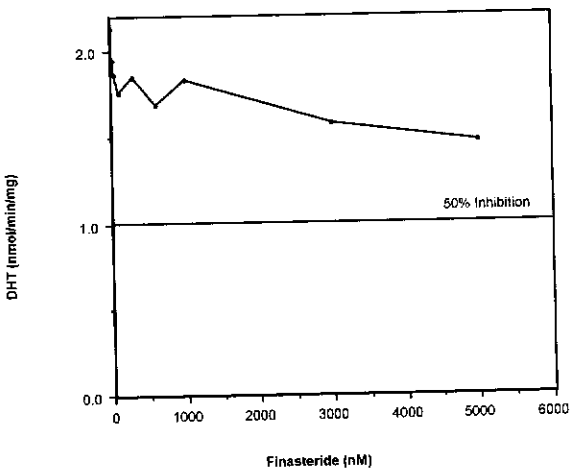

Figure 5.3.3b *Analysis of data (from 2 separate experiments) showed that 50% inhibition of 5AR activity expressed by CHO cells stably transfected with the mutants 5AR1G39A (C) or 5AR1G39D (D) could not be achieved with inhibitor concentrations of 5000nM.*

E

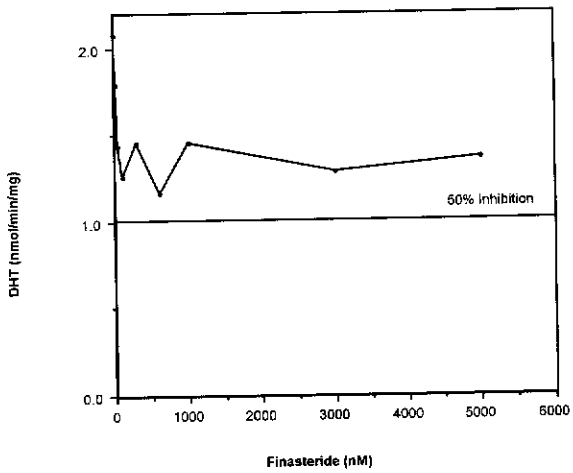

F

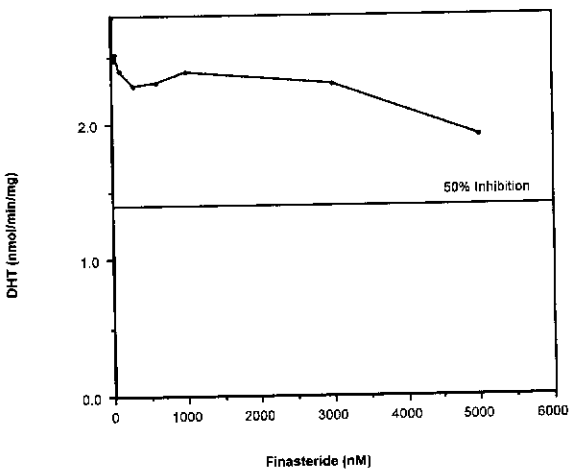

Figure 5.3.3c *Analysis of data (from 2 separate experiments) showed that 50% inhibition of 5AR activity expressed by CHO cells stably transfected with the mutants 5AR1G39E (E) or 5AR1G39N (F) could not be achieved with inhibitor concentrations of 5000nM.*

G

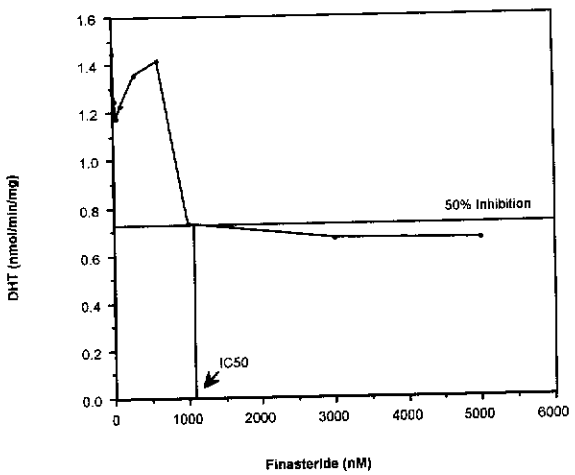

H

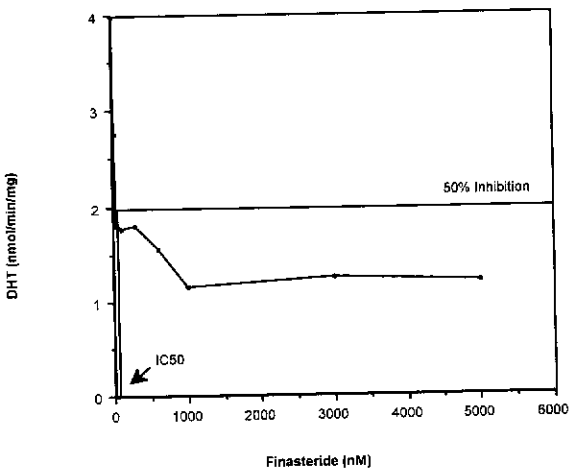

Figure 5.3.3d *Analysis of data (from 2 separate experiments) showed that 1100nM of Finasteride was required for 50% inhibition of the 5AR activity of CHO cells stably transfected with the mutant 5AR1G39Q (G). 50nM of Finasteride was required to inhibit the 5AR activity of CHO cells stably transfected with the mutant 5AR1G39R (H) by 50%.*

I

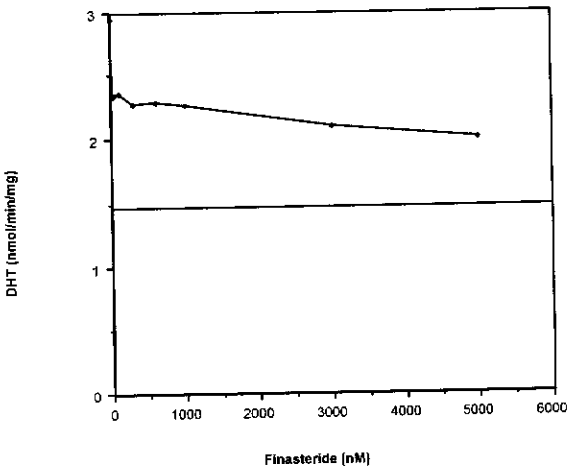

J

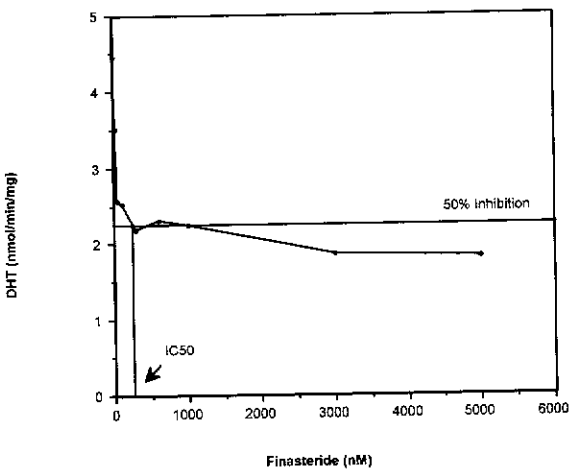

Figure 5.3.3e *Analysis of data (from 2 separate experiments) showed that 50% inhibition of 5AR activity expressed by CHO cells stably transfected with the mutant 5AR1H236R (I), could not be achieved with inhibitor concentrations of 5000nM. 267nM of Finasteride was required for 50% inhibition of the 5AR activity of CHO cells stably transfected with the mutant 5AR2G34A (J).*

K

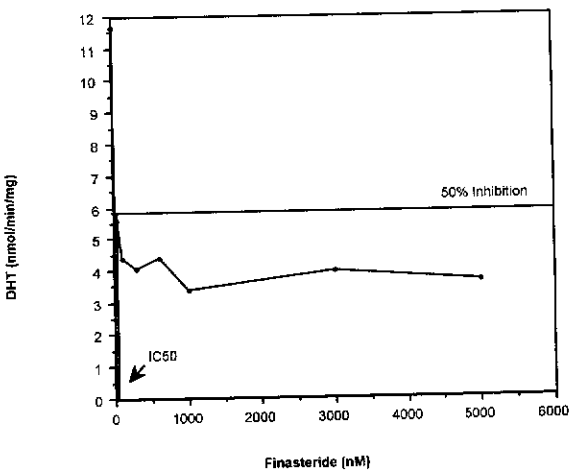

L

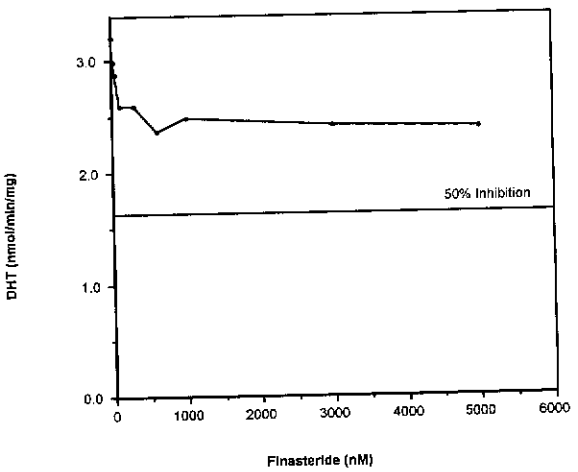

Figure 5.3.3f *Analysis of data (from 2 separate experiments) showed that 90nM of Finasteride was required to inhibit the 5AR activity of CHO cells stably transfected with the mutant 5AR2G34D (K) by 50%. 50% inhibition of 5AR activity expressed by CHO cells stably transfected with the mutant 5AR2G34E (L) could not be achieved with inhibitor concentrations of 5000nM.*

M

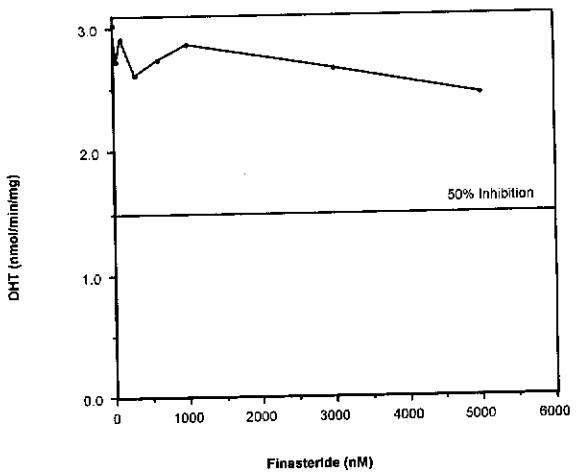

N

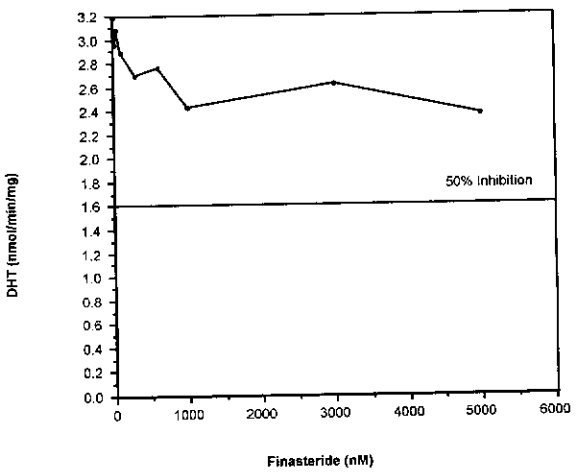

Figure 5.3.3g *Analysis of data (from 2 separate experiments) showed that 50% inhibition of 5AR activity expressed by CHO cells stably transfected with the mutants 5AR2G34N (M) or 5AR2G34Q (N) could not be achieved with inhibitor concentrations of 5000nM.*

O

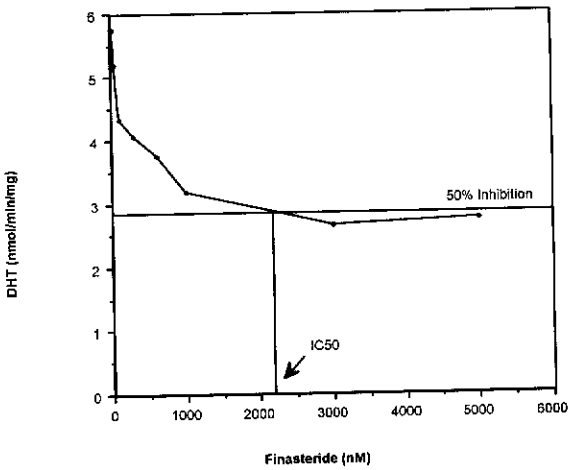

P

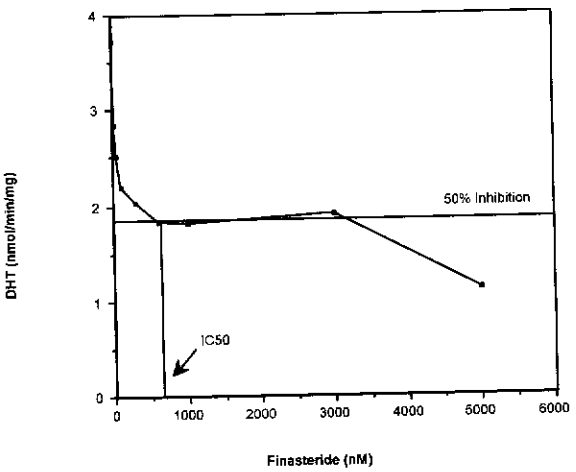

Figure 5.3.3h *Analysis of data (from 2 separate experiments) showed that 2140nM of Finasteride was required to inhibit the 5AR activity of CHO cells stably transfected with the mutant 5AR2G34R(O) by 50%. 615nM of Finasteride was required for 50% inhibition of the 5AR activity of CHO cells stably transfected with the mutant 5AR2H231R (P).*

5.3.4 pH Optima of Stably Transfected Cells

The pH optimum of the various 5AR1G39, 5AR1H236, 5AR2G34 and 5AR2H231 mutants was measured using cell sonicates prepared from CHO cells stably expressing these mutants. The pH optimum was determined from pH plots (Figures 5.3.4a to 5.3.4n) as the pH of the buffer in which maximum 5AR activity was seen.

A

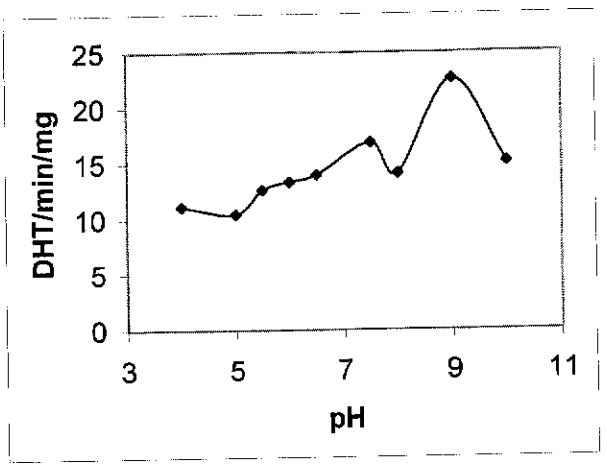

B

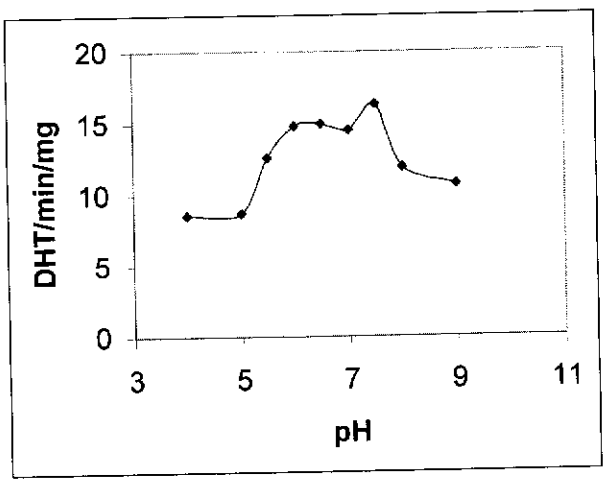

Figure 5.3.4a *The 5AR activity of CHO cells stably transfected with 5AR1G39A (A) or 5AR1G39D (B) was determined using sonicated cells incubated for 30 minutes at 37^{O}C with 1μM T in buffers ranging in pH from 4.0-9.0. For 5AR1G39A, a peak of maximum activity was seen at pH 9.0, whereas for 5AR1G39D a broad peak of maximum*

activity was seen between pH 6.0-7.5 with an optimum at pH 7.5.

C

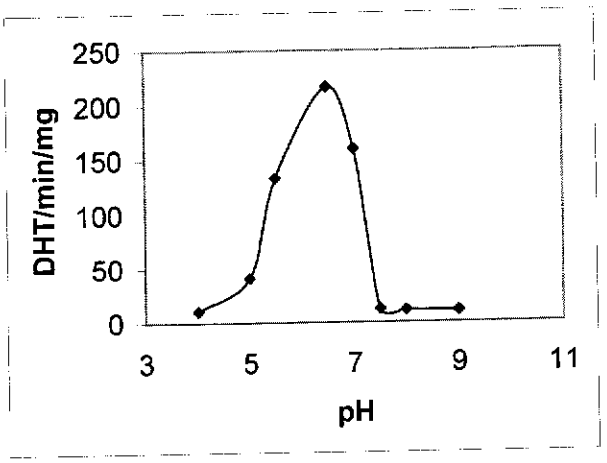

D

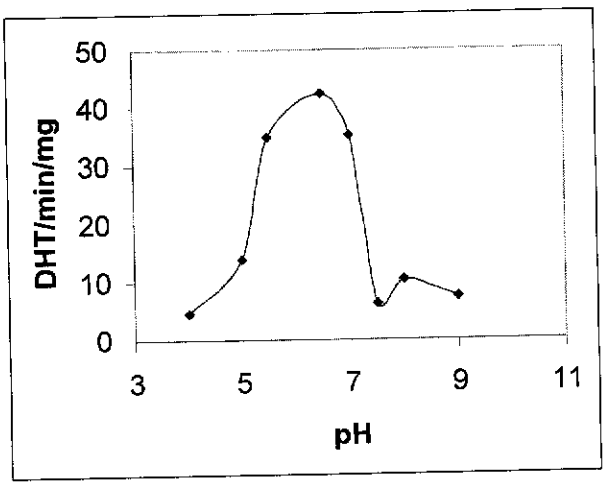

Figure 5.3.4b *The 5AR activity of CHO cells stably transfected with 5AR1G39E (C) or 5AR1G39N (D) was determined using sonicated cells incubated for 30 minutes at 37^{O}C with 1μM T in buffers ranging in pH from 4.0-9.0. For both 5AR1G39E and 5AR1G39N, a peak of maximum activity was seen at pH 6.5.*

E

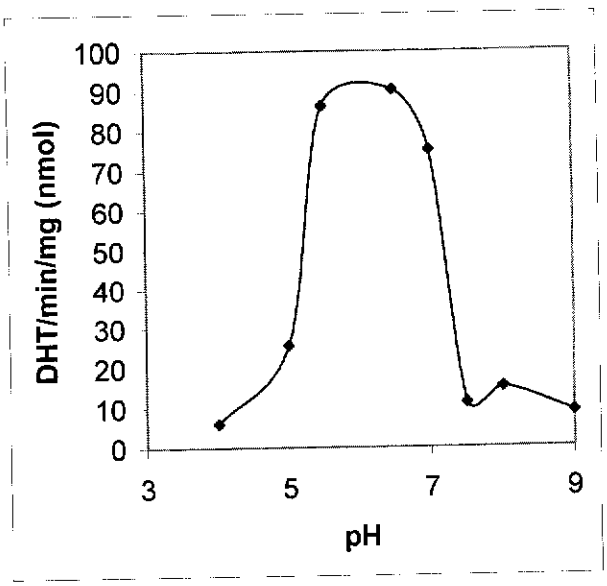

F

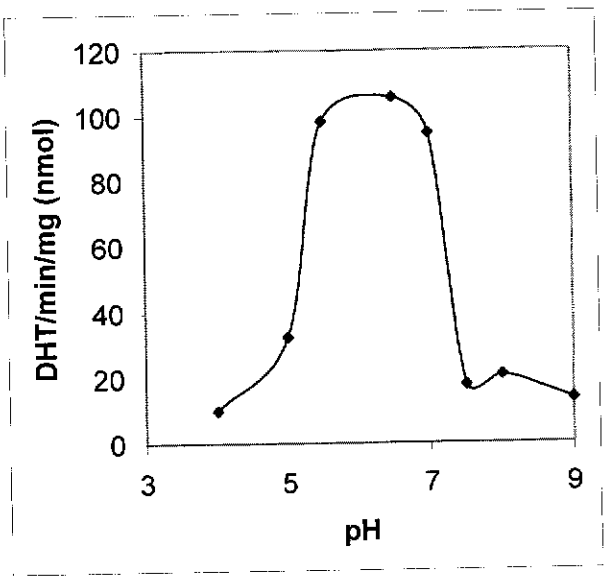

Figure 5.3.4c *The 5AR activity of CHO cells stably transfected with 5AR1G39Q (E) or 5AR1G39R (F) was determined using sonicated cells incubated for 30 minutes at 37^{O}C with 1μM T in buffers ranging in pH from 4.0-9.0. For both 5AR1G39Q and 5AR1G39R, a broad peak of maximum activity was seen at between pH 5.5-7.0 with an optimum at pH 6.5.*

G

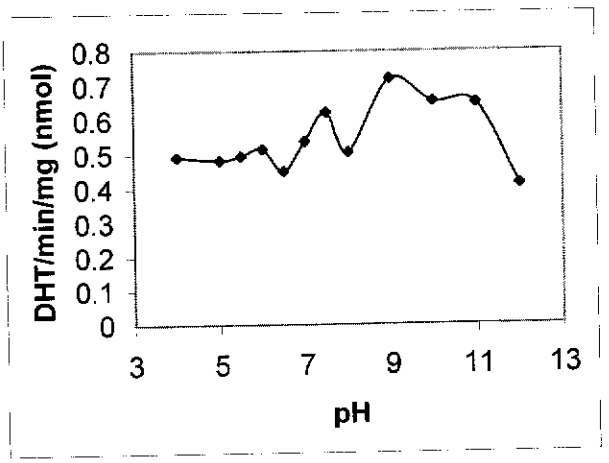

H

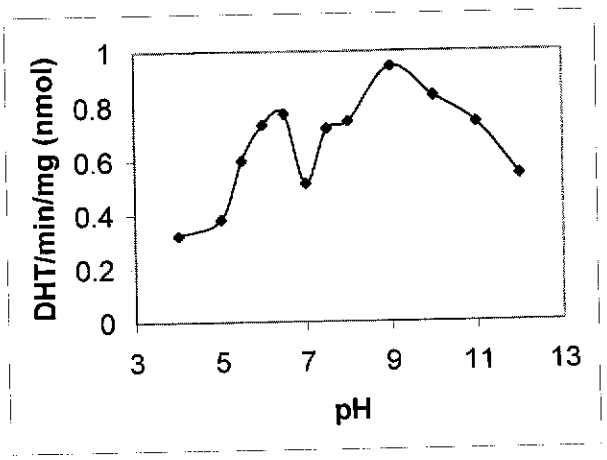

Figure 5.3.4d *The 5AR activity of CHO cells stably transfected with 5AR1H236R (G) or 5AR2G34A (H) was determined using sonicated cells incubated for 30 minutes at 37^{O}C with 1μM T in buffers ranging in pH from 4.0-12.0. For 5AR1H236R a broad peak of maximum activity was seen between pH 8.0-11.0 with an optimum at pH 9.0. For 5AR1G34A a broad peak with maximum activity at pH 9.0 was seen.*

I

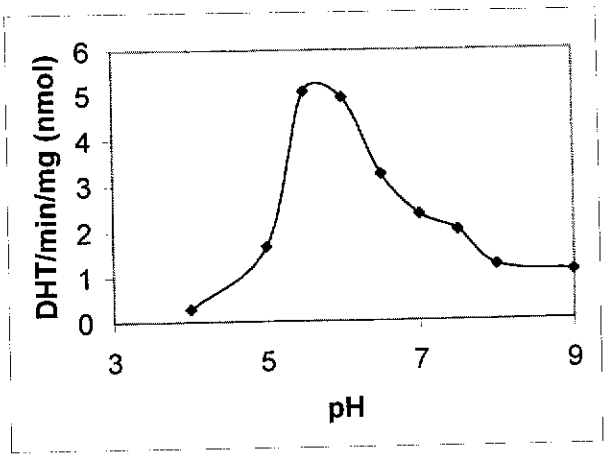

J

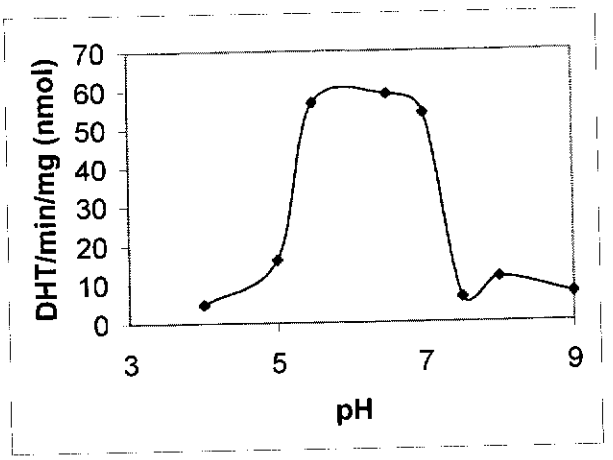

Figure 5.3.4e *The 5AR activity of CHO cells stably transfected with 5AR2G34D (I) or 5AR2G34E (J) was determined using sonicated cells incubated for 30 minutes at 37^{O}C with 1μM T in buffers ranging in pH from 4.0-9.0. For 5AR2G34D a broad peak was seen with maximum activity at pH 5.5. A broad peak of maximum activity was seen between pH 5.5-7.0 with an optimum at pH 6.5 for 5AR2G34E.*

K

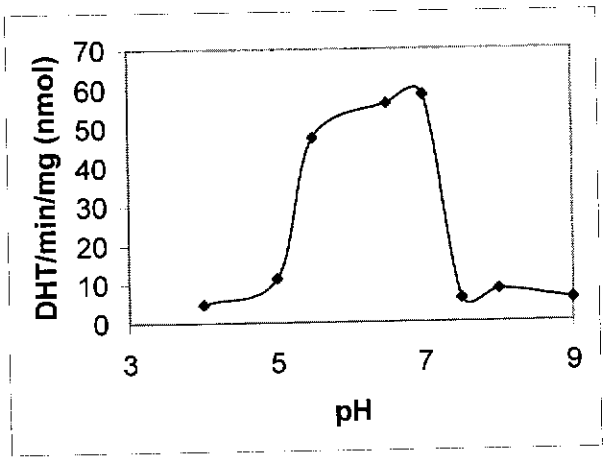

L

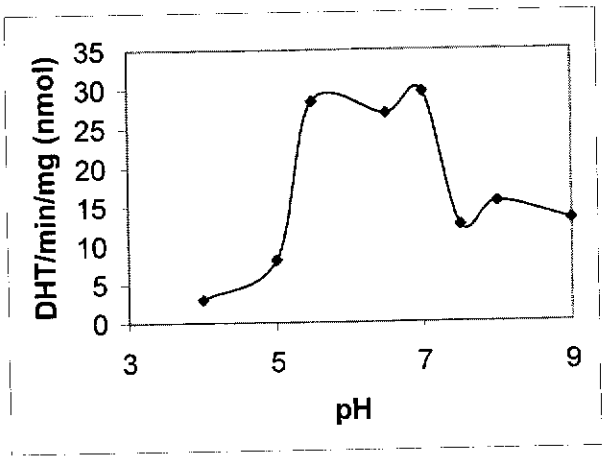

Figure 5.3.4f *The 5AR activity of CHO cells stably transfected with 5AR2G34N (K) or 5AR2G34Q (L) was determined using sonicated cells incubated for 30 minutes at 37^{O}C with 1μM T in buffers ranging in pH from 4.0-9.0. For both 5AR2G34N and 5AR2G34Q, a broad peak of maximum activity was seen between pH 5.5-7.0. The optimum for 5AR2G34N was at pH 6.5 and for 5AR2G34Q at pH 7.0.*

M

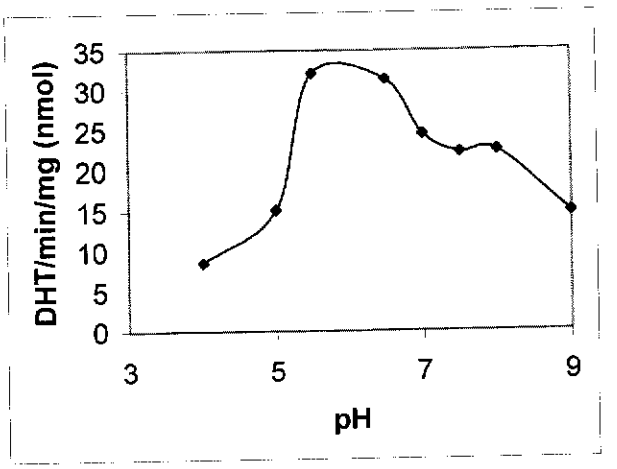

N

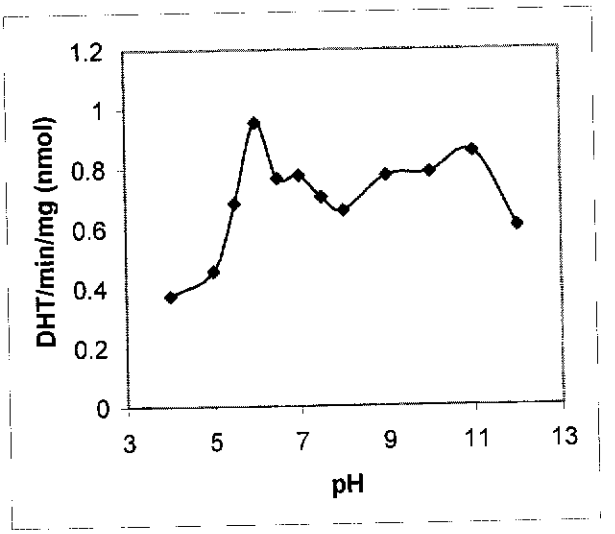

Figure 5.3.4g *The 5AR activity of CHO cells stably transfected with 5AR2G34R (M) or 5AR2H231R (N) was determined using sonicated cells incubated for 30 minutes at 37^{O}C with 1μM T in buffers ranging in pH from 4.0-12.0. 5AR2G34R had a broad peak of maximum activity between pH 5.5-6.5 with an optimum at pH 5.5. For 5AR2H231R a peak of maximum activity was seen at pH 6.0.*

Cell Line Expressing	Average % Conversion T to DHT	Km for T (μM)	Vmax (nmol DHT/min/mg)	Vmax/Km	IC50 (nM)	pH optimum
CHO control cells	0.85	18.67±1.19	42.07	2.25	-	-
Wild Type 5AR1	3.6	2.80±0.60	9.35	3.34	125	6
5AR1G39A	1.8	3.87±0.08	10.90	2.82	>5000	9
5AR1G39D	2.8	1.76±0.11	13.68	7.77	>5000	7.5
5AR1G39E	2.2	2.12±0.30	8.27	3.90	>5000	6.5
5AR1G39N	2.5	1.66±0.15	9.34	5.63	>5000	6.5
5AR1G39Q	2.2	3.06±0.06	11.85	3.87	1100	6.5
5AR1G39R	1.6	1.32±0.29	1.90	1.44	50	6.5
5AR1H236R	1.5	2.73±1.84	11.70	4.29	>5000	9
Wild Type 5AR2	21.2	0.45±0.31	6.58	14.62	19	5.5
5AR2G34A	6.1	2.45±0.64	22.94	9.36	257	9
5AR2G34D	5.1	2.83±0.63	14.55	5.14	90	5.5
5AR2G34E	1.9	2.01±0.64	8.29	4.12	>5000	6.5
5AR2G34N	2.1	1.63±0.17	9.00	5.52	>5000	6.5
5AR2G34Q	2.2	2.87±0.04	13.88	4.84	>5000	7
5AR2G34R	2.7	11.35±0.41	42.69	3.76	2140	5.5
5AR2H231R	1.4	12.51±2.88	16.10	1.29	615	6

Table 5.3.2: *Comparisons of the characteristics of mutant and wild type 5α-reductase enzymes*

5.4 DISCUSSION

The 80% efficiency claimed by the makers of the Quickchange™ kit was achieved for only half the mutant cDNAs created here, yet bacteria containing the various mutations were readily produced. The efficiency variation seen is attributable to differences in template DNA quantity and quality. Stratagene recommend cycling template quantities of 5-100ng to obtain maximum transformants and from previous reactions using the Quickchange™ kit (in our

laboratory), 50ng proved most successful. In some instances however no transformants were evident using 50ng of template, a problem successfully overcome by increasing template DNA usually from 50ng to 75ng.

Typically 5 transformants from each mutagenesis reaction were sent for DNA sequencing analysis to identify clones expressing the desired mutation. Following this, individual transformants expressing each mutation were selected and sequenced in their entirety to ensure no secondary mutations had occurred. CHO cells were then stably transfected with each mutant cDNA, by calcium phosphate precipitation and transfected cells selected for 14-16 days with neomycin sulphate (G418). Resistant cells were harvested into 24 well trays, grown to confluence and assayed for 5AR activity with cells expressing the greatest activity selected and expanded in tissue culture.

The Km and Vmax for the natural substrate T, IC_{50} for Finasteride and pH optimum were determined for each mutant enzyme. Comparisons were made between wild type and mutant enzymes and the mutational effects on enzyme function determined. Inhibitor constant (Ki) studies for Finasteride were initially performed on the 5AR1 and 5AR2 mutants but were met with limited success with the inhibitor plots themselves not resembling those for a competitive inhibitor and the Ki values obtained were negative. IC_{50} studies were then tried and more realistic results obtained. From these IC_{50} studies it became apparent Finasteride had very little inhibitory effect on most of the mutant enzymes, even at a concentration of 5μM. This marked Finasteride resistance may have contributed to the inability to obtain inhibitor plots and Ki values.

The Km for T of 11.35±0.41μM and pH optimum of 5.5 found here for the 5AR2G34R mutant, are in accord with previously published values for this mutant[63]. Comparisons of the values obtained here for this mutant and for wild type 5AR2 confirm this mutation has a significant effect on substrate binding by human 5AR2 but little effect on the pH optimum for this enzyme. The IC_{50} value of 2140nM for the competitive inhibitor Finasteride which is ~112-fold greater than the IC_{50} of 19nM for wild type 5AR2, also shows this

mutation has a significant effect on the binding of this inhibitor. This has not been previously reported.

Although the Vmax of the mutant enzyme of 42.69nmol DHT/min/mg cell protein is around 6.5-fold greater than that of 6.58nmol DHT/min/mg cell protein for the wild type enzyme, the Km of this mutant is ~25-fold greater than that of the wild type enzyme. Comparison of the Vmax/Km ratios of the mutant and wild type enzymes, 3.7 and 14.2 respectively, shows the mutant to be considerably less efficient than the wild type enzyme. In fact inspection of the Vmax/Km ratios shows this ratio for the 5AR2G34R mutant to be lower than seen for most of the other mutants.

Dayhoff's mutational odds matrix (Figure 5.4.1), states that amino acid residues close together in the matrix exhibit similar biochemical properties when expressed in proteins[147]. As is shown in the matrix, glycine and arginine are diagonally opposite and exhibit distinctly different properties. Glycine, which is the smallest of the amino acids, is uncharged and hydrophobic and its lack of a side chain enables it to influence protein conformation by adopting conformations sterically forbidden for other amino acids. In contrast, arginine is a large hydrophilic amino acid with a strong positive charge at physiological pH, which facilitates electrostatic interaction with negatively charged residues such as aspartate and glutamate. It could be therefore that the effects of the G34R mutation on substrate and inhibitor binding are due to conformational change and/or steric hindrance resulting from arginine's size and bulky side-chain. Alternatively, these effects could be due to arginine's positive charge.

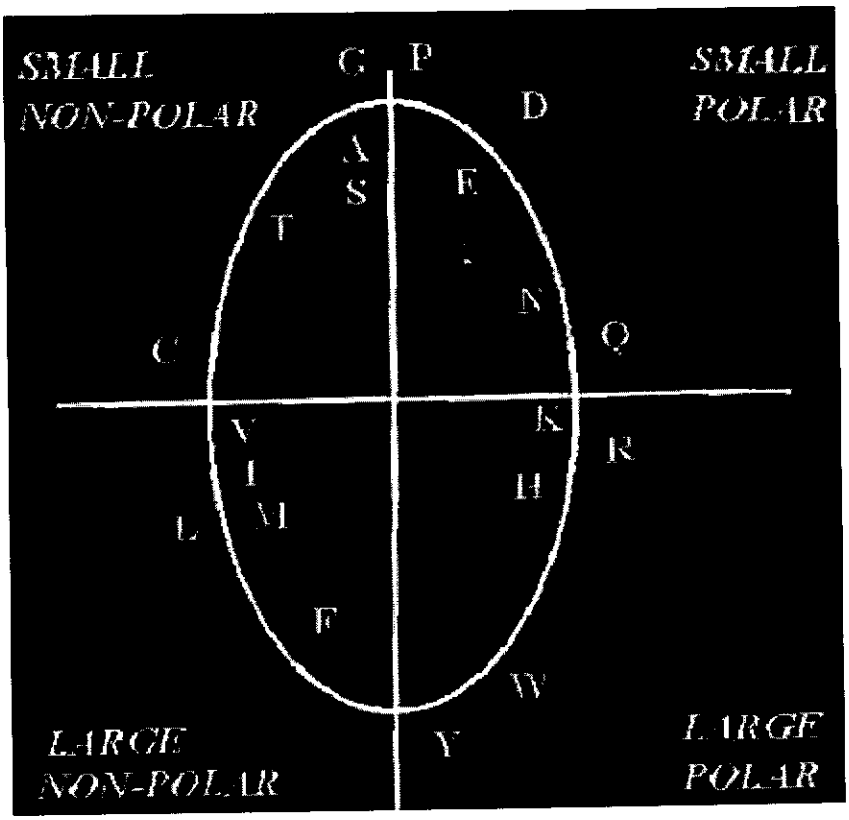

Figure 5.4.1 *Dayhoff's mutational odds matrix*[147].

To differentiate between these possibilities, a variety of mutations of 5AR2 were created, expressed in CHO cells and characterised. To determine the affects of size, the mutant G34A was constructed and charge and size effects were examined with the mutants G34D, G34E, G34N and G34Q.

Alanine is the substitution residue of choice for the determination of catalytic or functional role of amino acid residues as it eliminates the side chain beyond the β-carbon yet it does not alter the main chain conformation[148]. Additionally, alanine and glycine are close together in Dayhoff's matrix indicating they have similar properties.

Kinetic analysis of the 5AR2G34A mutant showed a 5.5-fold increase in Km (2.45μM compared with 0.45μM for wild type 5AR2) and a 14-fold increase in IC_{50} (267nM compared with 19nM). The Vmax/Km ratio of 9.2 for this mutant however, although lower than the 14.2 seen for the wild type enzyme, is 2 to

3-fold greater than the ratio seen for any of the 5AR2 mutants. This indicates that substitution of glycine by alanine has a lesser effect on 5AR2 than do the other mutations studied here. This is to be expected as both glycine and alanine are small hydrophobic amino acids ad it has been stated that alanine does not alter main chain conformation or impose extreme steric effects on protein structure[148]. The increase in Km and IC_{50} seen for the G34A mutant are considerably less than those seen for the G34R mutant. This indicates that size effects are responsible for at least part of the increase in Km and IC_{50} seen in the G34R mutant. The changes from wild type values seen in the 5AR2G34A mutant suggest these are due to direct effects on substrate/inhibitor binding rather than to conformational effects. It is probable therefore that G34 is actively involved in substrate/inhibitor binding by human 5AR2 as even the most conservative change at this residue has a marked effect on enzyme characteristics. Surprisingly, substitution of glycine with alanine had a marked effect on the pH optimum of 5AR2. In fact this substitution had the most marked effect of all the substitutions of 5AR2G34 assessed here. As the more radical substitution G34R, had no effect on this parameter the conclusion was that G34 possibly did not play a role in determining the pH optimum. A significant difference between alanine and glycine is their hydropathy indices, which are 1.8 and 0.4 respectively and it may be that this difference has caused the effect on the pH optimum. Without knowledge of the structure of 5AR2 however it is not possible to speculate as to why this conservative substitution had such a marked effect on pH optimum.

As mentioned above, the mutations G34D, G34E, G34N and G34Q were created to determine the effects of size and charge on substrate/inhibitor binding. The substitutions G34D and G34E increased the Km for T to a similar extent and the Vmax/Km ratios for the two mutants were not significantly different. Replacement of G34 by asparagine and glutamine, which are the uncharged amides of aspartate and glutamate respectively, again increased Km for T but although the Km for the G34N mutation was a little lower than Km values for G34D, G34E and G34Q, these values were much the same. Similarly, the Vmax/Km ratios for all of these mutants were

little different. This suggests charge does not play a role in substrate binding and that the reductions in affinity are due to size effects. The effects of these mutations on the binding of Finasteride were however somewhat different as the G34D mutant had an IC_{50} of 90nM compared with IC_{50} values of >5000nM for all of the other three mutants. This IC_{50} value of 90nM was in fact the lowest of all the 5AR2 mutants studied here and suggests there may be an electrostatic component in the binding of this inhibitor. The cause of the significant difference between the IC_{50} values obtained for G34D and G34E is unknown but may be due to differences in the pKa of the side chains of these amino acids. The pH optimum for the G34D mutant also was not different from that of the wild type enzyme whereas the pH optima for all of the other three mutants were more alkaline than for wild type 5AR2. Again the reasons for these differences are not clear but may reflect subtle changes in the microenvironment.

These studies suggest that glycine 34 contributes significantly to substrate and inhibitor binding by human 5AR2 and that this contribution is due to the unique nature of this amino acid. Mutation of glycine to larger amino acids, whether charged or not, reduces affinity for testosterone and sensitivity to Finasteride and even the conservative substitution by alanine, has a marked effect on these parameters.

The effects of the mutations to G39 in 5AR1, which is the analogous residue to G34 in 5AR2, have not previously been determined. Accordingly, the same mutations of this residue as those made for G34 in 5AR2 were created, expressed in CHO cells and characterised. In contrast to the G34R mutation in 5AR2, which markedly increased the Km for testosterone and the IC_{50} for Finasteride, the G39R mutation in 5AR1 gave a two-fold decrease in both the Km and the IC_{50}. In fact of all the mutations of 5AR1 that were assessed, this mutation gave the lowest values for Km and IC_{50}. However the Vmax/Km ratio of 1.5 was around two-fold lower than that of wild type 5AR1. These findings suggest the positive charge of arginine might have an effect on substrate and inhibitor binding and that the bulky arginine residue may reduce the efficiency of this mutant, possibly by altering its conformation.

Rather surprisingly, the mutation G39D, which gives a negative charge at this residue, also had a slightly lower Km than wild type 5AR1 although the IC_{50} of greater than 5000nM for this mutated showed it to be insensitive to Finasteride. These findings could indicate that a charge at this residue, whatever the nature of this charge is, has an effect on substrate and binding by 5AR1. However, this is contradicted as the G39N mutant also has a lower Km than wild type 5AR1. Overall, the changes made to G39 made little difference to Km and it is probable this residue is not significant for the binding of testosterone by 5AR1. As mutations to this residue had a marked effect on the sensitivity to Finasteride, it may be this residue is close to the substrate/inhibitor binding site and that alterations to this glycine affect inhibitor binding by altering the microenvironment. Interestingly, the G39A mutation, like the G34 mutation in 5AR2, has an optimum pH of 9.0 but as before, the reasons for this marked shift are unknown.

In comparison with wild type 5AR1, the H236R mutant showed no significant change in substrate affinity (Km =2.73±1.84μM) however a greater than 40-fold increase in IC_{50} was seen, with a Finasteride concentration of 5μM having no inhibitory effect on enzyme activity. This suggests that although H236 is not involved in substrate binding it is required for the binding of inhibitor. It is therefore apparent subtle differences exist between the substrate and inhibitor binding sites of 5AR1. The Vmax of the H236R mutant (11.7nmol DHT/min/mg of cell protein) is similar to that of wild type 5AR1 and the H236R mutation has not affected catalytic activity. The pH optimum of this mutant is 3.0 pH units greater than wild type 5AR1 and suggests H236 may determine this factor.

The H231R mutation in 5AR2 markedly reduced affinity for substrate by almost 28-fold (Km = 12.51±2.88μM), which is in agreement with earlier findings[63] and confirms the contribution of this residue to substrate binding by 5AR2. There have been no previous studies of the effects of this mutation on inhibitor binding. Comparisons with wild type 5AR2 showed a 32-fold increase in IC_{50} for the H231R mutant and the contribution of H231 to inhibitor

binding in 5AR2. The H231R mutation does not appear to have a pronounced effect on catalytic activity, differences in transfection efficiencies may again account for the 2.5-fold increase in Vmax. A difference of only 0.5 pH units between wild type and the H231R mutant suggests H231 does not determine the pH optimum of 5AR2.

As histidine and arginine are both large hydrophilic residues differing only in the charge they express at physiological pH (arginine is positive and histidine neutral)[147], electrostatic interactions may cause this reduced binding of substrate and inhibitor seen for H231. In many protein families, histidine residues commonly participate in metal-ion binding[147]. In human 5AR2, H231 is located within a stretch of three histidines and it has been suggested H231 may play a role in metal binding[63]. Results from the studies reported here and those of Wigley and colleagues[63] show that H231 is important for substrate and inhibitor binding in 5AR2. This together with the strict conservation of this residue between both isoenzymes and species suggests it is catalytically important in 5AR rather than involved in metal binding. This is in accord with the suggestion 5AR does not require metal ions for activity[9].

Mutational studies of G34 in 5AR2 have shown it to be an important residue for substrate and inhibitor binding. Mutation of G34 to a larger amino acid, be it charged or neutral, resulted in reduced affinity for substrate and increased resistance to Finasteride, suggesting this is the consequence of conformational change and steric hindrance. It is apparent therefore that at residue 34 in 5AR2 the small uncharged amino acid glycine is essential for optimal enzyme function. The similar loss of function seen when histidine is mutated to the positively charged amino acid arginine (H231R), also demonstrates its significance for both substrate and inhibitor binding by 5AR2. These studies have identified residues important for substrate and inhibitor binding by 5AR2 to the amino (G34) and carboxyl (H231) termini and support identification of the substrate and Finasteride binding sites of human 5AR2 as bipartite[127].

Chapter 6.0

Examining the Roles of Residues in the Tetrapeptide -AVFA- for Substrate/Inhibitor Binding in Human 5α- Reductase 1

6.1 INTRODUCTION

As discussed previously (Section 1.8), as the 4-aza steroids 4-MA and Finasteride are widely used for inhibition of 5AR, they have been extensively studied. It has been shown that substitutions at carbon 17 (C-17) of 4-azasteroids, such as the bulky t-butyl group of Finasteride, dramatically affects their ability to inhibit a given 5AR isoenzyme[19]. These authors suggested therefore that this t-butyl group may determine sensitivity of 5AR to Finasteride. In view of this is has been suggested[128] that the bulky phenylalanine residue in the tetrapeptide -AVFA- may be of particular significance with respect to the role of this tetrapeptide in determining the Finasteride sensitivity of human 5AR1.

Both of the aromatic amino acids phenylalanine and tyrosine contain delocalised electrons in their aromatic side chains that participate in weak electrostatic interactions. This may explain why these residues are expressed in regions associated with cofactor and substrate binding in 5AR. Tyrosine is a slightly polar amino acid that can participate in hydrogen bonding through its hydroxyl group, which can act as either an acceptor or a donor in hydrogen bonding[147]. In enzymes requiring NADP[H] as a cofactor, the hydroxyl function of tyrosine residues has been shown to be involved in cofactor binding and catalysis through mediation of hydride transfer from cofactor to substrate[134]. The involvement of tyrosine residues in cofactor binding by 5AR has been shown by Wang et al (1999)[133], who analysed the relative contributions of the highly conserved residues Y179 and Y189 to NADP[H] binding by rat 5AR1. These authors also showed that a phenylalanine residue (F187) is of importance for both cofactor and substrate binding.

All of this supports the suggestion[128] that F28 may also be of particular importance in those aspects of substrate/inhibitor binding by human 5AR1 that are mediated through the tetrapeptide -AVFA-. However, at the time there had been no studies examining the roles of various residues in this tetrapeptide. Again at the time only residues -AVFA- in human 5AR1 and the corresponding residues -VSIV- in 5AR1 rat had been identified as involved in substrate/inhibitor binding. To assess the roles of individual residues in the

tetrapeptide -AVFA-, all four residues were individually exchanged with their rat counterparts and the effects of these exchanges examined.

6.2 METHODS

6.2.1 PLASMID DNA EXTRACTION

The BRESAspin™ Plasmid Mini Kit (Bresatec) was used to extract all plasmid DNA, as described in section 3.2.1.1.

6.2.2 SITE-DIRECTED MUTAGENESIS

6.2.2.1 Reaction Components

Each reaction was set up as described section 4.2.2.1. Reaction components used to set up each reaction were as follows:

5μL	10X Reaction buffer
50ng	dsDNA template**
125ng	Oligonucleotide forward primer
125ng	Oligonucleotide reverse primer
1μL	dNTPs (10mM)
XμL	Sterile hpH_2O
50μL	

* Add 1μL of native *Pfu* DNA polymerase (2.5U/μL)

** 75ng of DNA template was used for all reactions except the 5AR1ASFA, 5AR1AVAA and 5AR1AVYA reactions for which 100ng and the 5AR1ASIV reaction for which 50ng of template DNA was cycled.

Nb. As each primer preparation had a different concentration, the amount rather than volume of primer used is given. The value of XμL for the volume of water used reflects the different volumes of primer solution added.

6.2.2.1a Primers

DNA sequences for the 5AR1AAFA, 5AR1AFVA, 5AR1ASFA, 5AR1ASIA, 5AR1ASIV, 5AR1AVAA, 5AR1AVFV, 5AR1AVIA, 5AR1AVYA, 5AR1VSIA and 5AR1VVFA primer pairs are listed below. All primers were synthesized by Pacific Oligonucleotides (New South Wales). Mutated residues are shown in bold type.

5AR1AAFA Primer Pair

5'- ^{24}GGC TGC GCG **GCG** TTC GCG CGG AAT CGT CAG ACG^{34} -3'

3'- ^{24}CCG ACG CGC **CGC** AAG CGC GCC TTA GCA GTC TGC^{34} -5'

5AR1AFVA Primer Pair

5'- ^{24}GGC TGC GCG **T**TC **G**TC GCG CGG AAT CGT CAG ACG^{34} -3'

3'- ^{24}CCG ACG CGC **A**AG **C**AG CGC GCC TTA GCA GTC TGC^{34} -5'

5AR1ASFA Primer Pair

5'- ^{24}GGC TGC GCG **TC**C TTC GCG CGG AAT CGT CAG ACG^{34} -3'

3'- ^{24}CCG ACG CGC **AG**G AAG CGC GCC TTA GCA GTC TGC^{34} -5'

5AR1ASIA Primer Pair

5'- ^{24}GGC TGC GCG **TC**C **A**TC GCG CGG AAT CGT CAG ACG^{34} -3'

3'- ^{24}CCG ACG CGC **AG**G **T**AC CGC GCC TTA GCA GTC TGC^{34} -5'

5AR1ASIV Primer Pair

5'- ^{24}GGC TGC GCG **TC**C **A**TC GT**C** CGG AAT CG^{32}-3'

3'- ^{24}CCG ACG CGC **AG**G **T**AG C**AG** GCC TTA GC^{32} -5'

5AR1AVAA Primer Pair

5'- ^{24}GGC TGC GCG GTC **GCG** GCG CGG AAT CGT CAG ACG^{34} -3'

3'- ^{24}CCG ACG CGC CAG **CGC** CGC GCC TTA GCA GTC TGC^{34} -5'

5AR1AVFV Primer Pair

5'- ^{24}GGC TGC GCG GTC TTC G**TC** CGG AAT CG^{32}-3'

3'- ^{24}CCG ACG CGC CAG AAG C**AG** GCC TTA GC^{32}-5'

5AR1AVIA Primer Pair

5'- ^{24}GGC TGC GCG GTC **A**TC GCG CGG AAT CGT CAG ACG^{34} -3'

3'- ^{24}CCG ACG CGC CAG **T**AG CGC GCC TTA GCA GTC TGC^{34} -5'

5AR1AVYA Primer Pair

5'- ^{24}GGC TGC GCG GTC T**A**C GCG CGG AAT CGT CAG ACG^{34} -3'

3'- ^{24}CCG ACG CGC CAG A**T**G CGC GCC TTA GCA GTC TGC^{34} -5'

5AR1VSIA Primer Pair

5'- ^{24}GGC TGC G**TC TC**C **A**TC GCG CGG AAT CG^{32}-3'

3'- ^{24}CCG ACG C**AG AG**G **T**AG CGC GCC TTA GC^{32}-5'

5AR1VVFA Primer Pair

5'- ^{24}GGC TGC G**TC** GTC TTC GCG CGG AAT CG^{32}-3'

3'- ^{24}CCG ACG C**AG** CAG AAG CGC GCC TTA GC^{32}-5'

6.2.2.2 Cycling Conditions

Cycling conditions for all mutations except the 5AR1ASIV mutation were:

1. 1 cycle at 95^{O}C for 30 seconds.
2. 16 cycles at 95^{O}C for 30 seconds.
3. 16 cycles at 55 ^{O}C for 1 minute.
4. 16 cycles at 68 ^{O}C for 14 minutes.
5. 4 ^{O}C overnight.

Cycling conditions for the 5AR1ASIV mutation were:

1. 1 cycle at 95^{O}C for 30 seconds.
2. 18 cycles at 95^{O}C for 30 seconds.
3. 18 cycles at 55 ^{O}C for 1 minute.
4. 18 cycles at 68 ^{O}C for 14 minutes.
6. 4 ^{O}C overnight.

6.2.2.3 Digesting the Product and Transformation into Epicurian Coli XL-1- Blue Supercompetent Cells.

Dpn I digestion and transformation of each 5AR1 mutagenesis reaction into Epicurian supercompetent *E.coli* were as described sections 4.2.2.3 and 4.2.2.4 respectively.

6.2.3 DNA SEQUENCING FOR MUTATION IDENTIFICATION

Automated DNA sequencing was as described in section 4.2.3, using a primer (T7EEV) specifically designed for the multiple cloning site of the pCI-neo vector. To enable sequencing of the entire cDNA, primers were also designed based on the sequences of 5AR1 or 5AR2 (AR1R and AR2R respectively).

6.2.4 CALCIUM PHOSPHATE TRANSFECTION

Calcium phosphate transfection of CHO cells with pCI-neo vector containing 5AR1 mutant cDNAs was as described section 3.2.12.

6.2.5 CHARACTERISATION OF STABLY TRANSFECTED CELLS - 5α- REDUCTASE ASSAYS

Determination of 5AR activity of transfected cells and of Km, Vmax, Ki, total protein assays and cell culture procedures were as described in sections 3.2.14 to 3.2.16.

6.3 RESULTS

6.3.1 Site-directed Mutagenesis of Wild Type 5AR1 cDNA

All 5AR1 mutant cDNAs were synthesised using the Quickchange™ site-directed mutagenesis kit with appropriate oligonucleotide primers. Ampicillin resistant bacteria from all transformations (Table 6.3.1), was sequenced for the presence of the desired mutation. Figures 6.3.1a to 6.3.1k are the automated DNA sequence chromatographs for the 5AR1AAFA, 5AR1AFVA, 5AR1ASFA, 5AR1ASIA, 5AR1ASIV, 5AR1AVAA, 5AR1AVFV, 5AR1AVIA, 5AR1AVYA, 5AR1VSIA and 5AR1VVFA mutations respectively.

Mutation	Colony Numbers on Transformation
5AR1AAFA	>250
5AR1AFVA	>250
5AR1ASFA	1
5AR1ASIA	>250
5AR1ASIV	100-200
5AR1AVAA	2
5AR1AVFV	100-200
5AR1AVIA	>250
5AR1AVYA	12
5AR1VSIA	5
5AR1VVFA	>250

Table 6.3.1 *Ampicillin resistant colony numbers resulting from the transformation of the various 5AR1 mutagenesis reactions, prepared using the Quickchange™ mutagenesis method.*

Figures 6.3.1a to 6.3.1k show the sequences, which confirm that the various mutations have been achieved. For each mutation shown the entire sequence data is given in appendix A.

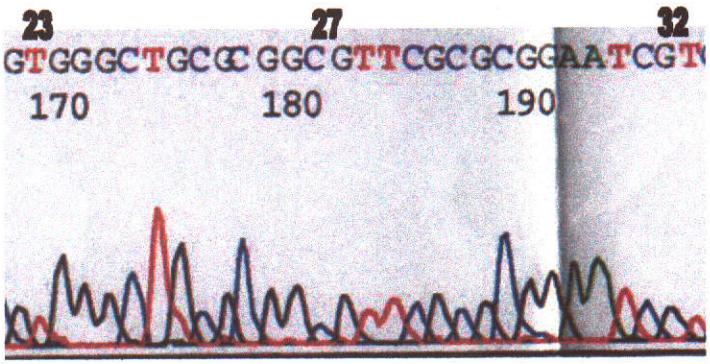

Figure 6.3.1a *DNA sequence chromatograph of 5AR1AAFA mutant clone with T7EEV primer. Residue 27 has been mutated from -GTC- to -**GCG**- and now encodes alanine.*

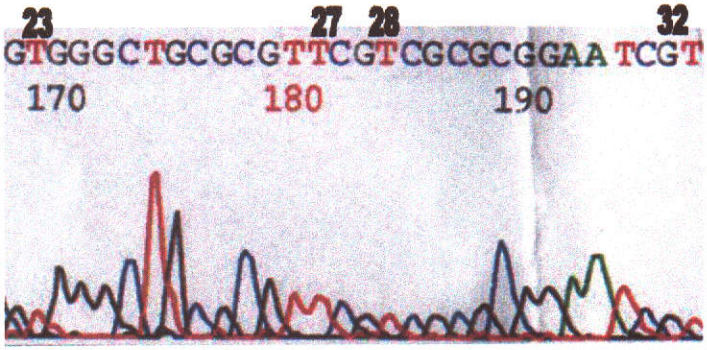

Figure 6.3.1b *DNA sequence chromatograph of 5AR1AFVA mutant clone with T7EEV primer. Residues 27 and 28 have been mutated from -GTC TTC- to -**TTC GTC**- and now encode phenylalanine and valine respectively.*

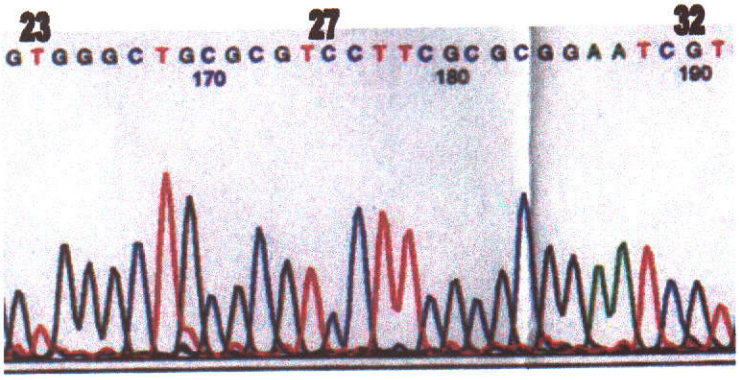

Figure 6.3.1c *DNA sequence chromatograph of 5AR1ASFA mutant clone with T7EEV primer. Residue 27 now encodes serine as a result of the mutation-GTC- to -**TCC**-.*

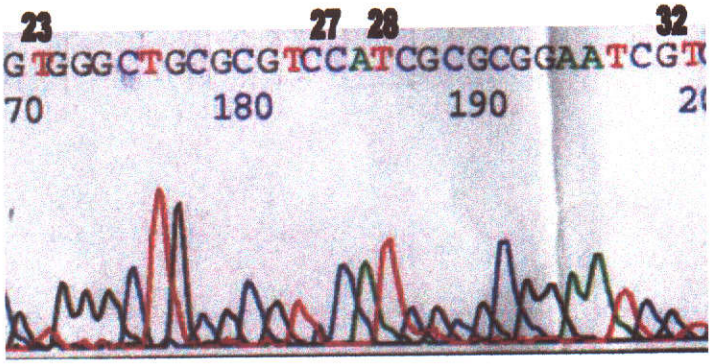

Figure 6.3.1d *DNA sequence chromatograph of 5AR1ASIA mutant clone with T7EEV primer. The presence of the sequence -**TCC ATC**- at residues 27 and 28 confirms the mutation of -AVFA- to -ASIA-.*

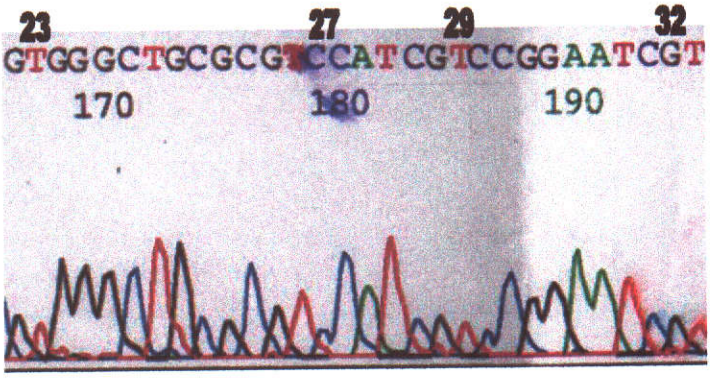

Figure 6.3.1e *DNA sequence chromatograph of 5AR1ASIV mutant clone with T7EEV primer. The sequence - **TCC ATC GTC**- at residues 27-29 confirms the mutation of -AVFA- to -ASIV.*

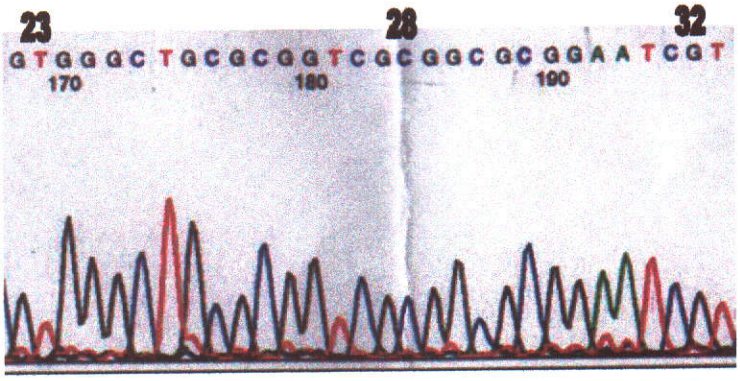

Figure 6.3.1f *DNA sequence chromatograph of 5AR1AVAA mutant clone with T7EEV primer. Residue 28 has been mutated from -TTC- to -**GCG**- and now encodes alanine.*

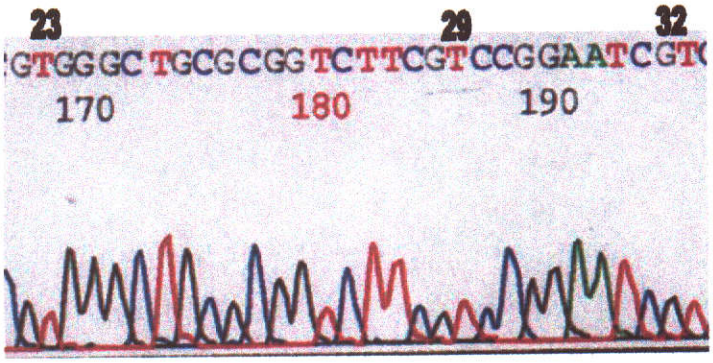

Figure 6.3.1g *DNA sequence chromatograph of 5AR1AVFV mutant clone with T7EEV primer. Residue 29 now encodes valine as a result of the mutation -GCG- to -G**TC**-.*

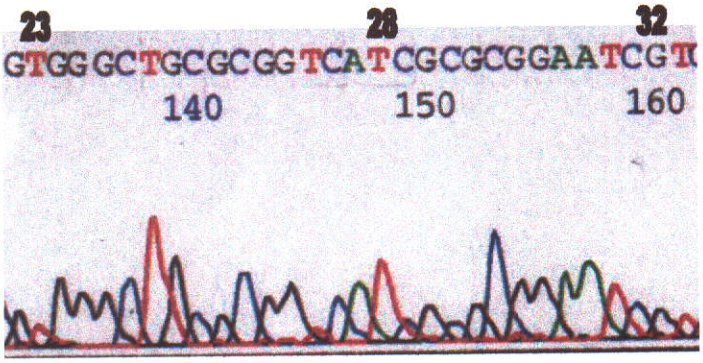

Figure 6.3.1h *DNA sequence chromatograph of 5AR1AVIA mutant clone with T7EEV primer. Residue 28 now encodes isoleucine as a result of the mutation -TTC- to -**A**TC-.*

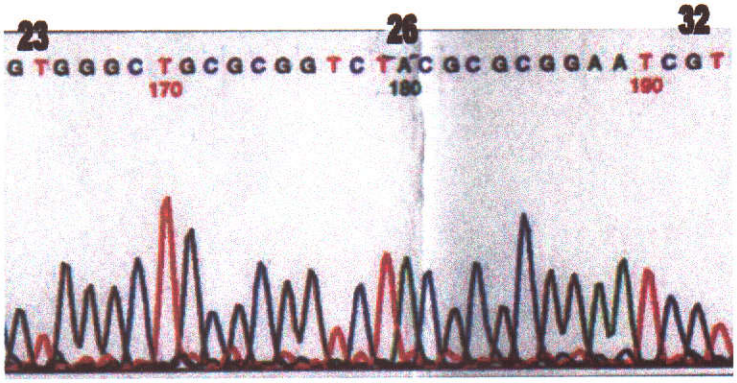

Figure 6.3.1i *DNA sequence chromatograph of 5AR1AVYA mutant clone with T7EEV primer. Residue 28 has been mutated from -TTC- to -**TAC**- and now encodes phenylalanine.*

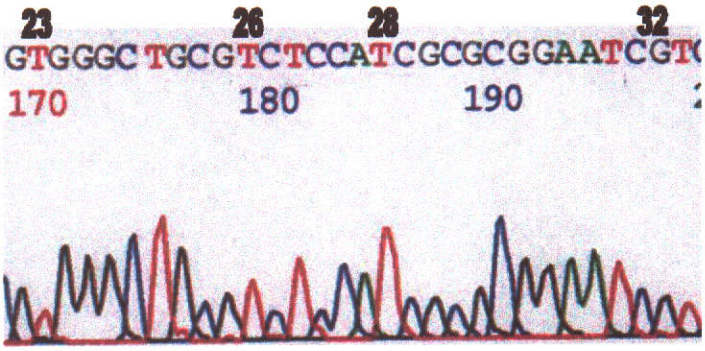

Figure 6.3.1j *DNA sequence chromatograph of 5AR1VSIA mutant clone with T7EEV primer. The sequence -G**TC TCC A**TC- at residues 26-28 confirms the mutation of -AVFA- to -VSIA.*

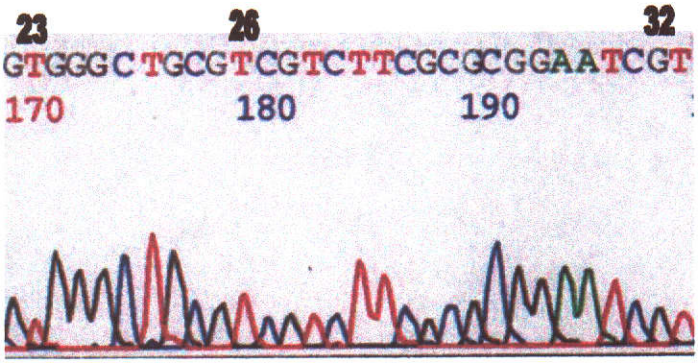

Figure 6.3.1k *DNA sequence chromatograph of 5AR1VVFA mutant clone with T7EEV primer. Residue 26 now encodes valine as a result of the mutation -GCG- to -G**TC**-.*

6.3.2 Characterisation of Stably Transfected Cells - Determination of Km and Vmax for Testosterone and Ki for Finasteride

As shown in the subsequent figures (6.3.2a to 6.3.2f) Km and Vmax values for each of the mutant enzymes were determined from Lineweaver-Burke plots constructed with the Enzyme Kinetics V1.5 program (Trinity Software, USA), all Km values are the calculated mean plus or minus the standard deviation. This program was also used to determine the inhibitor constant (Ki) for the competitive inhibitor Finasteride for each mutant (Figures 6.3.2g to 6.3.2l).

Mutants and the wild type 5AR1 used for comparisons, were stably transfected into CHO cells and the characteristics of the expressed enzymes were determined using pooled data from at least two, and more usually three or four, different experiments. All results are summarised in Table 6.3.2.

As is shown in table 6.3.2, the changes in characteristics of the mutants can be broadly divided into three groups. Those that had virtually no effect, those that increased Km and/or Ki and those that decreased Km and/or Ki. Additionally, many of the mutants had Vmax values different from wild type 5AR1.

Changes in Km ranged from an increased affinity for T of ~3.2-fold (mutant AVFV) to a decrease of ~4-fold (mutant AAFA). Changes in Ki ranged from a 1.7-fold increase (mutant ASIV) in sensitivity to Finasteride, to a 9 -fold decrease in sensitivity (mutant ASFA) to this competitive inhibitor. Changes in Vmax ranged from a 6-fold increase to a 1.3-fold decrease.

Increased affinity for T was seen in five mutants, with increases ranging from 1.8 to 3.2-fold. Increased sensitivity to Finasteride was seen in four mutants with these increases ranging from 1.2 to 1.7 -fold. Decreased affinity for T, 1.5 to 4-fold, was seen in four mutants and decreased sensitivity, 1.4 to 9-fold, to Finasteride in seven mutants.

In most instances changes in Km were accompanied with changes in Ki and again in most instances, the directional changes in Km and Ki were the same. Thus mutants with a decreased affinity for T had decreased sensitivity to Finasteride and increased affinity for T was accompanied by increased sensitivity to Finasteride. However this did not occur in every case and often changes in Km and Ki were of different magnitudes. Notably, the mutant 5AR1AAFA, which had the greatest decrease, 4-fold, in Km, had only a marginal decrease, 1.6-fold, in Finasteride sensitivity. Similarly, the mutant 5AR1ASFA, which had a 9-fold decrease in Finasteride sensitivity, had only a 2-fold decrease in affinity for T.

A

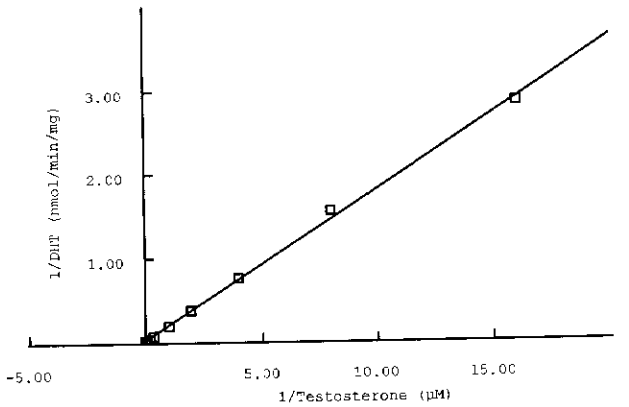

Figure 6.3.2a *Lineweaver-Burke plot of 5AR1AAFA (A) transfected CHO cells, derived from 2 separate experiments. Km and Vmax values were 11.24±1.40μM and 58.96nmol DHT/min/mg of cell protein (A).*

B

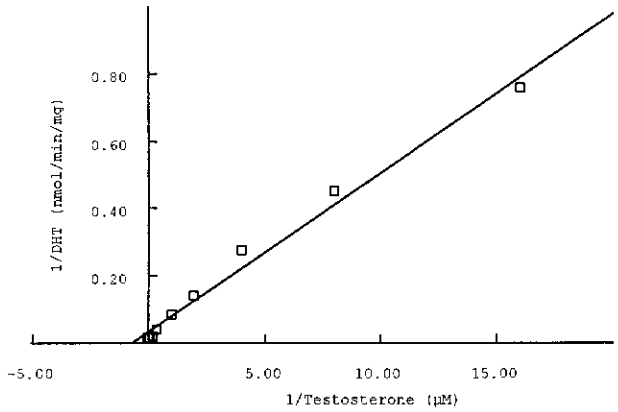

C

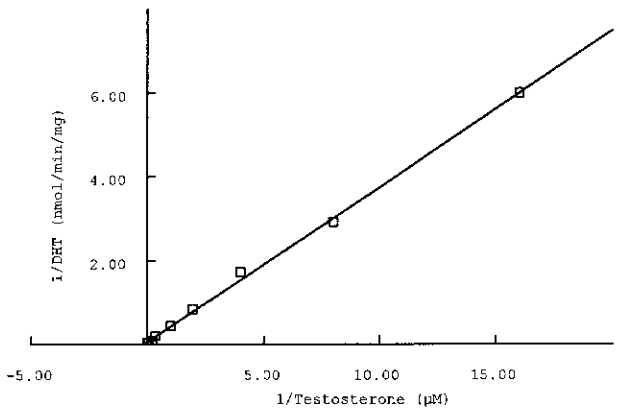

Figure 6.3.2b *Lineweaver-Burke plots of 5AR1AFVA (B) or 5AR1ASFA (C) transfected CHO cells, each derived from 2 separate experiments. Km and Vmax values were 1.61±0.81μM and 30.46nmol DHT/min/mg of cell protein (B) and 6.22±0.99μM and 16.59nmol DHT/min/mg of cell protein (C).*

D

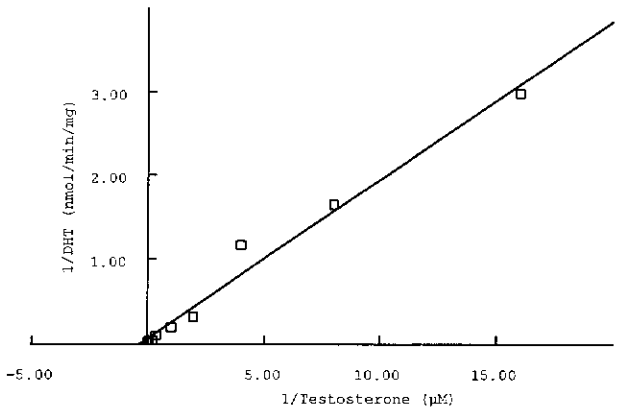

E

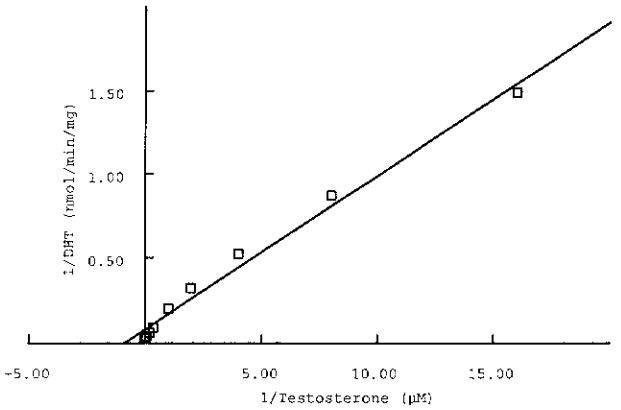

Figure 6.3.2c *Lineweaver-Burke plots of 5AR1ASIA (D) or 5AR1ASIV (E) transfected CHO cells, each derived from 2 separate experiments. Km and Vmax values were 2.92±0.001μM and 15.30nmol DHT/min/mg of cell protein (D) and 1.17±0.09μM and 12.76nmol DHT/min/mg of cell protein (E).*

F

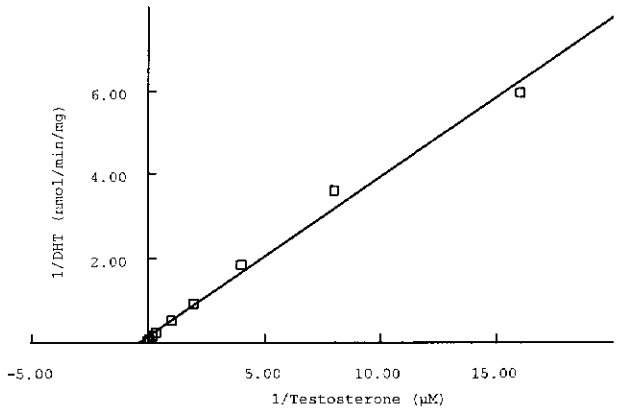

G

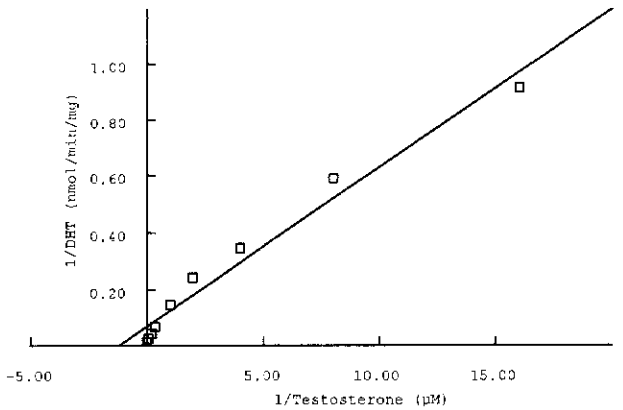

Figure 6.3.2d *Lineweaver-Burke plots of 5AR1AVAA (F) or 5AR1AVFV (G) transfected CHO cells, derived from 2 and 3 separate experiments respectively. Km and Vmax values were 2.73±0.86μM and 10.74nmol DHT/min/mg of cell protein (F) and 0.86±0.04μM and 15.07nmol DHT/min/mg of cell protein (G)*

H

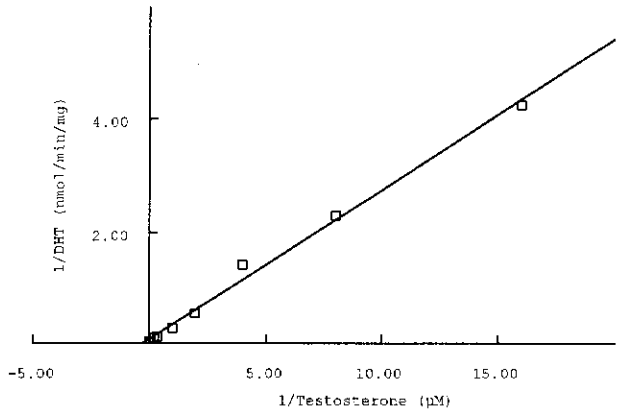

I

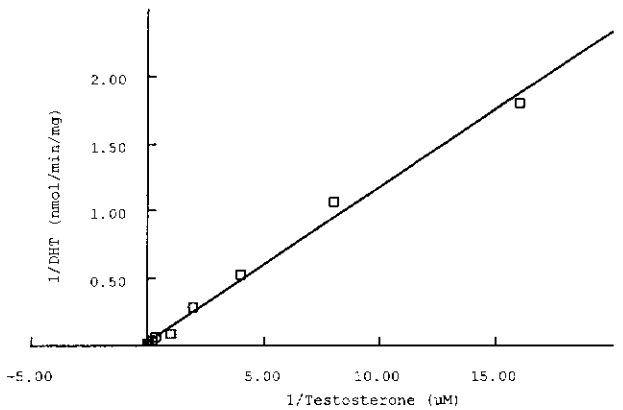

Figure 6.3.2e *Lineweaver-Burke plots of 5AR1AVIA (H) or 5AR1AVYA (I) transfected CHO cells, derived from 2 and 3 separate experiments respectively. Km and Vmax values were 4.13±0.38μM and 17.45nmol DHT/min/mg of cell protein (H) and 4.23±0.88μM and 36.54nmol DHT/min/mg of cell protein (I).*

J

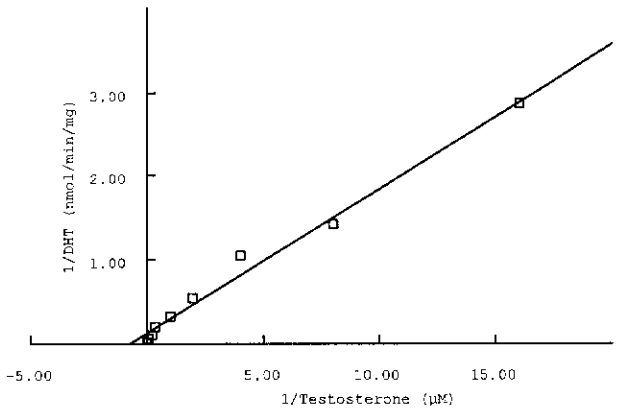

K

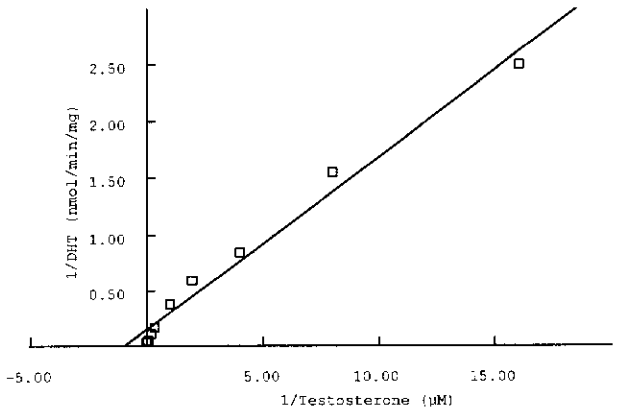

Figure 6.3.2f *Lineweaver-Burke plots of 5AR1VSIA (J) or 5AR1VVFA (K) transfected CHO cells, each derived from 2 separate experiments. Km and Vmax values were and 1.42±0.11µM and 8.30nmol DHT/min/mg of cell protein (J) and 1.10±0.06µM and 7.02nmol DHT/min/mg of cell protein (K).*

L

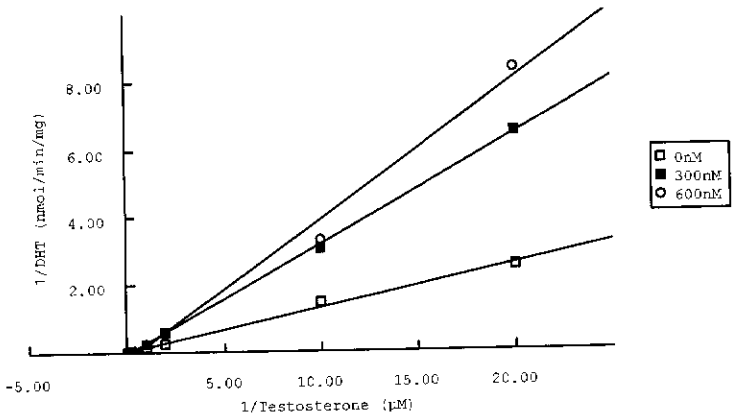

M

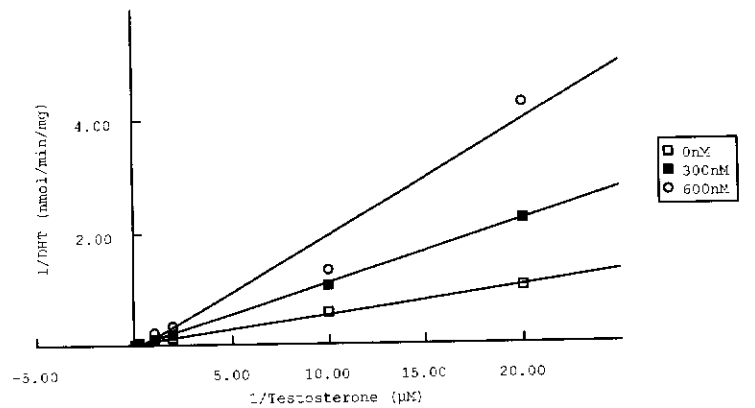

Figure 6.3.2g *From duplicate measurements of 5AR activity at T concentrations from 0.05-20μM and at 0, 300 and 600nM Finasteride, the Ki values derived for the 5AR1AAFA (L) and 5AR1AFVA (M) mutants respectively were 515.1nM and 233.2nM.*

N

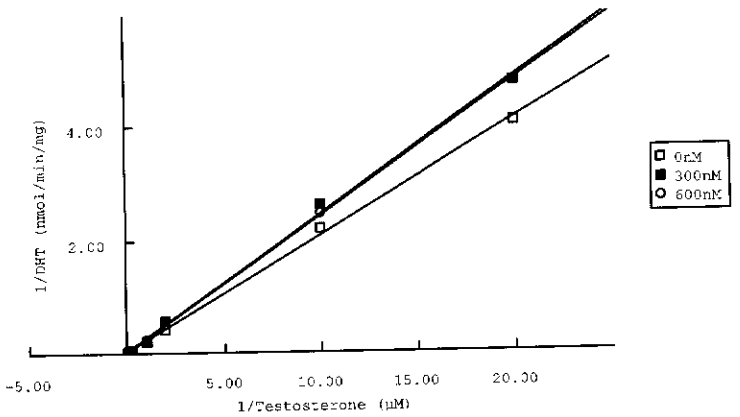

O

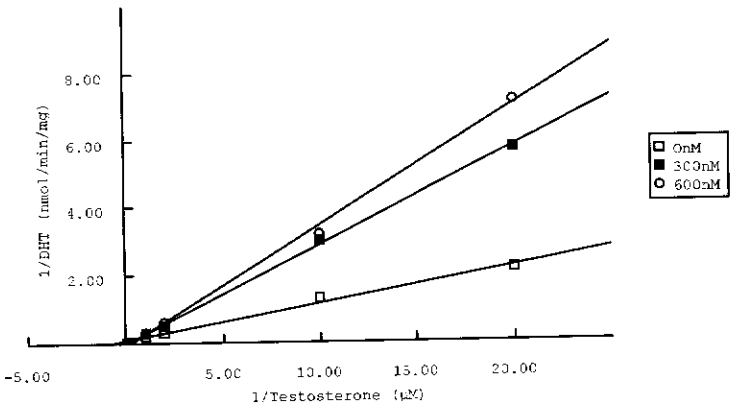

Figure 6.3.2h *From duplicate measurements of 5AR activity at T concentrations from 0.05-20μM and at 0, 300 and 600nM Finasteride, the Ki values derived for the 5AR1ASFA (N) and 5AR1ASIA (O) mutants respectively were 3001.5nM and 474.5nM.*

P

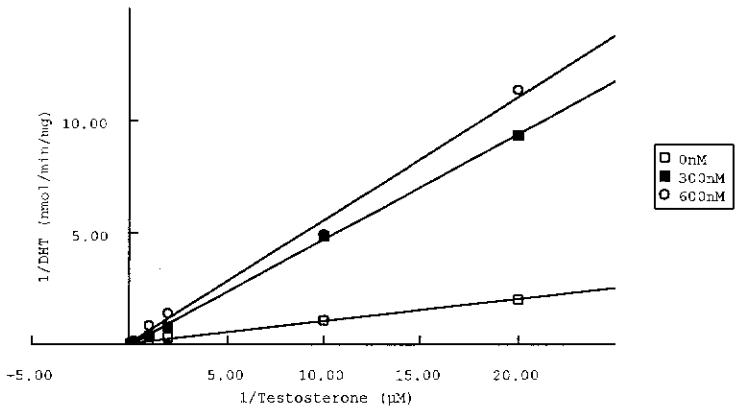

Q

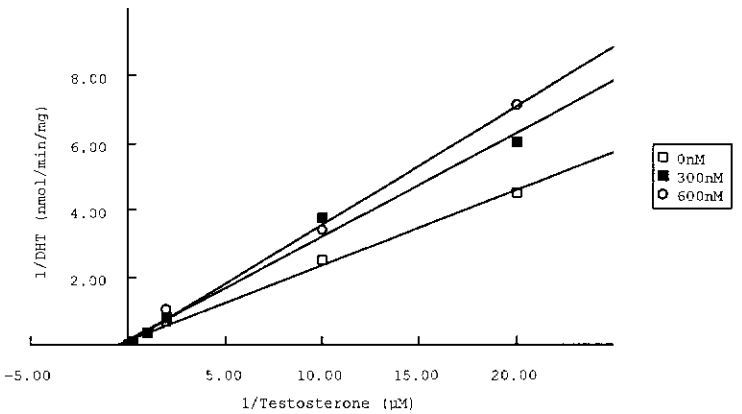

Figure 6.3.2i *From duplicate measurements of 5AR activity at T concentrations from 0.05-20μM and at 0, 300 and 600nM Finasteride, the Ki values derived for the 5AR1ASIV (P) and 5AR1AVAA (Q) mutants respectively were 187.5nM and 1151.0nM.*

R

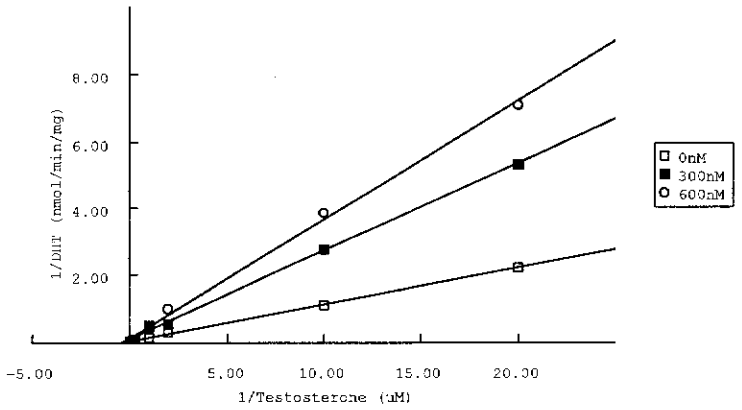

S

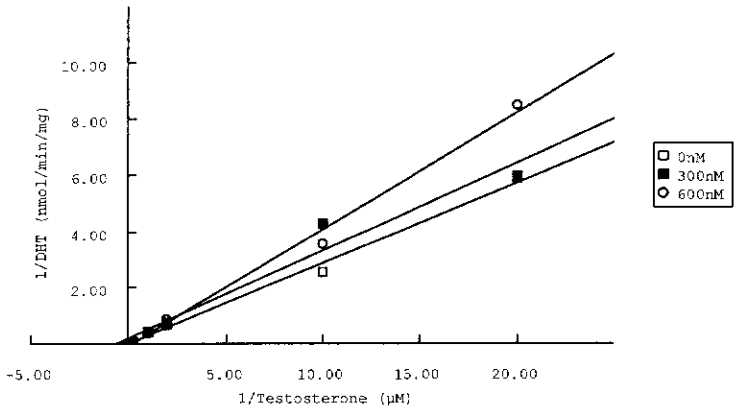

Figure 6.3.2j *From duplicate measurements of 5AR activity at T concentrations from 0.05-20µM and at 0, 300 and 600nM Finasteride, the Ki values derived for the 5AR1AVFV (R) and 5AR1AVIA (S) mutants respectively were 285.1nM and 1264.7nM.*

T

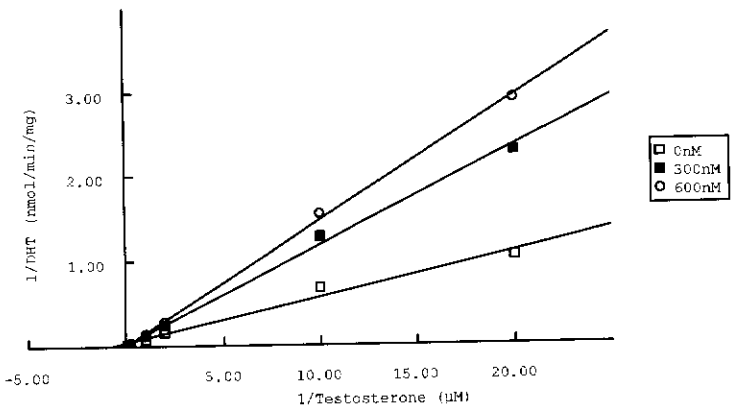

U

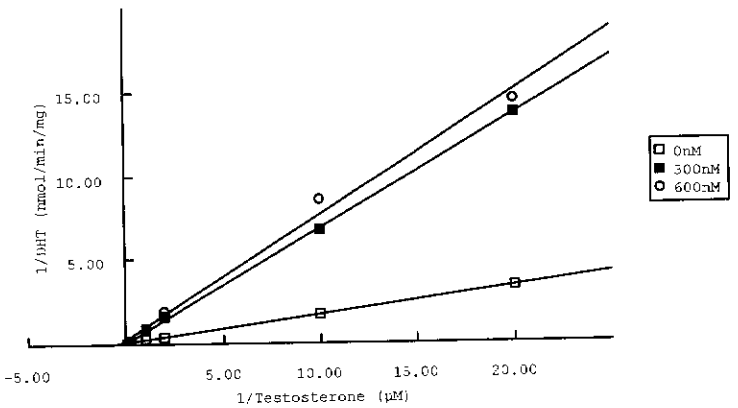

Figure 6.3.2k *From duplicate measurements of 5AR activity at T concentrations from 0.05-20μM and at 0, 300 and 600nM Finasteride, the Ki values derived for the 5AR1AVYA (T) and 5AR1VSIA (U) mutants respectively were 493.1nM and 254.4nM.*

V

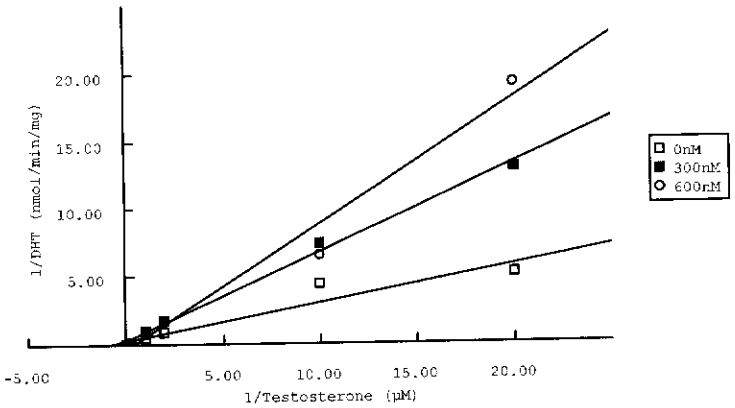

Figure 6.3.2l *From duplicate measurements of 5AR activity at T concentrations from 0.05-20μM and at 0, 300 and 600nM Finasteride, the Ki value derived for the 5AR1VVFA (V) mutant was 681.9nM.*

Enzyme	Average % Conversion T to DHT	Km for T (μM)	Vmax (nmol DHT/min/mg)	Vmax/Km	Ki for Finasteride (nM)
CHO cell control	0.85	18.67±1.19	42.07	2.25	-
Wild type human 5AR1	3.5	2.80±0.60	9.35	3.34	327.8
Wild type rat 5AR1[33, 128]	-	1.40	4.8	3.43	5.8
5AR1R	14.7	2.68±0.37	54.43	20.31	25.6
5AR1AAFA	6.2	11.24±1.40	58.96	5.25	515.1
5AR1AFVA	14.5	1.61±0.81	30.46	18.92	233.2
5AR1ASFA	2.3	6.22±0.99	16.59	2.67	3001.5
5AR1ASIA	5.6	2.92±0.001	15.30	5.24	474.5
5AR1ASIV	2.9	1.17±0.09	12.76	10.91	187.5
5AR1AVAA	2.3	2.73±0.86	10.74	3.93	1151.0
5AR1AVFV	9.0	0.86±0.04	15.07	17.52	285.1
5AR1AVIA	3.4	4.13±0.38	17.45	4.23	1264.7
5AR1AVYA	6.7	4.23±0.88	36.54	8.64	493.1
5AR1VSIA	3.7	1.42±0.11	8.30	5.85	254.4
5AR1VVFA	3.2	1.10±0.06	7.02	6.38	681.9

Table 6.3.2 *Summary table of the kinetic characterisation of mutant 5AR1 enzymes. Wild type rat and human 5AR1 and the 5AR1R mutant (replacement of -AVFA- in human with -VSIV- from rat 5AR1) are included for comparison.*

6.4 DISCUSSION

The number of transformants generated for each mutagenesis reaction varied, yet for all mutations bacteria expressing the desired mutations were produced. It was found that by varying the quantity of template DNA cycled, transformants could be produced. For most reactions 75ng of template proved successful, but for some mutations increasing template quantity to 100ng was necessary. Problems were encountered with the ASIV mutation with no transformants

evident with 50, 75 or 100ng of template. As recommended by the manufacturer, the annealing temperature was lowered to 50^{o}C and the extension time extended to 21 minutes (3min/kb plasmid), neither of which proved successful. By increasing the quantity of the forward and reverse primers to 1.5 times that recommended (187.5ng) and increasing the number of cycles from 16 to 18, transformants expressing the ASIV mutation were produced. For both the ASIV and VSIA mutation three alterations were required, 16 cycles and 125ng of each primer proved successful for the VSIA mutation and 18 cycles and 187.5ng of each primer for the ASIV mutation. It is notable that far less transformants (5) were generated for the VSIA compared with the ASIV mutation (100-200). This difference is thought probably to be due to the reduced cycle number and/or primer concentrations used for the ASIV mutation.

The tetrapeptides -AVFA- (r26-29) and -VSIV- (r22-25) have been shown to form part of the substrate/inhibitor binding domains of human and rat 5AR1 respectively[128]. However, the contribution to this binding of the individual amino acids comprising this tetrapeptide had not previously been determined. To gain some insight into the individual contributions of the four amino acids in the tetrapeptide -AVFA-, these residues were exchanged for the residues -VSIV- from rat 5AR1 using site-directed mutagenesis. Characterisation of the various mutants stably expressed by CHO cells enables this as the Ki for Finasteride of human 5AR1 is much greater than is the Ki of rat 5AR1 for this inhibitor. These exchanges permit a direct assessment for the contributions of the individual residues in human 5AR1 and an indirect assessment of the contributions of individual residues in rat 5AR1. Direct assessment of the contributions of residues of -VSIV- to substrate/inhibitor binding by rat 5AR1 was not possible, as the cDNA for rat 5AR1 was not available.

Although differences are seen between the Km for testosterone of 2.8μM obtained here for wild type human 5AR1 and the published value of ~1.4μM for rat 5AR1[128], a greater difference is seen between their sensitivities to the competitive inhibitor Finasteride. The Ki value obtained here for human 5AR1 of ~328nM for this inhibitor is markedly different from the published value of ~6nM for rat 5AR1[128]. Replacement of -AVFA- in human 5AR1 with the entire tetrapeptide -VSIV- gave a mutant with a Km of 2.7 μM and a Ki of 26nM

(Chapter 7.0). This increase (4-fold) in sensitivity to Finasteride is similar to that seen by others [128] and confirms their finding that these tetrapeptides are significantly involved in Finasteride binding. From Table 6.3.2 it is apparent that some of the mutants in which single amino acid changes were made, approach this level of sensitivity.

Significant variation was however seen between Vmax for all expressed mutants, which may reflect differences in the transfection efficiencies of CHO cells with these constructs. The Vmax/Km ratios of all mutants, except 5AR1ASFA, were greater than wild type 5AR1 and indicate enhanced enzyme efficiency. The ratio's of the 5AR1AVFV and 5AR1AFVA mutants were markedly increased, ~5.5-fold, with the smallest increase seen for the 5AR1AVAA and 5AR1AVIA mutants.

To determine their contribution to substrate/inhibitor binding in human 5AR1, residues 27 (valine) and 28 (phenylalanine) from the tetrapeptide -AVFA- were initially each mutated to alanine. A 1.5-fold reduction in sensitivity to Finasteride and 4-fold reduction in substrate affinity were seen when V27 was mutated to alanine (5AR1AAFA). It is therefore apparent V27 contributes to both substrate and inhibitor binding in human 5AR1, perhaps through conformational and steric effects imposed by its branched side chain.

Replacement of phenylalanine 28 with alanine (5AR1AVAA) had no effect on substrate binding, as the Km was similar to wild type 5AR1s. Delocalised electrons in the side chain of phenylalanine can electrostatically interact with other molecules. A loss of these interactions may account for the 3.5-fold increase in Finasteride resistance seen for the 5AR1AVAA mutant. To determine if this reduced sensitivity to Finasteride is the result of mutation to a non-aromatic residue, phenylalanine was mutated to the similarly aromatic residue tyrosine (5AR1AVYA). Studies of 5AR1AVYA showed no significant effects on substrate or inhibitor binding and suggest expression of an aromatic amino acid at residue 28 is required for the binding of Finasteride.

Residues comprising the tetrapeptide -AVFA- were next exchanged with their analogous residue from -VSIV- both individually and in combination. Replacing

A26 with V22 from rat 5AR1 (5AR1VVFA) resulted in a 2.5-fold increase in substrate affinity. The Km value for this mutant is similar to that of wild type rat 5AR1 and demonstrates the contribution of V22 to substrate binding in the rat enzyme. A 2-fold increase in resistance to Finasteride suggest V22 is not important for Finasteride binding in rat 5AR1, additionally these results show the importance of A26 for Finasteride binding in human 5AR1. Valine differs from alanine by its branched side chain, this increased resistance to Finasteride may therefore result from steric and conformational restrictions imposed by valine's branched side chain.

In the 5AR1ASFA mutation, the branched residue V27 in human 5AR1 was replaced with the unbranched residue S23 from rat 5AR1. Characterisation of this mutant showed the importance of V27 for both substrate and inhibitor binding in human 5AR1. Conformational change resulting from substitution to an unbranched residue may account for the 2.2-fold decrease in substrate affinity and 9-fold increase in Finasteride resistance seen. S23 does not appear important for substrate or inhibitor binding in rat 5AR1 as its introduction into human 5AR1 (-AVFA-) did not alter Km or Ki to values similar to those of wild type rat 5AR1.

A 1.5-fold reduction in substrate affinity and almost 4-fold increase in Finasteride resistance were seen when F28 in human 5AR1 was mutated to I21 from rat 5AR1 (5AR1AVIA). Although there was a reduction in substrate affinity, the Km remained within the widely accepted range of 1-5μM for wild type human 5AR1[10] and there has been no real effect on substrate binding. The increased Finasteride resistance was similar to that seen for the 5AR1AVAA mutant and reinforces the importance of F28 for Finasteride binding in human 5AR1. Introducing I24 into -AVFA- has not changed Km and Ki towards values of wild type rat 5AR1, suggesting this residue alone does not determine substrate/inhibitor binding in the rat enzyme.

The Km of the 5AR1ASIA mutant (residues V27 and F28 in human 5AR1 replaced with S23 and I24 from rat 5AR1) was not dissimilar from wild type human 5AR1. Changes to the Ki (1.4-fold) for 5AR1ASIA were not as great as those seen for other mutants eg. 5AR1ASFA (9.2-fold), suggesting either that

S23 and I24 are important for substrate/inhibitor binding in rat 5AR1 or alternatively that V27 and F28 are not important in human 5AR1. Results from studies of other mutations in this chapter have shown the latter not to be true and V27 and F28 are important for substrate/inhibitor binding in human 5AR1. It is therefore apparent S23 and I24 are important for both substrate and inhibitor binding in rat 5AR1.

Conservation of the terminal alanine of -AVFA- and mutation of the other three residues to -VSI- from rat 5AR1 (5AR1VSIA) changed Km towards wild type rat 5AR1, suggesting the tripeptide -VSI- is important for substrate binding in rat 5AR1. Similar results were seen from studies of the mutant in which -AVFA- was mutated to -ASIV- (5AR1ASIV) and suggest all four residues comprising the tetrapeptide -VSIV- contribute to substrate binding in rat 5AR1. Comparisons with wild type rat 5AR1 show a marked resistance to Finasteride for 5AR1VSIA and an increase in sensitivity to Finasteride for 5AR1ASIV, the tripeptide -SIV- is therefore of greater significance for Finasteride binding in rat 5AR1 than is -VSI-. Additionally the initial valine residue of the tetrapeptide -VSIV- does not appear to contribute to this binding.

Although these findings can only give an indirect assessment of the role of residues -VSIV- in rat 5AR1, they suggest all four residues of this tetrapeptide are of particular significance in substrate binding by this enzyme. The tripeptide -SIV- is important for Finasteride binding with the initial valine of -VSIV- playing no role in this binding.

Assessments of the contribution of residues in the tetrapeptide -AVFA- to substrate/inhibitor binding by human 5AR1 have shown;

1. The structural conformation of A26 is necessary for optimum binding of Finasteride, yet it is not required for substrate binding.
2. Conformational effects of the branched residue V27 are important for both substrate and inhibitor binding.
3. Electrostatic interactions by delocalised electrons in the aromatic side chain of phenylalanine are important for Finasteride binding.
4. The terminal alanine residue does not appear to have any functional significance.

These studies have only considered 5AR as a linear molecule, which of course it is not. The terminal alanine of -AVFA- may therefore be important for determining the secondary structure of the substrate/inhibitor binding site, rather than a direct involvement in binding.

Chapter 7.0

Assessment of the Role of the Tetrapeptide -GALA- in Substrate/Inhibitor Binding by Human 5α- Reductase 2

7.1 INTRODUCTION

Increased dihydrotestosterone (DHT) levels within the prostate are recognised as a major determinant for the development of benign prostatic hyperplasia (BPH). In males, BPH is the most common benign proliferative disorder and is due to histological changes occurring within the prostate as a result of prolonged androgen exposure. It has a 2% incidence in all males born and studies indicate that nearly all men will develop BPH if they live long enough[142]. Hyperplastic nodules form within the periurethral zone of the prostate eventually leading to urethral constriction[94] with resulting symptoms of hesitancy, dribbling, incomplete emptying, urgency, dysuria and straining. Although BPH is a non-malignant condition its associated symptoms can be highly distressing for the patient and necessitate treatment. As the enzyme 5α- reductase (5AR) through its action on testosterone (T), is responsible for increased DHT levels, a great deal of interest has been generated in the development of pharmacological inhibitors of this enzyme.

Many pharmacological inhibitors have been developed which can be classified as steroid derivatives, non-steroid derivatives and anti-androgen compounds. The anti-androgens, which include cyproterone acetate and flutamide although effective in reducing DHT levels, also reduce the levels of other androgens, notably T. As a result undesirable side effects relating to fertility and sexual function, such as impotence and loss of sex drive commonly result from treatment with these compounds.

The non-steroid derivatives share the heterocyclic ring structure of the steroid derivatives containing nitrogen and 3-oxo groups but without the characteristic fourth steroid ring. Non-steroid derivatives include the benzoylaminophenoxybutanoic acid derivatives and the benzoquinolones. ONO-3805 is an example of the benzoylaminophenoxybutanoic acid derivatives and exhibits potency against both rat prostatic and human 5AR[111] whereas the benzoquinolone LY191704 selectively inhibits human 5AR1[52].

The steroid derivatives are the largest class of 5AR inhibitors and include the extensively studied compounds 17β-[N,N-diethyl] carbamoyl-4-methyl-4-aza-5α-

androstan-3-one (4-MA) and 17β-[N-t-butyl] carbamoyl-4-aza-5α-androst-1-ene-3-one (Finasteride or MK-906). 4-MA contains a nitrogen (4-aza) instead of a carbon at position four of the heterocyclic ring and its reduction by 5AR leads to an inactive form of the enzyme[67].

Studies of 4-MA in rats demonstrate its ability to reduce DHT levels in the ventral prostate while simultaneously increasing T concentrations[105]. It has a low affinity for the AR and is unlikely to produce any undesirable side effects[149], unfortunately it inhibits the enzyme 3β- hydroxysteroid dehydrogenase resulting in hepatotoxicity[106].

Finasteride is the most studied of the 5AR inhibitors and as Proscar® is currently used for the treatment of BPH and more recently, as Propecia®, for male pattern baldness (MPB). Structurally, Finasteride differs from 4-MA by the presence of a double bond in the A-ring, a t-butyl amide group at position seventeen and the absence of a 4-methyl substitution[107]. It is a competitive inhibitor with greater efficacy for human 5AR2 than 5AR1. As it does not combine with the AR this reduces the incidence of undesirable side effects and treatment has no other inhibitory effects either on the formation or action of other steroid hormones [94, 143]. The recommended therapeutic dose of 5mg daily results in a 60-80% reduction in serum DHT levels[144] but a ~90% reduction of intraprostatic DHT levels[102]. This greater intraprostatic reduction seen is consistent with the predominant expression in the prostate of the type 2 enzyme, which is more sensitive to Finasteride than is 5AR1.

The role of Finasteride in the treatment of prostate cancer remains unclear, as there is no evidence yet of benefit to men with established cancer of the prostate[124, 145]. Finasteride treatment in patients with BPH however, is thought to prevent progression to more serious disease[67]. As mentioned previously, Finasteride is used for the treatment of dermatological disorders of 5AR expression including hirsutism, acne and male pattern baldness. There is some debate however regarding its usefulness in these conditions as they are predominantly associated with 5AR1, which is relatively insensitive to Finasteride.

Due to continuing inability to isolate 5AR from its membrane bound lipid environment and its very low expression levels even in androgen dependent tissue, little is known about the functional domains of 5AR. Consequently pharmacological inhibitors of 5AR have been largely based on the structure of the substrate testosterone, rather than the structure of the enzyme itself. The use of expression cloning techniques in the early 1990s isolated the cDNAs encoding two isoenzymes of 5AR in rat and man[1, 31, 32, 33]. Isolation of these cDNAs has enabled the study of 5AR at the molecular level, providing the means by which its functional domains may be elucidated.

Very few structure-function studies of human 5AR exist and to date there have been only three of merit[29, 63, 128]. A considerable amount of information regarding the substrate binding domains of 5AR has been obtained from studies of naturally occurring mutations in the gene encoding 5AR2 that are responsible for steroid 5AR deficiency. In these studies Wigley and colleagues[63] individually recreated each of the 22 mutations in an expressible cDNA construct (5AR2 cDNA). Human embryonic 293 cells were then transfected with each of the 22 constructs and the biochemical characteristics of the expressed enzymes determined. These studies showed that twelve of these mutations totally inactivated the enzyme while the remaining ten severely impaired enzyme activity. Significantly, all of the mutated residues studied are conserved between rat and human 5AR isoenzymes, which suggests they are important for enzyme function. Of the 10 mutations impairing enzyme function two, G34R and H231R, affected the ability of the enzyme to bind testosterone[63]. These two residues map to either end of the enzyme suggesting that the substrate binding domain constitutes nonlinear determinants. Recent studies of 5AR2[127] have also suggested that its substrate/Finasteride binding site is bipartite and there are distinct domains within the amino and carboxyl termini. If indeed both termini are involved in substrate/inhibitor binding, exactly how the amino terminus interacts with the carboxyl terminus to form this domain will necessitate isolation and crystallisation of the protein.

The remaining eight mutations identified[63] as severely impairing enzyme activity R145W, R171S, P181L, G183S, N193S, G196S, R246W and R246Q are all located within the carboxyl terminus and reduce the affinity of the enzyme for

NADPH. Although these mutations impair co-factor binding they do not affect substrate binding, suggesting both that enzyme denaturation is not a consequence of these mutations and that the two binding domains are discrete. 5AR does not have consensus NADPH selectivity residues or the adenine nucleotide binding sequences common to other reductase enzymes[131] and it is possible these eight residues comprise a unique class of NADPH binding sites.

In 1995, Bhattacharyya and colleagues[29] identified part of the NADP(H) binding site of rat liver 5AR1 using the probe [2'-^{32}P]-2N_3-NADP+, photolabelled to a peptide corresponding to the adenine binding domain. After exposure to the probe, the photolabelled enzyme was partially purified by preparative SDS gel electrophoresis and digested with trypsin before further purification of the [^{32}P]-labelled tryptic peptide using immobilised Al^{3+} affinity and reverse-phase high performance liquid chromatography (HPLC). Sequencing of the purified peptide showed it to comprise 11 amino acids identified as residues 170-180 of rat 5AR1. It was concluded these residues -^{170}N-L-X-K-P-G-E-T-G-Y-K^{180}- may form part of its NADP(H) binding domain[29].

Arginine 172 was the only unidentifiable residue (X) and appeared to be modified by the probe itself. Although this sequence shows little homology with the sequence -Gly-X-Gly-X-X-Gly/Ala- commonly associated with NAD[H] and NADP[H] binding enzymes[132, 146], it is still thought to contribute to cofactor binding. Significant conservation exists between rat and human 5AR isoenzymes with respect to these eleven residues. Hydropathy plots indicate that the peptide is in a solvent-exposed portion of 5AR1 enabling it to interact directly with the hydrophilic NADP[H]. A possible conclusion from these studies is that type 1 5ARs have a unique nucleotide binding sequence -Gly-X-X-Gly-X-X-X-X-X-Gly-Gly-[63]. Significantly there is considerable homology within this sequence for rat and human 5AR2 (Figure 7.1.2), however the second glycine is replaced with a serine in humans or isoleucine in rats.

Rat 5AR1	-[160]INIHSDHILR**NLRKPGETGYK**IPRGGLFEYV[190]-
Rat 5AR2	-[159]INIHSDYTLR**QLRKPGEVIYR**IPRGGLFTYV[189]-
Human 5AR1	-[164]INIHSDHILR**NLRKPGDTGYK**IPRGGLFEYV[194]-
Human 5AR2	-[159]INIHSDYILR**QLRKPGEISYR**IPQGGLFTYV[189]-

Figure 7.1.1 *Sequence alignment demonstrating conservation within and between species of the eleven amino acid peptide (underlined), proposed as the NADP[H] binding domain.*

Three of the eight mutations R171S, P181L and G183S, identified as affecting cofactor binding[63], all lie within the adenine binding domain proposed by Bhattacharyya and colleagues[29]. These residues are all highly conserved in rat and human isoenzymes, lending further support for the identification of the sequence -Gly-X-X-Gly-X-X-X-X-X-Gly-Gly-, as part of the cofactor binding domain of rat 5AR1.

In summary, the studies of naturally occurring mutations in 5AR2[63] indicate;

1. The cofactor-binding domain lies within the carboxyl terminus of 5AR.
2. Residues involved in substrate binding map to both the amino and carboxyl termini suggesting a domain composed of non-linear determinants.
3. Mutated residues are conserved between species thus demonstrating functional importance.

A further thirteen naturally occurring mutations of SRD5AR2 have been more recently identified using single stranded conformation polymorphism (SSCP)[127]. Each mutation was reconstructed in a mammalian expression vector (SRD5AR2 cDNA mammalian expression vector 5αR2) by site-directed mutagenesis, COS cells electroporated with the mutant constructs and their characteristics determined. Of these thirteen mutations, one coded for an enzyme with essentially unaltered kinetics from wild type 5AR2, three increased and nine reduced enzyme activity. Results from these studies were considered to suggest the substrate/Finasteride binding site of human 5AR2 is bipartite with the involvement of distinct amino acids both from the amino and carboxyl termini. The cofactor binding site however is confined largely to the enzyme's carboxyl terminus.

A significant study of the functional domains of 5AR was that of Thigpen and Russell[128]. In this study, differences in the sensitivities of rat and human 5AR1 to Finasteride were exploited to identify residues involved in substrate binding. Chimeric cDNAs coding for rat and human 5AR were created by oligonucleotide-directed loop-out mutagenesis, expressed in human embryonic kidney 293 cells and sensitivity to Finasteride of the chimeric enzymes determined. Chimeras containing exon 1 from the rat enzyme demonstrated a rat-like Finasteride sensitivity while those containing exon 1 from human 5AR1 exhibited a marked resistance to Finasteride, similar to that of the unaltered human enzyme[128]. These results suggested at least part of the substrate binding domain of both rat and human 5AR1 lies within exon 1. By exchanging progressively smaller segments the domain was located within the first 44 amino acids. Sequence analysis between rat and human 5AR1 identified two regions of non-identity within this region. Subsequent exchange of tri- and tetrapeptide sequences led to the identification of residues 22-25 in rat 5AR1 (-VSIV-) and 26-29 in human 5AR1 (-AVFA-) as contributing to the substrate binding domains of these enzymes[128].

From these studies it has been suggested[44, 128] that the analogous residues 21-24 (-GALA-) in human 5AR2 may form part of its substrate binding domain. These amino acids in 5AR2 lie close to the G34R mutation[63] suggesting at least part of the substrate binding domain of 5AR2 may map between residues 21-34 within the amino terminus.

To date however there is no experimental data to support this proposal[44, 128] and the substrate binding domain of 5AR2 remains unknown. To further investigate substrate binding by human 5AR2 we have created a series of mutant 5AR clones using the commercially available Quickchange™ method for site-directed mutagenesis.

Two mutant 5AR isoenzymes were created to determine the significance of the tetrapeptide sequences -AFVA- (r26-29) and -GALA- (r21-24), for substrate binding in human 5AR1 and 5AR2 respectively. These mutants were termed 5AR2M, residues 21-24 (-GALA-) in human 5AR2 mutated to the analogous residues 26-29 (-AVFA-) from human 5AR1 and 5AR1M in which residues 26-

29 (-AVFA-) in 5AR1 were replaced with the analogous residues 21-24 (-GALA) from 5AR2.

A third mutant also was created in which -AVFA- in human 5AR1 was mutated to the analogous residues -VSIV- (r22-25) from rat 5AR1. This mutant is that characterised by Thigpen and Russell[128], and was created in part to confirm the findings of these authors and in part as a control for the procedures performed here.

Following sequencing to ensure both that the expected mutations had occurred and there were no unexpected changes, mutant cDNAs were stably transfected into Chinese Hamster Ovary (CHO) cells and their characteristics determined.

7.2 METHODS

7.2.1 PLASMID DNA EXTRACTION

BRESAspin™ Plasmid Mini Kit (Bresatec) was used to extract all plasmid DNA, as described in section 3.2.1.1.

7.2.2 SITE-DIRECTED MUTAGENESIS

7.2.2.1 Reaction Components

Each reaction was set up as described section 4.2.2.1. Reaction components used in each reaction were:

5μL	10X reaction buffer
50ng	dsDNA template
125ng	Oligonucleotide forward primer
125ng	Oligonucleotide reverse primer
1 μL	dNTPs (10mM)

X μL sterile hpH_2O

---

50 μL

* 1μL of *Pfu* DNA polymerase (2.5U/μL), was added prior to cycling.

Nb. As each primer preparation had a different concentration, the amount rather than volume of primer used is given. The value of XμL for the volume of water used reflects the different volumes of primer solution added.

7.2.2.1a Primers

DNA sequences for the various mutagenesis primers are given below, with mutated residues in bold type. The primers used to create 5AR1M and 5AR2M were synthesized by Life Technologies (Queensland) and the primers used to create 5AR1R were from Operon Technologies (California).

5AR1M Primer Pair
5'- ^{22}GCC GTG GGC TGC **GGG GCA CTG** GCG CGG AAT CG^{32} -3'
3'- ^{22}CGG CAC CCG ACG **CCC CGT GAC** CGC GCC TTA GC^{32} -5'

5AR1R Primer Pair
5'- ^{22}GCC GTG GGC TGC **GTG TCC ATT GTG** CGG AAT CGT CAG^{33} -3'
3'- ^{22}CGG CAC CCG ACG **CAC AGG TAA CAC** GCC TTA GCA GTC^{33} -5'

5AR2M Primer Pair
5'- ^{18}GTC GCC CTT **GCG GTC TTC** GCG TTG TAC GTC GCG^{28} -3'
3'- ^{18}CAG CGG GAA **CGC CAG AAG** CGC AAC ATG CAG CGC^{28} -5'

7.2.2.2 Cycling Conditions

The 5AR1M, 5AR1R and 5AR2M mutagenesis reactions were cycled as below:

1. 1 cycle at 95^{o}C for 30 seconds.

2. 18 cycles at 95°C for 30 seconds.
3. 18 cycles at 55°C for 1 minute.
4. 18 cycles at 68°C for 16 minutes.
5. 4°C overnight.

7.2.2.3 *Product Digestion and Transformation into Bacteria*

Dpn I digestion and transformation of the product of each mutagenesis reaction into Epicurian supercompetent *E.coli* were as described in sections 4.2.2.3 and 4.2.2.4 respectively.

7.2.3 5' END LABELLING OF HYBRIDISATION PROBES

The protocol used to 5' end label the probes for the 5AR2 cDNA was as described in section 3.2.9.

7.2.4 HYBRIDISATION

Transfer of colonies to nylon membranes, hybridisation with radiolabelled probes, membrane washing, exposure to X-ray film and autoradiography were as described in sections 3.2.10.1 and 3.2.10.2.

7.2.5 DNA SEQUENCING FOR MUTATION IDENTIFICATION

Automated DNA sequencing was as described in section 4.2.3, using a primer (T7EEV) specifically designed for the multiple cloning site of the pCI-neo vector. To enable sequencing of the entire cDNA, primers were also designed based on the sequences of 5AR1 or 5AR2 (AR1R and AR2R respectively).

7.2.6 CALCIUM PHOSPHATE TRANSFECTION

Calcium phosphate transfection of CHO cells with pCI-neo vector containing 5AR1M, 5AR1R and 5AR2M mutant cDNAs was as described in section 3.2.12.

7.2.7 CHARACTERISATION OF STABLY TRANSFECTED CELLS - 5α- REDUCTASE ACTIVITY ASSAYS

Determination of the 5AR activity of transfected cells and of Km, Vmax, Ki, pH optima, total protein assays and cell culture procedures were as described in sections 3.2.14 to 3.2.16.

7.3 RESULTS

7.3.1 Site-directed mutagenesis of wild type 5AR1 and 5AR2 cDNAs

The 5AR1M, 5AR1R and 5AR2M mutant cDNAs were created using the Quickchange™ site-directed mutagenesis kit and appropriate oligonucleotide primers. Ampicillin resistant colonies from the 5AR2M transformation were first screened for the presence of the 5AR2 cDNA by hybridisation with specific $^{32}P_{\gamma}$ATP labelled probes (Section 3.2.9 and 3.2.10). The autoradiograph from this procedure is shown as Figure 7.3.1a. Plasmid DNA isolated from ampicillin resistant bacteria from all transformations (Table 7.3.1), was sequenced for the presence of the desired mutation. Figures 7.3.1b, 7.3.1c and 7.3.1d are the automated DNA sequence chromatographs for the 5AR1M, 5AR2M and 5AR1R mutations respectively.

Mutation	Colony Numbers on Transformation
5AR1M	>100
5AR1R	>100
5AR2M	24

Table 7.3.1 *Ampicillin resistant colony numbers resulting from the transformation of the 5AR1M, 5AR1R and 5AR2M mutagenesis reactions, prepared using the Quickchange™ mutagenesis method.*

Table 7.3.1 shows the number of ampicillin resistant colonies obtained following site-directed mutagenesis and transformation of the 5AR1M, 5AR1R and 5AR2M mutations into E.coli. 5AR2M clones were initially probed for the presence of the 5AR2 cDNA using a radiolabelled ($^{32P}\gamma$ATP) probe.

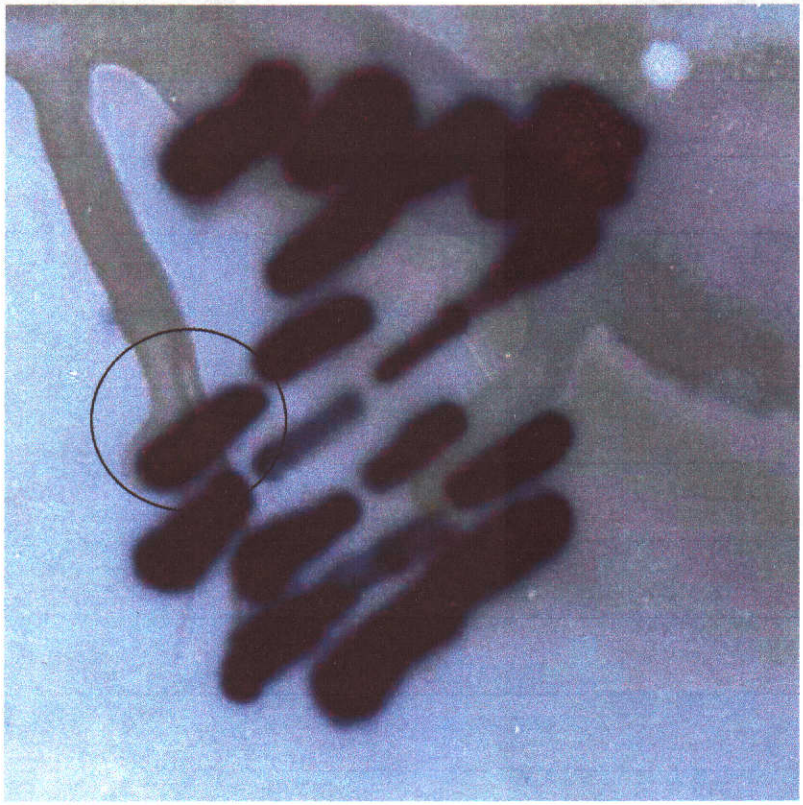

Figure 7.3.1a *Autoradiograph of 5AR2M transformants hybridised with $^{32p}\gamma$ATP-labelled probe for 5AR2. Clones containing the 5AR2 cDNA appear as black spots (circled).*

Figures 7.3.1b to 7.3.1d show the sequences, which confirm that the various mutations have been achieved. For each mutation shown the entire sequence data is given in appendix A.

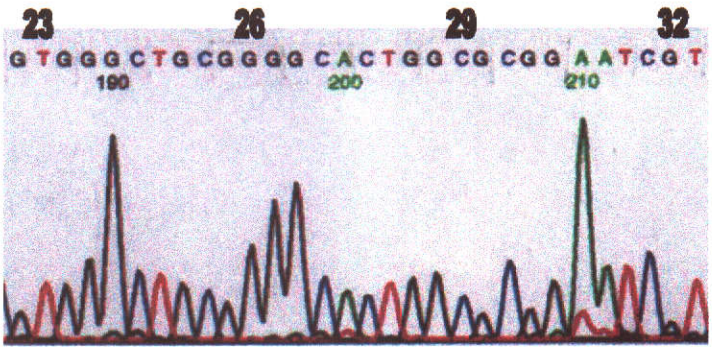

Figure 7.3.1b *DNA sequence chromatograph of 5AR1M mutant clone using the T7EEV primer. The presence of the sequence -GGG **GCA CTG**- at residues 26-28 confirms mutagenesis of -AVFA- (r26-29) in 5AR1 to -GALA- (r21-24) from 5AR2.*

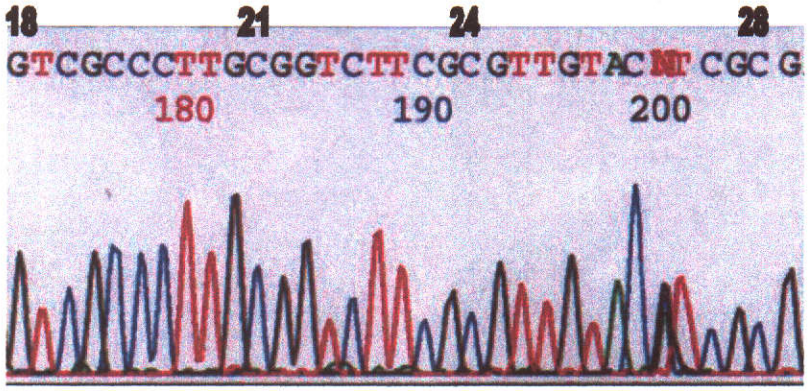

Figure 7.3.1c *DNA sequence chromatograph of 5AR2M mutant clone using the T7 EEV primer. Residues 21-23 have been mutated to -GCG GTC TTC- and now code for -AVFA-.*

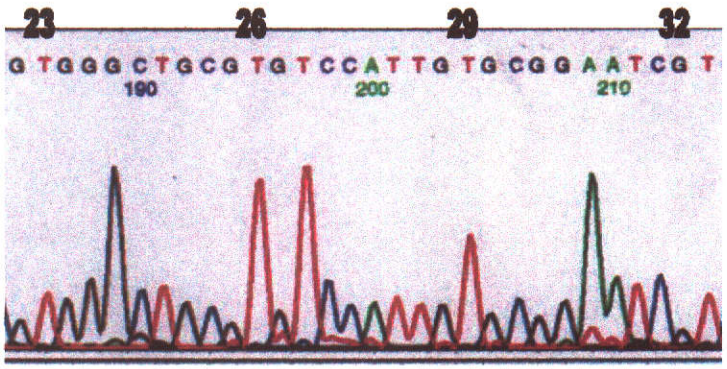

Figure 7.3.1d *DNA sequence chromatograph for 5AR1R mutant clone with the T7EEV primer. The sequence -GTG TCC ATT GTG- at residues 26-29 confirms the mutation of -AVFA- in human 5AR1 to VSIV (r21-24) from rat 5AR1.*

7.3.2 Characterisation of Stably Transfected Cells - Determination of Km and Vmax for Testosterone and Ki for Finasteride

Equilibrium constant (Km), maximum velocities (Vmax) and inhibition constants (Ki) for CHO cells stably transfected with the 5AR1M, 5AR1R or 5AR2M mutant cDNAs were determined as described sections 3.2.14.2 and 3.2.14.3. The Lineweaver-Burke plots constructed using the Enzyme Kinetics V1.5 programme are presented in Figures 7.3.2a to 7.3.2b and the inhibitor plots in Figures 7.3.2c to 7.3.2d. A summary table of the values obtained is given in

Table 7.3.2, all Km values are the calculated mean plus or minus the standard deviation.

A

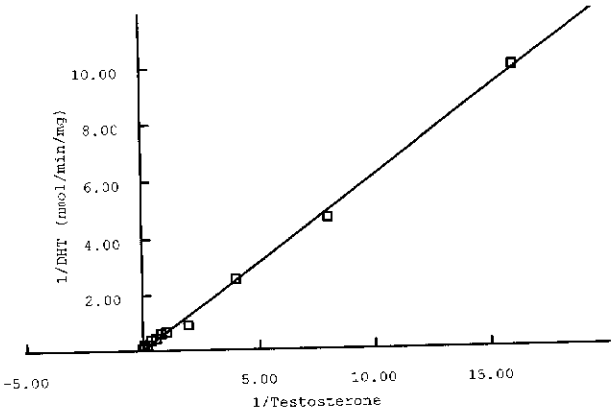

B

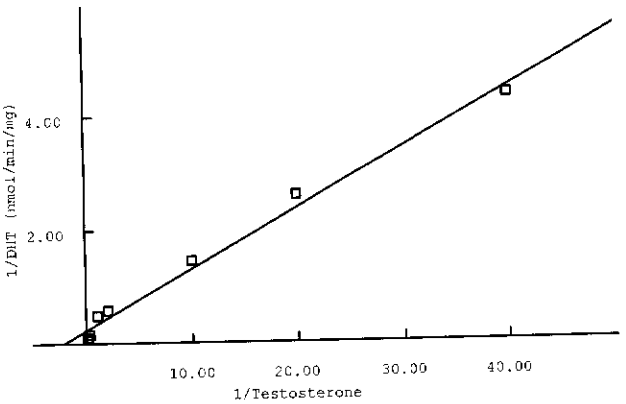

Figure 7.3.2a *Lineweaver-Burke plots of 5AR1M (A) or 5AR2M (B) transfected CHO cells, derived from 2 and 3 separate experiments respectively. Km and Vmax values were 9.26 ± 1.08μM and 15.43nmol DHT/min/mg of cell protein (A) and 0.43 ± 0.08μM and 3.21nmol DHT/min/mg of cell protein (B).*

C

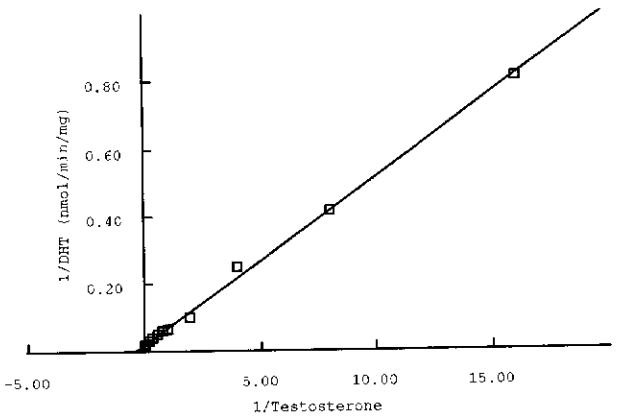

Figure 7.3.2b *Lineweaver-Burke plot of 5AR1R (C) transfected CHO cells derived using pooled data from 2 separate experiments. Km and Vmax values were 2.68±0.37μM and 54.43nmol DHT/min/mg of cell protein respectively.*

D

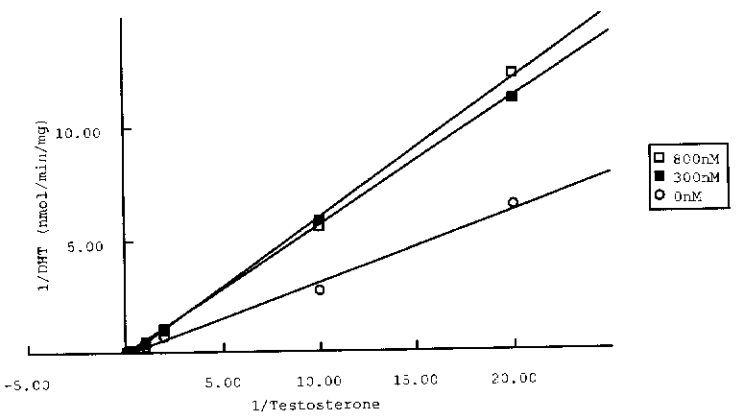

Figure 7.3.2c: *Inhibitor plot for the mutant 5AR1M (D) determined from duplicate measurements of 5AR activity at T concentrations from 0.05-20μM. At 0, 300 and 800nM Finasteride, a Ki of 1093.2nM was determined for 5AR1M.*

E

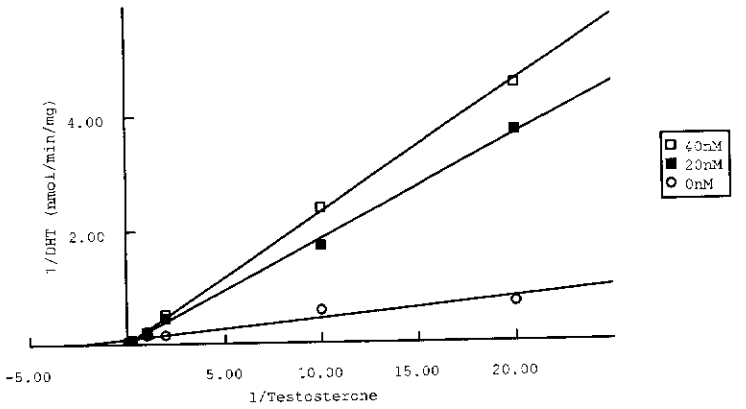

F

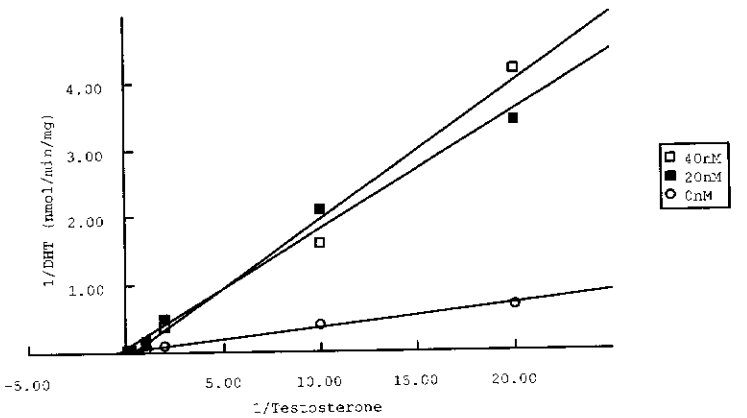

Figure 7.3.2d *Inhibitor plots for the mutants 5AR2M (E) and 5AR1R (F) determined from duplicate measurements of 5AR activity at T concentrations from 0.05-20μM. At 0, 20 and 40nM Finasteride, a Ki of 12.4nM was determined for 5AR2M and 25.6nM for 5AR1R.*

7.3.3 pH Optima of Stably Transfected Cells

Cell sonicates of transfected CHO cells were used to determine the pH optima of the mutants. These optima were determined from 5AR assays performed at pH values ranging from 4.0-9.0 (Figures 7.3.3a and 7.3.3b).

G

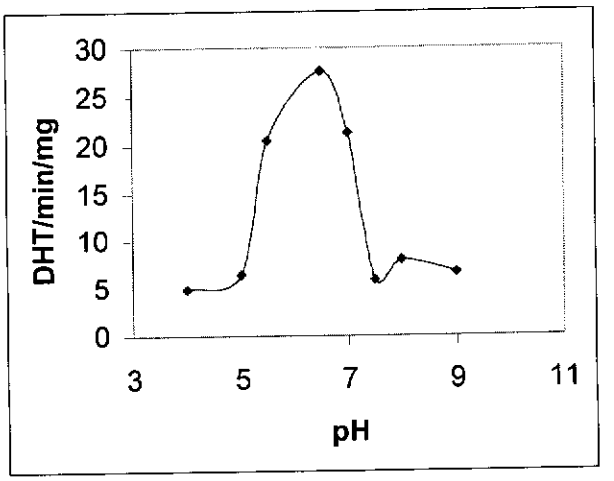

Figure 7.3.3a *The 5AR activity of CHO cells stably transfected with 5AR1M (G) was determined using sonicated cells incubated for 30 minutes at 37°C with 1μM T in buffers ranging in pH from 4.0-9.0. A sharp peak of maximum activity is seen at pH 6.5.*

H

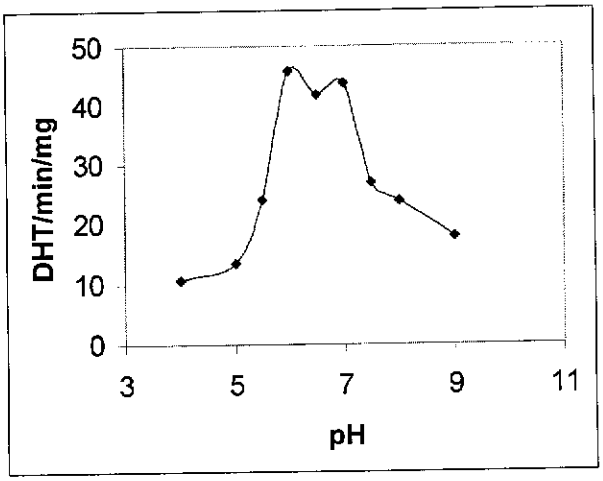

I

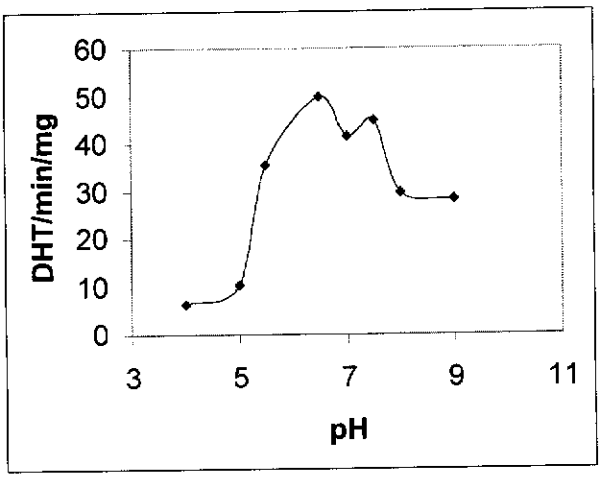

Figure 7.3.3b *The 5AR activity of CHO cells stably transfected with 5AR2M (H) or 5AR1R (I) was determined using sonicated cells incubated for 30 minutes at 37^{O}C with 1μM T in buffers ranging in pH from 4.0-9.0. For 5AR2M, a broad peak of maximum activity was seen between pH 6.0-7.0 with an optimum occurring at pH 6.0. Whereas for 5AR1R a peak of maximum activity was seen at pH 6.5.*

CHO cells Expressing	Average % Conversion T to DHT	Km for T (μM)	Vmax (nmol/min/ mg)	Vmax/Km	Ki for Finasteride (nM)	pH Optima
CHO cell control	0.85	18.67±1.19	42.07	2.25	-	-
Wild Type Human 5AR1	3.5	2.80±0.60	9.35	3.34	327.8	6.0
5AR1M	2.3	9.26±1.08	15.43	1.67	1093.2	6.5
5AR1R	14.7	2.68±0.37	54.43	20.31	25.6	6.5
5AR2M	13.0	0.43±0.08	3.21	7.47	12.4	6.0
Wild Type Human 5AR2	20.8	0.45±0.31	6.58	14.62	11.8	5.5

Table 7.3.2 *Comparisons of the characteristics of mutant and wild type 5α-reductase enzymes.*

7.4 DISCUSSION

Although the 80% efficiency claimed by the makers of the Quickchange™ mutagenesis procedure was not achieved, bacteria containing the mutants 5AR1R and 5AR2M were readily obtained. However considerable difficulties were experienced in mutating 5AR1 to 5AR1M (-AVFA- replaced with -GALA- from 5AR2). On many occasions no transformants were evident following transformation of the mutagenesis reaction, even though both the pWhitescript and pUC18 controls indicated satisfactory performance of the mutagenesis method.

It was considered initially that the quantity of DNA used for mutagenesis might be a causative factor as DNA quality and quantity concentrations were routinely determined by absorbance measurements at 260 and 280nM. Although commonly used, this method is known to be unreliable. However it is appropriate to note that problems were not encountered with the other mutants. In an attempt to overcome this possible cause of the problem, DNA for

mutagenesis was isolated electrophoretically in 1% agarose. This method enables both quantitative assessment from comparison with standards of known concentration and qualitative assessment from the appearance of the electrophoresed DNA.

Although the use of DNA obtained by electrophoresis did yield some colonies potentially containing 5AR1M transformants, sequence analysis showed they did not contain the desired mutation. This suggested the mutagenesis reaction conditions were still not optimal but various experiments conducted to identify the problem gave little insight into the cause(s) of the difficulties encountered.

Purchase of a new kit and increasing, by 5 fold, the amount of DNA used in the transformation reaction also failed to produce the desired result. Discussion with the manufacturers lead to the incorporation of 5% dimethyl sulphoxide (DMSO) into the reaction mix, to denature the secondary structure of the DNA which facilitates the action of the DNA polymerase. This approach was not successful. Other experiments were conducted in which the concentrations of both the forward and reverse primers were increased by 50%, the extension time at 68^{O}C was increased from 2 minutes/kb of DNA to 3 minutes/kb of DNA and the annealing temperature was reduced to 50 ^{O}C. These modifications were tried singly and in combination but were unsuccessful. The problem was finally overcome by the use of HPLC-purified primers, which generated over 100 transformants and bacteria containing the desired mutation were identified. It is not known why HPLC purified primes were required for this mutation but not for others.

Use of a radiolabelled probe to detect transformants containing the cDNA for 5AR was made only for the mutant 5AR2M. This was because this was the first mutant prepared and no experience had been obtained with the mutagenesis method. Of the 24 colonies probed, 18 were shown to contain the cDNA for 5AR2. However which of these transformants contained cDNA containing the desired mutation could not be determined with this probe. Five transformants were sequenced using the T7EEV sequence, which is 5' to the multiple cloning site (MCS) of the pCI-neo vector. All of the transformants sequenced contained the desired mutation. In view of the high percentage of colonies identified as

containing mutated 5AR cDNA and as the radiolabelled probe could not detect appropriately mutated transformants, it was decided to use only sequencing to identify other mutations.

Five transformants from each of the 5AR1M and 5AR1R mutations were also sequenced with the T7EEV primer and clones expressing the desired mutation identified. To check no unwanted secondary mutations had resulted from the mutagenesis procedure, clones expressing the 5AR2M, 5AR1M and 5AR1R mutation were selected and sequenced in their entirety with the AR1R or AR2R primer. These primers were derived from the cDNA sequence of 5AR1 or 5AR2 and are listed in section 4.2.3.

Mammalian cells can be either transiently (electroporation) or stably (calcium phosphate precipitation) transfected with foreign DNA. However, the stable transfection of CHO cells on average, resulted in the expression of much higher levels of 5AR than transiently transfected cells. For this reasons it was decided to stably transfect CHO cells with each of the mutant 5AR cDNAs for use in subsequent analyses. Selection of transfected cells was with neomycin sulphate (G418), resistance to which is encoded by the vector pCI-neo. Following 14-16 days incubation resistant clones were harvested into 24 well trays, grown to confluence and assayed for 5AR activity. Clones expressing the greatest 5AR activity were expanded in tissue culture and used for future analyses.

Kinetic characterisation of each mutant enzyme involved determination of affinity constant (Km) and maximum velocity for the natural substrate T, the inhibitor constant (Ki) for the 5AR inhibitor Finasteride and pH optima. Comparisons were made between mutant and wild type enzymes to determine whether the tetrapeptide -GALA- formed part of the substrate/inhibitor binding site of human 5AR2.

The 5AR1R mutation functioned as a control for both the mutagenesis procedure used to create and enzyme assays used to characterise the 5AR1M and 5AR2M mutant enzymes. Replacement of -AVFA- in human 5AR1 with -VSIV- from rat 5AR1 gave an enzyme with a Km of 2.68±0.37μM and Ki of 25.6nM. Although the Km was similar to that of wild type human 5AR1, the Ki

more closely resembled that of rat 5AR1 (Km = 1.4μM, Ki = 12nM). These results are similar to those obtained for the 5AR1R mutation by Thigpen and Russell[128] (Km = 2.9μM, Ki = 20nM), validating both the mutagenesis procedure and enzyme assays used here. The results for the 5AR1R mutation also confirmed for the first time the suggestion that -VSIV- is involved in substrate/inhibitor binding in rat 5AR1[128].

In comparison with wild type 5AR1, reduced affinity for substrate (Km = 9.26±1.08μM) and increased resistance to Finasteride (Ki = 1093.2nM) were seen when residues 26-29 (-AVFA-) in human 5AR1 were replaced with the analogous residues 21-24 (-GALA-) from 5AR2 (5AR1M mutant). These results demonstrate reduced ability to bind either substrate or inhibitor upon removal of the tetrapeptide -AVFA-. This supports its identification as part of the substrate/inhibitor binding site of human 5AR1[128]. Most significantly, replacement of -AVFA- in human 5AR1 with -GALA- from 5AR2 did not result in an enzyme with characteristics similar to those of wild type human 5AR2 ie. high affinity for T and sensitivity to Finasteride, which suggests the tetrapeptide -GALA- does not form part of the substrate/inhibitor binding site of human 5AR2.

Further evidence that residues 21-24 (-GALA-) do not form part of the substrate/inhibitor binding site of human 5AR2 was provided by the 5AR2M mutation in which -GALA- was replaced with the analogous residues -AVFA- from 5AR1. The Km and Ki values of 0.43±0.08μM and 12.4nM respectively determined for the 5AR2M mutant were not different from wild type 5AR2 (Km = 0.45±0.31μM, Ki = 11.8nM). Thus replacement of -GALA- with -AVFA- did not significantly alter either substrate affinity or sensitivity to Finasteride of 5AR2. This confirms that -GALA- does not form part of the substrate/inhibitor binding site of human 5AR2.

Although the various mutations did change the pH optimum, these changes were minimal. This suggests that although residues -AVFA- are clearly involved in substrate/inhibitor binding by human 5AR1, these residues do not have a significant role in determining the pH optimum of this enzyme. Indeed a similar increase of 0.5 pH units was seen in the 5AR2M mutant (-GALA- replaced with

-AVFA-) and it is clear the mutation in this enzyme does not involve residues that participate in substrate/inhibitor binding by human 5AR2. As all mutants showed an increase of 0.5 pH units, it may be these minimal changes are explained by procedural variation rather than any other cause.

These results do not support suggestions[44, 128] that -GALA- is involved in substrate/inhibitor binding by human 5AR2 and indicates that residues that are have yet to be identified. As residues forming part of the active site of both rat and human 5AR1 lie within the amino terminal region, it is probable that residues involved in substrate/inhibitor binding also are present in this region of human 5AR2. Some support for this is given by the reduction in substrate affinity due to the naturally occurring G34R mutation in human 5AR2[63]. These facts were taken into consideration in the design of the experiments performed to identify residues involved in substrate/inhibitor binding by human 5AR2. These experiments are presented elsewhere (Chapter 8.0) in this thesis.

Chapter 8.0

Determination of the Substrate/Inhibitor Binding Domain of Human 5α- Reductase 2, Using Site-Directed Mutagenesis

8.1 INTRODUCTION

To determine if in fact amino terminal residues are involved in substrate/inhibitor binding by human 5AR2, a chimera comprised of residues 1-41 of 5AR2 and 51-259 of 5AR1 was created. For this pCI-neo vectors containing the cDNAs coding for 5AR1 and 5AR2 were digested by the restriction enzymes *Not I*, *Sal I* and *NgoMIV*. After appropriate ligations the chimera (referred to as C2) was stably transfected into Chinese hamster ovary (CHO) cells and the expressed enzyme characterised. Details of the creation of the C2 chimera are given in Appendix B. Sasa Trivic created this chimera and performed the initial characterisation and this is gratefully acknowledged. The initial characterisation of the enzyme coded for by C2 indicated the presence of residues involved in substrate/inhibitor binding by 5AR2. Consequently it was considered necessary to construct, express and characterise further chimeric enzymes. These were prepared by site-directed mutagenesis using as template the altered cDNA coding for the mutant enzyme termed 5AR1M. This mutant is 5AR1 with residues 26-29 (-AVFA-) replaced with the analogous residues 21-24 (-GALA-) from 5AR2. These further mutations replaced the six residues before -GALA- (5AR1 residues 20-25), the six residues after -GALA- (5AR1 residues 30-35) and 5AR1 residues 36-41 with the analogous residues from 5AR2. Initial studies indicated the 5AR1/20-29 mutant (residues -QCAVGCAVFA- from 5AR1 replaced with -ATLVALGALA- from 5AR2) to be of particular interest and this was stably expressed in CHO cells and fully characterised. Further mutants termed 5AR1/20-22/26-29 (-QCA- and -AVFA- from 5AR1 replaced respectively with -VAL- and -GALA- from 5AR2) and 5AR1/20-22 (-QCA- from wild type 5AR1 replaced with -ATL- from 5AR2) were also prepared, stably expressed and characterised. Mutations also were made using the cDNA of wild type 5AR2 as template. These mutations, termed 5AR2/15-20, 5AR2/15-17 and 5AR2/18-20, respectively replaced -ATLVAL- in 5AR2 with -QCAVGC- from 5AR1, -ATL- in 5AR2 with -QCA- from 5AR1 and -VAL- in 5AR2 with -VGC- from 5AR1.

8.2 METHODS

8.2.1 PLASMID DNA EXTRACTION

The BRESAspin™ Plasmid Mini Kit (Bresatec) was used to extract all plasmid DNA using the methodology described in section 3.2.1.1.

8.2.2 SITE-DIRECTED MUTAGENESIS

8.2.2.1 Reaction Components

Each reaction was set up as described section 4.2.2.1. Reaction components used in each reaction were:

5μL	10X reaction buffer
75ng	dsDNA template**
125ng	Oligonucleotide forward primer
125ng	Oligonucleotide reverse primer
1μL	dNTPs (10mM)
XμL	hpH_2O
50μL	

* Add 1μL of native *Pfu* DNA polymerase (2.5U/L)

** 75ng of template DNA was cycled for all reactions with the exception being the 5AR2/15-17 reaction for which 50ng was cycled.

Nb. As each primer preparation had a different concentration, the amount rather than volume of primer used is given. The value of XμL for the volume of water used reflects the different volumes of primer solution added.

8.2.2.1a Primers

DNA sequences for the 5AR1/20-22, 5AR1/20-22/26-29, 5AR2/15-20, 5AR2/15-17 and 5AR2/18-20 primer pairs are given below with mutated residues in bold type. All primers were synthesized by Pacific Oligonucleotides (New South Wales).

5AR1/20-22 Primer Pair

5'- ^{17}GCC TAC CTG **GC**G **AC**C **CT**C GTG GGC TGC G^{26} -3'

3'- ^{17}CGG ATG GAC **CG**C **TG**G **GA**G CAC CCG ACG C^{26} -5'

5AR1/20-22/26-29 Primer Pair

5'- ^{17}GCC TAC CTG **GC**G **AC**C **CT**C GTG GGC TGC G^{26} -3'

3'- ^{17}CGG ATG GAC **CG**C **TG**G **GA**G CAC CCG ACG C^{26} -5'

5AR2/15-20 Primer Pair

5'- ^{14}C **CAG TGT GC**G GTC G**GC TGT** GGG GCA CTG G^{24} -3'

3'- ^{14}G **GTC ACA CG**C CAG C**CG ACA** CCC CGT GAC C^{24} -5'

5AR2/15-17 Primer Pair

5'- ^{11}G GCA GGC AGC **CAG TGT GC**G GTC GCC CTT G^{21} -3'

3'- ^{11}C CGT CCG TCG **GTC ACA CG**C CAG CGG GAA C^{21} -5'

5AR2/18-20 Primer Pair

5'- ^{15}GCC ACT TTG GTC G**GC TGT** GGG GCA CTG GC^{24} -3'

3'- ^{15}CGG TGA AAC CAG C**CG ACA** CCC CGT GAC CG^{24} -5'

8.2.2.2 Cycling Conditions

All mutagenesis reactions were cycled as follows:

1. 1 cycle at 95^{O}C for 30 seconds.
2. 18 cycles at 95^{O}C for 30 seconds.
3. 18 cycles at 55^{O}C for 1 minute.
4. 18 cycles at 68^{O}C for 14 minutes.
5. 4^{O}C overnight.

8.2.2.3 *Digesting the Product and Transformation into Epicurian Coli XL-1-Blue Supercompetent Cells.*

Dpn I digestion and transformation of the product of each mutagenesis reaction into Epicurian supercompetent *E.coli* were as described in sections 4.2.2.3 and 4.2.2.4 respectively.

8.2.3 DNA SEQUENCING FOR MUTATION IDENTIFICATION

Automated DNA sequencing was as described in section 4.2.3, using a primer (T7EEV) specifically designed for the multiple cloning site of the pCI-neo vector. To enable sequencing of the entire cDNA, primers were also designed based on the sequences of 5AR1 or 5AR2 (AR1R and AR2R respectively).

8.2.4 CALCIUM PHOSPHATE TRANSFECTION

Calcium phosphate transfection of CHO cells with pCI-neo vector containing mutated 5AR1 or 5AR2 cDNA was as described section 3.2.12.

8.2.5 CHARACTERISATION OF STABLY TRANSFECTED CELLS - 5α- REDUCTASE ACTIVITY ASSAYS

Determination of the 5AR activity of transfected cells and of Km, Vmax, Ki, pH optima, total protein assays and cell culture procedures were as described in sections 3.2.14 to 3.2.16.

8.3 RESULTS

8.3.1 Site-directed mutagenesis of wild type 5AR1 and 5AR2 cDNAs

Ampicillin resistant colonies were easily produced using the Quickchange™ site-directed mutagenesis method for the mutation of the 5AR cDNAs (Table 8.3.1). Plasmid DNA isolated from ampicillin resistant colonies was sequenced to identify those expressing the desired mutation (Figures 8.3.1a to 8.3.1e).

Mutation	Colony numbers on Transformation
5AR1/20-22 (-QCA- to -ATL-)	6
5AR1/20-22/26-29 (-QCA- to -ATL- and -AVFA- to -GALA-)	2
5AR2/15-20 (-ATLVAL- to -QCAVGC-)	~150
5AR2/15-17 (-ATL- to -QCA-)	48
5AR2/18-20 (-VAL- to -VGC-)	100-200

Table 8.3.1 *Ampicillin resistant colony numbers from the mutagenesis reactions used to obtain the mutants listed.*

Figures 8.3.1a to 8.3.1e show the sequences, which confirm that the various mutations have been achieved. For each mutation shown the entire sequence data is given in appendix A.

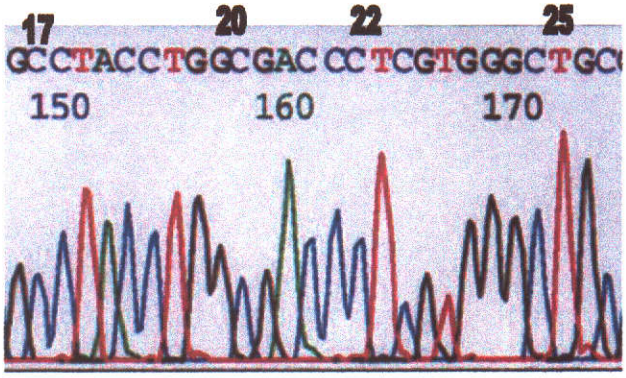

Figure 8.3.1a *Sequence chromatograph for the 5AR1/20-22 mutant with the T7EEV primer. Residues 20-22 (5'-CAG TGC GCC -3') have been mutated to the analogous residues 15-17 (5'- **GCG ACC CTC** -3') from 5AR2.*

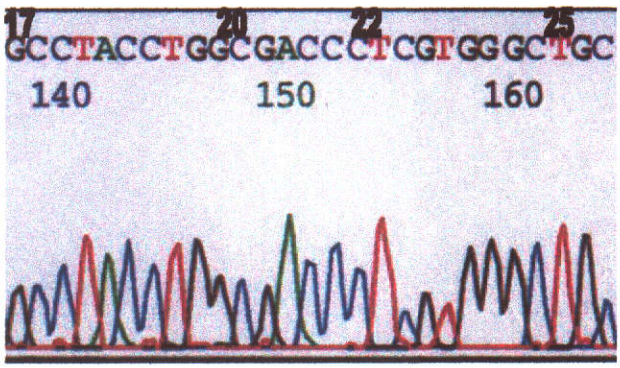

Figure 8.3.1b *Sequence chromatograph for the 5AR1/20-22/26-29 mutant with the T7EEV primer. Residues 20-22 (5'-CAG TGC GCC -3') have been mutated to the analogous residues 15-17 (5'- **GCG ACC CTC** -3') from 5AR2.*

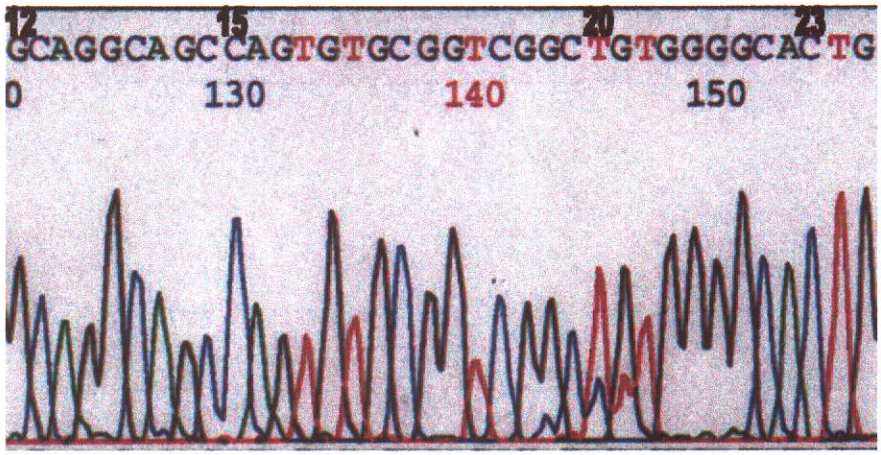

Figure 8.3.1c *DNA sequence chromatograph for the 5AR2/15-20 mutant using the T7EEV primer and showing the mutation of residues 15-20 -ATLVAL- (5'-GCC ACT TTG GTC GCC CTT-3') in 5AR2 to residues 20-25 -QCAVGC- (5'-**CAG TGT GCG** GTC GGC **TGT**-3') from 5AR1.*

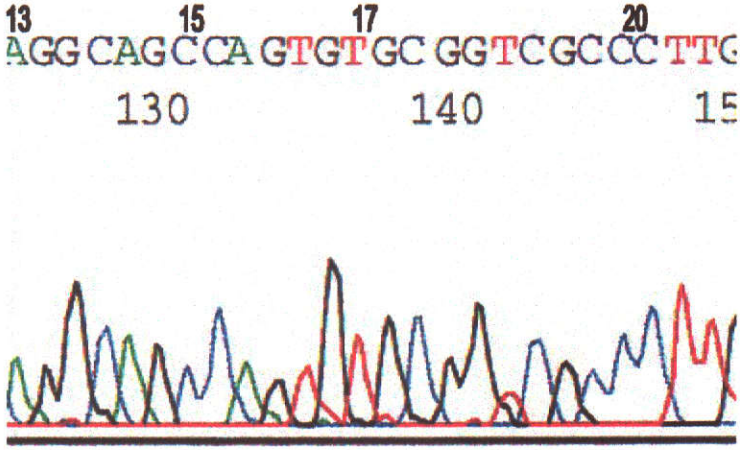

Figure 8.3.1d *Sequence chromatograph for the 5AR2/15-17 mutant with the T7EEV primer. Residues 15-17 (5'-GCC ACT TTG-3') have been mutated to the analogous residues 20-22 (5'-**CAG TGT GCG**-3') from 5AR1.*

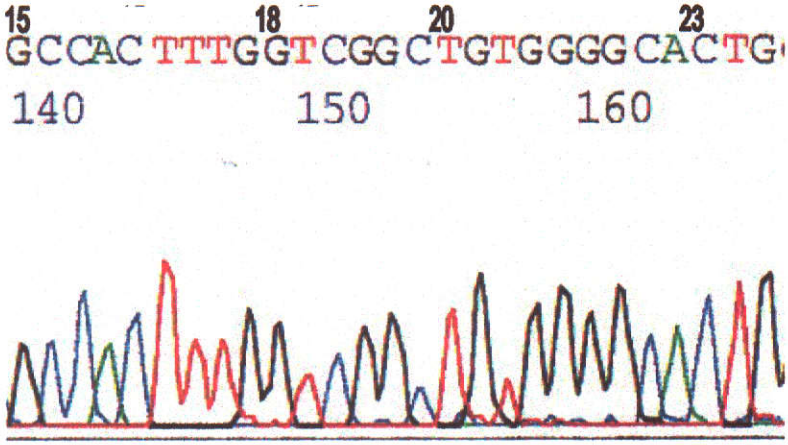

Figure 8.3.1e *DNA sequence chromatograph using the T7EEV primer for the 5AR2/18-20 mutant. The mutation of residues 18-20 (5'-GTC GCC CTT-3') to the analogous residues 23-25 (5'-GTC GGC **TG**T-3') from 5AR1 can be seen.*

8.3.2 Characterisation of Stably Transfected Cells - Determination of Km and Vmax for Testosterone and Ki for Finasteride

The Km and Ki for the C2 construct (comprising 5AR2 residues 1-41 and 5AR1 residues 51-259) are shown in Figure 8.3.2a. Comparisons of the Km of ~2.0μM and Ki of ~120nM with those of the wild type enzymes suggested residues in the amino terminus of human 5AR2 are involved in the substrate/inhibitor binding. Further investigations showed the 5AR1/20-29 mutant (residues -QCAVGCAVFA- from 5AR1 replaced with -ATLVALGALA- from 5AR2) to have Km and Ki values of ~1.2μM and ~36nM respectively (Figure 8.3.2b). These values are markedly different from those obtained for the 5AR1M mutant used as template for this mutation and are not dissimilar from those of wild type 5AR2. In addition, comparisons with wild type 5AR2 showed the mutant formed by replacing residues -ATLVAL- in 5AR2 with -QCAVGC- from 5AR1 to have marked reductions in affinity for testosterone and sensitivity to Finasteride (Figure 8.3.2c). The effects on the affinity for testosterone and sensitivity to Finasteride caused by replacing -QCA- with -ATL- in wild type 5AR1 and the mutant 5AR1M and replacing -ATL- with -QCA- or -VAL- with -VGC- in 5AR2 are shown in Figures 8.3.2d to 8.3.2g. A summary of the Km and Ki values for all of the mutant enzymes also is given in Table 8.3.2, all Km values are the calculated mean plus or minus the standard deviation.

A

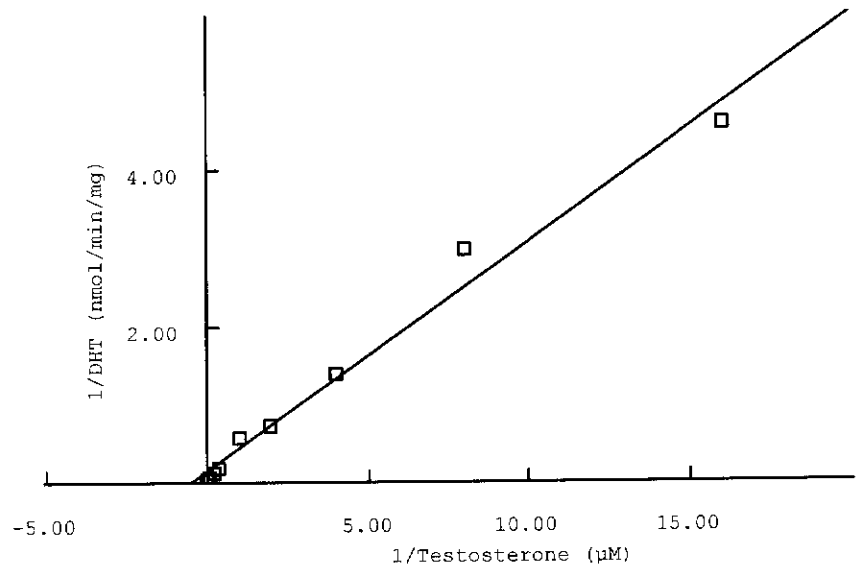

B

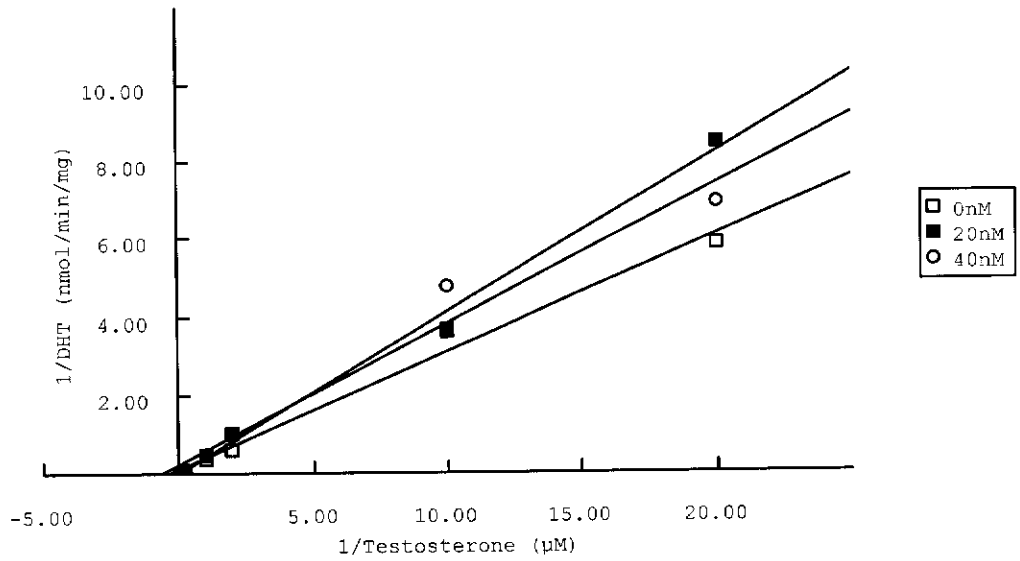

Figure 8.3.2a *Lineweaver-Burke plot (A) and inhibitor plot (B) of CHO cells stably expressing the C2 clone (5AR2 residues 1-41 and 5AR1 residues 51-259), each derived from 2 separate experiments. Km and Vmax values of 1.89±0.26µM and 5.49nmol DHT/min/mg of cell protein respectively and a Ki value of 119.8nM were obtained.*

C

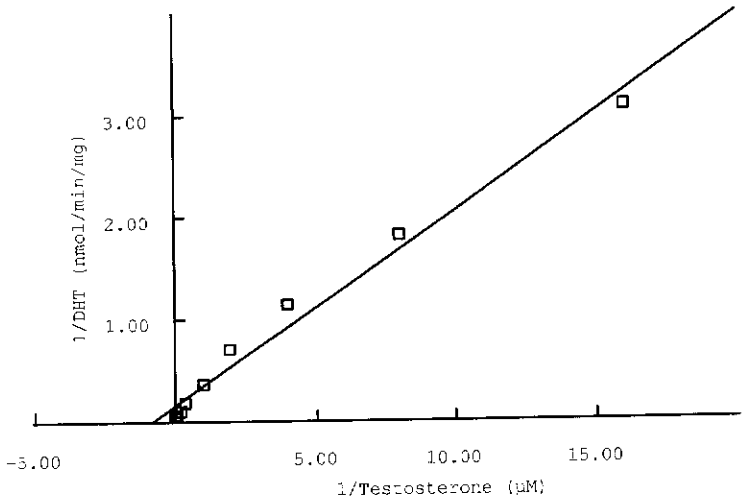

D

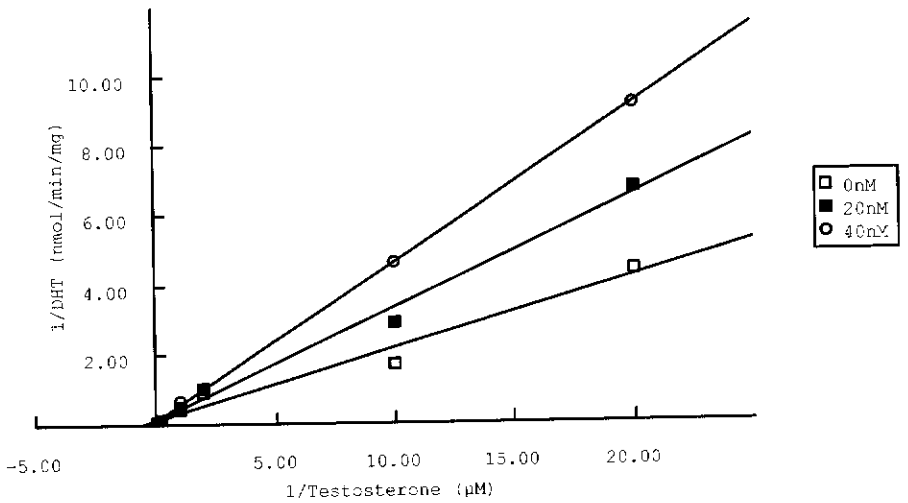

Figure 8.3.2b *Lineweaver-Burke plot (C) and inhibitor plot (D) of CHO cells stably expressing the 5AR1/20-29 mutant (residues -QCAVGCAVFA- from 5AR1 replaced with -ATLVALGALA- from 5AR2), derived from 2 and 3 separate experiments respectively. Km and Vmax values of 1.19±0.06µM and 6.19nmol DHT/min/mg of cell protein and a Ki value of 36.4nM were obtained.*

E

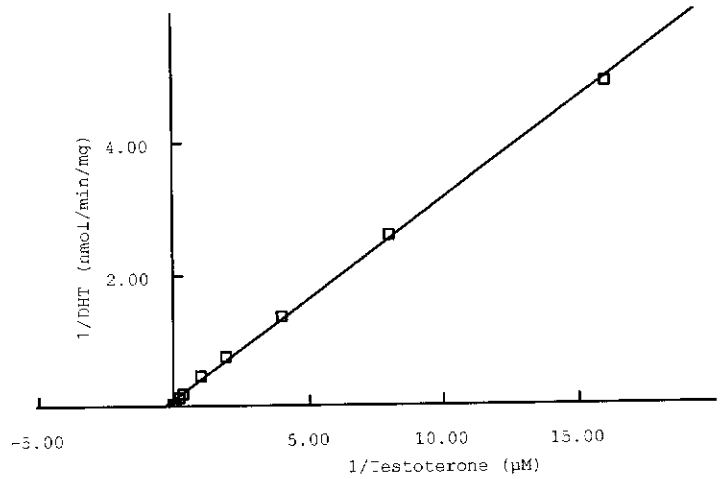

F

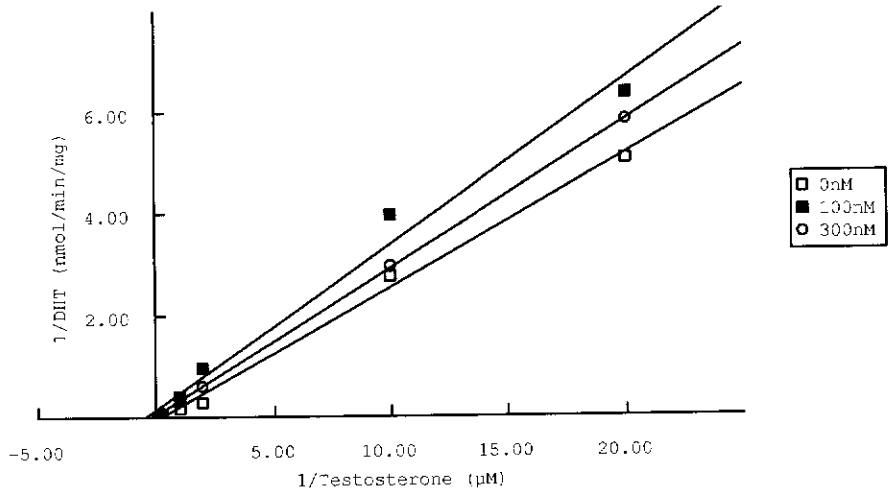

Figure 8.3.2c *Lineweaver-Burke plot (E) and inhibitor plot (F) of CHO cells stably expressing the 5AR2/15-20 mutant (residues -ATLVAL- in 5AR2 replaced with -QCAVGC- from 5AR1), each derived from 2 separate experiments. Km and Vmax values of 3.21±1.11μM and 11.86nmol DHT/min/mg of cell protein respectively and a Ki value of 745.3nM were obtained.*

G

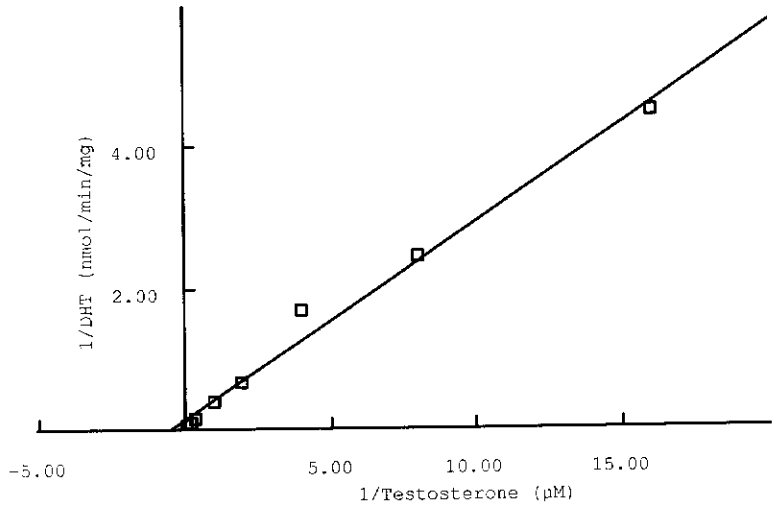

H

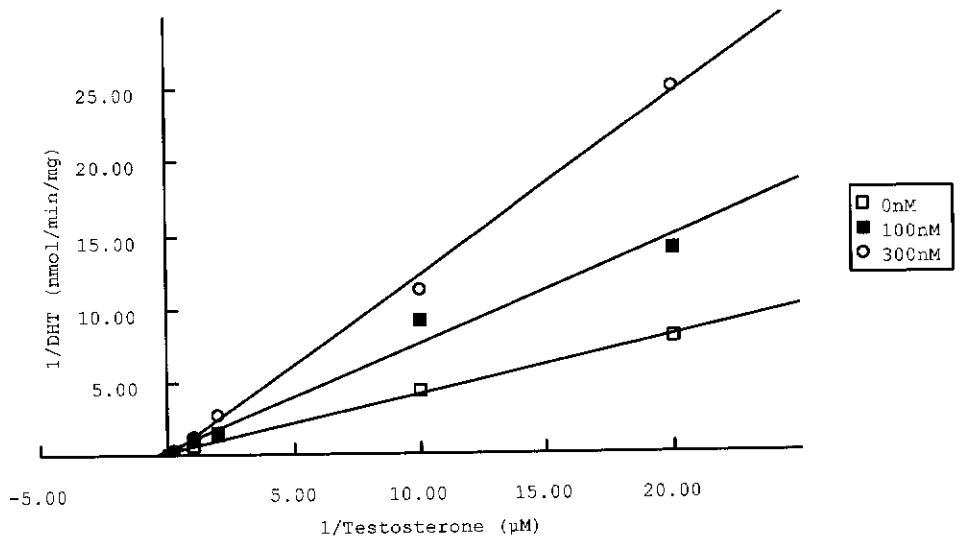

Figure 8.3.2d *Lineweaver-Burke plot (G) and inhibitor plot (H) of CHO cells stably expressing the 5AR2/15-17 mutant (replacement of residues -ATL- in 5AR2 with -QCA- from 5AR1), each derived from 2 separate experiments. Km and Vmax values of 2.58±0.31μM and 8.80nmol DHT/min/mg of cell protein respectively and a Ki value of 253.4nM were obtained.*

I

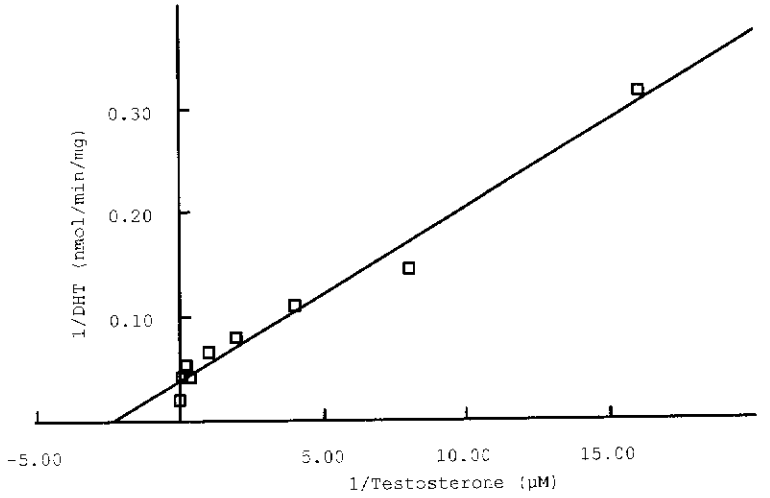

J

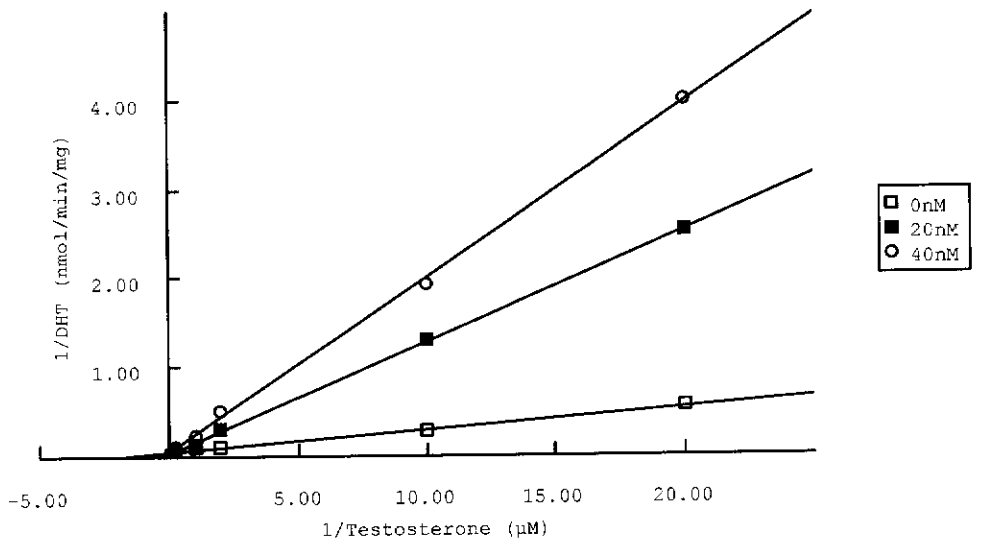

Figure 8.3.2e *Lineweaver-Burke plot (I) and inhibitor plot (J) of CHO cells stably expressing the 5AR2/18-20 mutant (replacement of residues -VAL- in 5AR2 with -VGC- from 5AR1), each derived from 2 separate experiments. Km and Vmax values of 0.43±0.02µM and 25.52nmol DHT/min/mg of cell protein respectively and a Ki value of 6.8nM were obtained.*

K

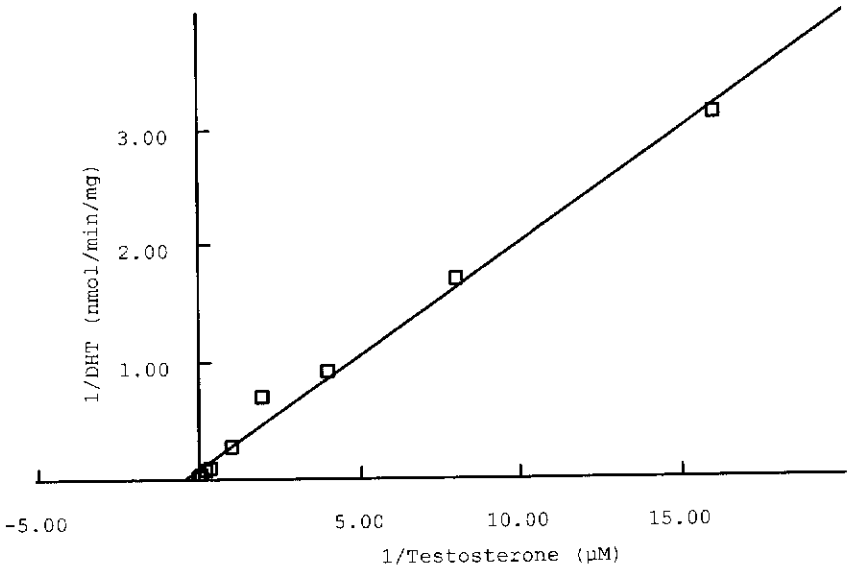

L

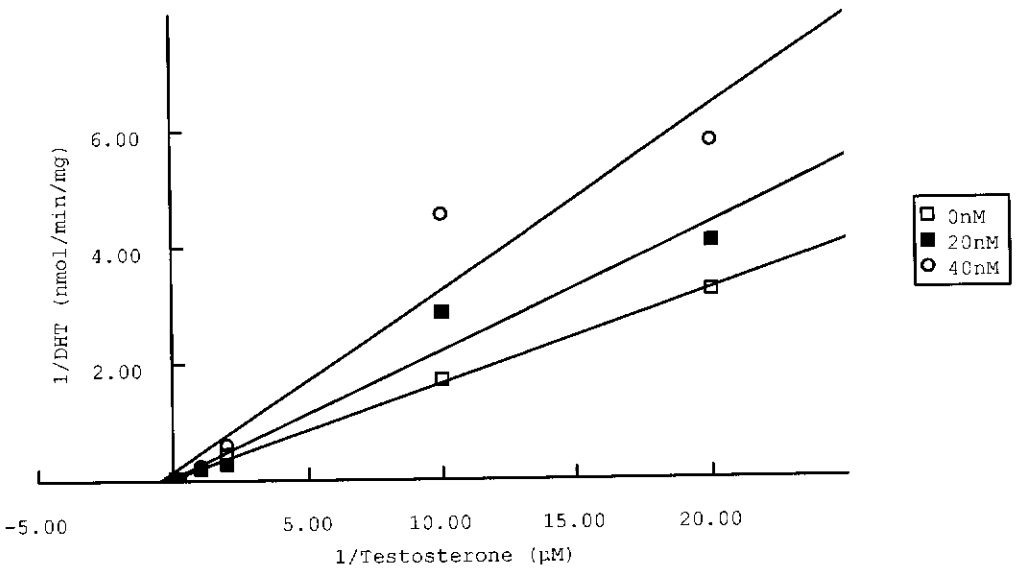

Figure 8.3.2f *Lineweaver-Burke plot (K) and inhibitor plot (L) of CHO cells stably expressing the 5AR1/20-22 mutant (residues -QCA- in 5AR1 replaced with -ATL- from 5AR2), each derived from 2 separate experiments. Km and Vmax values of 1.28±0.05µM and 56.55nmol DHT/min/mg of cell protein respectively and a Ki value of 46.8nM were obtained.*

M

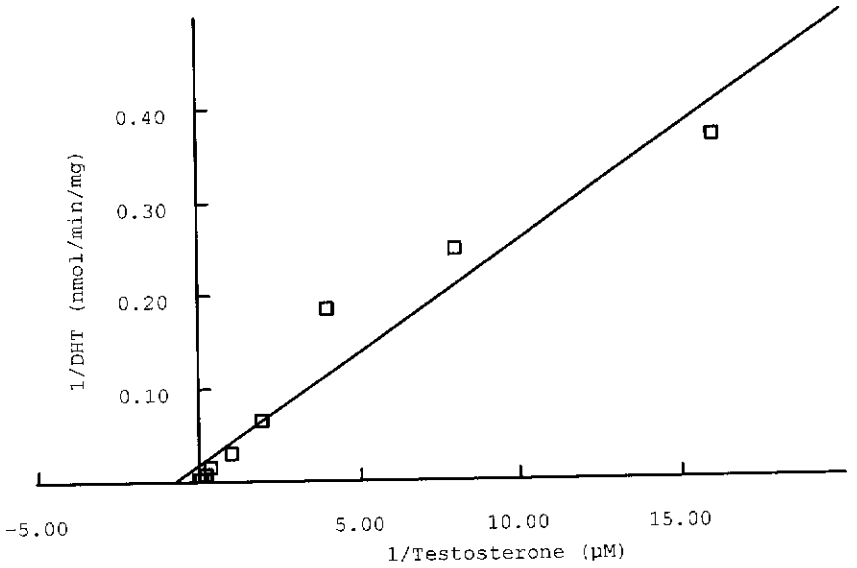

N

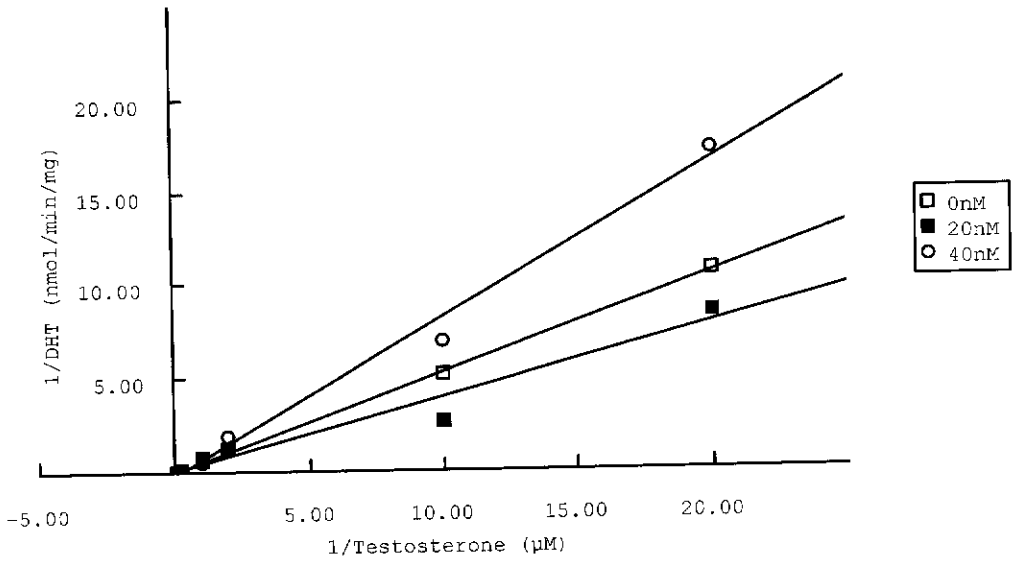

Figure 8.3.2g *Lineweaver-Burke plot (M) and inhibitor plot (N) of CHO cells stably expressing the 5AR1/20-22/26-29 mutant (residues -QCA- and -AVFA- in 5AR1 replaced respectively with -ATL- and -GALA- from 5AR2), each derived from 2 separate experiments. Km and Vmax values of 2.08 ±0.55µM and 10.82nmol DHT/min/mg of cell protein respectively and a Ki value of 53.1nM were obtained.*

8.3.3 pH Optima of Stably Transfected Cells

As well as the assessments referred to above, the effects of the various mutations on pH optima also were determined. These are shown in figures 8.3.3a to 8.3.3d and summarised in table 8.3.2. These studies were performed using cell sonicates prepared from CHO cells stably expressing each mutant enzyme.

O

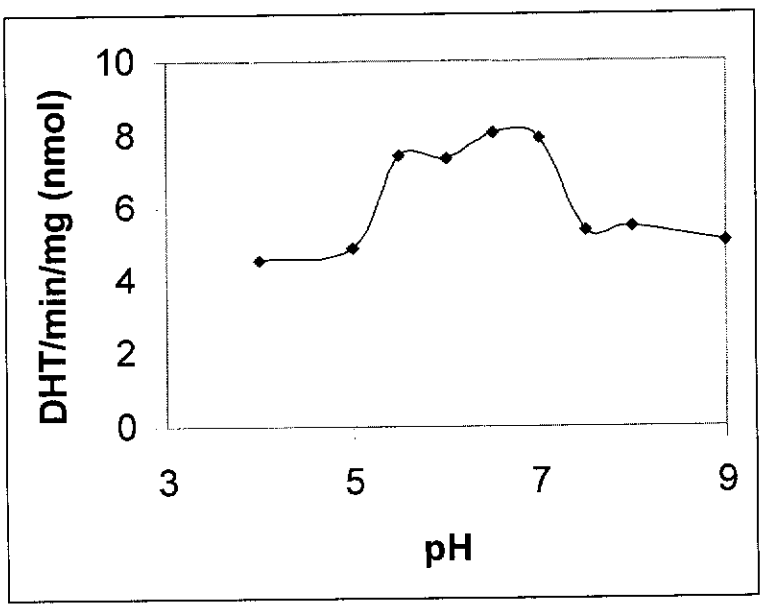

Figure 8.3.3a *The 5AR activity of CHO cells stably transfected with the C2 clone (5AR2 residues 1-41 and 5AR1 residues 51-259), was determined using sonicated cells incubated for 30 minutes at 37^{O}C with 1μM T in buffers ranging in pH from 4.0-9.0 (O). A broad peak of maximum activity was seen between pH 5.5-7.0 with an optimum at pH 6.5.*

P

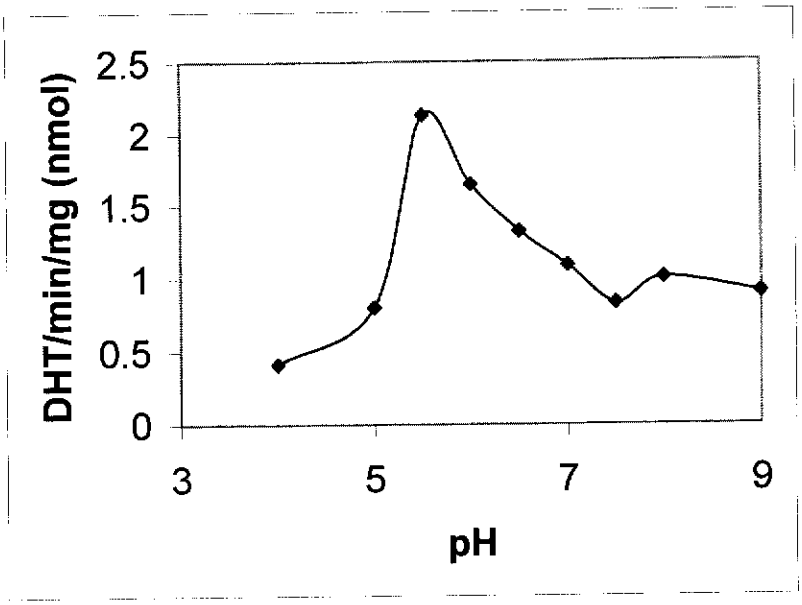

Q

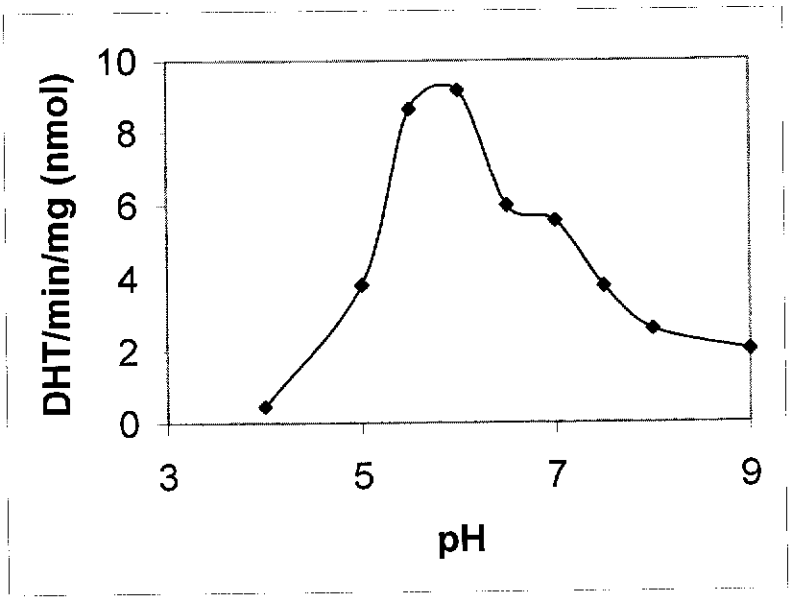

Figure 8.3.3b *The 5AR activity of CHO cells stably transfected with the 5AR1/20-29 (P) or 5AR2/15-20 (Q) mutants was determined using sonicated cells incubated for 30 minutes at 37^{O}C with 1μM T in buffers ranging in pH from 4.0-9.0. A peak of maximum activity was seen at pH 5.5 for 5AR1/20-29 and at pH 6.0 for 5AR2/15-20.*

R

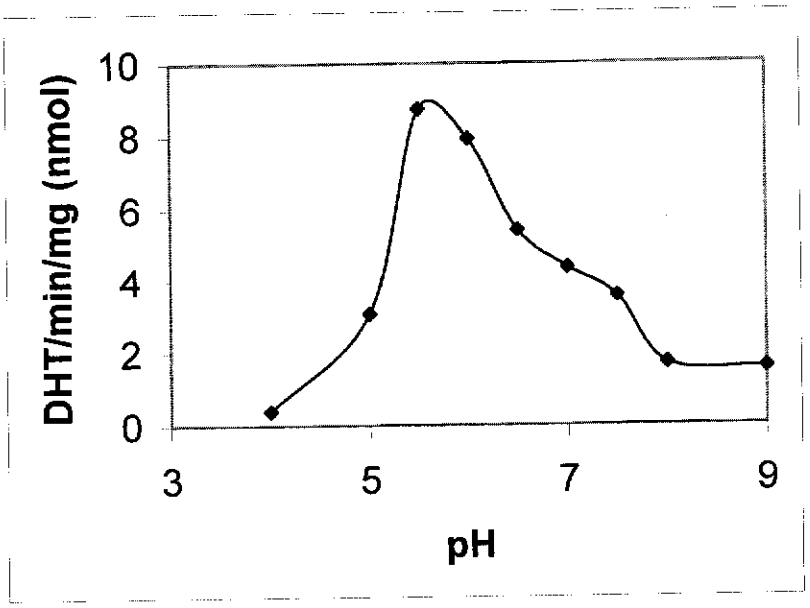

S

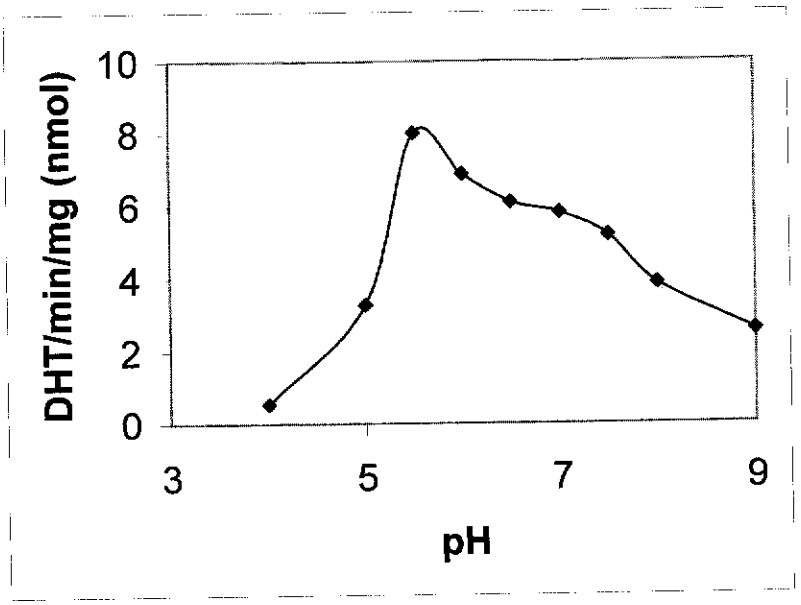

Figure 8.3.3c *The 5AR activity of CHO cells stably transfected with 5AR2/15-17 (R) or 5AR2/18-20 (S) mutants was determined using sonicated cells incubated for 30 minutes at 37^{O}C with 1μM T in buffers ranging in pH from 4.0-9.0. For both mutants, a peak of maximum activity was seen at pH 5.5.*

T

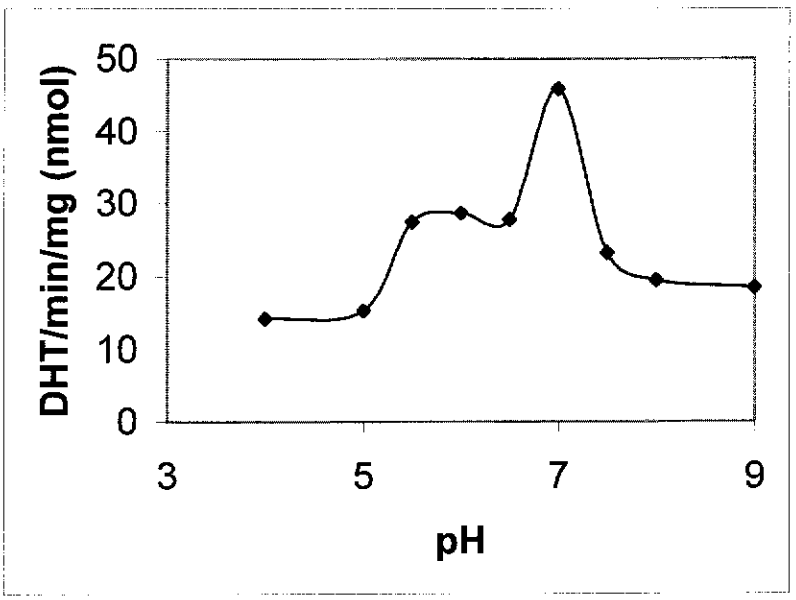

U

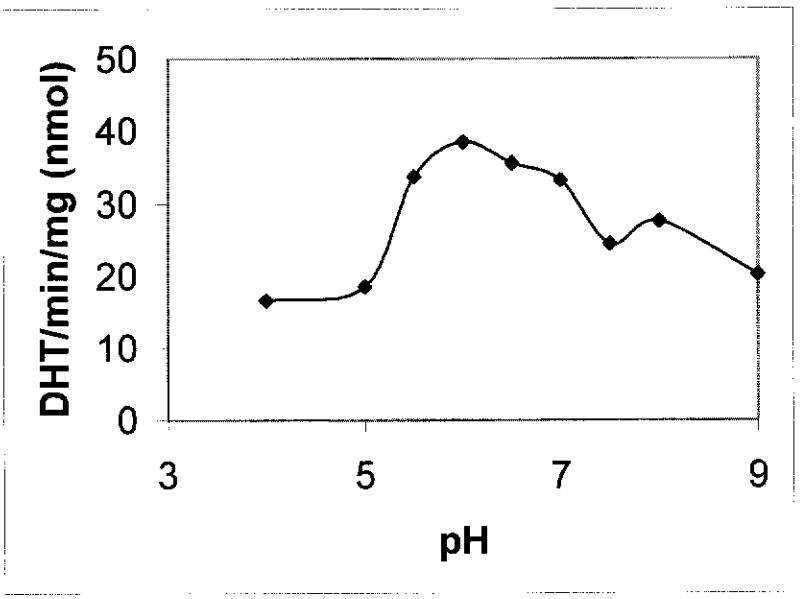

Figure 8.3.3d *The 5AR activity of CHO cells stably transfected with 5AR1/20-22 (T) or 5AR1/20-22/26-29 (U) mutants was determined using sonicated cells incubated for 30 minutes at 37^{O}C with 1μM T in buffers ranging in pH from 4.0-9.0. For 5AR1/20-22, a peak of maximum activity was seen at pH 7.0 whereas for 5AR1/20-22/26-29 a broad peak of maximum activity was seen between pH 5.5-7.0 with an optimum at pH 6.0.*

Cell Line Expressing	Average % Conversion T to DHT	Km for T (μM)	Vmax (nmol DHT/min/mg)	Vmax/Km	Ki for Finasteride (nM)	pH Optima
CHO cell control	0.85	18.67±1.19	42.07	2.25	-	-
Wild type 5AR1	3.5	2.80±0.60	9.35	3.34	327.8	6.0
Wild type 5AR2	20.8	0.45±0.31	6.58	14.62	11.8	5.5
5AR1M	2.3	9.26±1.08	15.43	1.67	1093.2	6.5
5AR2M	13.0	0.43±0.08	3.21	7.47	25.6	6.5
C2	1.2	1.89±0.26	5.49	2.91	119.8	6.5
5AR1/20-29	2.9	1.19±0.06	6.19	5.20	36.4	5.5
5AR1/20-22	2.9	1.28±0.05	56.55	44.18	46.8	7.0
5AR1/20-22/ 26-29	2.3	2.08±0.55	10.82	5.20	53.1	6.0
5AR2/15-20	1.5	3.21±1.11	11.86	3.70	745.3	6.0
5AR2/15-17	1.0	2.58±0.31	8.80	3.41	253.4	5.5
5AR2/18-20	19.1	0.43±0.02	25.52	59.35	6.8	5.5

Table 8.3.2 *Comparisons of the characteristics of mutant and wild type 5α-reductase enzymes*

8.4 DISCUSSION

The suggestions[44,128] that -GALA- forms part of the substrate/inhibitor binding site of human 5AR2 are not substantiated. As described in chapter 7, replacing -AVFA- in human 5AR1 with the analogous residues -GALA- from 5AR2 (5AR1M) did not confer any 5AR2 type characteristics, rather there was a significant reduction in binding of both substrate and inhibitor. Similarly replacing -GALA- from 5AR2 with -AVFA- had no effect on either substrate or inhibitor binding nor did this mutant (5AR2M) have any 5AR1 type characteristics. Additionally the pH optima of the two mutants (5AR1M and 5AR2M) were not significantly different from those of the wild type enzymes.

These studies clearly indicated -GALA- is not involved in substrate/inhibitor binding by 5AR2. Consequently the C2 chimera comprising residues 1-41 of 5AR2 and 51-259 of 5AR1 and was constructed to determine if in fact any N-terminal residues of 5AR2 were involved in substrate/inhibitor binding. The Km of 1.89±0.26μM and Ki of 119.8nM determined for the C2 chimera were sufficiently different from those obtained for wild type 5AR1 to suggest N-terminal residues are involved in substrate/inhibitor binding by 5AR2.

Comparisons of the N-terminal regions of human 5AR1 and 5AR2 showed little homology and it was decided to alter 6 residues at a time, using the 5AR1M mutant cDNA as a template. This mutant was chosen as its Km for testosterone of 9.26μM and Ki for Finasteride of 1093.2nM are markedly different both from the Km and Ki values of 2.80μM and 327.8nM respectively of wild type 5AR1 and of 0.45μM and 11.8nM of wild type 5AR2. The rationale was that these greater differences in Km and Ki of 5AR1M might enable a more sensitive detection of changes toward 5AR2 type Km and Ki values caused by residue replacement.

As the Quickchange^{TM} site-directed mutagenesis kit was only capable of mutating up to 18 nucleotides during a single reaction, 6 residue clusters were selected for mutation. Constructs were made in which 5AR1 residues 20-25 or 30-35 or 36-41 were exchanged for their analogous residues from 5AR2. Characterisation of these constructs showed that replacing 5AR1 residues 20-29 (-QCAVGCAVFA-) with the analogous residues 15-24 (-ATLVALGALA-), gave a mutant with a Km of 1.19±0.06μM, Ki of 36.4nM and pH optimum of 5.5. These values are markedly different from the Km and Ki for the template 5AR1M and are approaching those of wild type 5AR2, suggesting 5AR2 residues 15-20 are involved in substrate/inhibitor binding. This suggestion was strengthened by the reverse exchange replacing residues 15-20 (-ATLVAL-) in 5AR2 with the analogous residues 20-25 (-QCAVGC-) from 5AR1, which gave a mutant (5AR2/15-20) with a Km, Ki and pH much more like wild type 5AR1 than 5AR2 (Table 8.3.2).

Further studies of these residues were made by exchanging -VAL- in 5AR2 with

-VGC- from 5AR1 to give the mutant 5AR2/18-20. This replacement had little effect on substrate/inhibitor binding indicating -VAL- is not involved. However, replacing -ATL- in 5AR2 with -QCA- from 5AR1 gave a mutant (5AR2/15-17) with characteristics similar to wild type 5AR1. These reductions in affinity for testosterone and sensitivity to Finasteride strongly suggested that -ATL- is involved in substrate/inhibitor binding by 5AR2. This was confirmed as replacing -QCA- with -ATL- in either 5AR1M or wild type 5AR1 (5AR1/20-22/26-29 and 5AR1/20-22 respectively), markedly increased both the affinity for testosterone and sensitivity to Finasteride.

Although it is certain that the substrate/inhibitor binding site of 5AR2 is comprised of residues other than those (-ATL-) identified here, these residues do seem of particular significance for the binding of Finasteride. Replacing these residues in 5AR2 with the analogous residues from 5AR1 and vice versa, had a greater effect on Ki than on Km. Replacing -QCA- with -ATL- in wild type 5AR1 increased Km by around 2-fold but increased Ki by around 7-fold. Similarly replacing -ATL- with -QCA- in 5AR2 decreased Km by around 6-fold and Ki by 21-fold. Interestingly, the ratios of the new values for Ki and Km are similar in the two mutants, suggesting -ATL- is of particular significance for Finasteride binding. Replacing -QCA- with -ATL- in the 5AR1M mutant, in which -AVFA- is replaced with -GALA-, increases the Km 4.4-fold and the Ki 21-fold giving a ratio of 4.8:1 for the new Ki and Km values. This not only strengthens the suggestion that the tripeptide -ATL- is of particular significance for Finasteride binding but also indicates it has greater affinity for the inhibitor than does the tetrapeptide -AVFA-. It seems reasonable to suppose therefore that the differences between 5AR1 and 5AR2 both in the Km for Testosterone and the Ki for Finasteride are due, at least in part, to differences in interaction of substrate and inhibitor with the tripeptide -ATL- and the tetrapeptide -AVFA-. It is apparent that replacing -AVFA- with -ATL and vice versa, would enhance the assessment of the relative roles of these peptides. However despite very many attempts and for reasons unknown, these mutations proved impossible to achieve in the time frame of this study.

Interestingly and perhaps coincidentally, the decreases in Km and Ki seen when -ATL- in 5AR2 is replaced with -QCA-, are very similar to the increases in Km and Ki that occur when -QCA- is replaced by -ATL- in the 5AR1M mutant (-AVFA- replaced with -GALA-). In 5AR1M, in which at least part of the active site has been removed, there is a 3-fold reduction in both Km and Ki when compared to wild type 5AR1. When -ATL- is introduced into this relatively inactive mutant however, there is a 4.4-fold increase in Km and a 21-fold increase in Ki. Thus in both the reactivation of 5AR1M and inactivation of 5AR2 there are changes of similar magnitude in both Km and Ki, although of course these changes are in opposite directions in the two enzymes. It is tempting to speculate that as these changes are so similar, this indicates there could be unexpected similarities in the conformation of the active sites of 5AR1 and 5AR2. Whether or not this is in fact the case requires further studies such as those referred to above.

Despite the obvious significance of -ATL- in substrate/inhibitor binding, the alterations to enzyme characteristics when exchanging the hexapeptides -ATLVAL- from 5AR2 and -QCAVGC- from 5AR1 suggest involvement of other residues. Although replacing -ATLVAL- with -QCAVGC- decreases the Km by around 7-fold compared with a decrease of around 6-fold when -ATL- is replaced with -QCA-, hexapeptide exchange decreases the Ki by 62-fold compared with a decrease of 21-fold from exchange of tripeptides. It could be argued that this marked change in Ki is due to structural disruption but this seems unlikely in view of the Km value. In addition, exchanging -QCAVGC- for -ATLVAL- in 5AR1M gives around an 8-fold increase in Km and a 30-fold increase in Ki compared with increases of 4.4-fold and 21-fold in Km and Ki respectively, when -QCA- is changed to -ATL-. These findings clearly indicate that the changes seen on exchanging the hexapeptides are not due to structural disruption. It is unclear however, exactly why exchanging the hexapeptides has more effects than exchanging the tripeptides -ATL- and -QCA- as replacing -VAL- with -VGC- has no effect on Km, although rather suprisingly it slightly increases the Ki. Although the identification of -AVFA- by Thigpen and Russell[128] suggests a tetrapeptide might have more effect than a tripeptide, this seems unlikely to be the case here as the valine is common to both 5AR1 and 5AR2. It may be therefore that the two carboxy terminal residues subtly alter

the conformation of the hexapeptides and thus the binding of substrate and inhibitor. Again it is clear that elucidation of the roles of the individual residues in these hexapeptides requires the assessment of further mutations.

Although the studies reported in this chapter quite clearly show the residues -ATL- have a significant role in substrate/inhibitor binding by 5AR2, it seems unlikely that these residues have a major role in determining the pH optimum. With the possible exception of 5AR1/20-29 where the pH optimum changed to 5.5 from the 6.0 of wild type 5AR1, none of the mutants showed a clear cut change. This is not really surprising however as it is probable many residues contribute to the pH optimum. Other studies of 5AR mutations have demonstrated alterations in substrate binding without significant change to the pH optima. Studies of naturally occurring mutations in the SRD5AR2 gene by Wigley and colleagues (1994)[63] demonstrated 5AR2 mutants with significantly reduced affinity for substrate, with all but one mutation resulting in a basic shift in the pH optimum from 5.0 to between 5.1-6.5. The majority of mutants studied however demonstrated only a slight shift in pH optimum to between 5.1-5.5, a difference of only 0.5 a pH unit.

A recent article by Makridakis and associates (2000)[127] claims to have defined the substrate and cofactor binding sites of human 5AR2. These authors however do not identify exactly which residues comprise the substrate and cofactor binding domains, rather they simply state that the substrate binding site is bipartite involving amino and carboxyl terminal residues and the cofactor binding site is confined largely to the carboxyl terminal third. In contrast the studies reported here have identified a tripeptide involving residues 15-17 (-ATL-) in the amino terminus of human 5AR2, that form a significant part of its substrate/inhibitor binding domain.

Chapter 9.0

Conclusions

9.0 CONCLUSION

The rationale for undertaking these studies has been discussed on many occasions throughout this thesis. The initial impetus was to determine if residues in human 5AR2, -GALA-, were involved in substrate/inhibitor binding by this enzyme. As the analogous residues in rat and human 5AR1 had been shown involved in this binding, it had been suggested these residues (GALA) also were involved in substrate/inhibitor binding by human 5AR2 [44,128]. These suggestions however had been made without any supporting experimental evidence. Some experiments in this study therefore were designed to test these suggestions.

Although the tetrapeptide -AVFA had been shown to be involved in substrate/inhibitor binding by human 5AR1[128], the relative roles of the individual amino acids comprising this tetrapeptide had not been assessed at the commencement of the studies reported here. As those who initially identified the tetrapeptide had suggested this assessment to be necessary, studies to achieve this were undertaken here. Studies also were made of the 5AR2 residues G34 and H231 as these had also been identified as being involved in substrate binding by this enzyme[63]. However, the roles of these residues in inhibitor binding by 5AR2 had not been examined and neither had the roles of the analogous residues in 5AR1 been determined. Similarly, others had noted that the mechanism of Finasteride inhibition exhibited by rat 5AR1 differed both from that of rat 5AR2 and human 5AR1 and 5AR2. It had been suggested that this difference might be due to expression of cysteine at position 146 in rat 5AR1 rather than the arginine expressed at the analogous position in rat 5AR2 and in both types of human 5AR[115]. Studies to examine this suggestion were considered of interest and suitable experiments were designed and performed.

It is apparent that changes due to site directed mutagenesis cannot be evaluated without reference to the wild type enzymes. Establishment and characterisation of the wild type enzymes is reported in chapter 3.0. The superiority of stable (calcium phosphate precipitation) over transient (electroporation) transfection of CHO cells was demonstrated from these studies. Additionally, the characteristics (Km and Ki) determined for cells

expressing the wild type enzymes were similar to those previously reported in the literature. An early lesson was learnt that all that is written is not gospel. The primer sequences from the article by Boudon et al, 1995[53], were shown to be cited the wrong way around such that the primer for 5AR1 was actually complementary to 5AR2 and vice versa. This provided much frustration in early hybridisation experiments, which subsequently proved highly successful upon resolution of this author's error. It was also determined from these studies that the mammalian expression vector pCI-neo was well suited for the purpose for which it was chosen.

As mentioned above the effects of the arginine to cysteine change were assessed (Chapter 4.0). The purpose of this was two-fold, firstly to determine the suitability of the Quickchange™ site-directed mutagenesis kit for our needs and secondly to determine the effects of the arginine to cysteine mutation. It is apparent that possession of the rat enzymes would have provided a more definitive answer, however only the human enzymes were readily available. These studies showed the suitability of the Quickchange™ site-directed mutagenesis kit for future studies and that cysteine alone was not responsible for the differences in Finasteride inhibition of the rat and human enzymes.

Residues G34 and H231 of 5AR2 had been shown to be important for substrate binding[63], the significance of these residues for Finasteride binding and that of the analogous residues in 5AR1 (G39 and H236) however have not been assessed. Experiments designed to determine these factors showed G34 and H231 not only to be important for substrate but also Finasteride binding. The analogous residues in 5AR1 however proved significant for Finasteride but not substrate binding highlighting that although they are largely similar, subtle differences exist between the substrate and inhibitor binding sites.

It had been suggested the reduced substrate binding seen for the G34R mutant resulted from substitution of a small, uncharged amino acid (G) to a large, bulky charged residue (R)[63]. The mechanism of this reduced binding were therefore investigated by mutation of G34 to a variety of residues differing in size and charge (Chapter 5.0). From these studies, conformational change and steric

hindrance rather than electrostatic interactions were shown to be the main cause of this reduced binding.

This study is the first confirmation of the identification of -AVFA- as part of the substrate/inhibitor binding site of human 5AR1. The authors of the original study although noting that determination of the individual contributions of residues in this tetrapeptide was necessary, did not make these determinations[128]. Experiments designed to address this were therefore carried out and are presented in Chapter 6. Amongst other findings, these studies showed the tripeptide -AVF- to be of greater functional significant than the tetrapeptide -AVFA- in substrate/inhibitor binding by human 5AR1.

The most significant information obtained was that regarding substrate/inhibitor binding by human 5AR2. As mentioned previously the substrate/inhibitor binding site of this enzyme had not been elucidated but the involvement of the tetrapeptide -GALA- had been suggested[44,128]. This suggestion was based on the finding that the tetrapeptides -AVFA- and -VSIV- were involved in substrate/inhibitor binding by human and rat 5AR1 respectively. As -GALA- is the analogous tetrapeptide in human 5AR2, it was considered this tetrapeptide might be involved in substrate/inhibitor binding by this enzyme. As experiments to test this suggestion had not been performed mutant enzymes therefore were constructed, transfected and characterised. The results of this, reported in Chapter 7, showed no involvement of these four residues in substrate/inhibitor binding by human 5AR2. However as residues involved in substrate/inhibitor binding by both human and rat 5AR1 map to the amino terminus, it seemed likely those of 5AR2 would also.

To determine this, chimeric constructs of human 5AR1 and 5AR2 were created and the characteristics of these chimeras assessed. This showed residues involved in substrate/inhibitor binding by human 5AR2 to be present in the first 40 amino terminal residues of this enzyme. A series of mutant enzymes therefore was created to identify these residues

As discussed in Chapter 8, replacing the hexapeptide QCAVGC (residues 20-25) in 5AR1 with ATLVAL (residues 15-20) from 5AR2 decreased the Km from

9.3μM to 1.2μM and the Ki from 1093nM to 36nM. These values approach those obtained for wild type 5AR2 and indicate a significant role for this peptide in substrate/inhibitor binding. Replacing residues VAL in wild type 5AR2 with VGC from 5AR1 had no significant effect on either Km or Ki. However, replacing ATL in 5AR2 with QCA from 5AR1 altered the Km to 2.0μM from 0.48μM and the Ki to 136nM from 11.4nM. These findings show residues 15-17 of type 2 5AR participate in inhibitor/substrate binding by human 5AR2 whereas residues 18-20 do not.

To date this is the only report identifying residues involved in substrate/inhibitor binding by human 5AR2. As this is enzyme is known to be involved in diseases of the prostate, particularly benign prostatic hyperplasia, identification of these residues may assist in the development of new and improved therapeutics for these diseases. This is of obvious significance.

In conclusion, the studies of human 5AR presented here not only answer some of the questions generated from previous studies but also provide new information which will be of value in further studies of these clinically significant enzymes.

Chapter 10.0

References

10.0 REFERENCES

1. Andersson, S., Russell, DW. 1990. Structural and Biochemical Properties of Cloned and Expressed Human and Rat 5α- Reductases. *Proc. Natl. Acad. Sci USA.* 87:3640-3644.
2. Schneider, JJ., Hortsmann, PM. 1951. *J. Biol. Chem.* 191:327-338. (Cited from reference 10, Russell and Wilson, 1994).
3. Schneider, JJ. 1952. Conversion of Deoxycortisone to Four Allopregnane Metabolites by Rat Liver *in vitro*. *J. Biol. Chem.* 199:235-244.
4. Tomkins, GM. 1957. *J. Biol. Chem.* 225:13-24 (Cited from reference 10, Russell and Wilson, 1994).
5. McGuire, JS., Tomkins, GM. 1960a. The Heterogeneity of Δ^4-3-Ketosteroid Reductases (5α). *J. Biol. Chem.* 235:1634-1638.
6. McGuire, JS., Hollis, VW., Tomkins, GM. 1960b. *J. Biol. Chem.* 235:3112-3116.
7. Fisher, LK., Kogut, MD., Moore, RJ., Goebelsmann, U., Weitman, JJ et al. 1978. Clinical Endocrinological and Enzymatic Characterisation of Two Patients with 5α- Reductase Deficiency: Evidence that a Single Enzyme is Responsible for the 5α- Reduction of Cortisol and Testosterone. *J. Clin. Endocrinol. Metab.* 45:653-664.
8. Bondy, PK. 1981. In *Williams Textbook of Endocrinology*, ed. JD Wilson, DW Foster, pp. 816-890. Philadelphia:Saunders.
9. Wilson, JD. 1975. Metabolism of Testicular Androgens. In *Handbook of Physiology*, ed. RO, Greep., EB, Astwood., pp491-508. American Physiology Society, Washington DC.
10. Russell, DW., Wilson, JD. 1994. Steroid 5α- Reductase: Two Genes/Two Enzymes. *Annu. Rev. Biochem.* 63:25-61.
11. Wilson, JD., Griffin, JE., Russell, DW. 1993. Steroid 5α- Reductase 2 Deficiency. *Endocrine Reviews.* 14(5):577-593.
12. Jost, A. 1970. Hormonal Factors in the Sex Differentiation of the Mammalian Foetus. *Philos. Trans. R. Soc. Lond[Biol].* 259:119-130.

13. Koopman, P., Gubbay, J., Vivain, N., Goodfellow, P., Lovell-Badge, R. 1991. Male Development of Chromosomally Female Mice Transgenic for *Sry*. *Nature*. 351:117-121.
14. Josso, N., Boussin, L., Knebelmann, B., Nihoul-Fekete, C., Picard, JY. 1991. Anti-Mullerian Hormone and Intersex State. *Trends Endocrinol. Metab.* 2:227-233.
15. Donahoe, PK., Cate, RL., MacLaughlin, DT., Epstein, J., Fuller, AF., Takahashi, M., Coughlin, JP., Ninfa, EG., Taylor, LA. 1987. Mullerian Inhibiting Substance Gene Structure and Mechanism of Action of a Foetal Regressor. *Recent Prog. Horm. Res.* 43:431-467.
16. Griffin, JE., Wilson, JD. 1989. The Androgen Resistance Syndromes: 5α-Reductase Deficiency, Testicular Feminization and Related Syndromes. In *The Metabolic Basis of Inherited Disease*. ed. CR, Scriver., AL, Beaudet., WS, Sly., D, Valle., pp1919-1944. McGraw-Hill/New York.
17. Moore, RJ., Griffin, JE., Wilson, JD. 1975. Diminished 5α- Reductase Activity in Extracts of Fibroblasts Cultured from Patients with Familial Incomplete Male Pseudohermaphroditism. *J. Biol. Chem.* 250:7168-7172.
18. Moore, RJ., Wilson, JD. 1976. Steroid 5α- Reductase in Cultured Human Fibroblasts. *J. Biol. Chem.* 251:5895-5900.
19. Liang, T., Cascieri, MA., Cheung, AH., Reynolds, GF., Rasmusson, GH. 1985. Species Differences in Prostatic Steroid 5α- Reductase of Rat, Dog and Human. *Endocrinology*. 117:571-579.
20. Frederiksen, DW., Wilson, JD. 1971. Partial Characterization of the Nuclear Reduced Nicotinamide Adenine Dinucleotide Phosphate: Δ^4-3-ketosteroid 5α-oxidoreductase of Rat Prostate. *J. Biol. Chem.* 246:2584-2593.
21. Moore, RJ., Wilson, JD. 1972. Localization of the Reduced Nicotinamide Adenine Dinucleotide Phosphate: Δ^4-3-ketosteroid 5α-oxidoreductase in the Nuclear Membrane of the Rat Ventral Prostate. *J. Biol. Chem.* 247:958-967.
22. Moore, RJ., Wilson, JD. 1974. Extraction of the Reduced Nicotinamide Adenine Dinucleotide Phosphate: Δ^4-3-ketosteroid 5α-oxidoreductase of Rat Prostate with Digitonin and Potassium Chloride. *Biochemistry*. 13:450-456.

23. Liang, T., Heiss, CE., Ostrove, S., Rasmusson, GH., Cheung, A. 1983. Binding of a 4-Methyl-4-Aza-Steroid to 5α- Reductase of Rat Liver and Prostatic Microsomes. *Endocrinology*. 112:1460-1468.
24. Houston, B., Chisholm, GD., Habib, FK. 1985. Solubilisation of Human Prostatic 5α- Reductase. *J. Steroid Biochem.* 22:461-467.
25. Ichihara, K., Tanaka, C. 1987. Some Properties of Progesterone 5α-Reductase Solubilised from Rat Liver Microsomes. *Biochem. Int.* 15:1005-1011.
26. Enderle-Schmitt, U., Neuhaus, C., Aumüller, G. 1989. Solubilisation of Nuclear Steroid 5α- Reductase from Rat Ventral Prostate. *Biochem. Biophys. Acta*. 987:21-28.
27. Levy, MA., Brandt, M., Greway, AT. 1990. Mechanistic Studies with Solubilised Rat Liver Steroid 5α- Reductase: Elucidation of the Kinetic Mechanism. *Biochemistry*. 29:2808-2815.
28. Sargent, NSE., Habib, FK. 1991. Partial Purification of Human Prostatic 5α-Reductase in a Stable and Active Form. *J. Steroid Biochem. Molec. Biol.* 38:73-77.
29. Bhattacharyya, AK., Chavan, AJ., Haley, BE., Taylor, MF., Collins, DC. 1995. Identification of the NADP[H] Binding Site of Rat Liver Microsomal 5α-Reductase (Isozyme 1): Purification of a Photolabel Peptide Corresponding to the Adenine Binding Domain. *Biochemistry*. 34(11):3663-3669.
30. Farkash, Y., Soreq, H., Orly, J. 1988. Biosynthesis of Catalytically Active Rat Testosterone 5α- Reductase in Microinjected *Xenopus* oocytes: Evidence for Tissue Specific Differences in Translatable mRNA. *Proc. Natl. Acad. Sci. USA*. 85:5824-5828.
31. Andersson, S., Bishop, RW., Russell, DW. 1989. Expression Cloning and Regulation of 5α- Reductase, an Enzyme Essential for Male Sexual Differentiation. *J. Biol. Chem.* 264(27):16249-16255.

32. Andersson, S., Berman, DM., Jenkins, EP., Russell, DW. 1991. Deletion of Steroid 5α- Reductase 2 Gene in Male Pseudohermaphroditism. *Nature.* 354:159-161.
33. Normington, K., Russell, DW. 1992. Tissue Distribution and Kinetic Characteristics of Rat Steroid 5α- Reductase Isozymes. *J. Biol. Chem.* 267(27):19548-19554.
34. Market, CL., Moller, F. 1959. *Proc. Natl. Acad. Sci. USA.* 45:753-763. (Cited from reference 10, Russell and Wilson, 1994).
35. Labrie, F., Sugimoto, Y., Luu-The, V., Simard, J., Lachance, Y., Bachvarov, D., Levianc, G., Durocher, F., Paquet, N. 1992. Structure of the Human Type II 5α- Reductase Gene. *Endocrinology.* 131(3):1571-1573.
36. Jenkins, EP., Hsieh, C., Milatovich, A., Normington, K., Berman, DM., Francke, U., Russell, DW. 1991. Characterisation and Chromosomal Mapping of a Human Steroid 5α- Reductase Gene and Pseudogene and Mapping of the Mouse Homologue. *Genomics.* 11:1102-1112.
37. Thigpen, AE., Cala, KM., Russell, DW. 1993b. Characterisation of Chinese Hamster Ovary Cell Lines Expressing Human Steroid 5α- Reductase Isozymes. *J. Biol. Chem.* 268(23):17404-17412.
38. Griffin, JE., Wilson, JD. 1989. In *The Metabolic Basis of Inherited Disease*, ed. CR Scriver, AL Beaudet, WS Sly, D Valle., pp1919-1944. McGraw-Hill: New York.
39. Span, PN., Smals, GH., Sweep, GJ., Benraad, TJ. 1995. Rat Steroid 5α- Reductase Kinetic Characteristics: Extreme pH-dependency of the Type 2 Isozyme in Prostate and Epididymis Homogenates. *J. Steroid Biochem. Molec. Biol.* 54(3/4):185-192.
40. Span, PN., Benraad, TJ., Sweep, GJ., Smals, GH. 1996b. Kinetic Analysis of Steroid 5α- Reductase Activity at Neutral pH in Benign Prostatic Hyperplasia Tissue: Evidence for Type 1 Isozyme Activity in the Human Prostate. *J. Steroid Biochem. Molec. Biol.* 57(1/2):103-108.

41. Smith, CM., Ballard, SA., Worman, N., Buettner, R., Masters, JRW. 1996. 5α- Reductase Expression by Prostate Cancer Cell Lines and Benign Prostatic Hyperplasia *In Vitro*. *J. Clin. Endocrinol. Metab.* 81(4):1361-1366.
42. Imperato-McGinley, J., Peterson, RE., Gautier, T., Sturla, E. 1979. Male Pseudohermaphroditism Secondary to 5α- Reductase Deficiency- a Model for the Role of Androgens in Both the Development of the Male Phenotype and the Evolution of Male Gender Identity. *J. Steroid Biochem.* 11:637-648.
43. Ellsworth, KP., Azzolina, BA., Cimis, G., Bull, HG., Harris, GS. 1998. Cloning, Expression and Characterization of Rhesus Macaque Types 1 and 2 5α- Reductase: Evidence for Mechanism-Based Inhibition by Finasteride. *J. Steroid Biochem. Molec. Biol.* 66(5/6):271-279.
44. Levy, MA., Brandt, M., Sheedy, KM., Holt, DA., Heaslip, JI., Trill, JJ., Ryan, PJ., Morris, RA., Garrison, LM., Bergsman, DJ. 1995. Cloning, Expression and Functional Characterisation of Type 1 and Type 2 Steroid 5α- Reductase from *Cynomolgus* Monkey: Comparisons with Human and Rat Isoenzymes. *J. Steroid Biochem. Molec. Biol.* 52(4):307-319.
45. Thigpen, AE., Silver, RI., Guileyardo, JM., Casey, ML., McConnell, JD., Russell, DW. 1993a. Tissue Distribution and Ontogeny of Steroid 5α- Reductase Isozyme Expression. *J. Clin. Invest.* 92:903-910.
46. Eicheler, W., Aumüller, G., Happle, R., Hoffmann, R. 1996. Immunolocalisation of Steroid 5α- Reductase Isoenzymes in Human Foetal Skin. *Europ. J. Derm.* 6(2):132-134.
47. Levine, AC., Wang, JP., Ren, MY., Eliashvili, E., Russell, DW., Kirschenbaum, A. 1996. Immunohistochemical Localization of Steroid 5α- Reductase 2 in the Human Male Foetal Reproductive Tract and Adult Prostate. *J. Clin. Endocrinol. Metab.* 81(1):384-389.
48. Berman, DM., Russell, DW. 1993. Cell-type-specific Expression of Rat Steroid 5α- Reductase Isozymes. *Proc. Natl. Acad. Sci. USA.* 90:9359-9363.
49. Span, PN., Sweep, GJ., Benraad, TJ., Smals, GH. 1996c. Differential Subcellular Distribution of Rat Prostatic Steroid 5α- Reductase Isozyme Activities. *Europ. J. Endocrinol.* 134(3):386-392.

50. Span, PN., Benraad, TJ., Sweep, GJ., Smals, GH. 1996a. Kinetic Analysis of Rat Steroid 5α- Reductase Activity in Prostate and Epididymis Homogenates at Neutral pH: Evidence for Type 1 Activity in Epididymis. *J. Steroid Biochem. Molec. Biol.* 57(1/2):395-414.
51. Bonnet, P., Reiter, E., Bruyninx, M., Sente, B., Dombrowicz, D., de Leval, J., Closset, J., Hennen, G. 1993. Benign Prostatic Hyperplasia and Normal Prostate Aging: Differences in Types I and II 5α- Reductase and Steroid Hormone Receptor Messenger Ribonucleic Acid (mRNA) Levels, but not in Insulin-Like Growth Factor mRNA levels. *J. Clin. Endocrinol. Metab.* 77:1203-1208.
52. Hirsch, KS., Jones, CD., Audia, JE, Andersson, S., McQuaid, L., Stamm, NB., Neubauer, BL., Pennington, P., Toomey, RE., Russell, DW. 1993. LY191704: a Selective, Non-Steroidal Inhibitor of Human Steroid 5α-Reductase Type 1. *Proc. Natl. Acad. Sci. USA.* 90:5277-5281.
53. Boudon, P., Lobaccaro, JM., Lechevallier, E., Mottet, N., Gibelin, B., Sultan, C. 1995b. 5α- Reductase Activity in Cultured Epithelial and Stromal Cells from Normal and Hyperplastic Human Prostates- Effects of Finasteride (PROSCAR), a 5α- Reductase Inhibitor. *Cellular and Molec. Biol.* 41(8):1007-1015.
54. Delos, S., Carsol, JL., Ghazarossian, E., Raynaud, JP., Martin, PM. 1995. Testosterone Metabolism in Primary Cultures of Human Prostate Epithelial Cells and Fibroblasts. *J. Steroid Biochem. Molec. Biol.* 55(3/4)375:383.
55. Kaefer, M., Audia, JE., Bruchovsky, N., et al. 1996. Characterization of Type 1 Steroid 5α- Reductase in DU145 Human Prostatic Adenocarcinoma Cells. *J. Steroid Biochem. Molec. Biol.* 58(2):195-205.
56. Sutkowski DM. Audia JE. Goode RL. Hsiao KC. Leibovitch IY. McNulty AM. Neubauer BL. 1996. Responses of LNCaP Prostatic Adenocarcinoma Cell Cultures to LY300502, a Benzoquinolone Human Type I 5α-Reductase Inhibitor. *Prostate -Suppl.* 6:62-6.
57. Bruchovsky, N., Sadar, MD., Akakura, K., Goldenburg, SL., Matsuoka, K., Rennie, PS. 1996. Characterisation of 5α- Reductase Gene Expression in

Stroma and Epithelium of Human Prostate. *J. Steroid Biochem. Molec. Biol.* 59(5/6):397-404.

58. Silver, RI., Wiley, EI., Thigpen, AE., Guileyardo, JM., McConnell, JD., Russell, DW. 1994. Cell Type Specific Expression of Steroid 5α- Reductase 2. *J. Urology.* 152:438-442.
59. Miyamoto, T., Tsuro, Y., Kagawa, S., Yokoi, H., Ishimura, K. 1996. Immunolocalisation of Steroid 5α- Reductase type 2 in Human Prostate, Seminal Vesicles and Vas-Deferens- Light and Electron Microscopic Immunohistochemistry. *Acta Histochemica et Cytochemica.* 29(1):29-37.
60. Russell, DW., Berman, DM., Bryant, JT., Cala, KM., Davis, DL., Landrum, CP., Prihoda, JS., Silver, RI., Thigpen, AE., Wigley, WC. 1994. The Molecular Genetics of Steroid 5α- Reductase. *Recent Prog. Horm. Res.* 49:275-284.
61. George, FW., Russell, DW., Wilson, JD. 1991. Feed-forward Control of Prostate Growth: Dihydrotestosterone Induces Expression of its own Biosynthetic Enzyme, Steroid 5α- Reductase. *Proc. Natl. Acad. Sci. USA.* 88:8044-8047.
62. Imperato-McGinley, J., Guerrero, L., Gautier, T., Peterson, RE. 1974. Steroid 5α- Reductase Deficiency in Man: An Inherited Form of Male Pseudohermaphroditism. *Science.* 186:1213-1215.
63. Wigley, WC., Prihoda, JS., Mowszowicz, I., Mendoca, BB., New, MI., Wilson, JD., Russell, DW. 1994. Natural Mutagenesis Study of the Human Steroid 5α- Reductase 2 Isozyme. *Biochemistry.* 33:1265-1270.
64. Nowakowski, H., Lenz, W. 1961. Genetic Aspects in Male Hypogonadism. *Recent Prog. Horm. Res.* 17:53-95.
65. Walsh, PC., Madden, JD., Harrod, MJ., Goldstein, JL., MacDonald, PC., Wilson, JD. 1974. Familial Incomplete Male Pseudohermaphroditism Type 2. Decreased Dihydrotestosterone Formation in Pseudovaginal Perineoscrotal Hypospadias. *N. Eng. J. Med.* 291:944-949.
66. Wilson, JD. 1999. The Role of Androgens in Male Gender Role Behaviour. *Endocrine Rev.* 20(5):726-737.

67. Schroder, FH. 1994. 5α- Reductase Inhibitors and Prostatic Disease. *Clin. Endocrinol.* 41:139-147.

68. Sinnecker, GHG., Hiort, O., Dibbelt, L., Albers, N., Dorr, HG., Hauss, H., Hienrich, U., Hemminghaus, M., Hoepffner, W., Holden, M., Schnabel, D., Kruse, K. 1996. Phenotypic Classification of Male Pseudohermaphroditism due to Steroid 5α- Reductase Type 2 Deficiency. *Amer. J. Med. Genetics.* 63(1):223-230.

69. Forti, G., Galchetti, A., Santoro, S., Davis, DL., Wilson, JD., Russell, DW. 1996. Steroid 5α- Reductase 2 Deficiency: Virilisation in Early Infancy may be due to Partial Function of Mutant Enzyme. *Clin. Endocrinol.* 44:477-482.

70. Boudon, C., Lumbroso, S., Lobaccaro, JM., Szarras-Czapnik, M., Romer, TE., Garandeau, P., Montoya, P., Sultan, C. 1995a. Molecular Study of the 5α-Reductase Type 2 Gene in Three European Families with 5α- Reductase Deficiency. *J. Clin. Endocrinol. Metab.* 80(7):2149-2153.

71. Griffin, JE., Wilson, JD. 1992. Disorders of Sexual Differentiation. In *Campbell's Urology*, ed. PC Walsh, AB, Retik, TA Stamey, IR Vaughan, pp. 1509-1542. Philadelphia:Saunders.

72. Keenan, BS., Eberle, AJ., Sparrow, JT., Greger, NG., Panko, WB. 1987. Dihydrotestosterone Heptanoate: Synthesis, Pharmacokinetics and Effects on Hypothalamic-Pituitary-Testicular Function. *J. Clin. Endocrinol. Metab.* 64:557-562.

73. Carpenter, TO., Imperato-McGinley, J., Boulware, SD., Weiss, RM., Shackelton, C., Griffin, JE., Wilson, JD. 1990. Variable Expression of 5α-Reductase Deficiency: Presentation with Male Phenotype in a Child of Greek Origin. *J. Clin. Endocrinol. Metab.* 71:318-322.

74. Price, P., Wass, JAH., Griffin, JE., Leshin, M., Savage, MO., Large, DM, Bu'Lock, DE., Andersson, DC., Wilson, JD., Besser, GM. 1984. High Dose Androgen Therapy in Male Pseudohermaphroditism due to 5α- Reductase Deficiency and Disorders of the Androgen Receptor. *J. Clin. Invest.* 74:1496-1508.

75. Liao, S., Liang, T., Fang, S., Castaneda, E., Shao, TC. 1973, Steroid Structure and Androgenic Activity: Specificities Involved in the Receptor Binding and Nuclear Retention of Various Androgens. *J. Biol. Chem.* 248:6154-6162.

76. Schweikert, HU., Wilson, JD. 1974. Regulation of Human Hair Growth by Steroid Hormones. *J. Clin. Endocrinol. Metab.* 38:811-819.

77. Bingham, KD., Shaw, DA. 1973. The Metabolism of Testosterone by Human Scalp Skin. *J. Endocrinol.* 87:111-121.

78. Jenkins, EP., Andersson, S., Imperato-McGinley, J., Wilson, JD., Russell, DW. 1992. Genetic and Pharmacological Evidence for More than One Human Steroid 5α- Reductase. *J. Clin. Invest.* 89:293-300.

79. Dallob, AL., Sadick, NS., Unger, W., Lipert, S., Geissler, LA., Gregoire, SL., Nguyen, HH., Moore, EC., Tanaka, WK. 1994. The Effect of Finasteride, a 5α- Reductase Inhibitor, on Scalp Skin Testosterone and Dihydrotestosterone Concentrations in Patients with Male Pattern Baldness. *J. Clin. Endocrinol.* Metab. 79(3):703-706.

80. Diani, AR., Mulholland, MJ., Shull, KL., et al. 1992. Hair Growth Effects of Oral Administration of Finasteride, a Steroid 5α- Reductase Inhibitor, Alone and in Combination with Topical Minoxidil in the Balding Stumptail Macaque. *J. Clin. Endocrinol. Metab.* 74:345-350.

81. Ebling, FJG. 1986. Hair Follicles and Associated Glands as Androgen Targets. *J. Endocrinol. Metab.* 15:319-339.

82. Miles, RA., Cassidenti, DI., Carmina, E., Gentzshein, E., Stanczyk, FZ., Lobo, AR. 1992. Cutaneous Application of an Androstenedione Gel as *in vivo* Test of 5α- Reductase Activity in Women. *Fertil. Steril.* 58:708-712.

83. Serafini, P., Ablan, F., Lobo, RA. 1985. 5α- Reductase Activity in the Genital Skin of Hirsute Women. *J. Clin. Endocrinol. Metab.* 60:349-535.

84. Johnson, L., George, FW., Neaves, WB., Rosenthal, IM., Christensen, RA., Decristoforo, A., Schweikert, HU., Sauer, MV., Leshin, M., Griffin, JE., Wilson, JD. 1986. Characterisation of the Testicular Abnormality in 5α- Reductase Deficiency. *J. Clin. Endocrinol. Metab.* 63:1091-1099.

85. Thiboutot, DM., Demers, LM., Lookingbill, DP. 1992. Quantitation of Androgens in Sebum. *J. Invest. Dermatol.* 98:581.

86. Imperato-McGinley, J., Gautier, T., Cai, LQ., Yee, B., Epstein, J., Pochi, P. 1993. The Androgen Control of Sebum Production: Studies of Subjects with Dihydrotestosterone Deficiency and Complete Androgen Insensitivity. *J. Clin. Endocrinol. Metab.* 76:524-528.

87. Cunha, GR 1976. Epithelial-Stromal Interactions in Development of the Urogenital Tract. *Int. Rev. Cytol.* 47:137-194.

88. Cowan, RA., Cowan, SK., Grant, JK., Elder, HY. 1977. Biochemical Investigations of Separated Epithelium and Stroma from Benign Hyperplastic Tissue. *J. Endocrinol.* 74:111-115.

89. Hudson, RW. 1987. Comparison of Nuclear 5α- Reductase Activities in the Stromal and Epithelial Fractions of the Human Prostatic Tissue. *J. Steroid Biochem.* 26:349-353.

90. Kreig, M., Klözl, G., Kaufmann, J., Voight, KD. 1981. Stroma of Human Prostatic Hyperplasia: Preferential Tissue for Androgen Metabolism and Oestrogen Binding. *Acta Endocrinol.* 96:422-432.

91. Rennie, PS., Bruchovsky, N., McLoughlin., MG., Batzold, FH., Dunstan-Adams, EE. 1983. Kinetic Analysis of 5α- Reductase Isoenzymes in Benign Prostatic Hyperplasia. *J. Steroid Biochem.* 19:169-173.

92. Wilkin, RP., Bruchovsky, N., Shnitka, TK., Rennie, PS., Comeau, TL. 1980. Stromal 5α- Reductase Activity is Elevated in Benign Prostatic Hyperplasia. *Acta. Endocrinol.* 94:284.

93. Tunn, S., Hochstrate, H., Grunwald, I., Flüchter, SH and Kreig, M. 1988. Effect of Aging on Kinetic Parameters of 5α- Reductase in Epithelium and Stroma of Normal and Hyperplastic Human Prostate. *J. Clin. Endocrinol. Metab.* 67:379-385.

94. Rittmaster, RS. 1994. Finasteride. *New Engl. J. Med.* 330(2):120-125.

95. Ruijter, E., Van De Kaa, C., Miller, G., Ruiter, D., Debruyne, F., Schalken, J. 1999. Molecular Genetics and Epidemiology of Prostate Cancer. *Endocrine Rev.* 20(1):22-45.

96. Ross RK, Bernstein L, Lobo RA, Shimizu FZ, Stanczyk FZ, Pike MC, Henderson BE. 1992. 5α-Reductase Activity and Risk of Prostate Cancer Among Japanese and US White and Black Males. Lancet 339:887–889

97. Makridakis, NM., Ross, RK., Pike, MC., Crocitto, LE., Kolonel, LN., Pearce, CL., Henderson, BE., Reichardt, KV. 1999. Association of Mis-sense Substitution in SRD5A2 Gene with Prostate Cancer in African-American and Hispanic Men in Los Angeles, USA. *Lancet.* 354:975-978.

98. Bruchovsky, N., Leiskovsky, G. 1979. Increased ratio of 5α- Reductase: 3α(β)- Hydroxysteroid Dehydrogenase Activities in the Hyperplastic Human Prostate. *J. Endocrinol.* 80:289.

99. Isaacs, JT., Brendler, CB., Walsh, PC. 1983. Changes in the Metabolism of Dihydrotestosterone in the Hyperplastic Human Prostate. *J. Clin. Endocrinol. Metab.* 56:139-145.

100. Walsh, PC., Hutchins, GM., Ewing, LL. 1983. Tissue Content of Dihydrotestosterone in Human Prostatic Hyperplasia is not Supranormal. *J. Clin. Invest.* 72:1772-1777.

101. Geller, J. 1991. Benign Prostatic Hyperplasia: Pathogenesis and Medical Therapy. *J. Am. Geriatr. Soc.* 39:1208-1216.

102. McConnell, JD., Wilson, JD., George, FW., Geller, J., Pappas, F., Stoner, E. 1992. Finasteride, an Inhibitor of 5α- Reductase, Suppresses Prostatic Dihydrotestosterone in Males with Benign Prostatic Hyperplasia. *J. Clin. Endocrinol. Metab.* 74:505-508.

103. Gustafsson, O., Norming, U., Gustafsson, S., Eneroth, P., Astrom, G., Nyman, CR. 1996. Dihydrotestosterone and Testosterone Levels in Men Screened for Prostate Cancer - A Study of a Randomised Population. *British J. Urol.* 77(3):433-440.

104. Lamb, JC., English, H., Levandoski, PL., Rhodes, GR., Johnson, RK., Isaccs, JT. 1992. Prostatic Involution in Rats Induced by a Novel 5α-Reductase Inhibitor, SK and F-105657: Role for Testosterone in the Androgenic Response. *Endocrinol.* 130:685-694.

105.Brooks, JR., Baptista, EM., Berman, C., Ham, EA., Hichens, M., et al. 1981. Response of Rat Ventral Prostate to a New and Novel 5α- Reductase Inhibitor. *Endocrinol.* 109(3):830-836.

106.Brandt, M., Levy, MA. 1989. 3 Beta-Hydroxy-Delta 5-Steroid Dehydrogenase/3-Keto-Delta 5 Steroid Isomerase from Bovine Adrenals: Mechanism of Inhibition by 3-Oxo-4-Aza Steroids and Kinetic Mechanism of the Dehydrogenase. *Biochemistry.* 28:140-148.

107.Rasmusson, GH., Reynolds, GF., Utne, T., Jobson, RB., Primka, RL., et al. 1984. Azasteroids as Inhibitors of Rat Prostatic 5α- Reductase. *J. Med. Chem.* 27:1690-1701.

108.Faller, B., Farley, D., Nick, H. 1993. Finasteride: A Slow-binding 5α-Reductase Inhibitor. *Biochemistry.* 32(21):5705-5710.

109.Hausler, A., Allegrini, PR., Biollaz, M., Batzl, C., Schidegger, E., Bhatnagar, AS. 1996. CGP 53153: A New Potent Inhibitor of 5α- Reductase. *J. Steroid Biochem. Molec. Biol.* 57(3/4):187-195.

110.Metcalf, BW., Holt, DA., Levy, MA., Erb, JM., Heaslip, JI., Brandt, M., Oh, HJ. 1989. Potent Inhibition of Human Steroid 5α- Reductase (EC 1.3.1.30) by 3-androsten-3-carboxylic acids. *Bioorg. Chem.* 17:372-376.

111.Naki, H., Terashima, H., Arai, Y. 1988. *Eur. Patent No.* 0291245A2.

112.McNulty, AM., Audia, JE., Bemis, KG., Goode, RL., Rocco, VP., Neubauer, BL. 2000. Kinetic Analysis of LY 320236: Competitive Inhibitor of Type I and Non-competitive Inhibitor of Type II Human Steroid 5α- Reductase. *J. Steroid Biochem. Molec. Biol.* 72(1/2):13-21.

113.Tian, I., Stuart, JD., Moss, ML., Domanico, PL., Bramson, HN,. Patel, IR., Kadwell, SH., Overton, LK., Kost, TA., Mook, RA., Frye, SV., Batchelor, KW., Wiseman, JS. 1994. 17β-(N-*tert*-butylcarbamoyl)-4-aza-5α-androstan-1-ene-3-one Is an Active Site-Directed Slow Time-Dependent Inhibitor of Human Steroid 5α- Reductase 1. *Biochemistry.* 33:2291-2296.

114.Bull, HG., Garcia-Calvo, M., Andersson, S., et al. 1996. Mechanism-Based Inhibition of Human Steroid 5α- Reductase by Finasteride - Enzyme-

Catalysed Formation of NADP-Dihydrofinasteride, a Potent Bisubstrate Analogue Inhibitor. *J. Am. Chem. Soc.* 118:2359-2365.

115.Azzolina, B., Ellsworth, k., Andersson, S., Geissler, W., Bull, HG., Harris, GS. 1997. Inhibition of Rat α-Reductases by Finasteride: Evidence for Isozyme Differences in the Mechanism of Inhibition. *J. Steroid Biochem. Molec. Biol.* 61(1/2):55-64.

116.Weisser, H., Tunn, S., Debus, M., Kreig, M. 1994. 5α- Reductase Inhibition by Finasteride (Proscar) in Epithelium and Stroma of Human Benign Prostatic Hyperplasia. *Steroids.* 59:616-620.

117.Rittmaster, RS., Norman, RW., Thomas, LN., Rowden, G. 1996. Evidence for Atrophy and Apoptosis in the Prostates of Men Given Finasteride. *J. Clin. Endocrinol. Metab.* 81(2):814-819.

118.Lobaccaro, JM., Boudon, C., Lechevallier, E., Mottet, N., Rebillard, X., Lumbroso, S., Gibelin, B., Sultan, C. 1996. Effect of Finasteride (PROSCAR) on the Proliferation of Cultured Epithelial and Stromal Cells form Normal and Hyperplastic Human Prostates. *Cellular and Molec. Biol.* 42(4):511-518.

119.Stoner, E. 1994. 5α- Reductase Inhibitors for the Treatment of Benign Prostatic Hyperplasia. *Recent Prog. Horm. Res.* 49:285-292.

120.Steiner, JE. 1996. Clinical Pharmacokinetics and Pharmacodynamics of Finasteride. *Clin. Pharmacokinetics.* 30(1):16-27.

121.Bruchovsky, N., Rennie, PS., Batzold, FH., Goldenberg, SL., Fletcher, T., McLoughlin, MG. 1988. Kinetic Parameters of 5α- Reductase Activity in Stroma and Epithelium of Normal, Hyperplastic and Carcinomatous Human Prostates. *J. Clin. Endocrinol. Metab.* 67(4):806-816.

122.Brendler, CB. 1985. Hormonal Therapy of Prostate Cancer. *J. Urol.* 133:650-651.

123.Hudson, RW., Wherrett, D. 1990. Comparisons of Nuclear 5-alpha Reduction of Testosterone and Androstenedione in Human Prostatic Carcinoma and Benign Prostatic Hyperplasia. *J. Steroid Biochem.* 35:231-236.

124.Presti, JC., Fair, WR., Andriole, G., Sogani, PC., Seidmon, E., Ferguson, D., Ng, J., Gormley, GJ. 1992. Multicentre, Randomized, Double-blind, Placebo Controlled Study to Investigate the Effect of Finasteride (MK-906) on Stage D Prostate Cancer. *J. Urol.* 145:1201-1204.

125.Fruzzetti, F., DeLorenzo, D., Parrini, D., Ricci, C. 1994. Effects of Finasteride, a 5α- Reductase Inhibitor, on Circulating Androgens and Gonadotrophin Secretion in Hirsute Women. *J. Clin. Endocrinol. Metab.* 79(3):831-835.

126.Moghetti, P., Castello, R., Magnani, CM., Tosi, F., Negri, C., Armanini, D., Bellotti, G., Muggeo, M. 1994. Clinical and Hormonal Effects of the 5α-Reductase Inhibitor Finasteride in Idiopathic Hirsutism. *J. Clin. Endocrinol. Metab.* 79(4):1115-1120.

127.Makridakis, NM., Di Salle, E., Reichardt, JKV. 2000. Biochemical and Pharmacogenetic Dissection of Human Steroid 5α- Reductase Type II. *Pharmacogenetics.* 10:407-413.

128.Thigpen, AE., Russell, DW. 1992. Four-amino Acid Segment in Steroid 5α-Reductase 1 Confers Sensitivity to Finasteride, a Competitive Inhibitor. *J. Biol. Chem.* 267(12):8577-8583.

129.Bhattacharyya, AJ., Wang, M., Rajagopalan, K., Taylor, MF., Hiipakka, R., Liao, S., Collins, DC. 1999. Analysis of the Steroid Binding Domain of Rat Steroid 5α- Reductase (Isozyme-1) The Steroid D-ring Binding Domain of 5α-Reductase. *Steroids.* 64:197-204.

130.Südhof, TC., Goldstein, JL., Brown, MS., Russell, DW. 1985. The LDL Receptor Gene: A Mosaic of Exons Shared with Different Proteins. *Science.* 228:815-822.

131.Perham, RN., Scrutton, NS., Berry, A. 1991. New Enzymes for Old: Redesigning the Coenzyme and Substrate Specificities of Glutathione Reductase. *BioEssays.* 13:515-525.

132.Baker, PJ., Britton, LK., Rice, DW., Rob, A., Stillman, TJ. 1992. Structural Consequences of Sequence Patterns in the Fingerprint Region of the Nucleotide Binding Fold. *J. Mol. Biol.* 228:662-671.

133.Wang, M., Bhattacharyya AJ., Taylor, MF., Tai, HH., Collins, DC. 1999. Site-Directed Mutagenesis Studies of the NADPH-binding Domain of Rat Steroid 5α- Reductase (isozyme-1) I: Analysis of Aromatic and Hydroxylated Amino Acid Residues. *Steroids.* 64:356-362.

134.McKinley-McKee, JS., Winberg, JO., Pettersson, G. 1991. Mechanism of Action of *Drosophila melanogaster* Alcohol Dehydrogenase. *Biochem. Int.* 25:879-885.

135.Lauvergeat, V., Kennedy, K., Feuillet, JH., McKie, L., Baltas, M., Boudet, AM., Grima-Pettanati., Douglas, KT. 1995. Site-directed Mutagenesis of a Serine Residue in Cinnamyl Alcohol Dehydrogenase, a Plant NADPH Dependent Dehydrogenase, Affects the Specificity for the Coenzyme. *Biochemistry.* 34:12426-12434.

136.Sambrook, J., Fritsch, EF., Maniatis, T. 1989. Molecular Cloning, A Laboratory Manual. Cold Spring Harbour Laboratory Press, USA.

137.Benore-Parson., Anderson, L. 1995. Purification of DNA Fragments from Lyophilised Agarose Gels. *Nucleic Acid Research.* 23(23):4926-4927.

138.Brown, TA. 1990. Gene Cloning an Introduction. Chapman and Hall, London.

139.Simmons, DL. 1993. Cellular Interactions in Development. Oxford University Press, New York.

140.Papworth, C., Bauer, JC., Braman, J., Wright, DA. 1996. Site-Directed Mutagenesis in One Day with >80% Efficiency. *Strategies.* 8:3-4.

141.Stratagene. 1996. Quickchange™ Site-Directed Mutagenesis Kit.

142.Berry, SJ., Coffery, DS. 1994. The Development of Human Benign Prostatic Hyperplasia with Age. *J Urol.* 132:474-479.

143.Stoner, E. 1990. The Clinical Development of a 5α- Reductase Inhibitor, Finasteride. *J Steroid Biochem. Mol. Biol.* 37:375-378.

144.Gormley, GJ., Stoner, E., Rittmaster, RS., et al. 1990. Effects of Finasteride (MK-906), a 5α- Reductase Inhibitor on Circulating Androgens in Male Volunteers. *J. Clin. Endocrinol. Metab.* 70:1136-1141.

145.Gormley, GJ. 1991. Role of 5α- Reductase Inhibitors in the Treatment of Advanced Prostatic Carcinoma. *Urol. Clin. North Am.* 18:93-98.

146.Segal, AW., West, I., Wientjes, F., Nugent, J., Chavan, AJ., Haley, BE., Garcia, RC., Rosen, H., Scrace, G. 1992. Cytochrome b-245 is a Flavocytochrome Containing FAD and the NADP[H]-Binding Site of the Microbial Oxidase of Phagocytes. *Biochem. J.* 284:781-788.

147.www.cryst.bbk.ac.uk

148.Baquero, MR., Bouzon, M., Quintel, JC., Ayala, JA., Moreno, F. 1996. *dacD*, an *Escherichia coli* Gene Encoding a Novel Penicillin-Binding Protein (PBP66) with DD-Carboxypeptidase Activity. *J. Bacteriol.* 178:7106-7111.

149.Liang, T., Heiss, C., Cheung, AH., Reynolds., GF., Rasmusson, GH. 1984. 4-Azasteroidal 5α- Reductase Inhibitors. *J. Steroid Biochem.* 19:385-390.

150.Wilson, JD. 1980. The Pathogenesis of Benign Prostatic Hyperplasia. *Am. J. Med.* 68:745-756.

151.Daughday, WH., Lowry, OH., Rosebrough, NJ., Fields, WS. 1952. Determination of Cerebrospinal Fluid Protein with the Folin Phenol Reagent. *J. Lab. Clin. Med.* 39:663-665.

Appendix A

Sequence Data

I

II

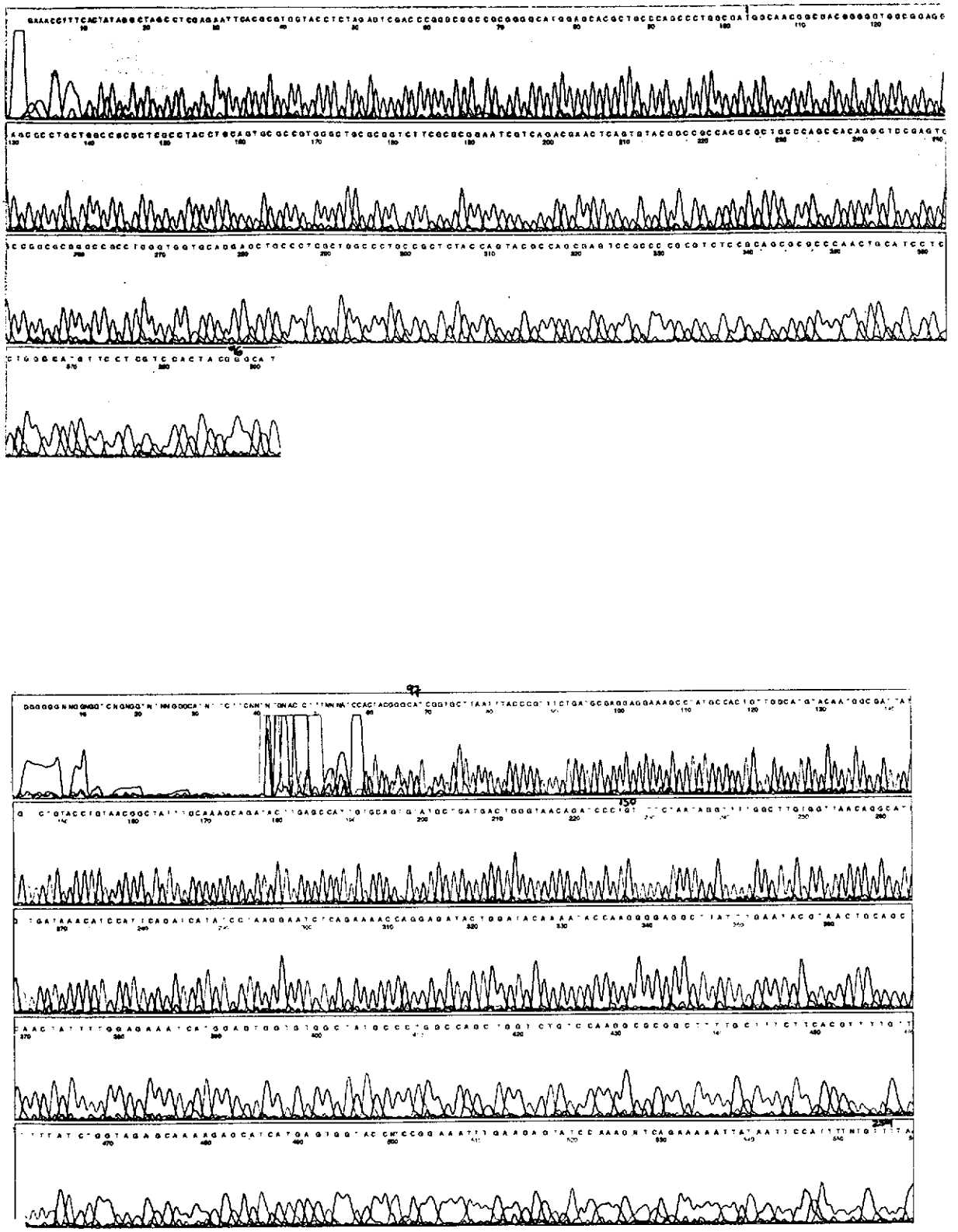

Figure A1: DNA sequence chromatographs of 5AR1RC mutant clone using the T7EEV (I) and AR1R (II) primers. Other than the mutation at residue 150 (-CGT- to -TGT-), no additional alterations to the wild type cDNA were seen.

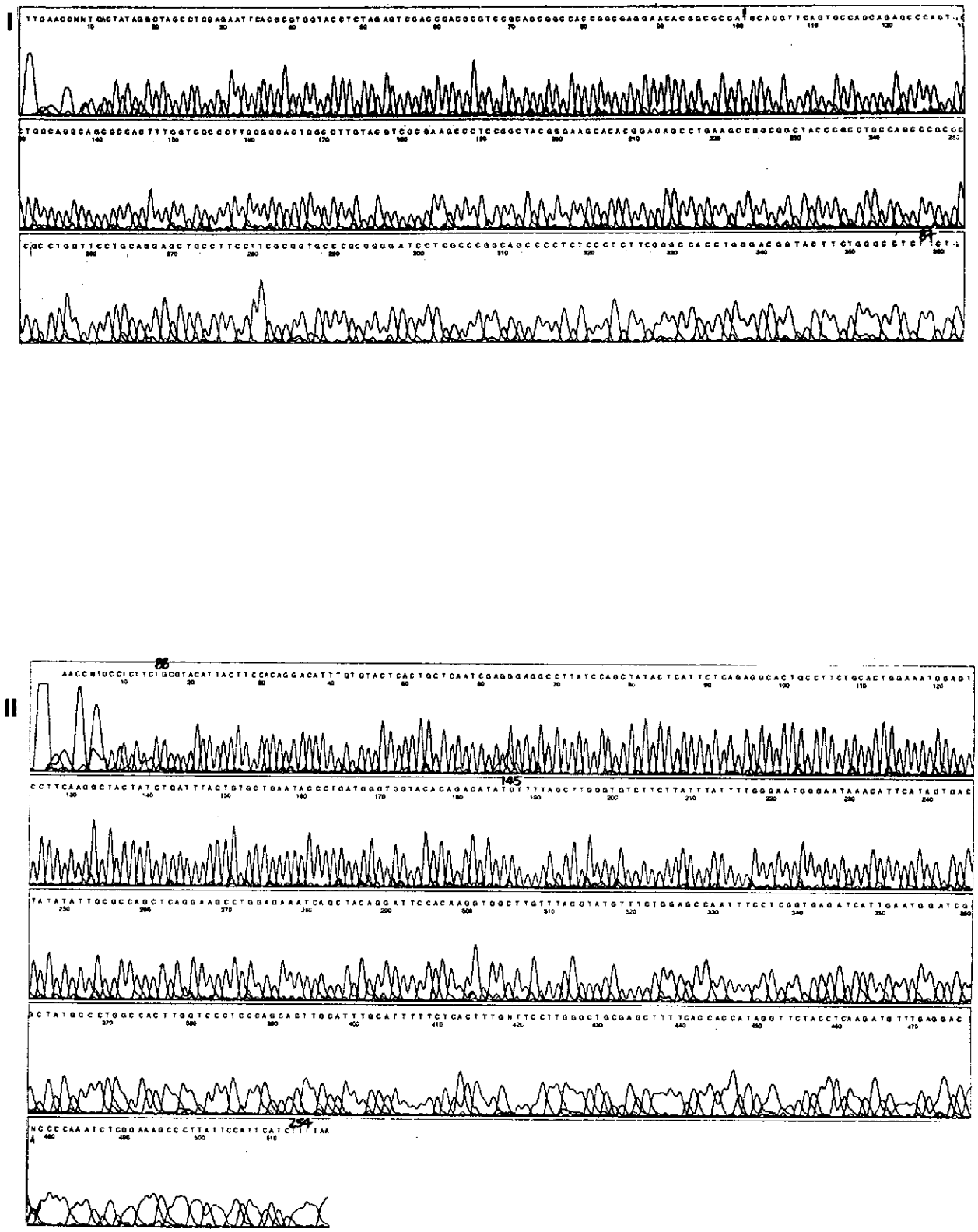

Figure A2: DNA sequence chromatographs of 5AR2RC mutant clone using the T7EEV (I) and AR2R (II) primers. Other than the mutation at residue 145 (-CGG- to -TGT-), no additional alterations to the wild type cDNA were seen.

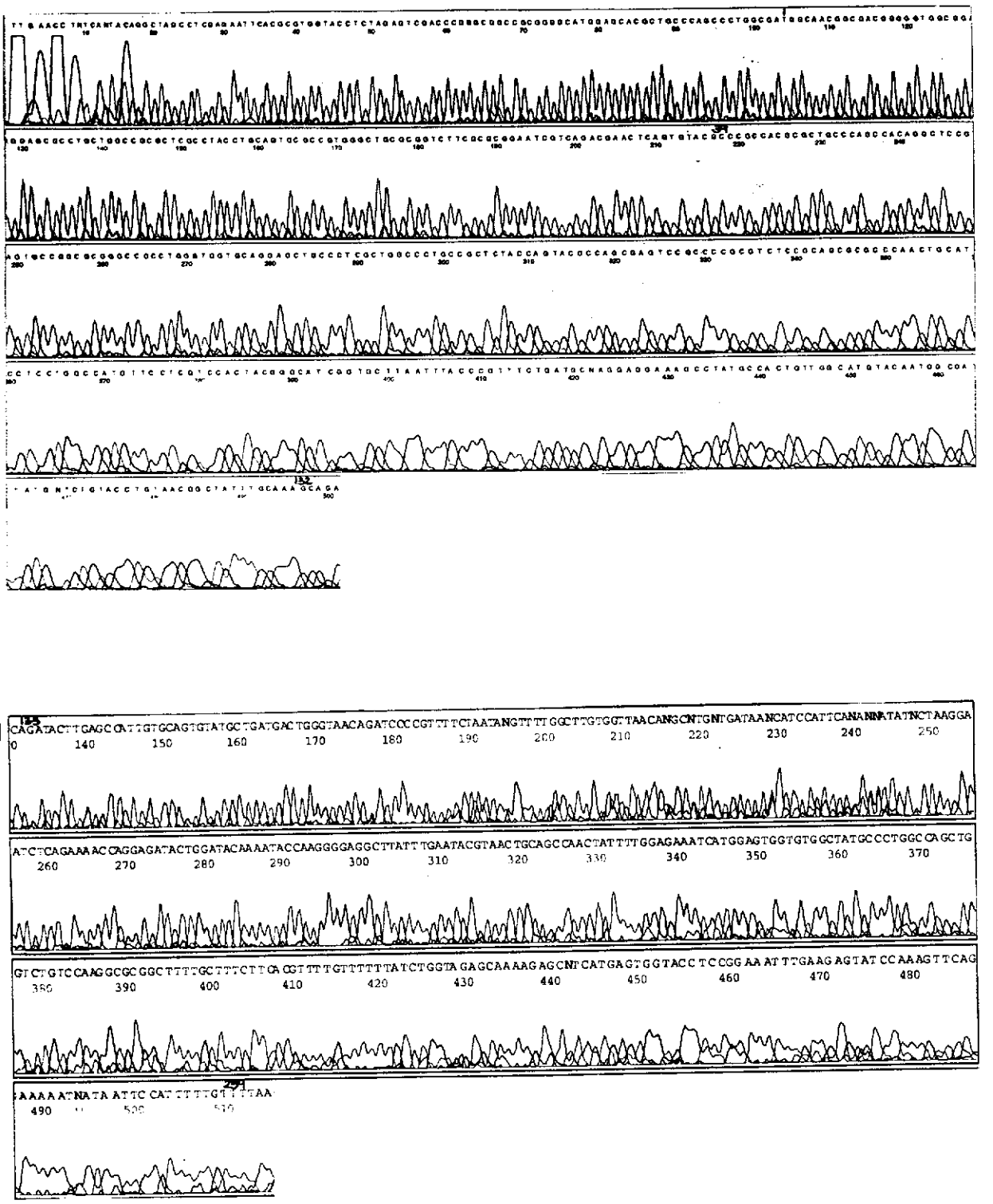

Figure A3: DNA sequence chromatographs of 5AR1G39A mutant clone using the T7EEV (I) and AR1R (II) primers. Other than the mutation at residue 39 (-GGC- to -GCC-), no additional alterations to the wild type cDNA were seen.

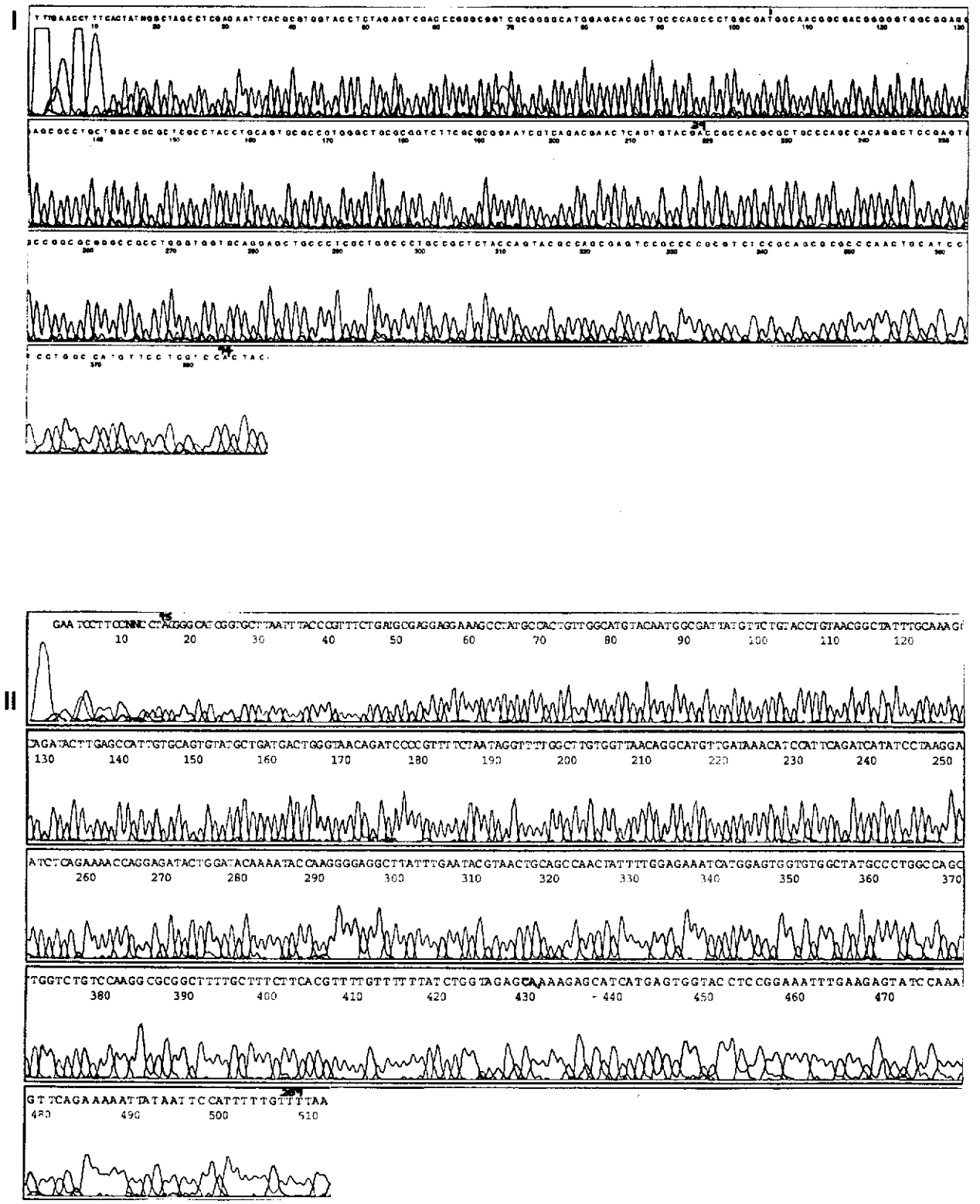

Figure A4: DNA sequence chromatographs of 5AR1G39D mutant clone using the T7EEV (I) and AR1R (II) primers. Other than the mutation at residue 39 (-GGC- to -GAC-), no additional alterations to the wild type cDNA were seen.

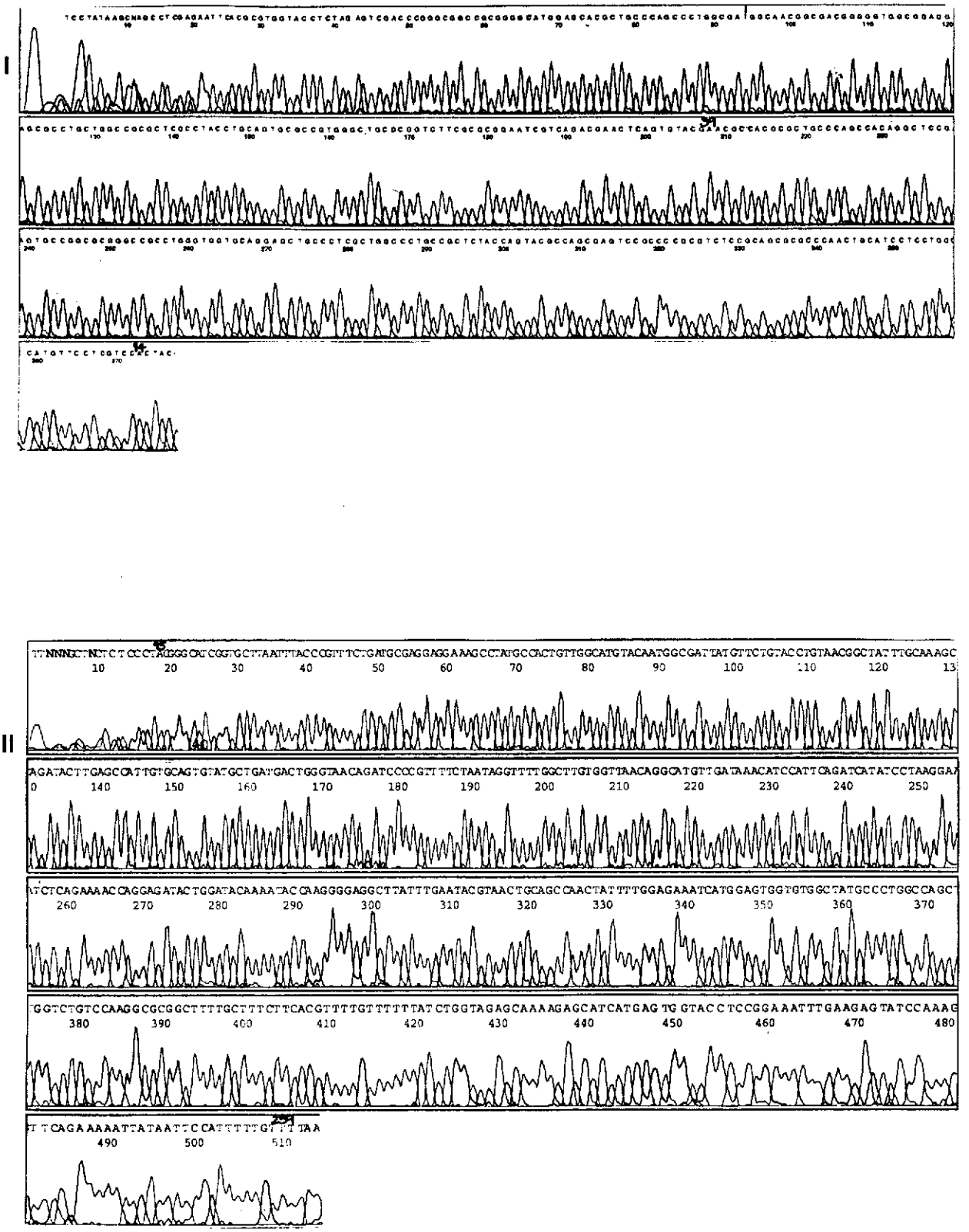

Figure A5: DNA sequence chromatographs of 5AR1G39E mutant clone using the T7EEV (I) and AR1R (II) primers. Other than the mutation at residue 39 (-GGC- to -GAA-), no additional alterations to the wild type cDNA were seen.

av

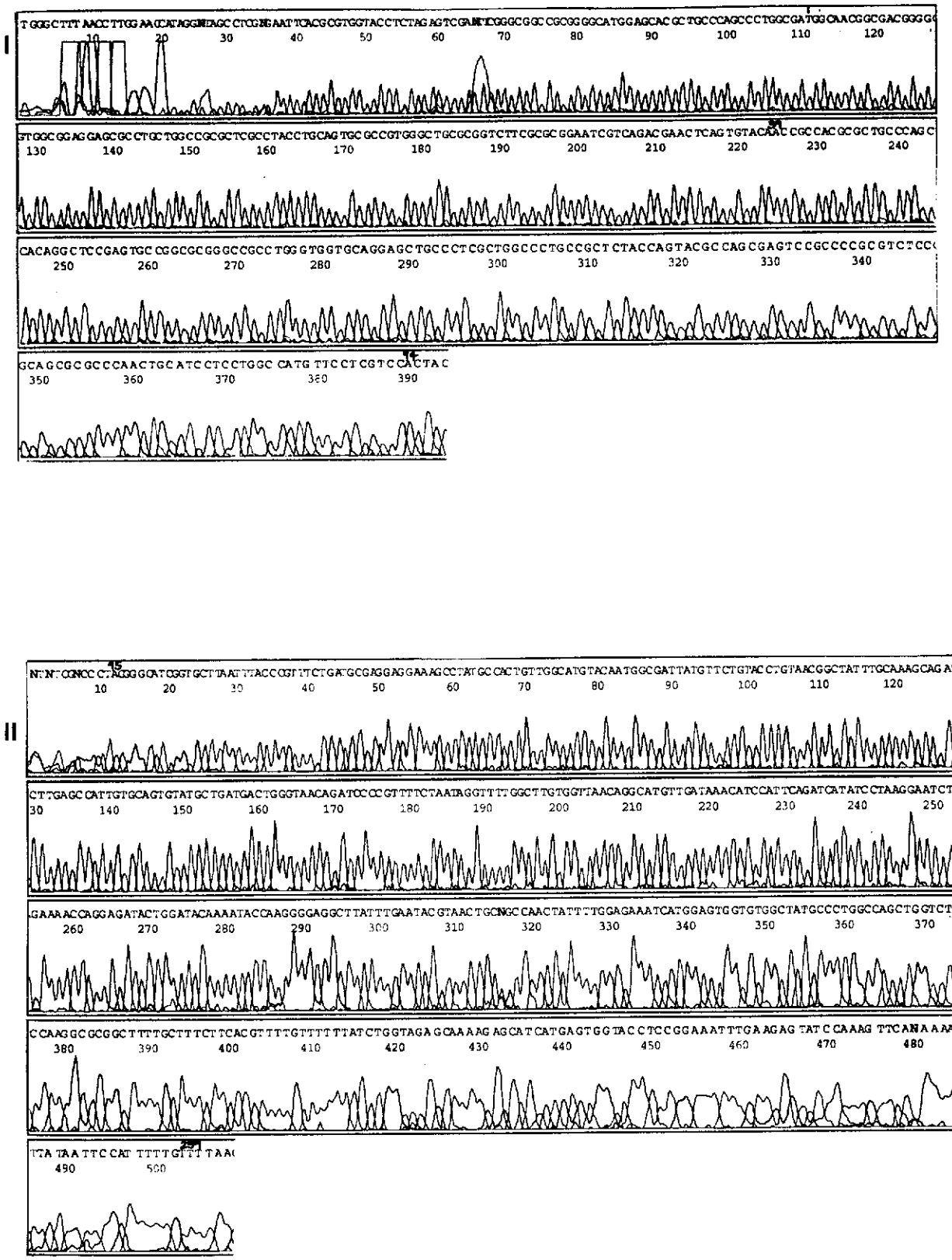

Figure A6: DNA sequence chromatographs of 5AR1G39N mutant clone using the T7EEV (I) and AR1R (II) primers. Other than the mutation at residue 39 (-GGC- to -AAC-), no additional alterations to the wild type cDNA were seen.

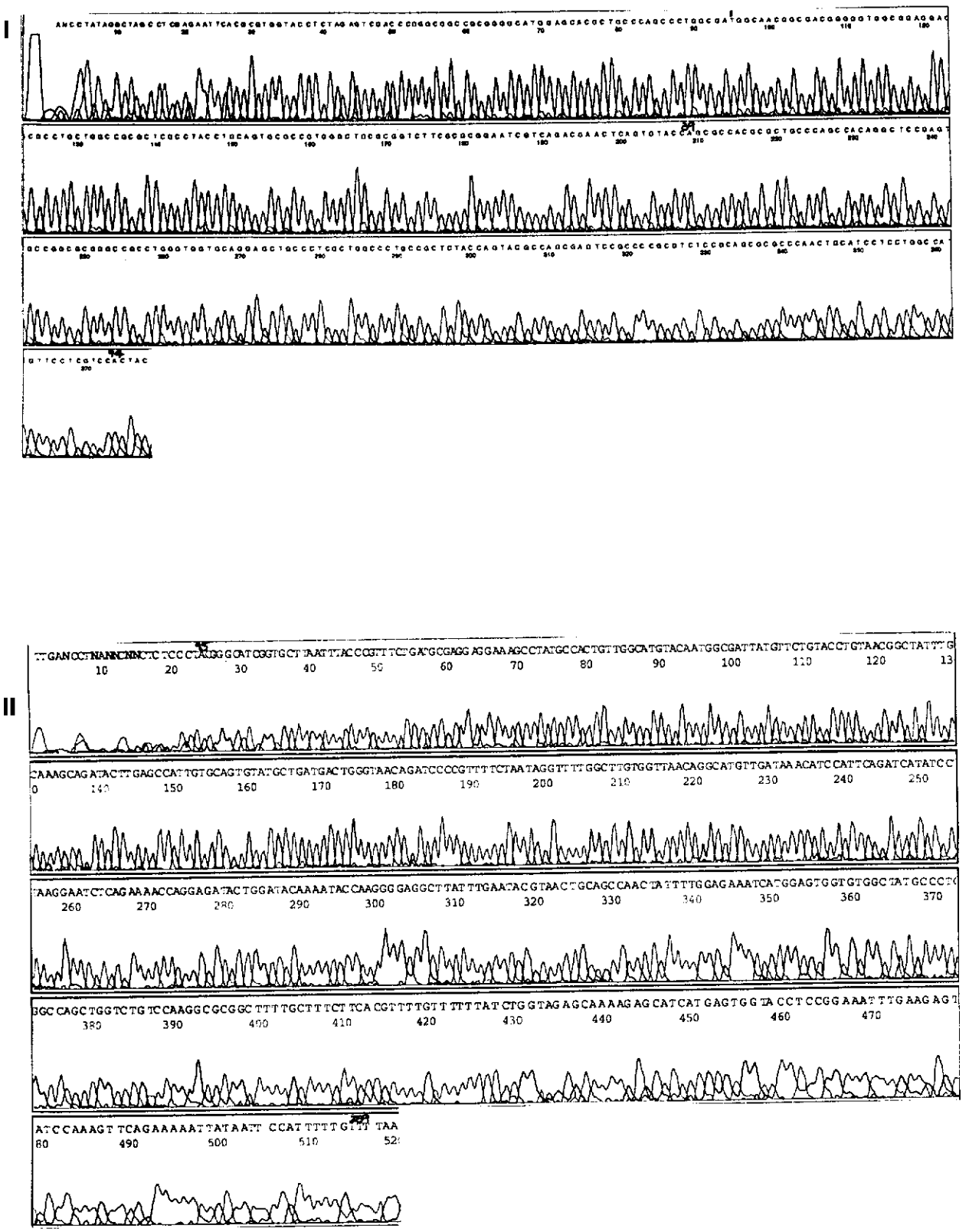

Figure A7: DNA sequence chromatographs of 5AR1G39Q mutant clone using the T7EEV (I) and AR1R (II) primers. Other than the mutation at residue 39 (-GGC- to -CAG-), no additional alterations to the wild type cDNA were seen.

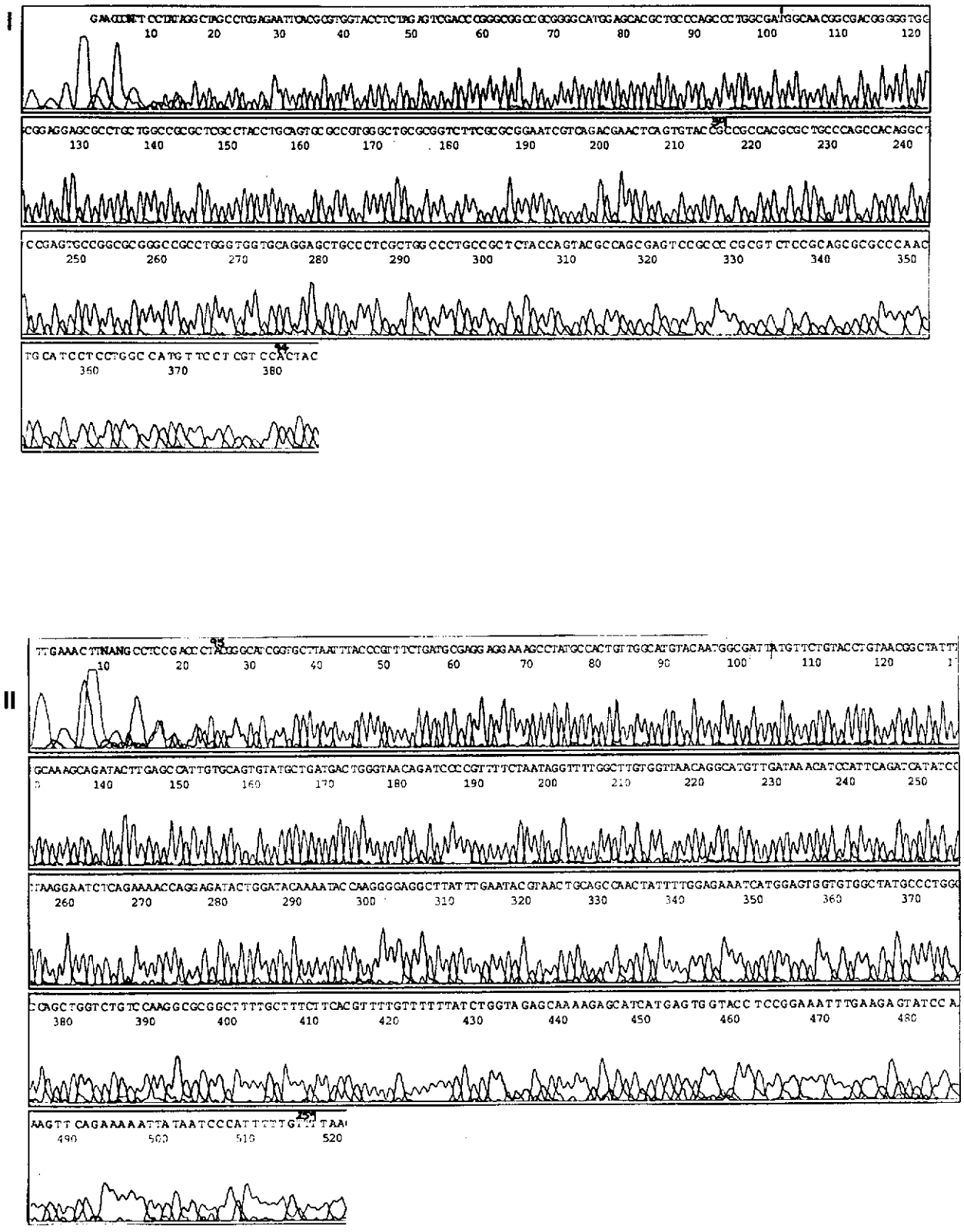

Figure A8: DNA sequence chromatographs of 5AR1G39R mutant clone using the T7EEV (I) and AR1R (II) primers. Other than the mutation at residue 39 (-GGC- to -CGC-), no additional alterations to the wild type cDNA were seen.

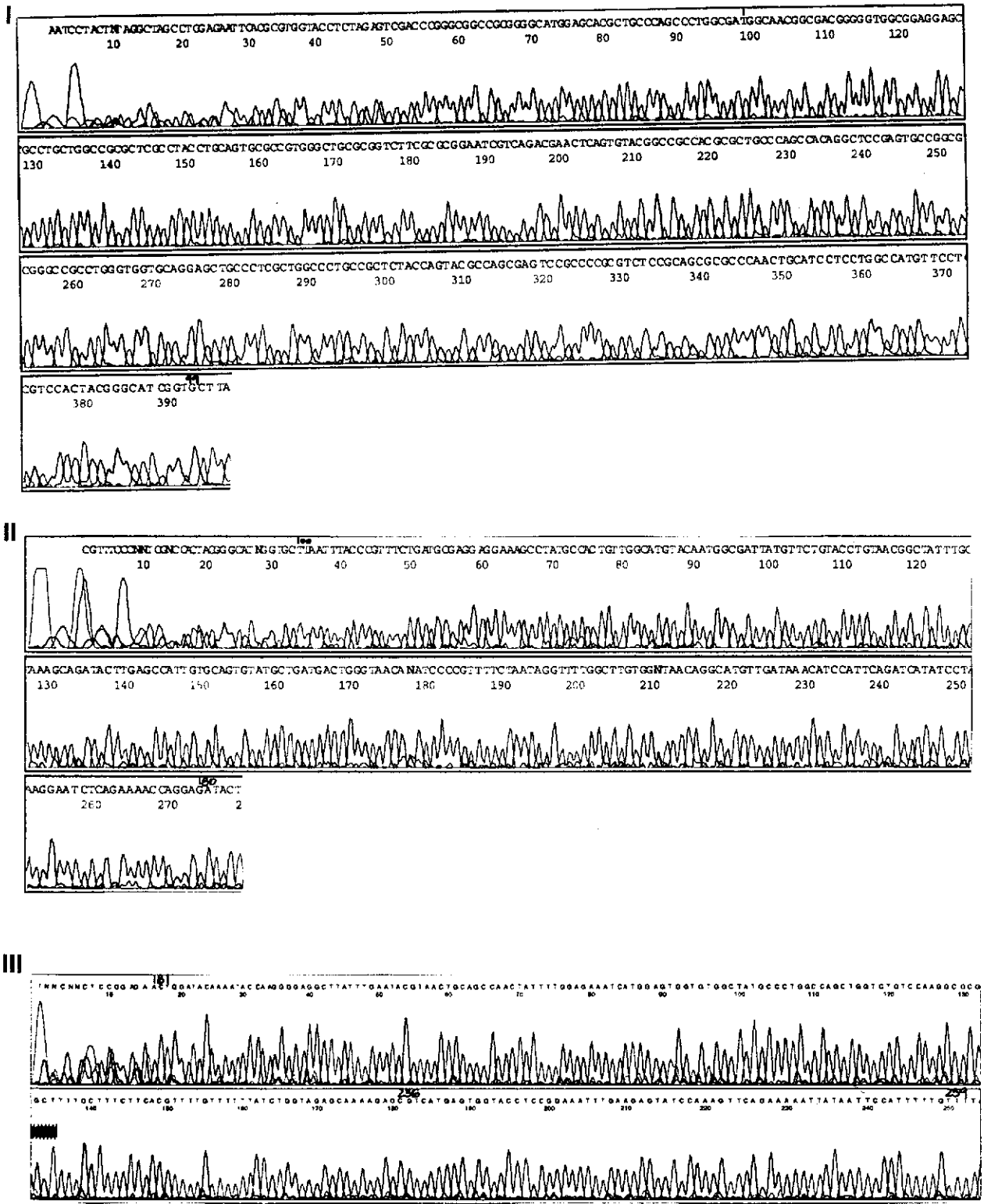

Figure A9: DNA sequence chromatographs of 5AR1H236R mutant clone using the T7EEV (I), AR1R (II) and AR1H (III) primers. Other than the mutation at residue 236 (-CAT- to -CGT-), no additional alterations to the wild type cDNA were seen.

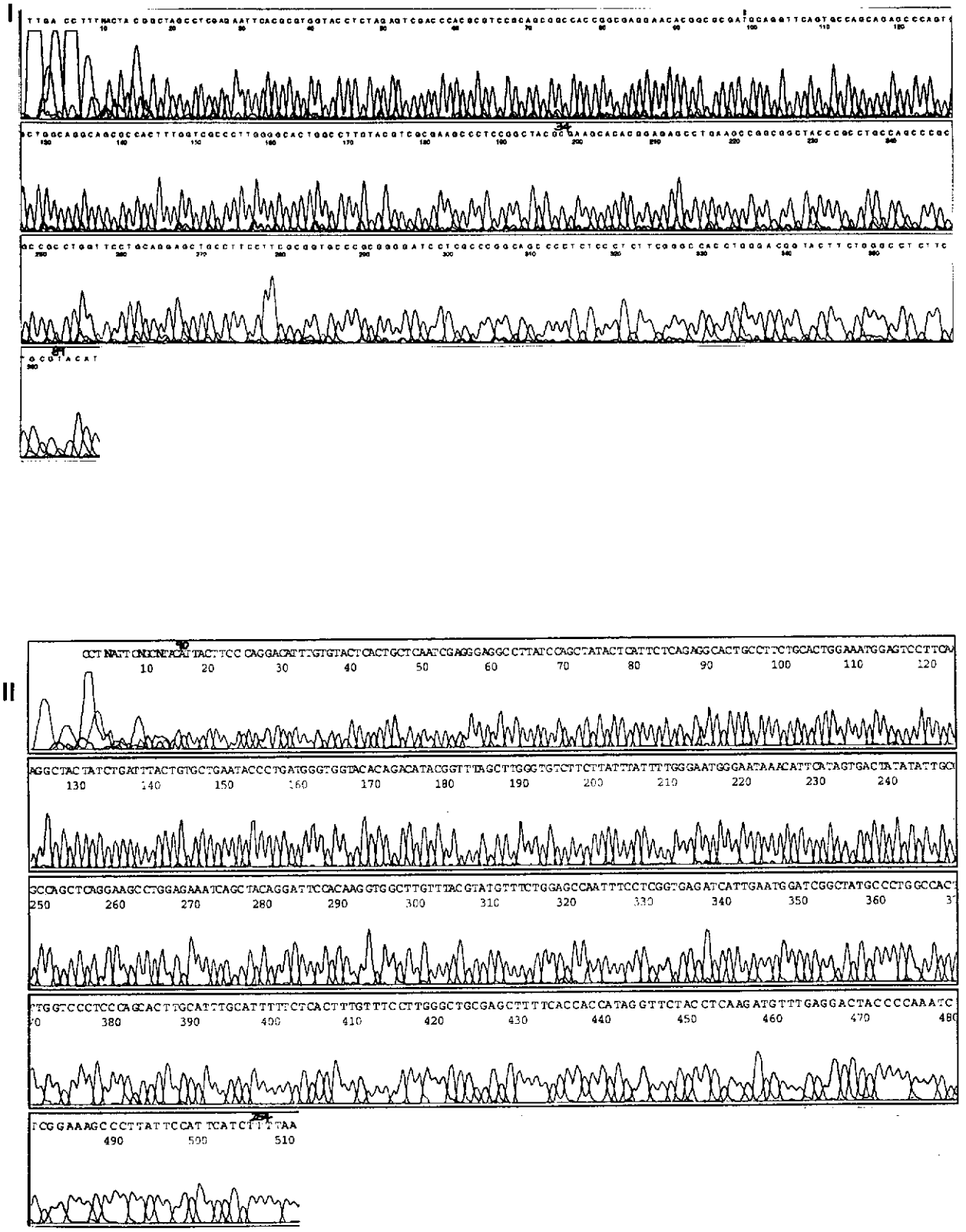

Figure A10: DNA sequence chromatographs of 5AR2G34A mutant clone using the T7EEV (I) and AR2R (II) primers. Other than the mutation at residue 34 (-GGG- to -GCG-), no additional alterations to the wild type cDNA were seen.

ax

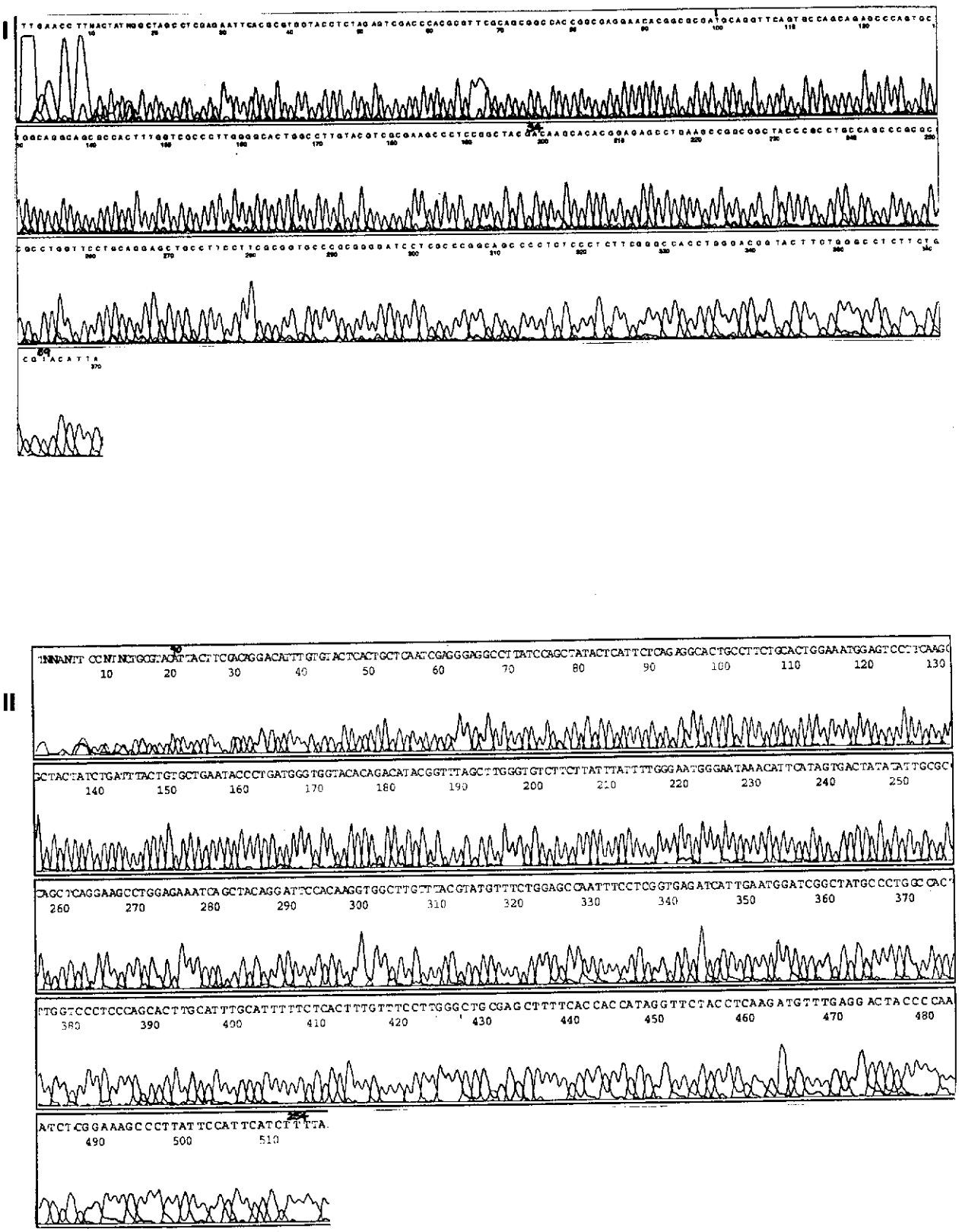

Figure A11: DNA sequence chromatographs of 5AR2G34D mutant clone using the T7EEV (I) and AR2R (II) primers. Other than the mutation at residue 34 (-GGG- to -GAC-), no additional alterations to the wild type cDNA were seen.

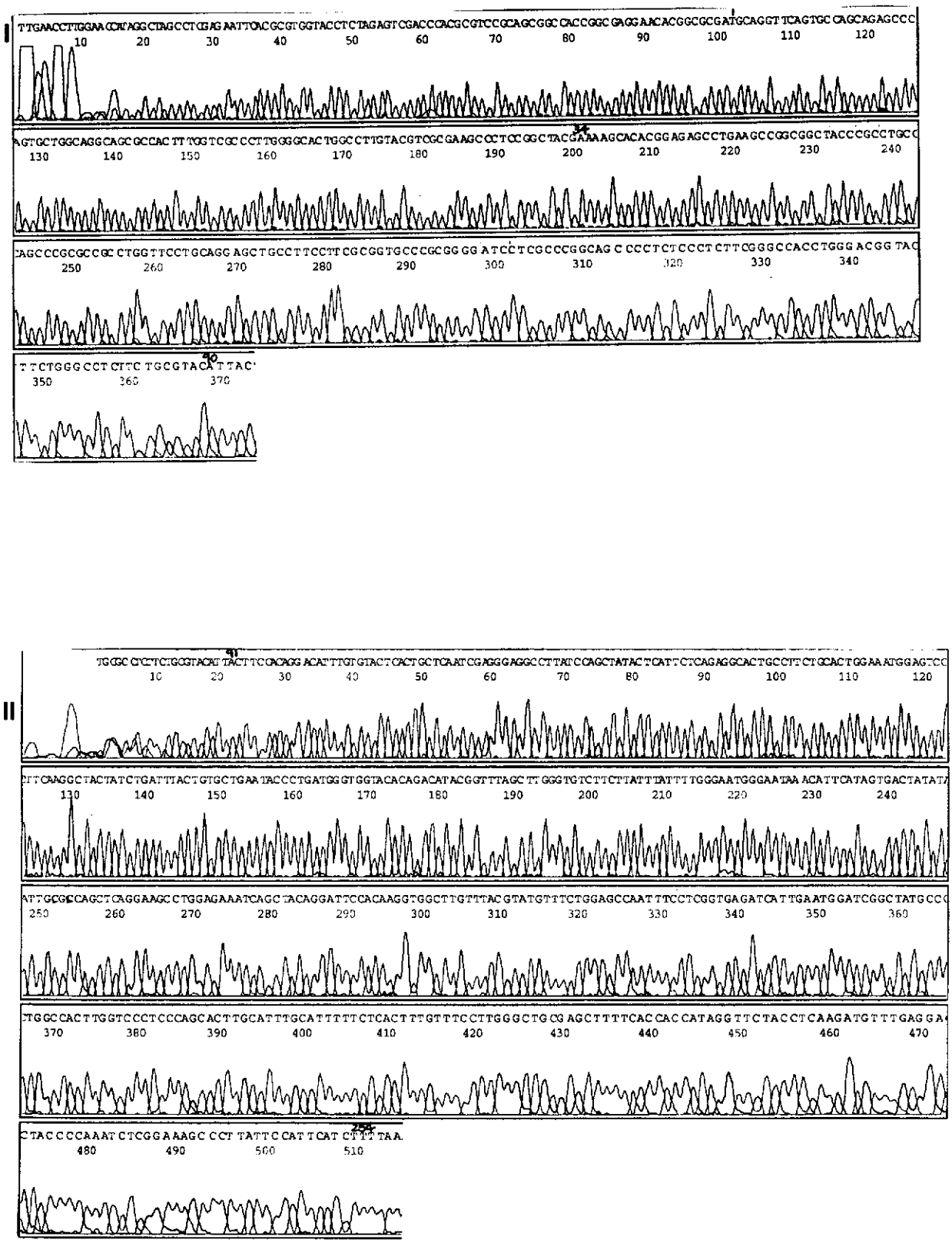

Figure A12: DNA sequence chromatographs of 5AR2G34E mutant clone using the T7EEV (I) and AR2R (II) primers. Other than the mutation at residue 34 (-GGG- to -GAA-), no additional alterations to the wild type cDNA were seen.

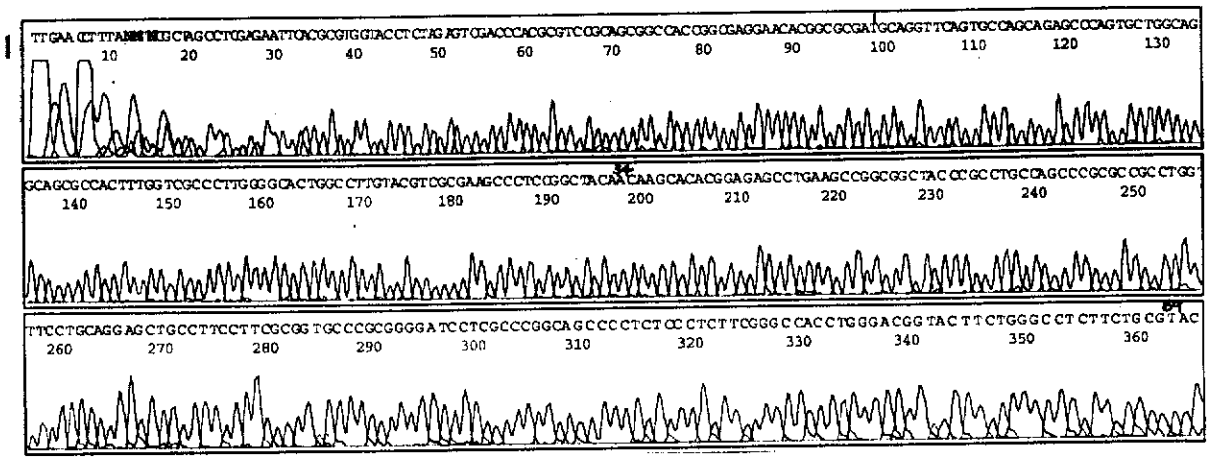

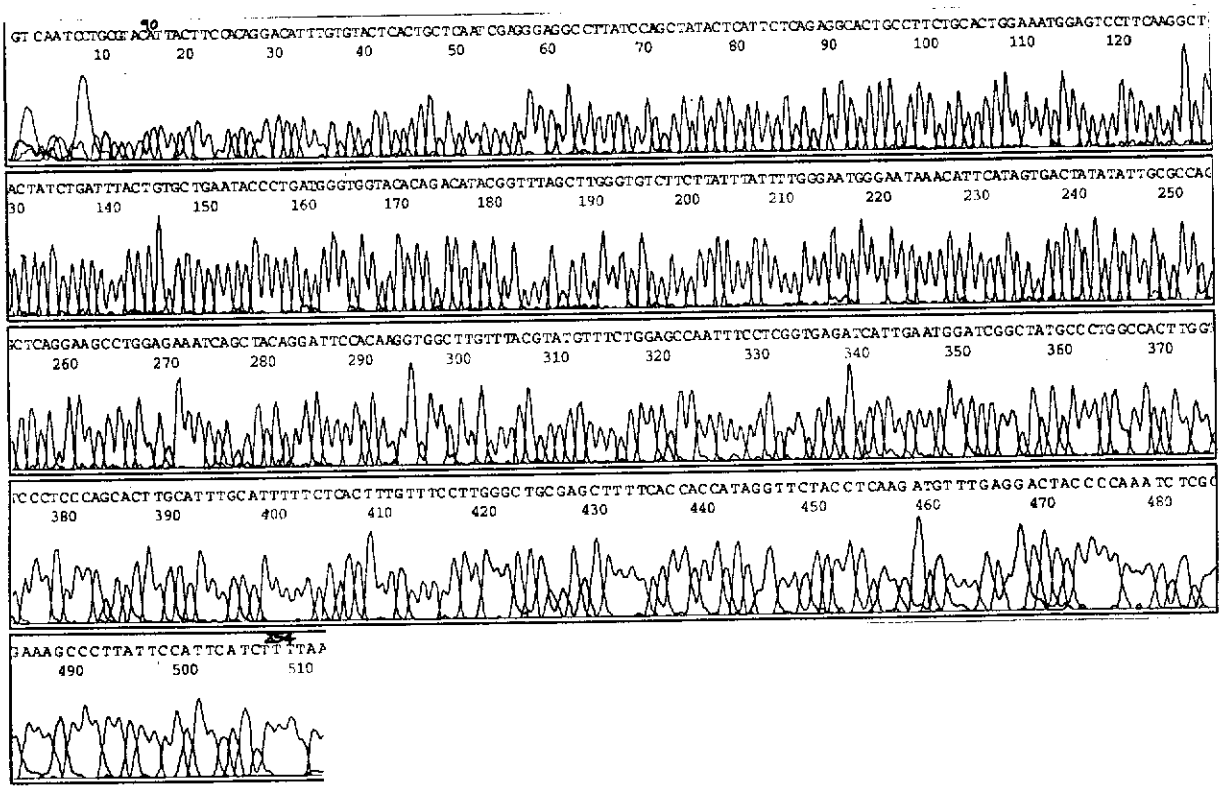

Figure A13: DNA sequence chromatographs of 5AR2G34N mutant clone using the T7EEV (I) and AR2R (II) primers. Other than the mutation at residue 34 (-GGG- to -AAC-), no additional alterations to the wild type cDNA were seen.

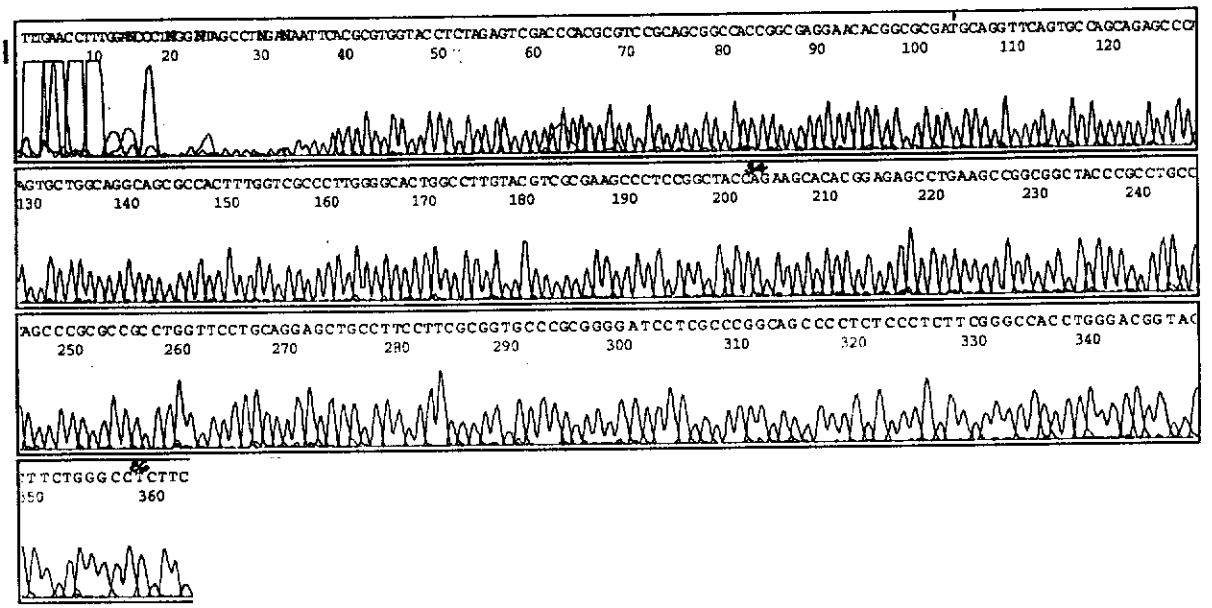

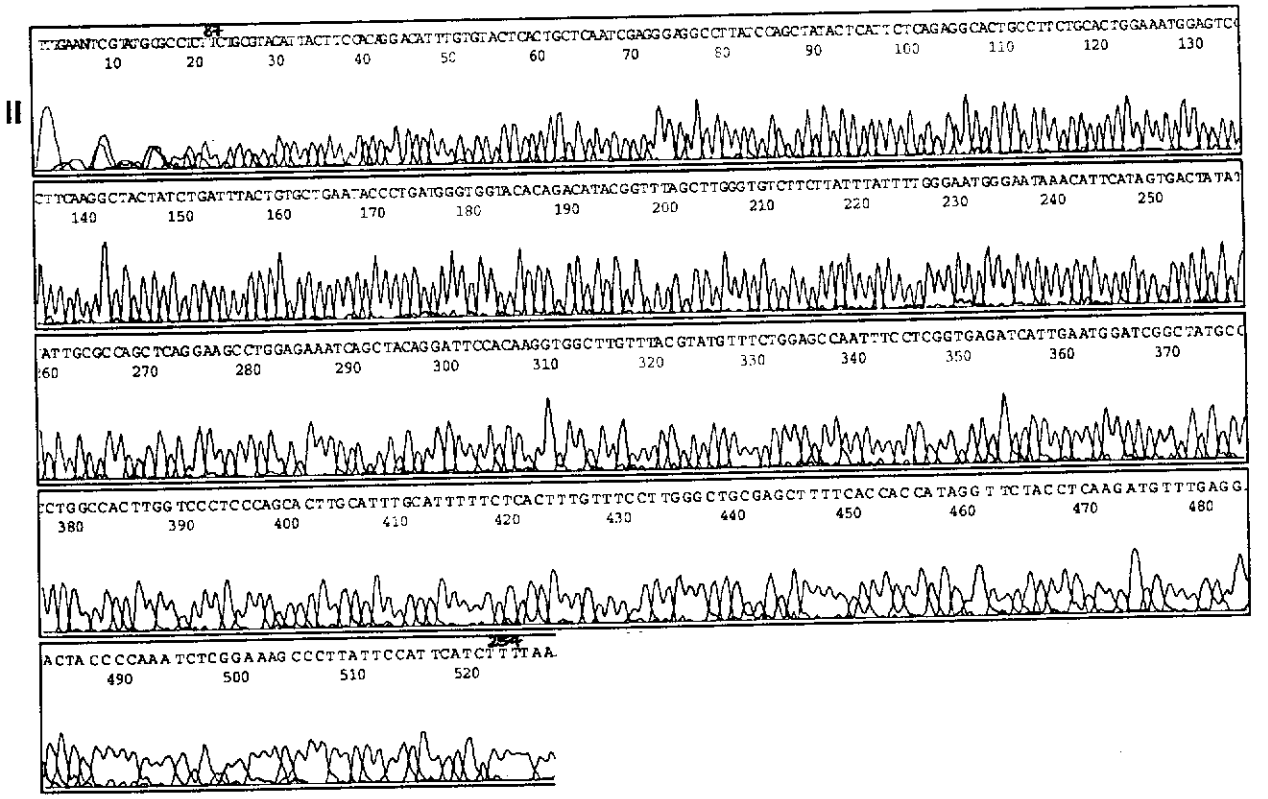

Figure A14: DNA sequence chromatographs of 5AR2G34Q mutant clone using the T7EEV (I) and AR2R (II) primers. Other than the mutation at residue 34 (-GGG- to -CAG-), no additional alterations to the wild type cDNA were seen.

I

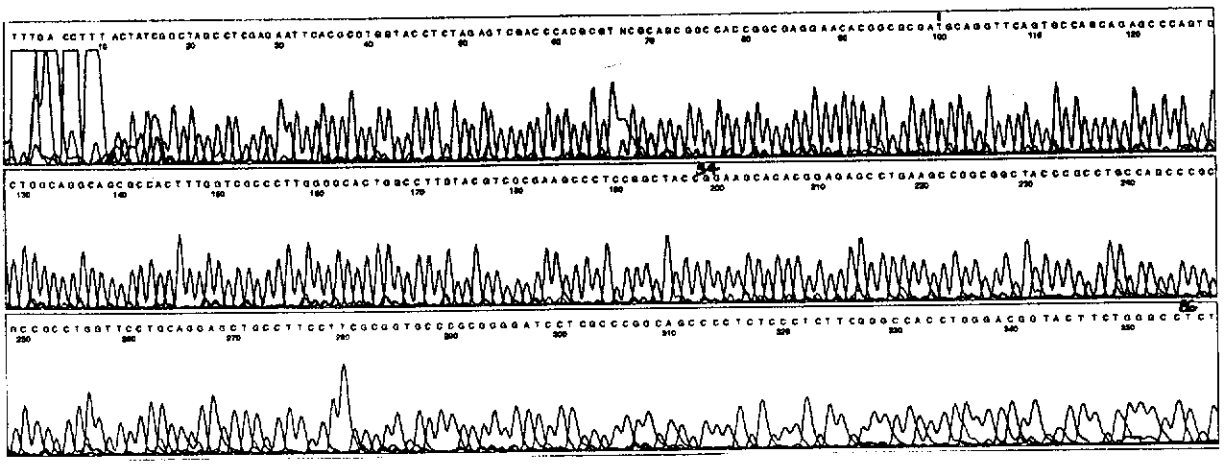

II

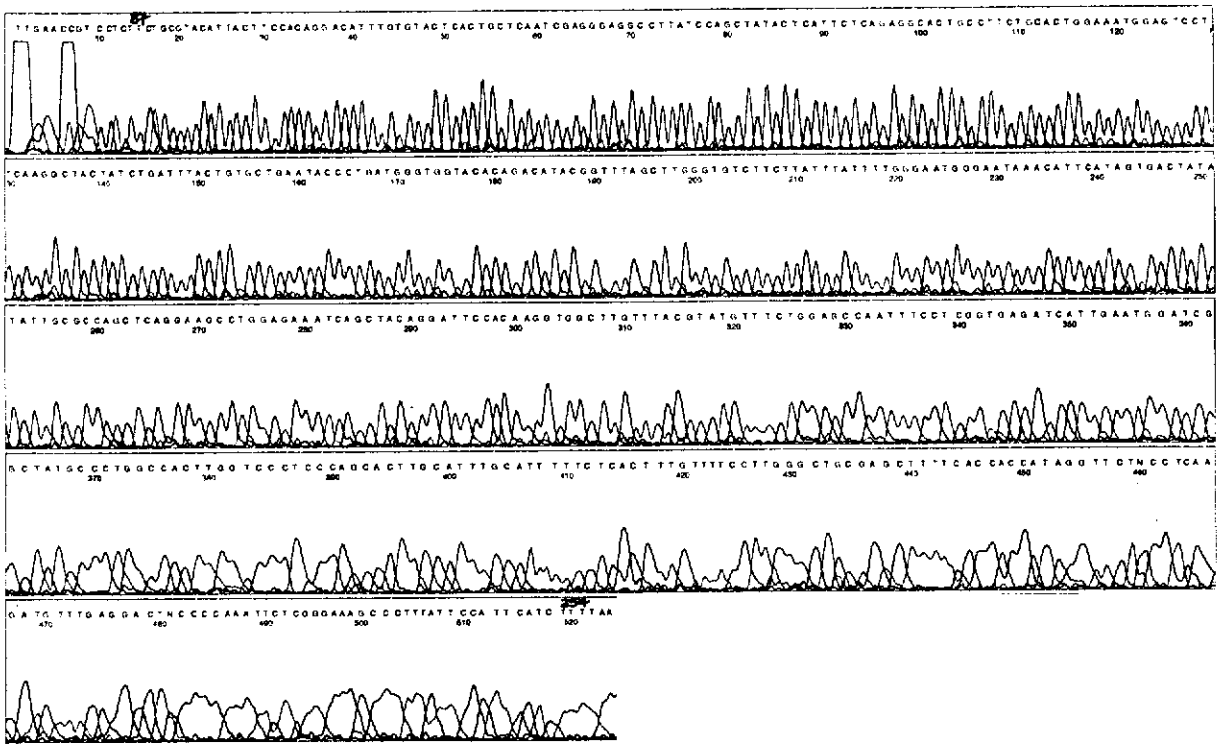

Figure A15: DNA sequence chromatographs of 5AR2G34R mutant clone using the T7EEV (I) and AR2R (II) primers. Other than the mutation at residue 34 (-GGG- to -CGG-), no additional alterations to the wild type cDNA were seen.

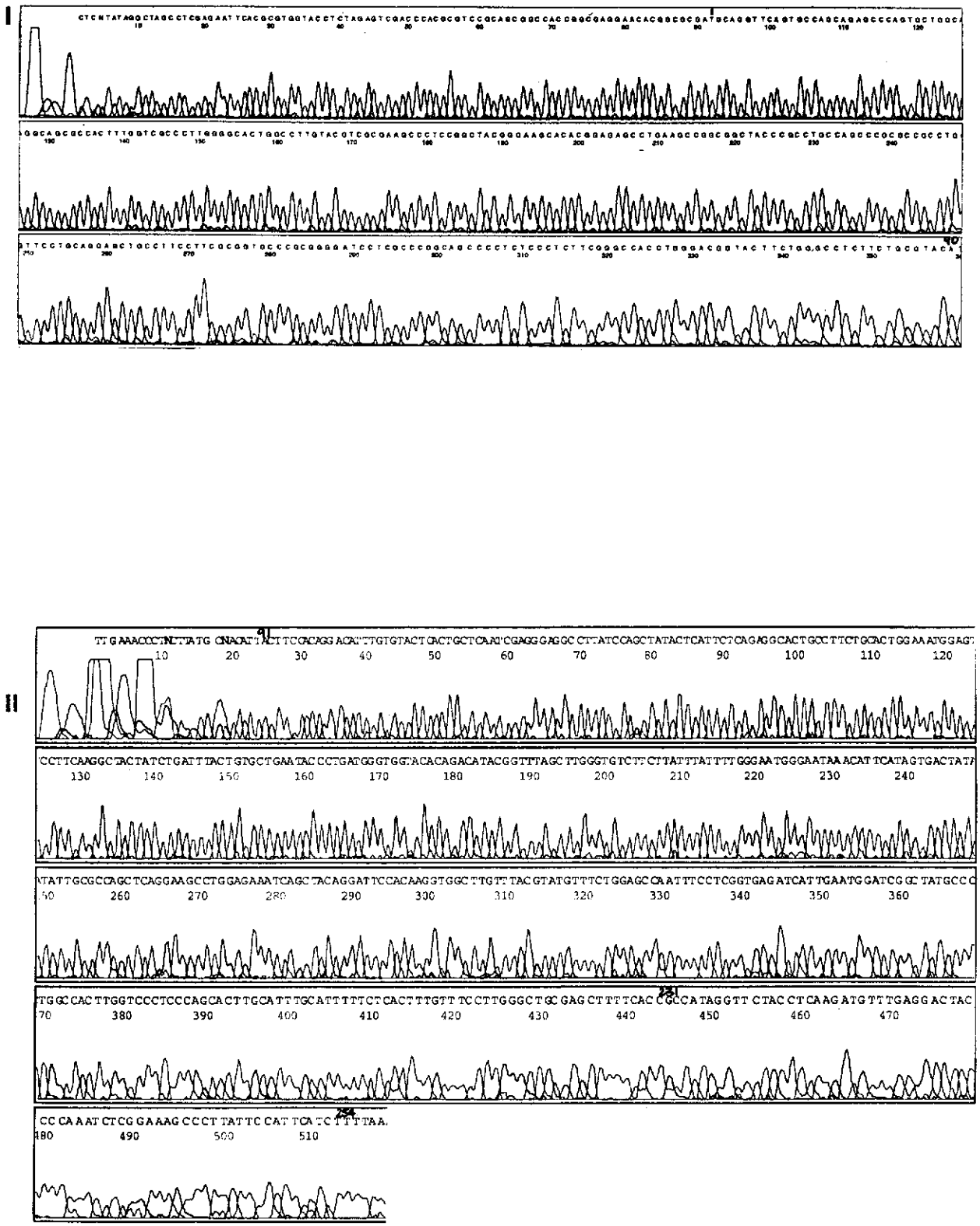

Figure A16: DNA sequence chromatographs of 5AR2H231R mutant clone using the T7EEV (I) and AR2R (II) primers. Other than the mutation at residue 231 (-CAC- to -CGC-), no additional alterations to the wild type cDNA were seen.

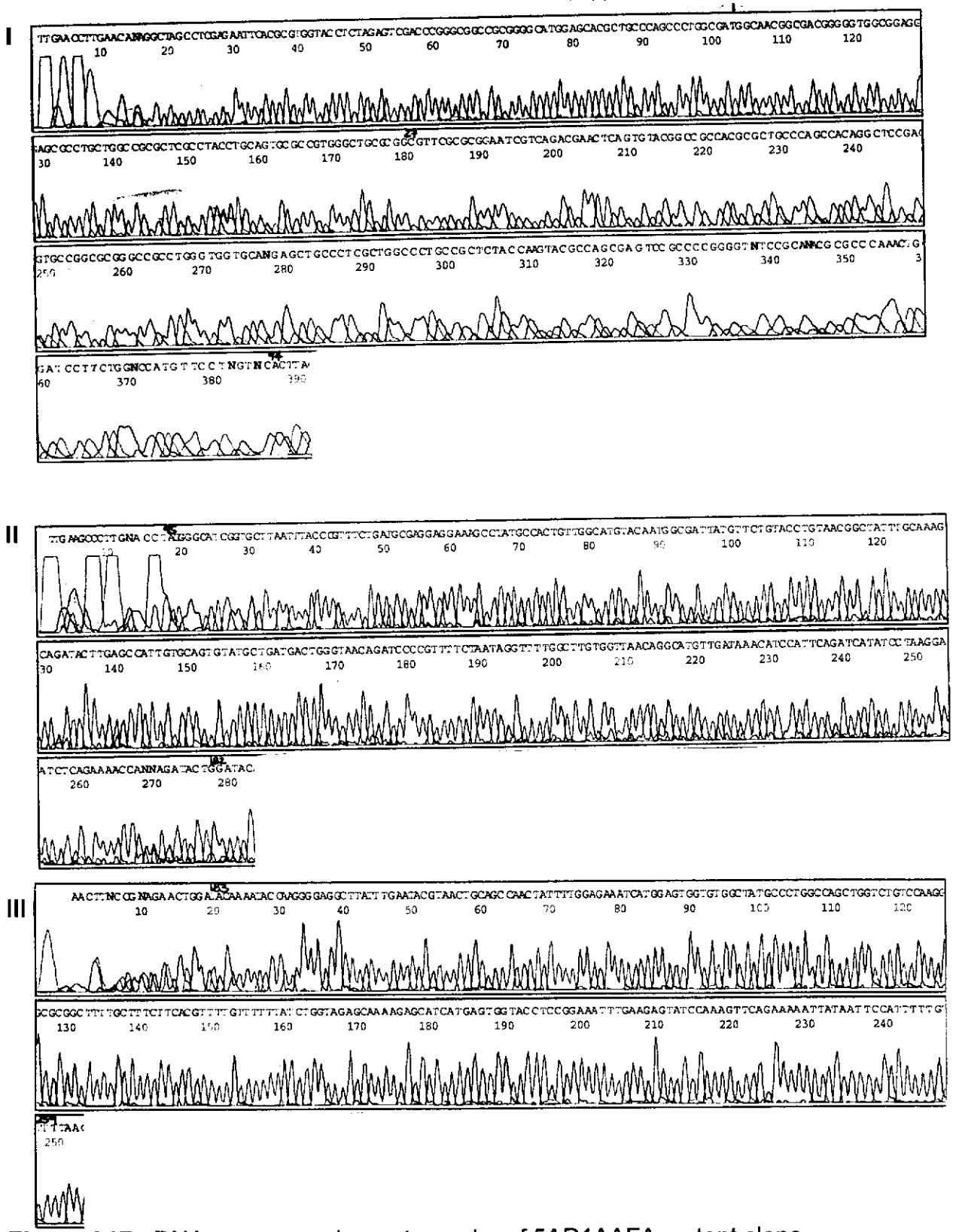

Figure A17: DNA sequence chromatographs of 5AR1AAFA mutant clone using the T7EEV (I), AR1R (II) and AR1H (III) primers. Other than the mutation at residue 27 (-GTC- to -GCG-), no additional alterations to the wild type cDNA were seen.

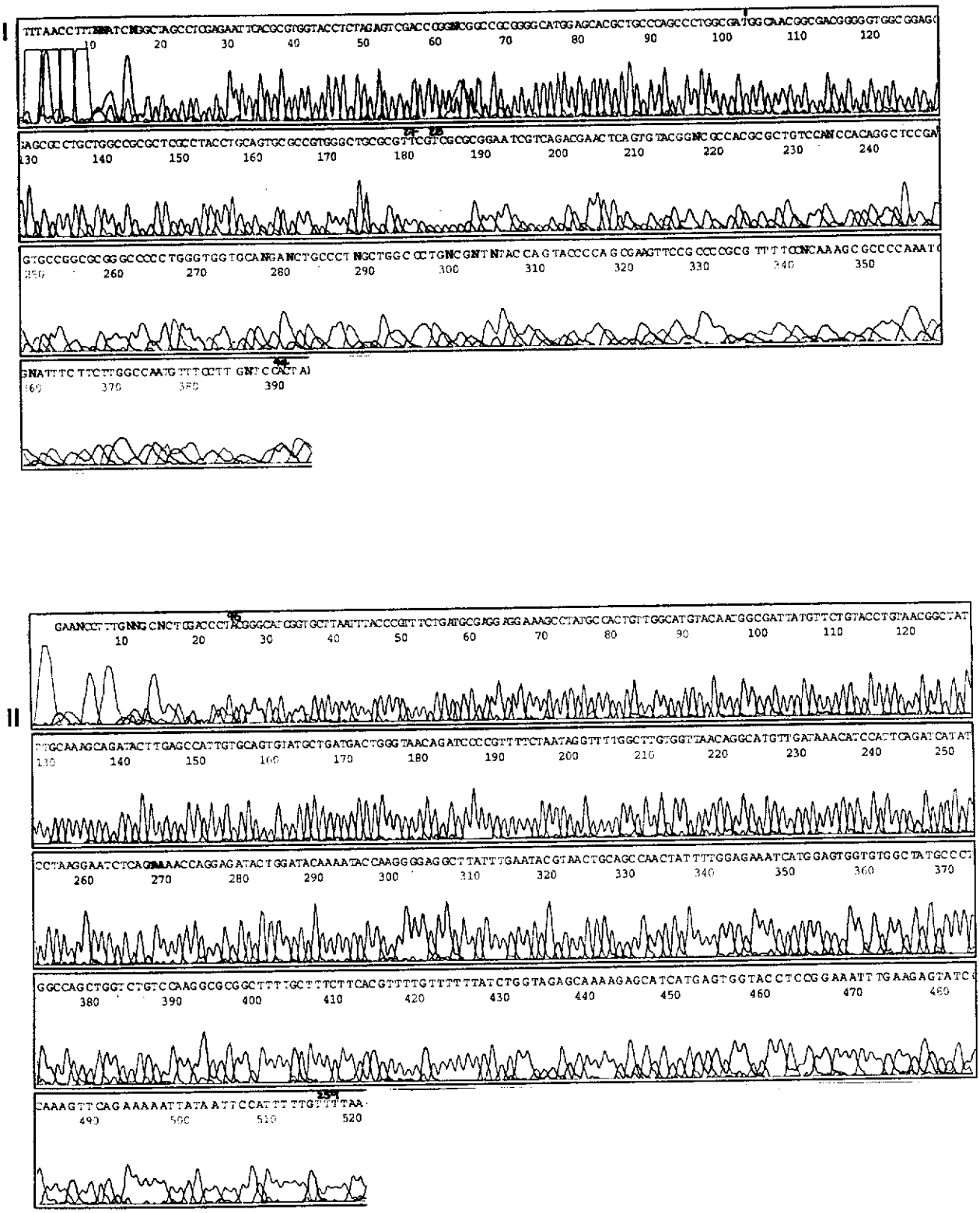

Figure A18: DNA sequence chromatographs of 5AR1AFVA mutant clone using the T7EEV (I), and AR1R (II) primers. Other than the mutations at residues 27 (-GTC- to -TTC-) and 28 (-TTC- to -GTC-), no additional alterations to the wild type cDNA were seen.

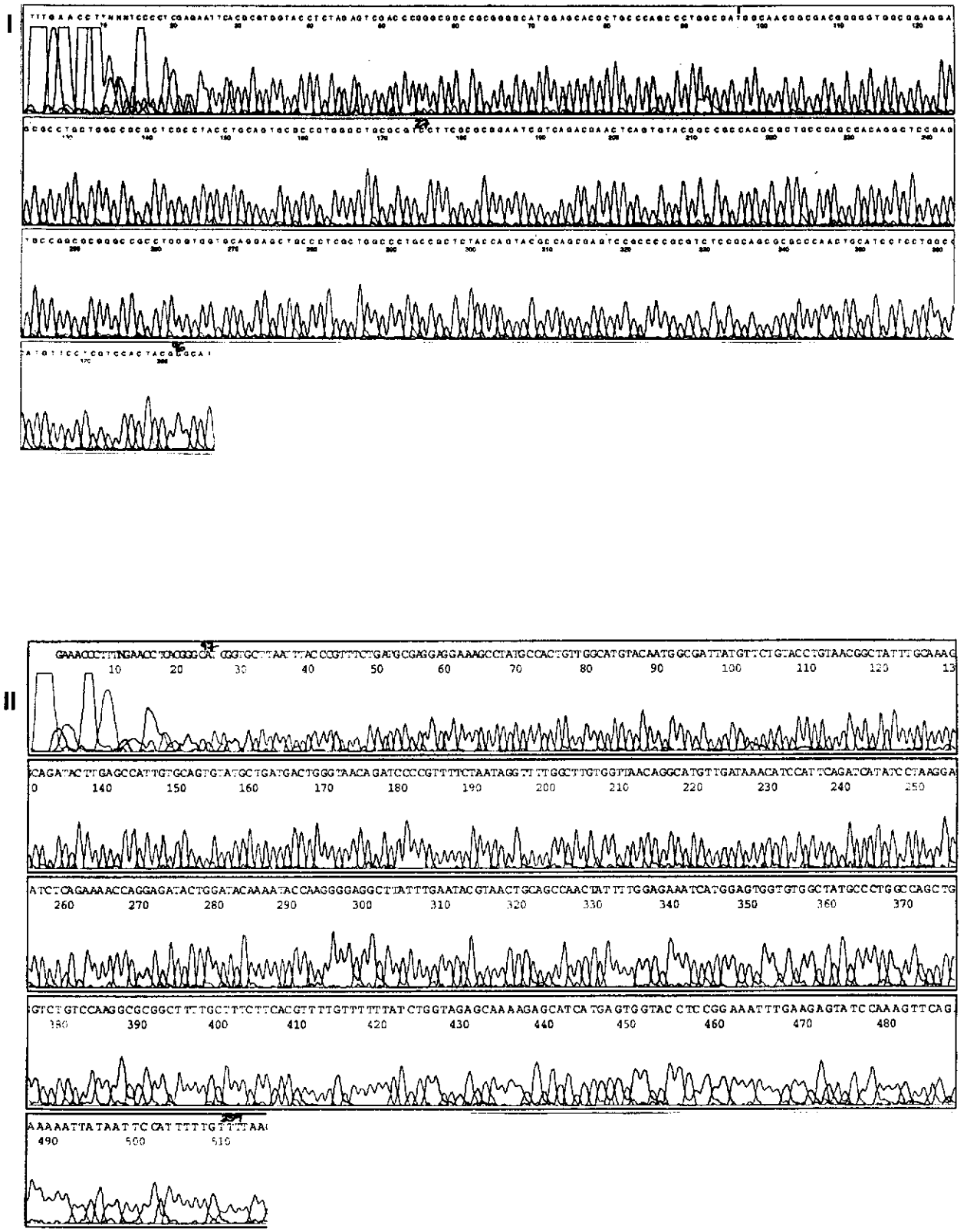

Figure A19: DNA sequence chromatographs of 5AR1ASFA mutant clone using the T7EEV (I), and AR1R (II) primers. Other than the mutation at residue 27 (-GTC- to -TCC-), no additional alterations to the wild type cDNA were seen.

axix

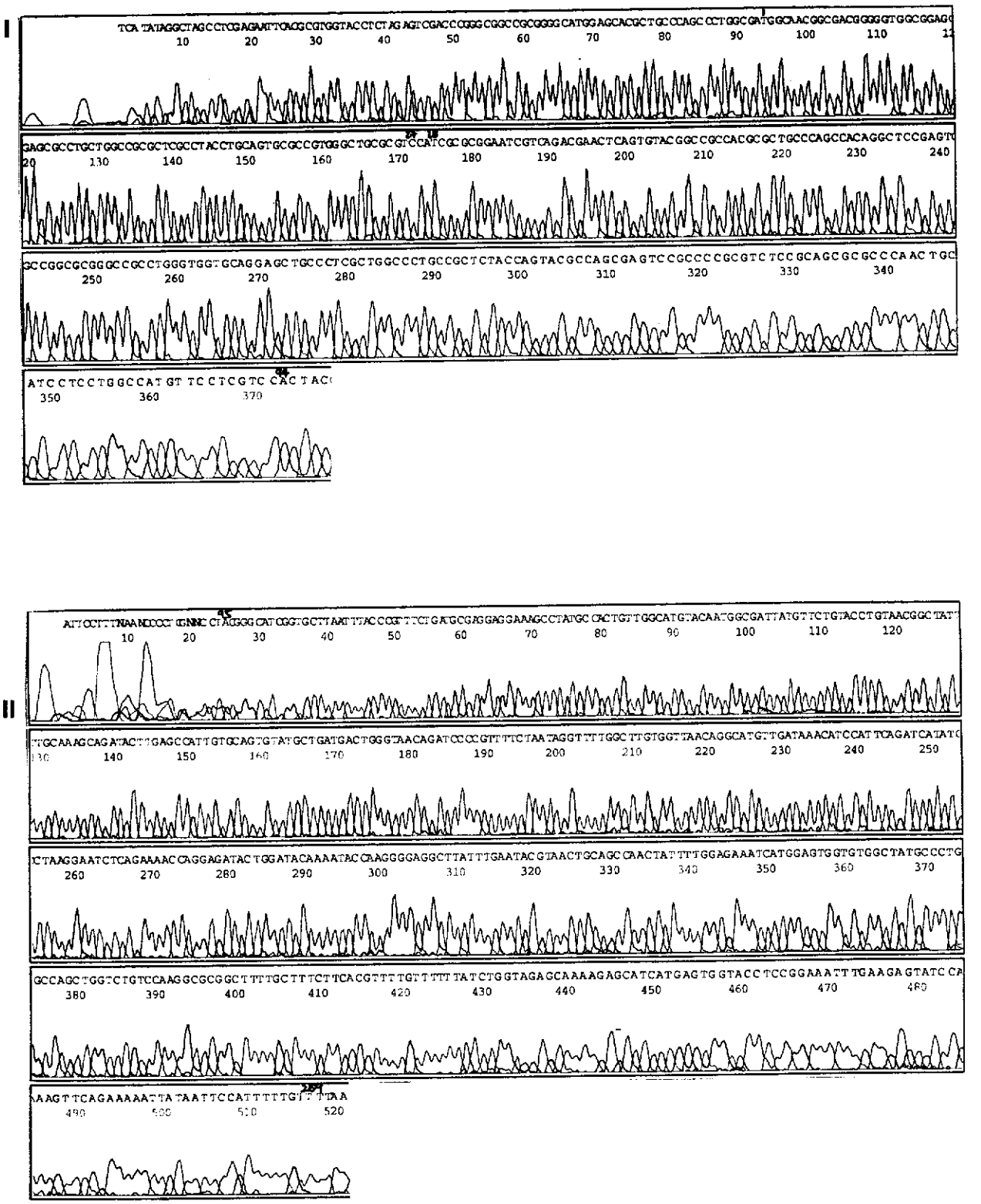

Figure A20: DNA sequence chromatographs of 5AR1ASIA mutant clone using the T7EEV (I), and AR1R (II) primers. Other than the mutations at residues 27 (-GTC- to -TCC-) and 28 (-TTC- to -ATC-), no additional alterations to the wild type cDNA were seen.

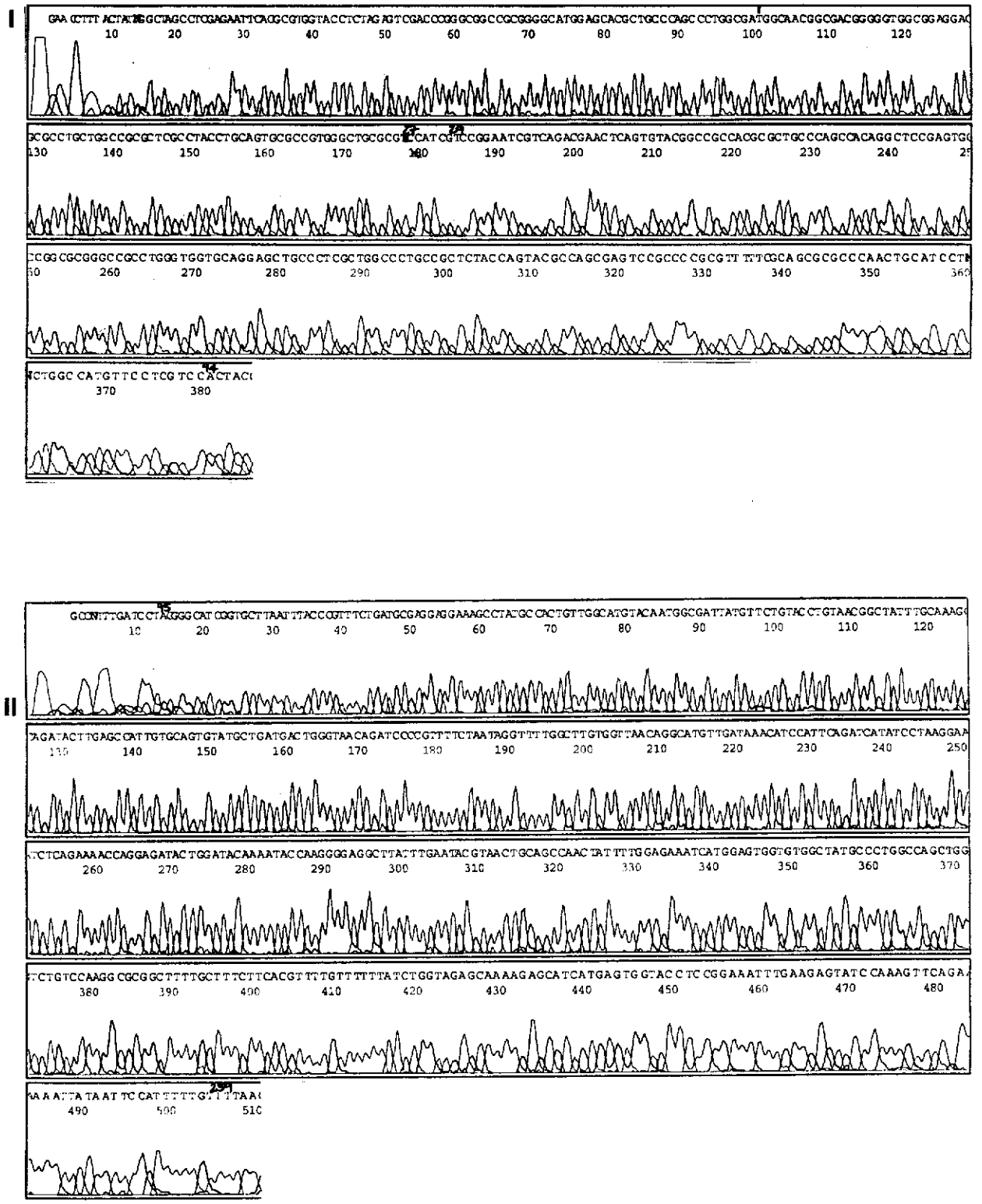

Figure A21: DNA sequence chromatographs of 5AR1ASIV mutant clone using the T7EEV (I), and AR1R (II) primers. Other than the mutations at residues 27 to 29 (-GTCTTCGCG- to -TCCATCGTC-), no additional alterations to the wild type cDNA were seen.

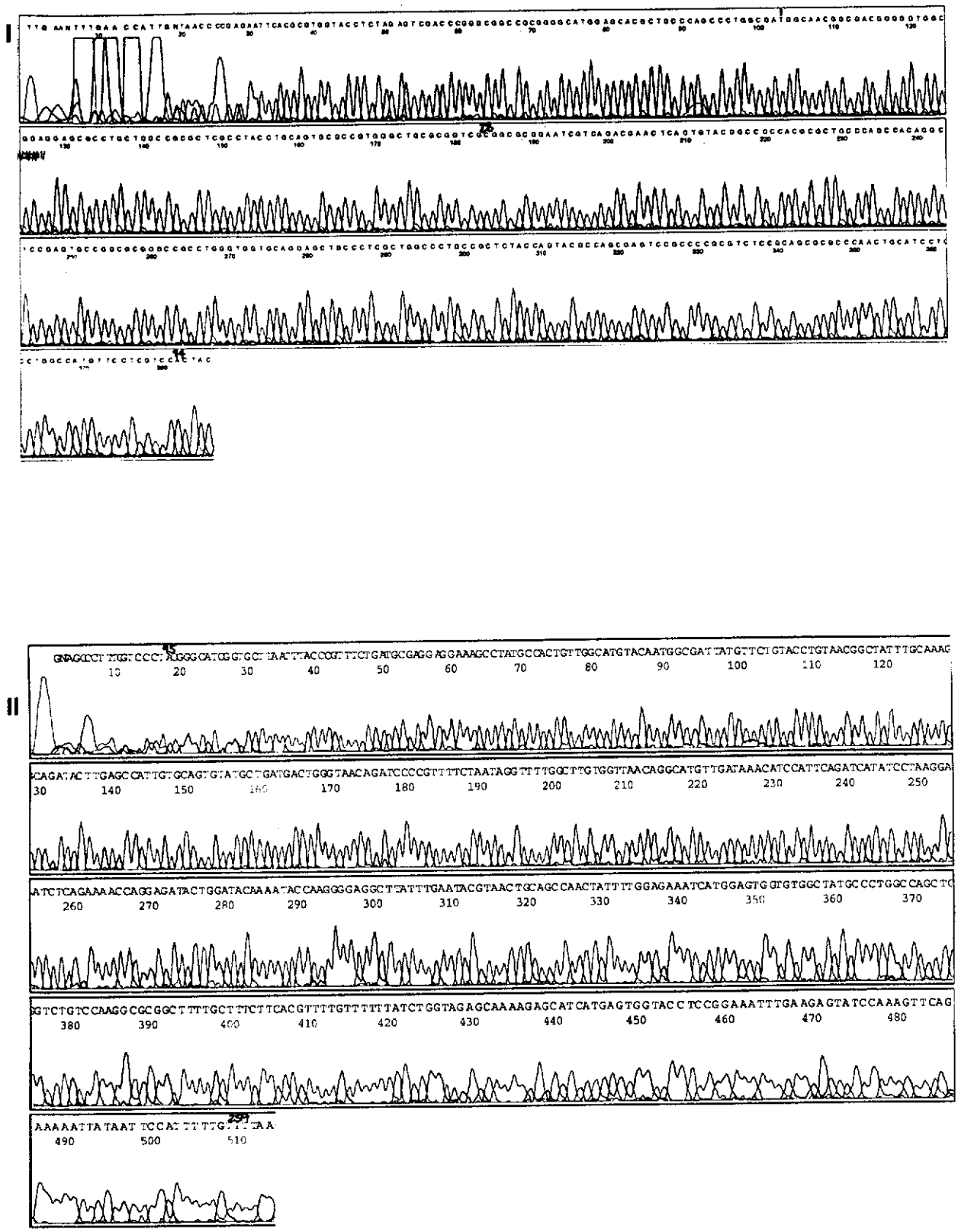

Figure A22: DNA sequence chromatographs of 5AR1AVAA mutant clone using the T7EEV (I), and AR1R (II) primers. Other than the mutation at residue 28 (-TTC- to -GCG-), no additional alterations to the wild type cDNA were seen.

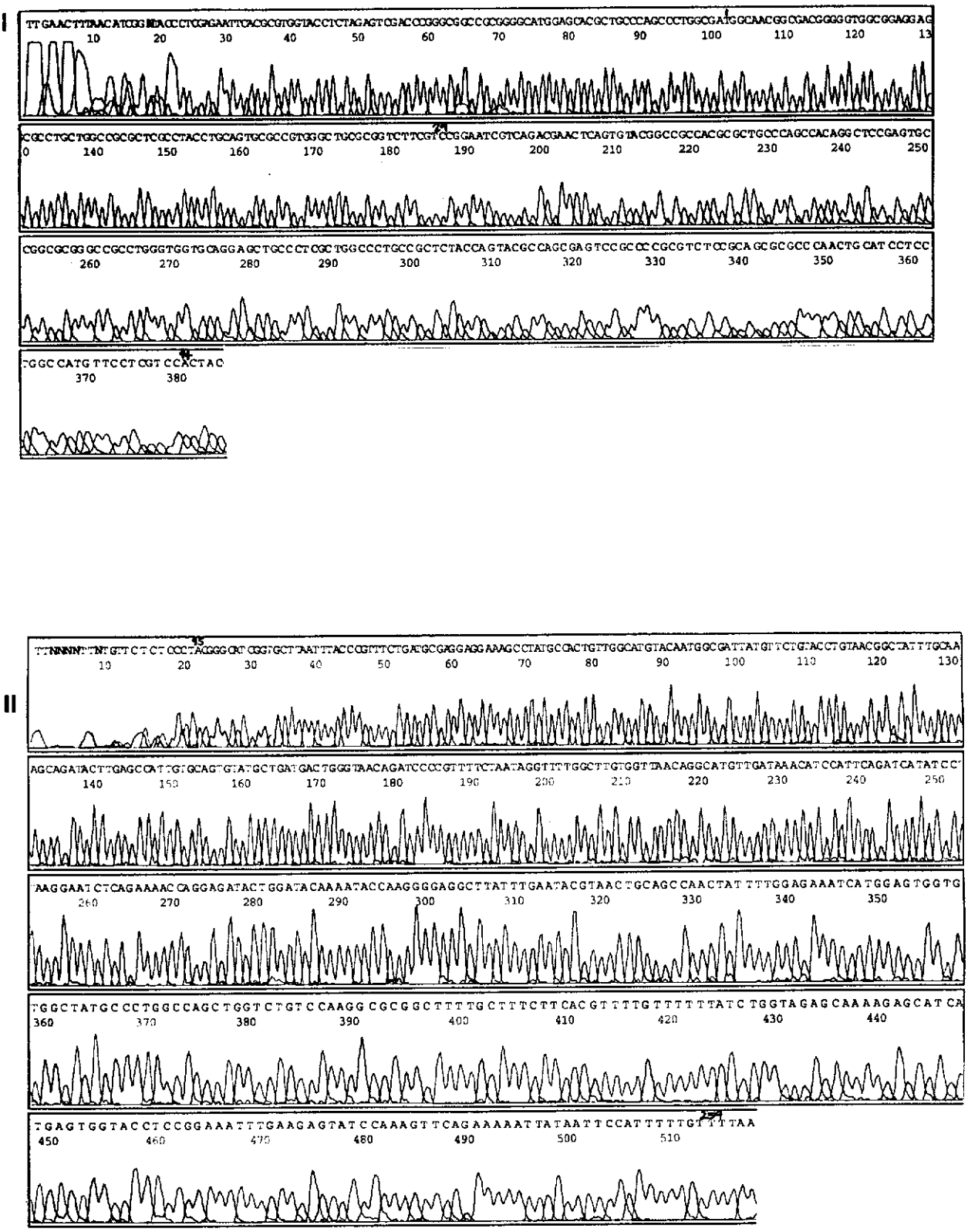

Figure A23: DNA sequence chromatographs of 5AR1AVFV mutant clone using the T7EEV (I), and AR1R (II) primers. Other than the mutation at residue 29 (-GCG- to -GTC-), no additional alterations to the wild type cDNA were seen.

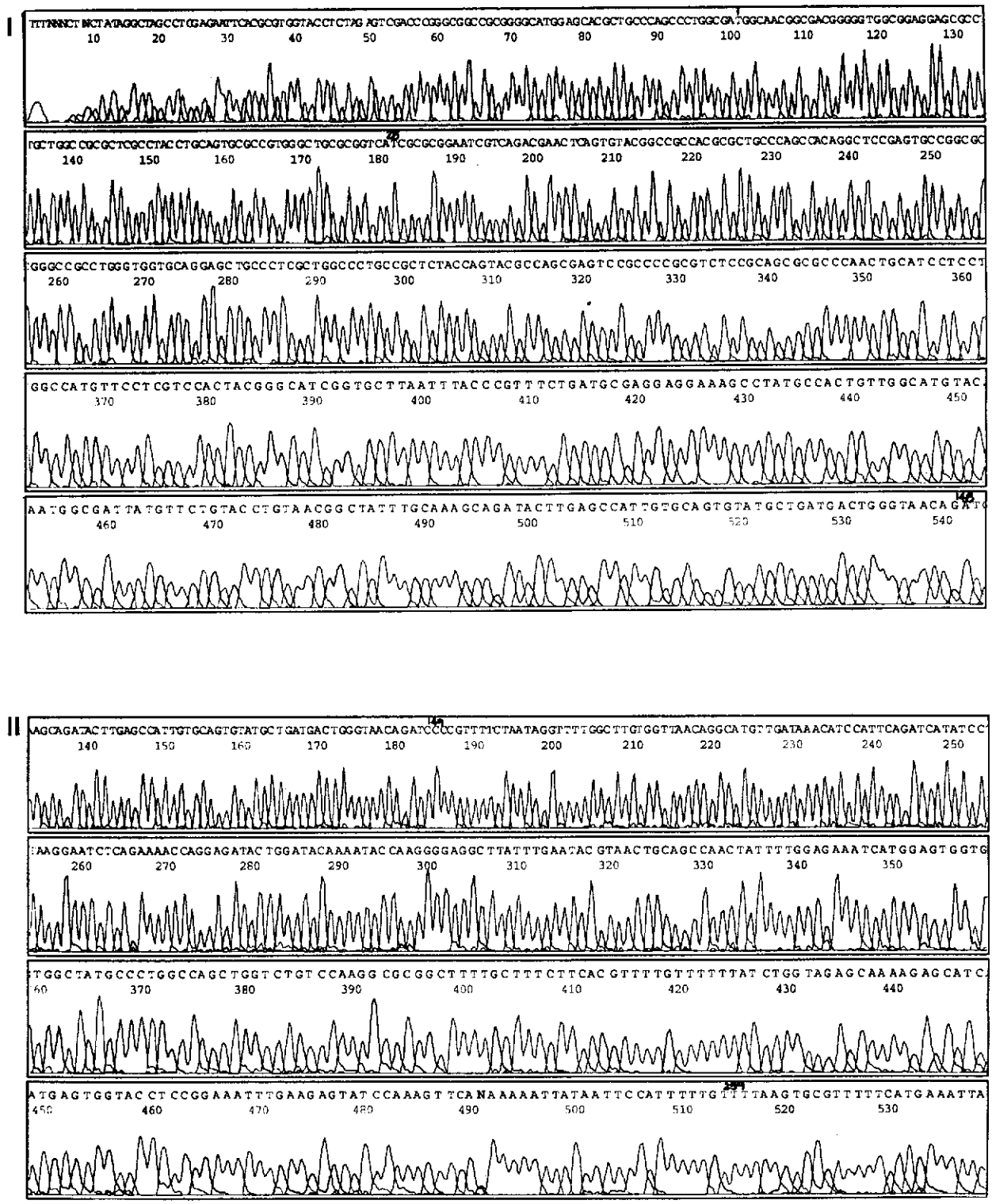

Figure A24: DNA sequence chromatographs of 5AR1AVIA mutant clone using the T7EEV (I), and AR1R (II) primers. Other than the mutation at residue 28 (-TTC- to -ATC-), no additional alterations to the wild type cDNA were seen.

I

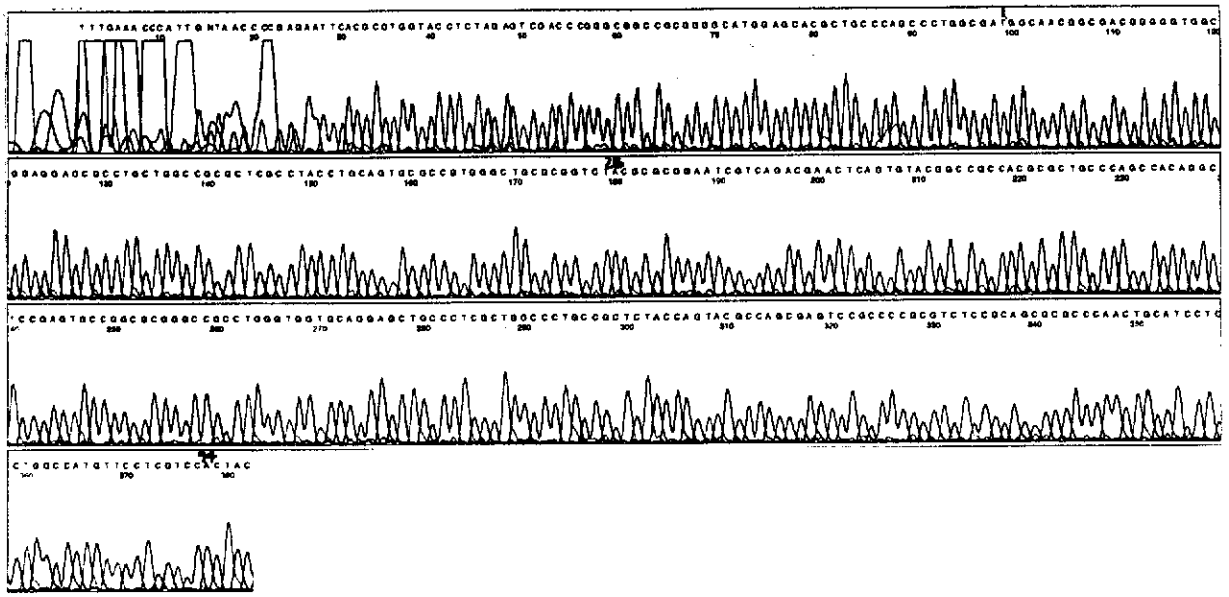

II

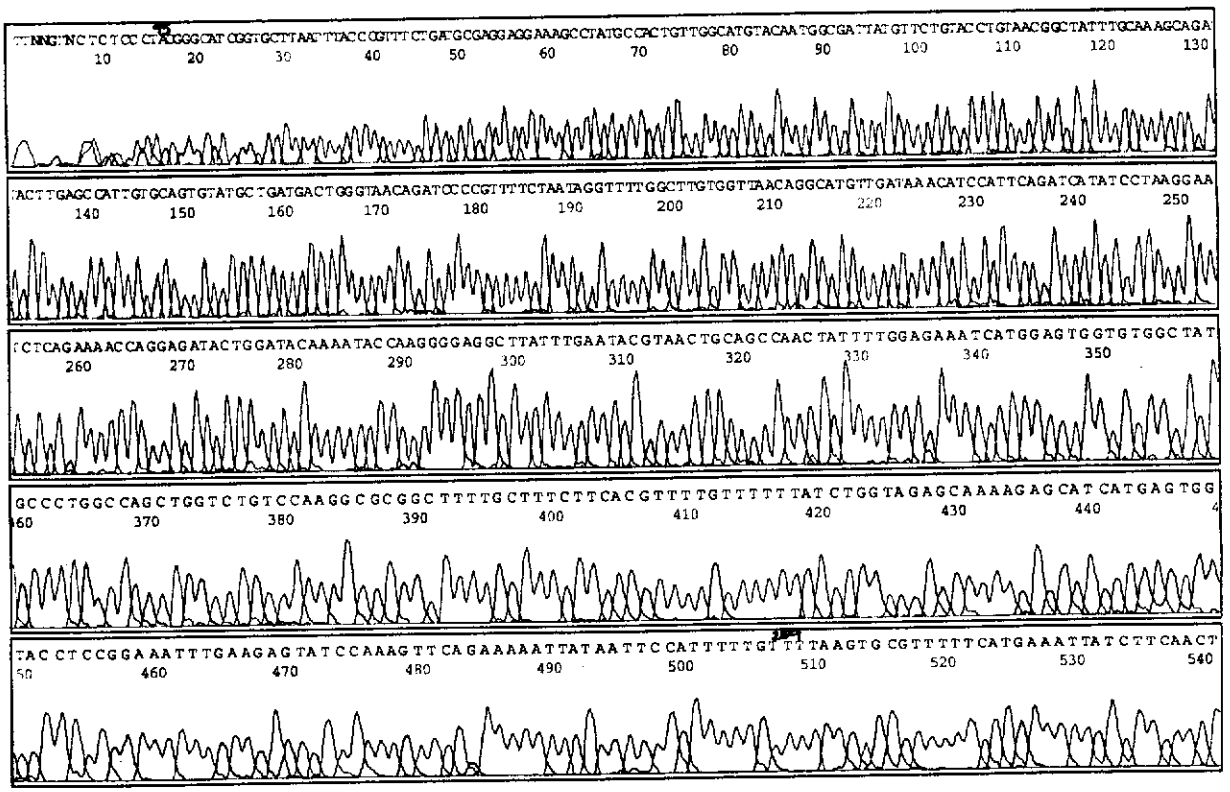

Figure A25: DNA sequence chromatographs of 5AR1AVYA mutant clone using the T7EEV (I), and AR1R (II) primers. Other than the mutation at residue 28 (-TTC- to -TAC-), no additional alterations to the wild type cDNA were seen.

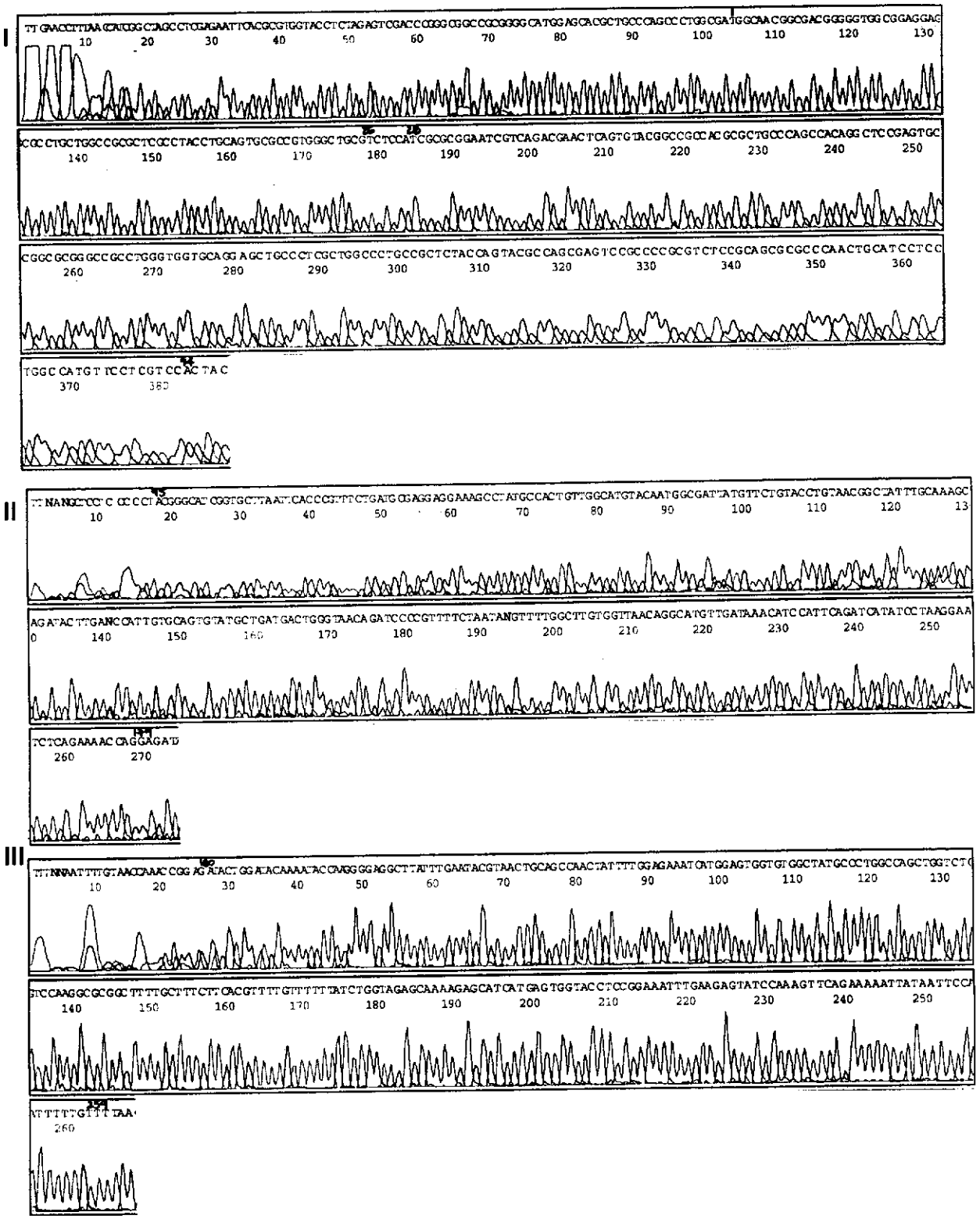

Figure A26: DNA sequence chromatographs of 5AR1VSIA mutant clone using the T7EEV (I), AR1R (II) and AR1H (III) primers. Other than the mutation at residues 26 to 28 (-GCGGTCTTC- to -GTCTCCATC-), no additional alterations to the wild type cDNA were seen.

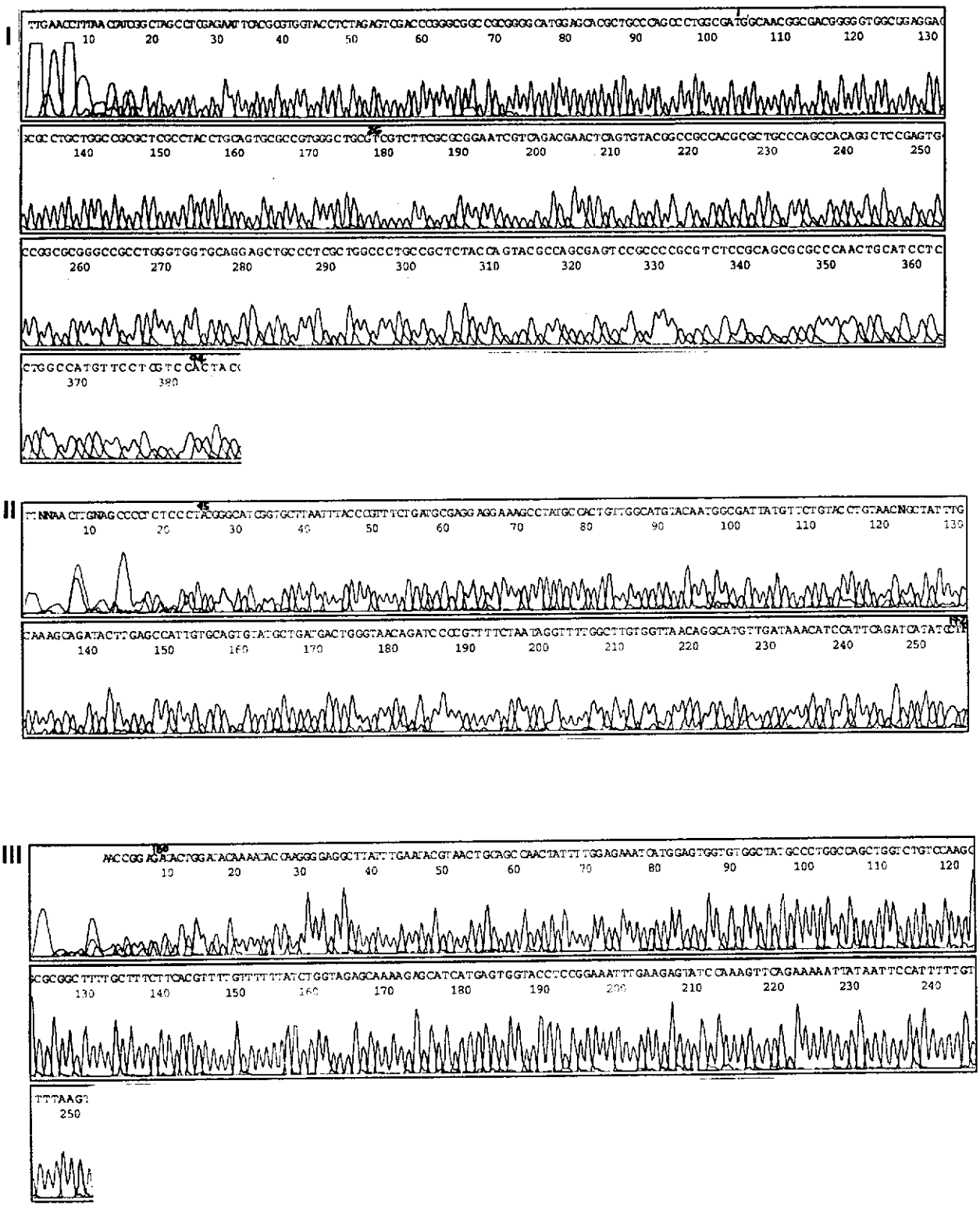

Figure A27: DNA sequence chromatographs of 5AR1VVFA mutant clone using the T7EEV (I), AR1R (II) and AR1H (III) primers. Other than the mutation at residue 26 (-GCG- to -GTC-), no additional alterations to the wild type cDNA were seen.

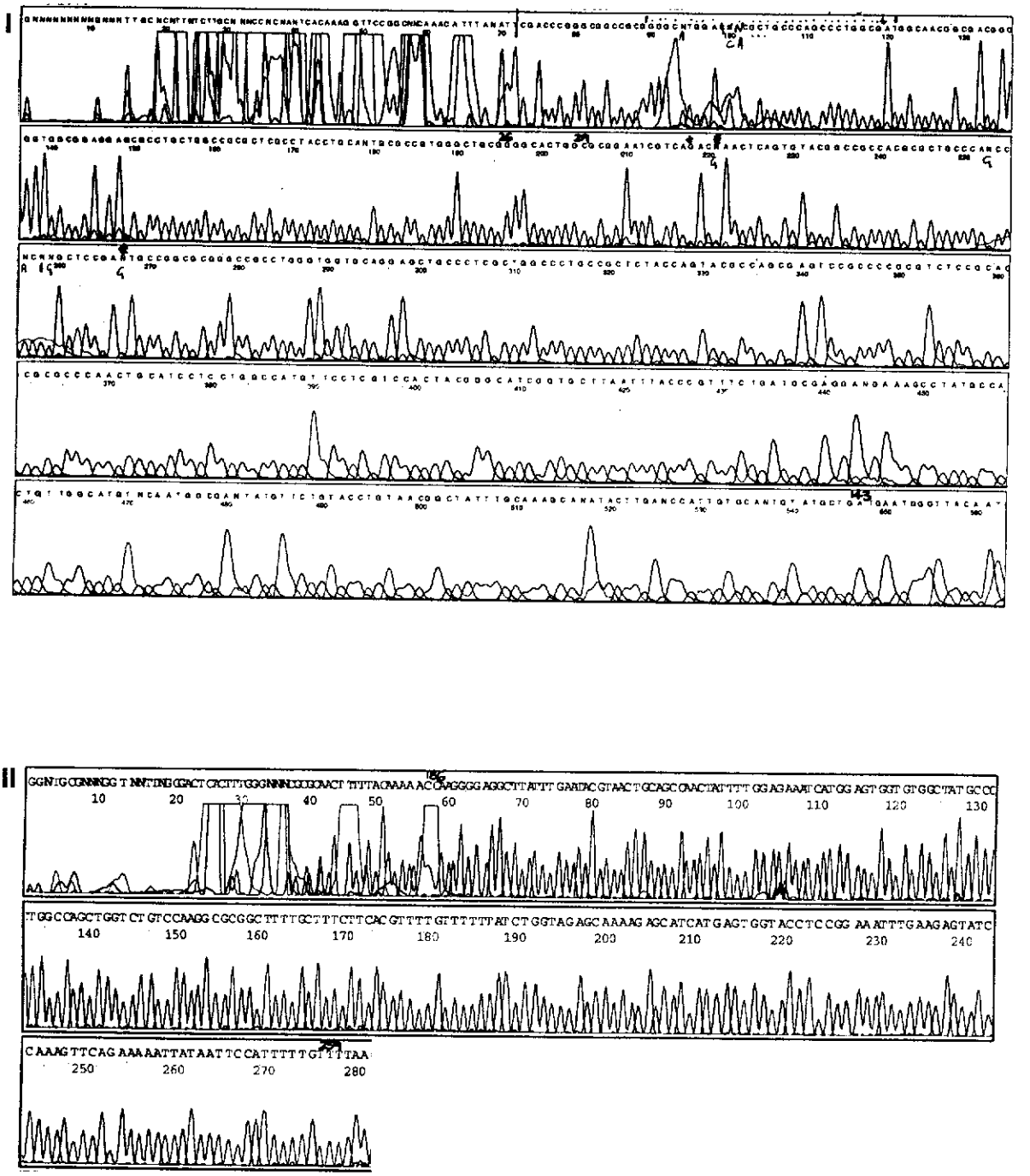

Figure A28: DNA sequence chromatographs of 5AR1M mutant clone using the T7EEV (I) and AR1H (II) primers. Other than the mutation at residues 26 to 29 (-GCGGTCTTCGCG- to -GGGGCACTG GCG-), no additional alterations to the wild type cDNA were seen. Sequencing of residues 143-186 was however not possible using these primers.

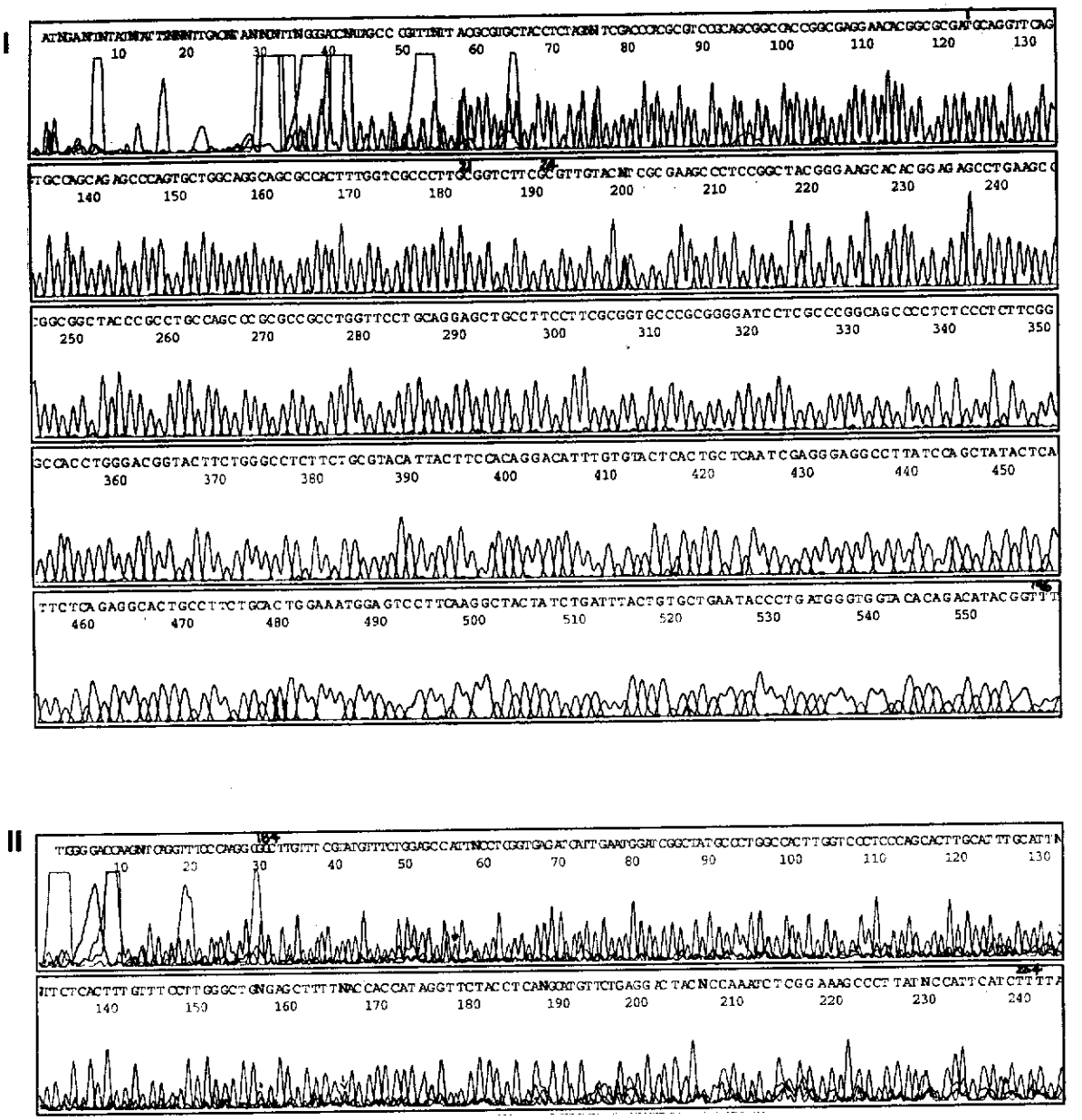

Figure A29: DNA sequence chromatographs of 5AR2M mutant clone using the T7EEV (I) and AR2H (II) primers. Other than the mutation at residues 21 to 24 (-GGCGCACTGGCC- to -GCGGTCTTC GCG-), no additional alterations to the wild type cDNA were seen. Sequencing of residues 146-184 was however not possible using these primers.

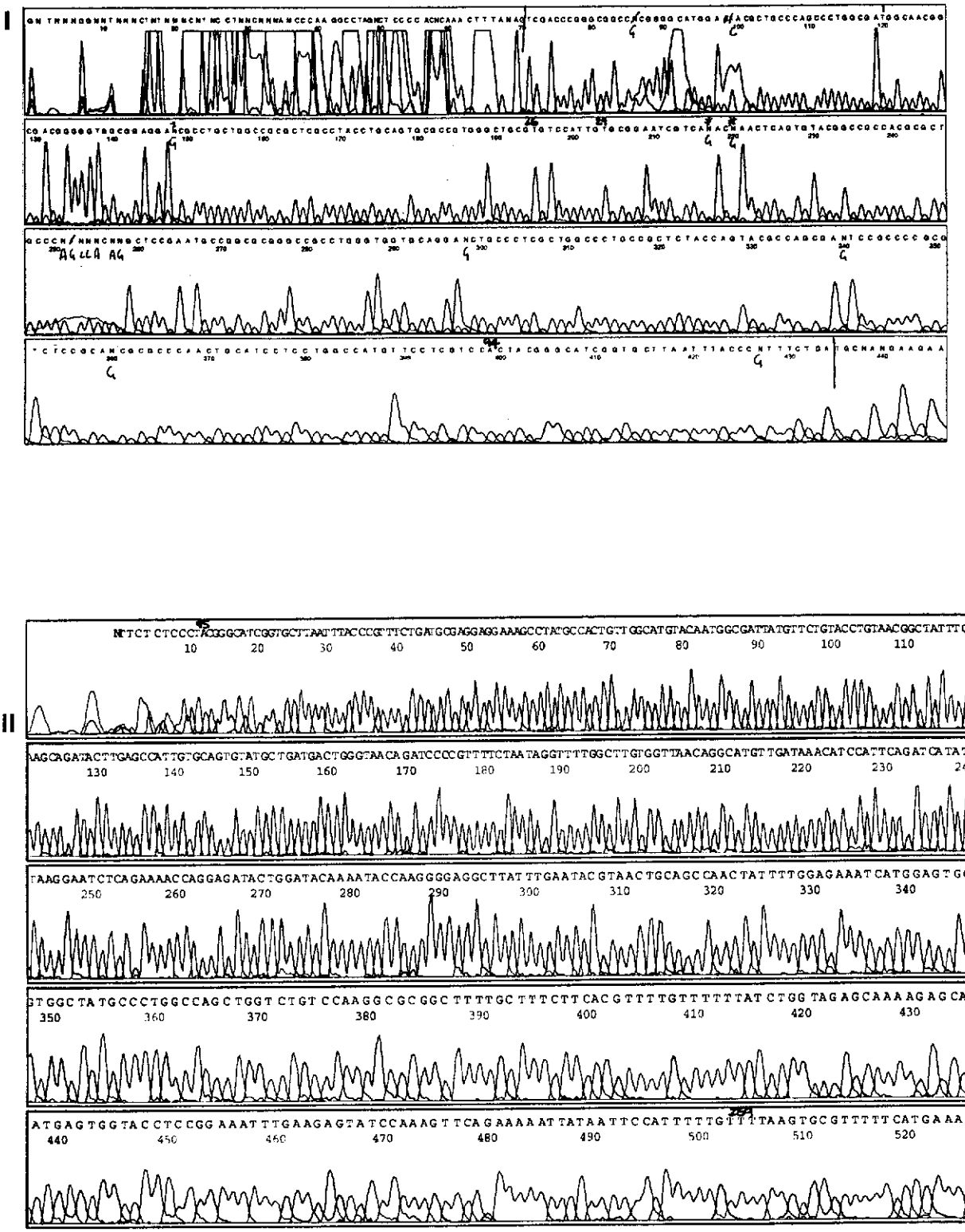

Figure A30: DNA sequence chromatographs of 5AR1R mutant clone using the T7EEV (I) and AR1R (II) primers. Other than the mutation at residues 26 to 29 (-GCGGTCTTCGCG- to -GTGTCCATT GTG-), no additional alterations to the wild type cDNA were seen.

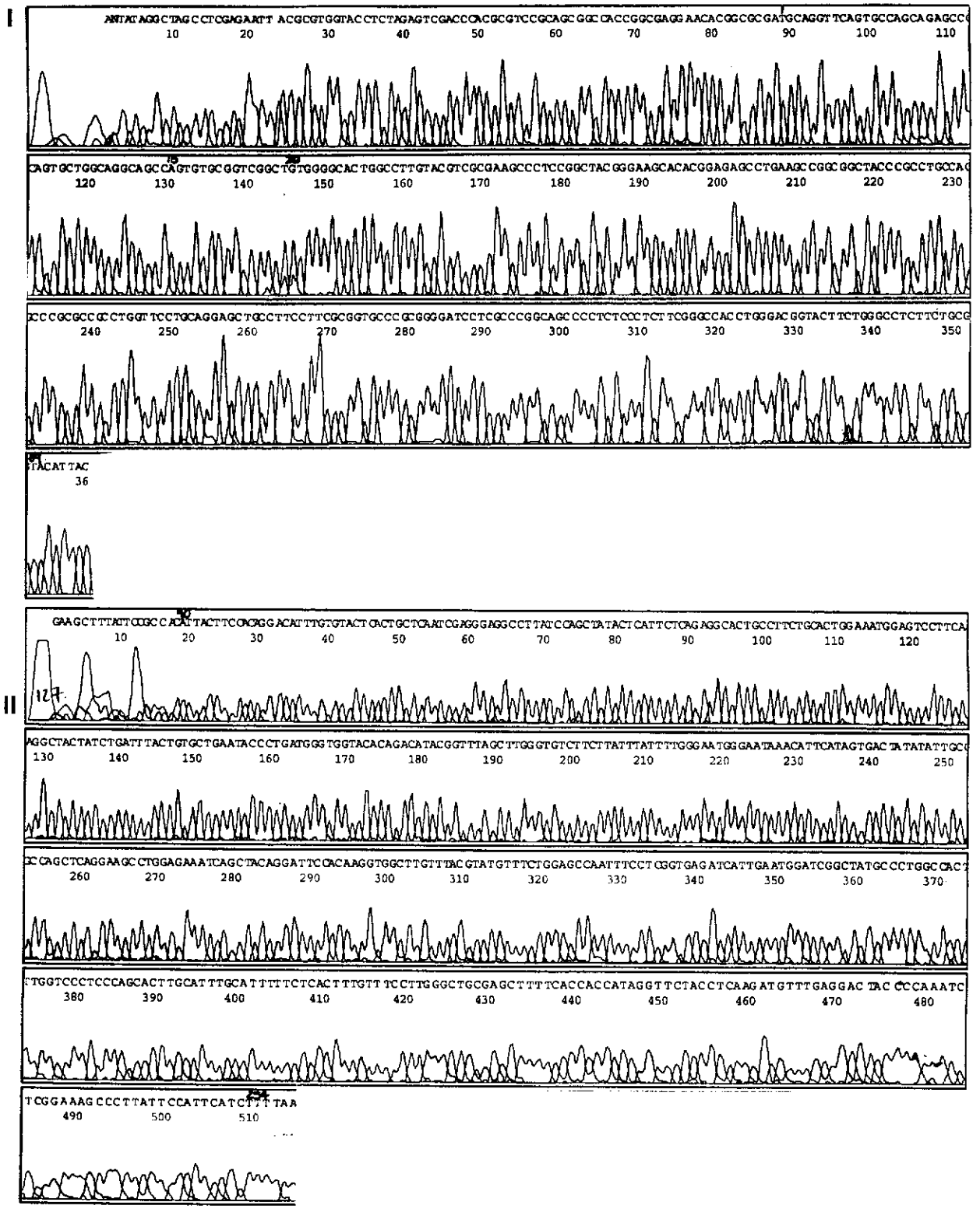

Figure A31: DNA sequence chromatographs of 5AR2/15-20 mutant clone using the T7EEV (I) and AR2R (II) primers. Other than the mutation at residues 15 to 20 (-GCCACTTTGGTCGCCCTT- to -CAGTGTGCGGTCGGCTGT-), no additional alterations to the wild type cDNA were seen.

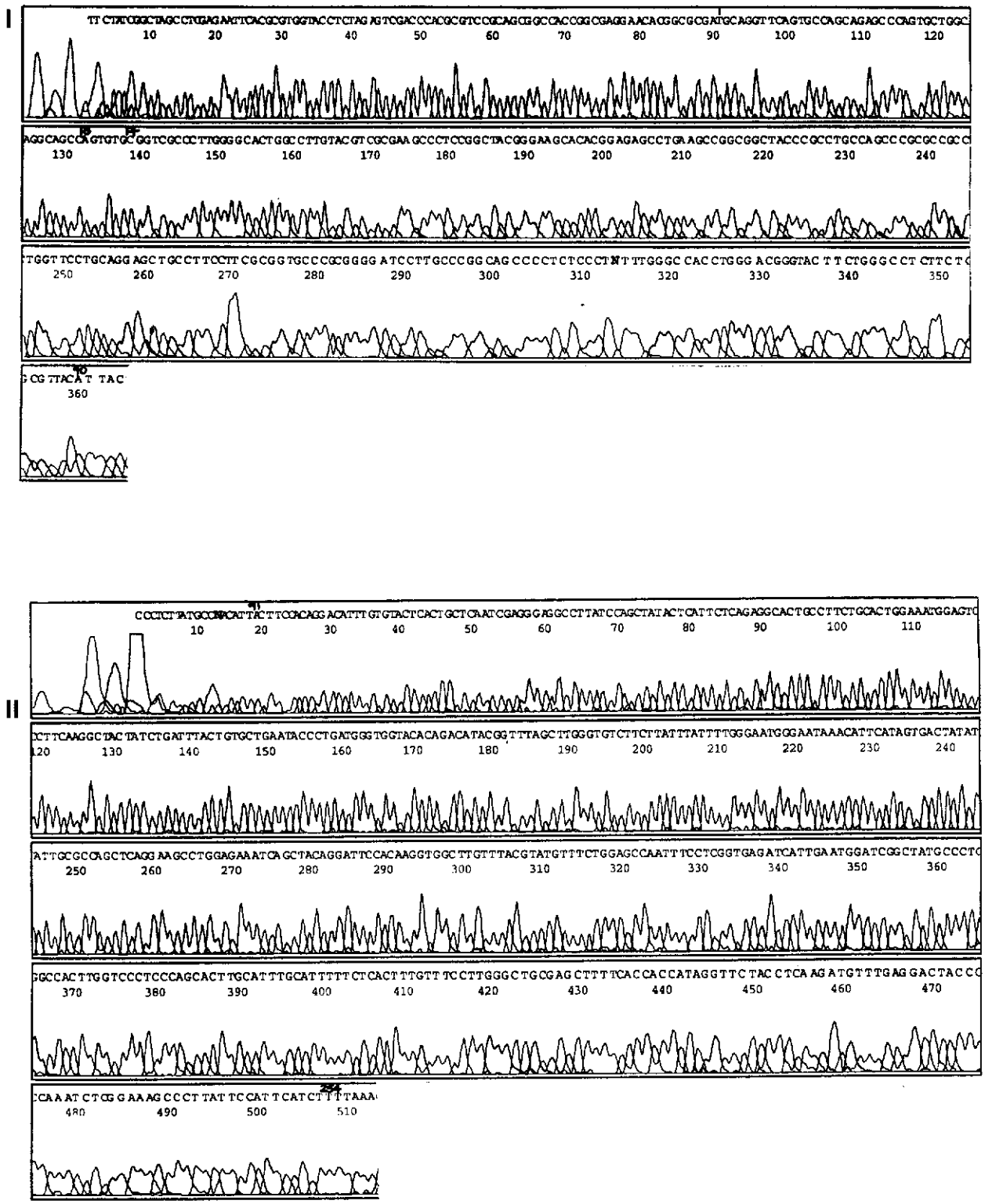

Figure A32: DNA sequence chromatographs of 5AR2/15-17 mutant clone using the T7EEV (I) and AR2R (II) primers. Other than the mutation at residues 15 to 17 (-GCCACTTTG- to -CAGTGTGCG-), no additional alterations to the wild type cDNA were seen.

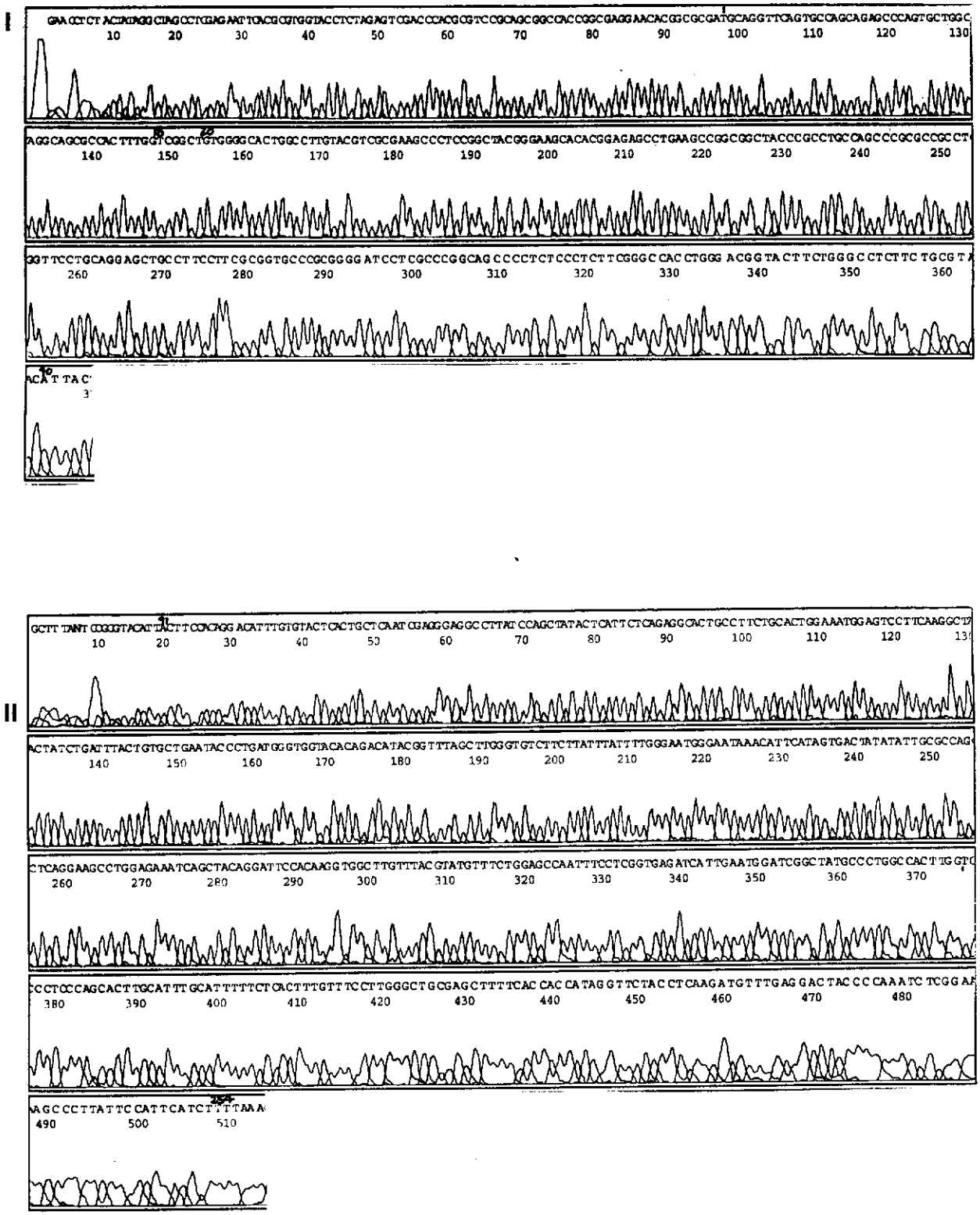

Figure A33: DNA sequence chromatographs of 5AR2/18-20 mutant clone using the T7EEV (I) and AR2R (II) primers. Other than the mutation at residues 18 to 20 (-GTCGCCCTT- to -GTCGGCTGT-), no additional alterations to the wild type cDNA were seen.

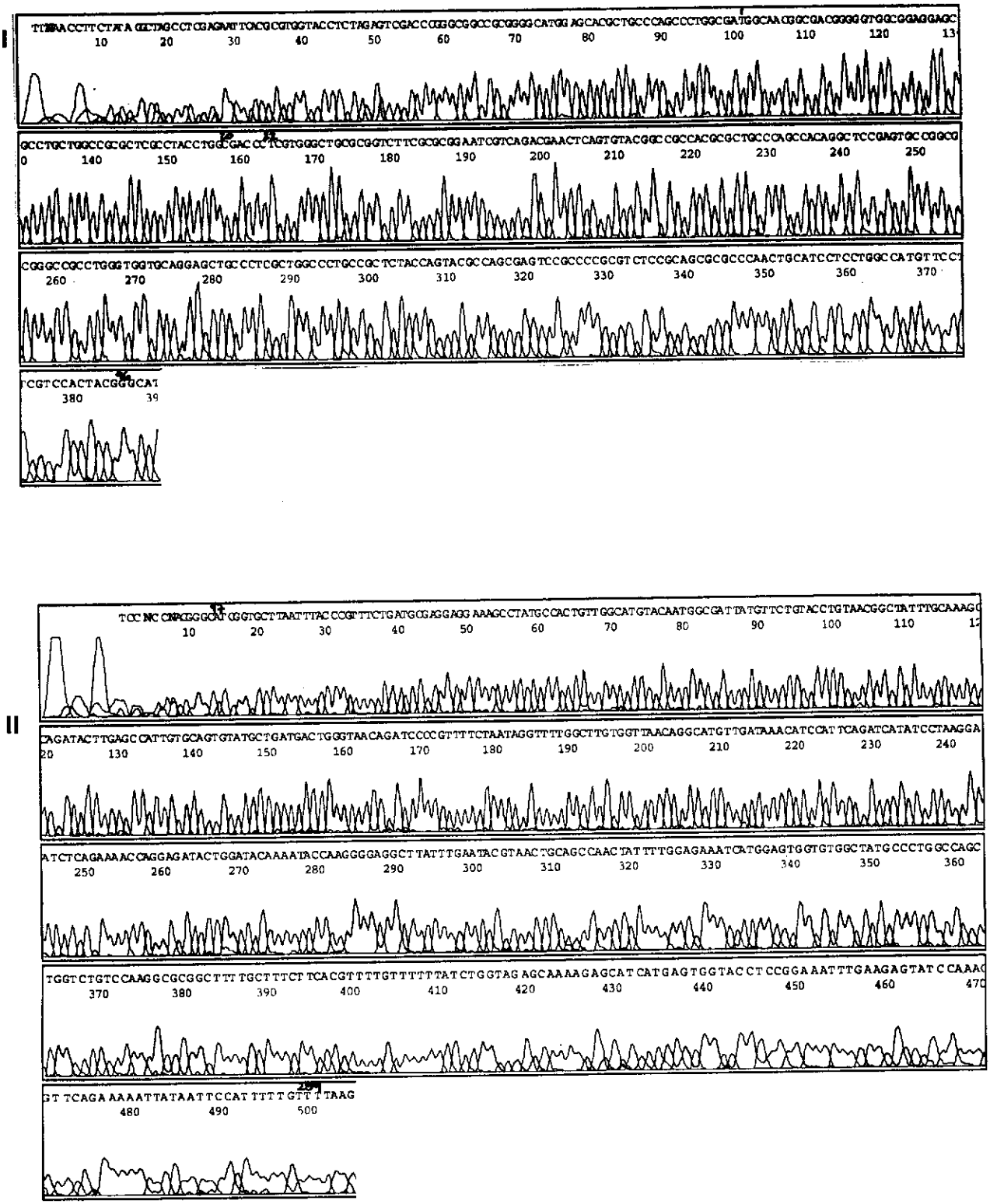

Figure A34: DNA sequence chromatographs of 5AR1/20-22 mutant clone using the T7EEV (I) and AR1R (II) primers. Other than the mutation at residues 20 to 22 (-CAGTGCGCC- to -GCGACCCTC-), no additional alterations to the wild type cDNA were seen.

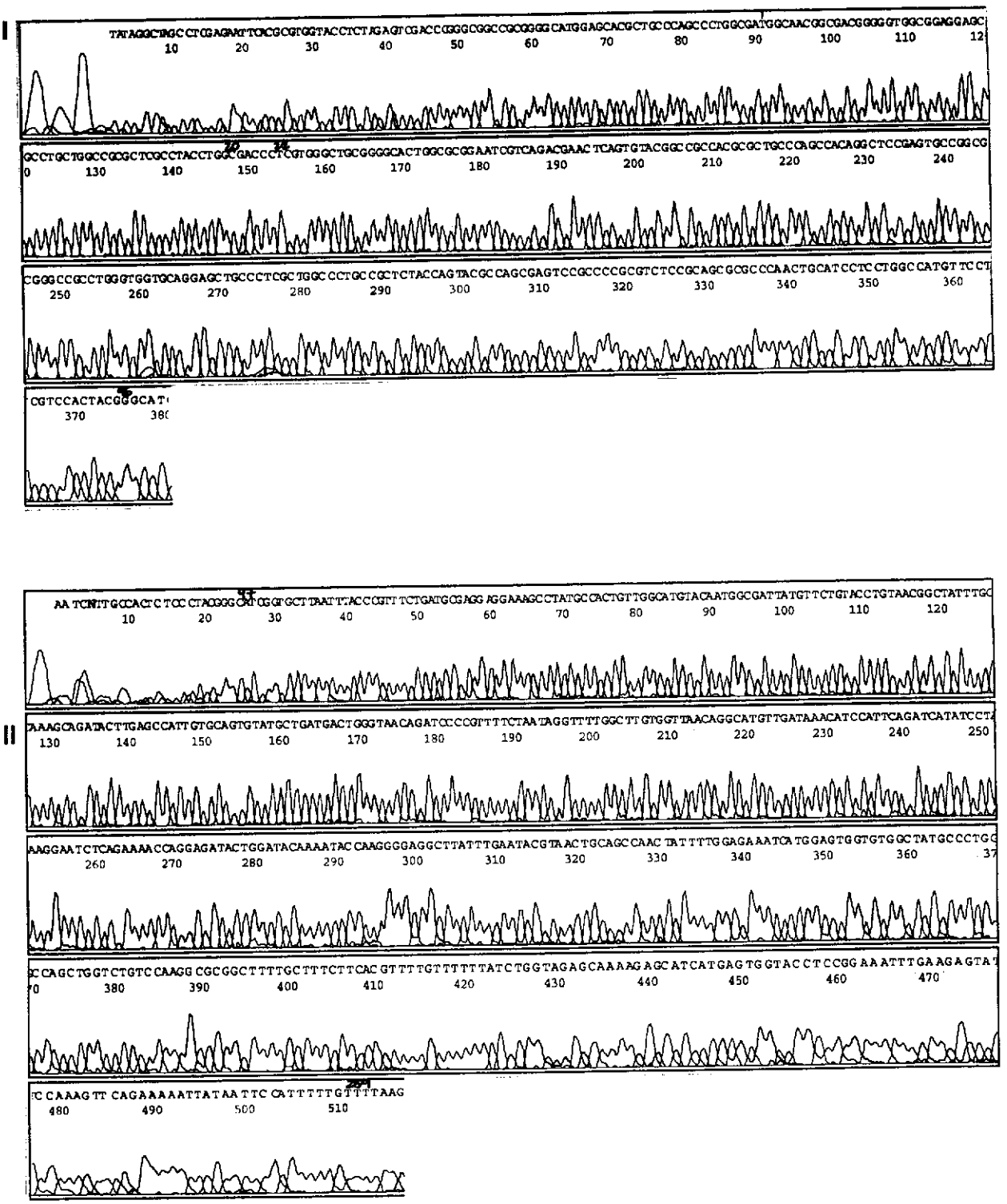

Figure A35: DNA sequence chromatographs of 5AR1/20-22/26-29 mutant clone using the T7EEV (I) and AR1R (II) primers. Other than the mutations at residues 20 to 22 (-CAGTGCGCC- to -GCGACCCTC-) and 26 to 29 (-GCGGTCTTCGCG- to -GGGGCACTGGCG-), no additional alterations to the wild type cDNA were seen.

Appendix B

C1 and C2 Constructs

APPENDIX B

Chimeric constructs of the human 5AR1 and 5AR2 cDNAs in the mammalian expression vector pCI-neo were created, for which the amino terminus of 5AR1 was ligated with the carboxyl terminus of 5AR2 and vice versa. *Ngo MIV* was selected for restriction digests of the 5AR cDNA inserts in pCI-neo as it cuts both 5AR cDNAs once only, at residue 50 for 5AR1 and 41 for 5AR2. *Ngo MIV* digestion of pCI-neo plus either 5AR insert generated three large fragments of 3.5, 2.4 and 1.5kb for 5AR1 and 3.5, 2.7 and 1.5kb for 5AR2 (figure B1).

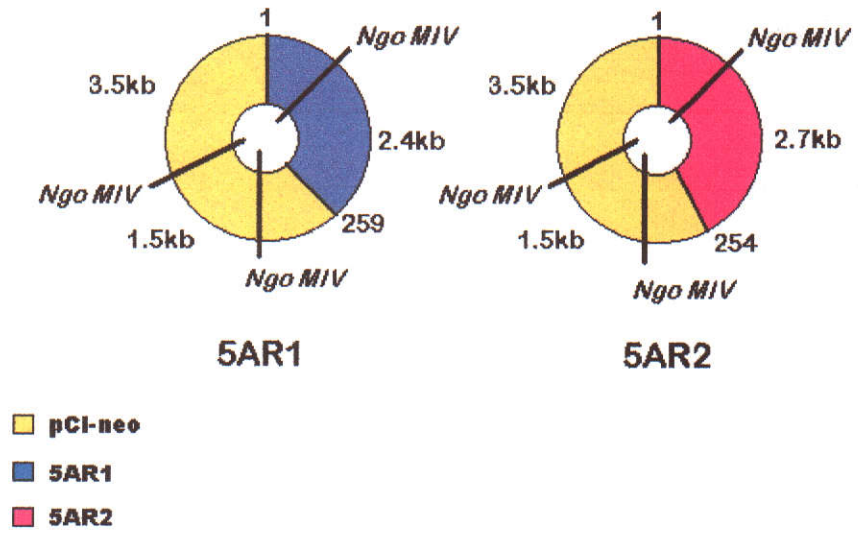

Figure B1 *Restriction digest fragments resulting from Ngo MIV digestion of pCI-neo/5AR1 and pCI-neo/5AR2.*

The 3.5kb fragment from the 5AR1/*Ngo MIV* digest was ligated with the 2.7kb fragment from the 5AR2/*Ngo MIV* digest and in doing so ligated r1-50 from 5AR1 with r42-254 from 5AR2, giving the preliminary C1 clone. The 3.5kb fragment from the 5AR2/*Ngo MIV* digest was ligated with the 2.4kb fragment from the 5AR1/*Ngo MIV* digest and in doing so ligated r1-41 from 5AR2 with r51-259 from 5AR1, giving the preliminary C2 clone (figure B2).

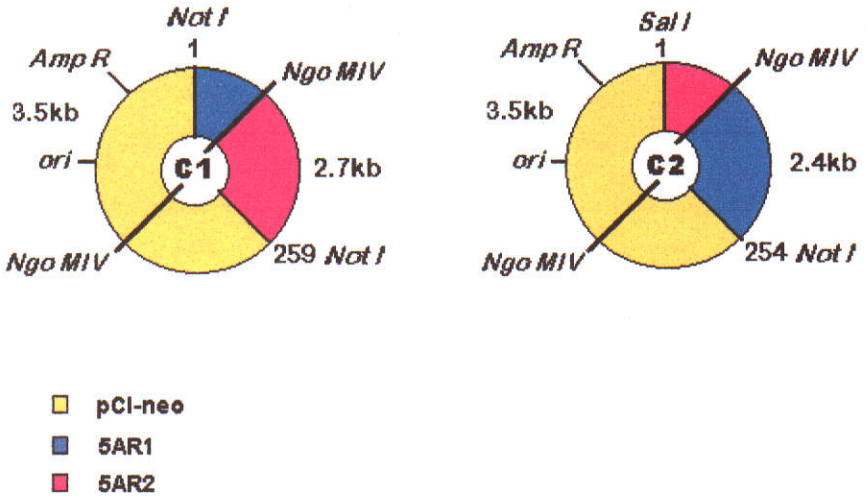

Figure B2 *Preliminary C1 and C2 sub-clones.*

These preliminary C1 and C2 clones contain both an origin of replication and ampicillin resistance gene enabling their transformation into *E.coli* and subsequent selection, however they lacked a neomycin resistance gene preventing their selection in mammalian cells. The preliminary constructs were therefore digested with *Not I* for C1 and *Not I/Sal I* for C2. Unmodified pCI-neo vector was simultaneously digested. The C1 sub-clone was then religated into *Not I* digested pCI-neo and C2 sub-clone into *Not I/Sal I* digested pCI-neo to generate the final C1 and C2 constructs (figure B3). Our main focus was the C2 chimeric construct expressing the amino terminus of 5AR2, this was stably transfected into CHO cells and the characteristics of the expressed enzyme determined.

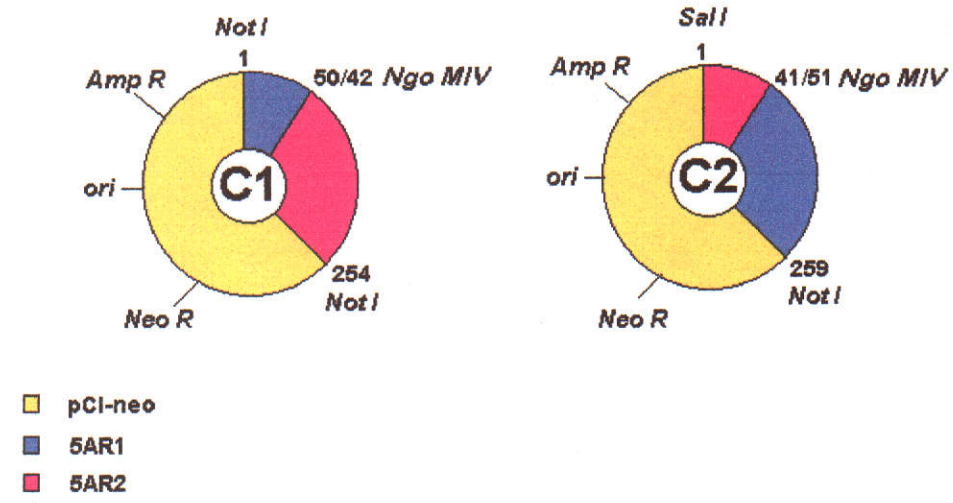

Figure B3 *Final chimeric constructs of C1 and C2.*